ANAEROBIC FILTER TREATMENT

OF

WINE DISTILLERY WASTE

by

Mario G. Capri, B.Sc.(Eng) (Cape Town)

A thesis submitted in partial fulfilment of the requirements for the Degree of Master of Science in the Faculty of Engineering, University of Cape Town.

Department of Civil Engineering,
UNIVERSITY OF CAPE TOWN.

April 1973.

DECLARATION OF CANDIDATE

I, Mario Capri, hereby declare that this thesis is my own work and that it has not been submitted for a degree at another university.

Signed by candidate

April 1973.

SYNOPSIS

In the Western Cape, the high strength wine distillery wastes (approximate COD of 24 000 mg/l) are stabilized by the anaerobic contact process. This process requires fairly close operational control, and a degree of technical competence which is often lacking in many small plants. McCarty has recently developed the submerged anaerobic filter as an effective means for treating low strength wastes. As the filter was found to require little supervision to ensure efficient and stable operation, it was decided to enquire into the suitability of the filter for the treatment of wine distillery waste.

The specific objectives of the investigation were to:

1. Compare the performance and behaviour of the anaerobic filter with those of the contact process.

2. Investigate the effect of different filter media on the process performance.

3. Apply the general kinetic model for biological systems to the anaerobic filter process.

4. Investigate the factors controlling the pH in an anaerobic process.

Three bench-scale anaerobic filters containing quartzite, clinker and combined plate-sand media were operated on wine distillery waste. A high recirculation rate ensured that the contents were kept completely mixed and thus eliminated the low pH conditions which tend to develop at the bottom of a filter. The temperature was controlled at $35^{o}C$. Waste loading rates were incrementally increased over a period of about 120 days from an initial low value of 1,5 kg COD/day/m^3 of total reactor volume, to the maximum load capacity for the filters - approximately 15,0 kg COD/day/m^3. The treatment efficiencies and general performances were measured for each loading rate once 'steady-state' conditions were achieved.

The treatment efficiencies and capacities of the anaerobic filters were found to be almost identical to those of the full-scale anaerobic contact process in operation at present. In both, a loading rate of 2,0 kg COD/day/m^3 of total reactor volume ensured stable operation with 98,5% COD reductions. From this study, there does not appear to be any significant advantage in replacing the contact by the filter process. Research should preferably be oriented towards improvement in the solid-liquid separation mechanism in the contact process.

The stabilization process in the filters appears to be situated mainly in the interstices provided by the media, and is not greatly affected by the surface area of the media. Although the clinker had a far greater surface area than the quartzite, the clinker filter was able to attain only a 20% increase over the maximum load capacity of quartzite filter. The filter with perforated plate media operated satisfactorily, with a maximum load capacity in the same range as that of the stone and clinker media filters. The sand media eventually proved useless since it choked with biological solids.

It was found that the continuous culture kinetic model can be usefully applied to the anaerobic filter process. As for the contact system, the solids retention time proved to be the controlling parameter for predicting (i) the treatment efficiency, (ii) the stability of a process, (iii) the solid concentrations in the reactor and effluent, and (iv) the response of the filter to shock loads. The solids concentration in the effluent was found to be a particularly sensitive parameter for the control of the solids retention time, and consequently, of the process performance. Small changes in the average solids concentration in the effluent can have such marked effect on the process performance, that it is proposed that a positive method for solids retention in a reactor, such as centrifuging of solids from the effluent, be employed. Implementation of this proposal would probably increase the loading capacity of a reactor.

The pH in an anaerobic process (operating in the pH range 6,0 to 7,5) was found to be established by the carbonic, ammonia and volatile fatty acids weak acid/base systems, and by some strong base released in the process. It was experimentally verified that the buffer capacity in the pH range 6,0 to 7,5 is provided only by the carbonic

weak acid system. A pH conditioning diagram showing the effect various dosing chemicals have on pH was developed. The diagram was experimentally verified for additions of NaOH, Na_2CO_3, and $NaHCO_3$. The limitation which $CaCO_3$ solubility places on pH was verified with $Ca(OH)_2$ additions to de-ionized water samples. In anaerobic liquid samples, pH was found not to be limited by the $CaCO_3$ solubility. This is due to $CaCO_3$ precipitation being inhibited by orthophosphates. It was experimentally shown that pH adjustment to 7,0 with $Ca(OH)_2$ is possible only if $CaCO_3$ precipitation is inhibited. Orthophosphate was isolated as causing the inhibition mechanism in both spent wine and domestic sludge digestors. Any orthophosphate concentration greater than 1×10^{-3} moles/l ensures that about 45% of $Ca(OH)_2$ added is not precipitated out. With concentrations below 1×10^{-3} moles/l, the danger exists that the orthophosphate itself may precipitate out, and in so doing, remove the inhibitory effect on $CaCO_3$ precipitation. Should this happen, pH adjustment to near 7,0 with further $Ca(OH)_2$ additions becomes impossible; there is in fact a reduction in pH to the value associated with the maximum permissible Ca concentration in pure water.

ACKNOWLEDGEMENTS

I wish to express my gratitude to the following:

Professor G.v.R. Marais, Water Resources and Public Health Engineering, University of Cape Town, under whose supervision and guidance this research was conducted. His enthusiastic encouragement and advice throughout this work is very much appreciated.

Mr. R.F. Beverton, laboratory technician in the Department of Civil Engineering, whose expertise in constructing the apparatus (and patience in making belated modifications) made this work possible.

Miss P. Preston and Mr. T. Lakay for their cheerful technical assistance in the laboratory.

The Council for Scientific and Industrial Research, who donated a monetary grant, without which, this work could not have been carried out.

Finally, Miss. F. Godet, Miss I. Williams and Mr. C. Basson, who produced the manuscript.

TABLE OF CONTENTS

SYNOPSIS

CHAPTER I : ANAEROBIC TREATMENT OF WINE DISTILLERY WASTE

INTRODUCTION 1
Objectives 2

ANAEROBIC TREATMENT OF WINE DISTILLERY WASTE 5
Characteristics of Spent Wine 5
Characteristics of the Process 8

THE ANAEROBIC FILTER 13
Conventional Digestor System 13
The Anaerobic Contact System 16
The Anaerobic Filter 18

DESCRIPTIONS OF FILTERS AND APPARATUS 21
Filter Media 21
Solid-Liquid Separation Mechanisms 24
Stone Media 24
Clinker Media 24
Perforated Plate Media 26
Sand Media 26
General Apparatus 26

OPERATING PROCEDURES 31

RESULTS 37

DISCUSSION 47
Steady-State Treatment Efficiencies and Capacities 47
Surface Area Effect 54
Comparison Between the Three Filters 56
Comparison of the Filters with Other Systems 61
Contact Process Treating Spent Wine 61
Anaerobic Filters Treating Synthetic Wastes 62
Kinetic Model and Applications 63
Fundamental Growth Kinetics 63
Yield of micro-organisms 64
Micro-organism decay 65
Unbiodegradable fraction of micro-organisms 65
Rate of substrate utilization 65

Process Kinetic Model 66
Experimental Approximation of Growth Constants 71
Diagrammatic Representation of Model 75
Treatment Efficiency 77
Shock Loads 78
Solids Concentration in the Reactor 80
Solids Concentration in the Effluent 81
Effluent Quality 84
Conclusions 84
Substrate Removal in Aerobic and Anaerobic Processes 86
Behavioural Characteristics 88
Process Response 88
Start-Up 89
Loading Rate Fluctuations 90
Temperature Fluctuations 91
General Comment 92
Operational Behaviour 92
Mixing Conditions 93
Blockages of Voids 93
Reactivation 95
Spent Wine Composition 96
General 96

CHAPTER II : pH CONTROL IN ANAEROBIC DIGESTION

MECHANISM OF ANAEROBIC TREATMENT 97

pH CONTROL BY ORGANISMS 101

WEAK ACID-BASE SYSTEMS 102
Dissociation and Equilibrium 102
pH Buffer Capacity 105

EXPERIMENTAL VERIFICATION OF BUFFER CAPACITY 111

pH ESTABLISHMENT AND CONTROL 120

pH ADJUSTMENT 127

pH CONDITIONING DIAGRAM 129

pH Conditioning Diagram for Completely Soluble Dosing Chemicals 129

Ionic Equilibrium Movement for the Addition of a Strong Base or Acid 132

Ionic Equilibrium Movement for the Addition of a Carbonate 133

Ionic Equilibrium Movement for the Addition of a Bicarbonate 136

Ionic Equilibrium Movement for the Addition or Removal of Carbonic Acid (Dissolved CO_2) 137

Upward Adjustment of pH 138

Experimental Verification of the pH Conditioning Diagram for the Addition of Soluble Dosing Chemicals 139

Downward Adjustment of pH 144

pH Conditioning Diagram Incorporating $CaCO_3$ Solubility 145

INHIBITION OF $CaCO_3$ PRECIPITATION 152

COMPARISON OF DOSING CHEMICALS 160

pH AND THE MECHANISM OF FAILURE 162

Operating Procedure 162

Results 163

Discussion 167

CONCLUSIONS 171

APPENDIX I A.1

APPENDIX II A.4

APPENDIX III A.6

APPENDIX IV A.9

APPENDIX V A.10

APPENDIX VI A.18

REFERENCES

CHAPTER I

ANAEROBIC TREATMENT OF WINE DISTILLERY WASTE IN THE ANAEROBIC FILTER

A. INTRODUCTION

Wine distillery waste, or spent wine, is the residue left after ethyl alcohol or brandy has been distilled from fermented grape juice. It contains organic acids, soluble proteins and carbohydrates, as well as various inorganic compounds which are normal constituents of grape juice. The polluting potential of the spent wine is mainly the COD of 23 000 mg/l, the nitrogen content of 360 mg/l, and the phosphorus content of 100 mg/l.

Twenty distilleries in the Western Cape district produce an estimated 370 million litres of spent wine per year. Treatment capacity of individual plants for the disposal of the spent wine in the 14 towns faced with this problem ranges from 25 to 90 million litres per year.

Wine distillation is a seasonal operation with a 4 to 7 month period of activity, but even during the active period, operation is generally intermittent. A plant treating wine distillery waste must be able to accommodate various operational characteristics such as shock loads, long dormant periods and fast reactivation after the dormant period. Since the majority of plants are small and not supervised by highly trained personnel, the plants should be simple to operate.

The high organic content of spent wine (23 000 mg/l as COD) excludes treatment by aerobic processes as economically not feasible. Aerobic treatment processes would require long retention times and high aeration inputs, which respectively increase the volumetric size of the plant and the running costs. Consequently, in the past, attention has been focussed on treating the spent wine by the anaerobic process.

Anaerobic processes rely on the activities of the micro-organism population for the stabilization of the wastewater. The key to successful and efficient operation of the process is in maintaining a high mass of micro-organisms in the system relative to the waste mass treated, i.e. a low food/micro-organism ratio. This implies long

retention times for the micro-organisms in the process. One of the major problems of anaerobic systems is the difficulty in retaining the micro-organisms. The designs of anaerobic systems have been dictated largely by this requirement.

The principal anaerobic system employed for the treatment of spent wine is the anaerobic 'activated sludge' or 'contact' system[1]. Solids (including micro-organisms) are retained in the process reactor by solid-liquid separation of the reactor effluent in a sedimentation tank, and the return of the separated solids to the reactor. This system has operated fairly successfully on wine distillery waste, but is hampered by the poor settling characteristics of the micro-organisms in the sedimentation tank; in fact the treatment capacity of this system appears to be limited chiefly by the efficiency of the solid-liquid separation in the settling tank. Operation of the system, and in particular the sedimentation tank, requires close control.

The anaerobic filter system, which has been developed only recently[2], has been put forward as providing a simple and efficient system for retaining micro-organisms in a process reactor. Wastewater is passed upward through a submerged bed of rocks which retain the micro-organisms on the rock surface and in the interstices. The solid-liquid separation unit is thus integrated with the process reactor. This eliminates the problems involved with the sedimentation tank unit, and generally reduces operational control to a minimum. Although this system has been used successfully in the treatment of dilute wastes, it has not been applied to the treatment of concentrated wastes such as wine distillery wastes.

Objectives

Primary objectives of this investigation were to:

1. Determine whether wine distillery waste is amenable to treatment in the anaerobic filter.

2. Compare the treatment efficiency and general behavioural characteristics of an anaerobic filter process treating spent wine with the anaerobic contact system as operated at present[1].

To achieve these objectives, consideration of the following aspects of anaerobic digestion in the anaerobic filter system was required:

1. The retention of micro-organisms in an anaerobic filter is the vital factor governing the performance of the process, and it is thus of interest to investigate the solid-liquid separation phenomena in the anaerobic filter. In order to investigate whether the dominant site of the micro-organisms, and therefore the fermentation process, is on the surface or in the interstitial volumes of the filter media, it is necessary to test the effect of media with different shapes and surface areas on the process efficiency.

2. The continuous culture kinetic model is widely used to simulate the anaerobic process, and especially in describing the steady-state operation and performance. It would be useful to determine in what manner this theory, as it is understood today, applies to the anaerobic filter system.

3. Anaerobic processes require well defined environmental conditions for their optimal operation, and are susceptible to sudden and complete failures under adverse environmental conditions. The reasons for, and the mechanism of failure are not always apparent; hence enquiry into the behaviour of the filter under stress would be of value. This can be achieved by monitoring some of the parameters reputed to govern the anaerobic process, i.e. solids retention time, volatile fatty acid concentration and pH. Observations during periods of instability in the process, induced during start-up, and during temperature and loading rate fluctuations, would be of particular interest.

   The hydrogen ion concentration, or pH, features prominently in the mechanism of most process failures, and is probably the single most important control parameter of the anaerobic process. To investigate the effects of this parameter on anaerobic digestion, an enquiry was necessary into the following aspects:

   (a) significance of pH in anaerobic fermentation,

(b) factors which establish and control the pH in an anaerobic process,

(c) relation of pH with the mechanism of process failure,

(d) methods for controlling the pH.

These investigations into the significance of pH are not limited to the treatment of wine distillery waste in an anaerobic filter, but apply to anaerobic processes in general. Because this aspect of the investigation tends to deviate somewhat from the main intent of the objectives of the thesis, it is reported as a separate section (Chapter II).

B. ANAEROBIC TREATMENT OF WINE DISTILLERY WASTE

Research in the field of anaerobic digestion of wine distillery waste seems to have been confined almost entirely to South Africa. Fundamental investigations were conducted by Stander in 1950[3], and since then, fundamental and applied research has been continued by members of the South African Council for Scientific and Industrial Research (CSIR)[1]. These investigations have shown that spent wine is amenable to treatment in the anaerobic contact process, and have delineated some of the optimum conditions required for efficient operation.

Characteristics of Spent Wine

An analysis of the main chemical components of wine distillery waste is summarized in Table I. In relation to anaerobic treatment, the composition of spent wine yields the following information:

1. The macro-nutrients, carbon, nitrogen and phosphorus are present in relative abundance, and in approximately the correct proportions: based on the average chemical formulation of the cell ($C_5 H_7 O_2 N$)[4] and a cell yield of 0,1 mg per mg COD of substrate utilized, the ratio by weight of carbon (as COD) to nitrogen to phosphorus should be 1000 : 11 : 2. In wine distillery waste the ratio is 100 : 15,3 : 4,8. Thus, phosphorus and nitrogen nutrient additions to a process treating spent wine are unnecessary - the carbon source is the limiting macro-nutrient in the spent wine.

2. Spectrographic analysis of trace elements has indicated that these are probably present in sufficient quantity to meet the metabolic requirements of the micro-organisms[1].

3. Toxic materials have not been detected in any significant concentration[1]. An examination by the CSIR of laboratory scale processes which had failed, did not disclose any permanent toxins, such as heavy metals or sulphides, which could have been the cause of failure.

TABLE I

Average Composition of Wine Distillery Waste (mainly after the CSIR[1]).

Test		Composition
COD - Total	mg/l	23 500
COD - Soluble	mg/l	21 400
COD - Suspended Solids	mg/l	2 100
5-Day BOD	mg/l	23 000
Organic Nitrogen	mg/l as N	350
Ammonia Nitrogen	mg/l as N	10
Total Phosphorus	mg/l as PO_4	300
Total Suspended Solids	mg/l	1 500
Volatile Suspended Solids	mg/l	1 500
Total Solids	mg/l	15 000
pH		4,6
Volatile Fatty Acids	mg/l as acetic acid	850
Conductivity	milli siemens	5,5

4. A comparison of the COD (23 500 mg/l) and the 5 day BOD (23 000 mg/l) indicates that the waste is easily and virtually completely biodegradable. Results obtained on the aerobic treatment of anaerobically digested spent wine indicate that only 1,5% of the COD of wine distillery waste is unbiodegradable[1]. Treatment efficiency, measured as percentage COD removal of influent waste, should take due account of this unbiodegradable fraction of COD.

5. Inorganic suspended solids are either absent or present in negligible concentrations.

6. The organic suspended solid concentration, as measured by the volatile suspended solids test, is low (1500 mg/l) relative to the COD strength of the waste. Also, the suspended solids are almost entirely solubilized and biodegraded during anaerobic treatment. This is evident from the following:

   If it is assumed that the unbiodegradable fraction of the total COD (i.e. 1,5% of 23 500 = 300 mg/l) is completely derived from the volatile suspended solids, then the COD associated with solids (2100 mg/l COD) will be reduced by 86%. Thus, the maximum possible unbiodegradable solids concentration in spent wine influent which can accumulate in a process reactor is 210 mg/l (14% of 1500 mg/l).

   Spent wine can thus be considered to be a virtually completely soluble waste.

7. The low pH of 4,6 in unstabilized spent wine tends to inhibit biological activity - storage of spent wine does not appear to alter its characteristics or COD concentration. It has been observed that spent wine in holding dams undergoes little or no change in a 4 to 6 month period.

8. The high dissolved solids concentration (13 500 mg/l) and high conductivity (5,5 milli siemens) are indicative of a high ionic concentration. pH, which is an important control parameter in the anaerobic process, is significantly affected by such high ionic strengths. Consequently, the true hydrogen ion concentration differs from the effective hydrogen ion concentration as measured by a pH meter.

Characteristics of the Process

The following information on the behavioural characteristics of an anaerobic process treating spent wine was abstracted from experimental investigations conducted on laboratory, pilot and full-scale plants by the CSIR[1]. This information on the optimum operating conditions for the process is substantiated, or supplemented, wherever possible with the conditions observed in anaerobic processes in general.

1. In the mesophilic temperature range, the optimum temperature for long-term stable operation of the anaerobic process treating spent wine is about 35°C[1]. Relative to the maximum permissible loading rate at 35°C, loading rates had to be decreased by 66% and 30% for operating temperatures of 15°C and 45°C respectively. Outside these limits the process deteriorated rapidly. These characteristics are in agreement with those observed in anaerobic processes in general[5][6].

   Short-term temperature effects on the anaerobic process were not investigated by the CSIR. However, other reports indicate that sudden short-term temperature changes from stable operating temperature have a very pronounced effect on the activity of the anaerobic organisms[7]. Activity declines rapidly as the process is cooled from 35°C, to cease completely when a temperature of 20°C is reached. If the process is heated from 35°C to 45°C, the activity increases, but degenerates rapidly at higher temperatures.

   One concludes that for anaerobic treatment of spent wine:

   (a) Stable process operation is obtained over a 15°C to 45°C range in temperature, providing the temperature does not fluctuate.

   (b) The optimum temperature for long-term stable operation is about 35°C.

   (c) Fluctuations in temperature (short-term changes) significantly affect the performance of a process, and should thus be kept to a minimum for stable operation.

2. Although thermophilic operation of a process treating spent wine was more efficient than mesophilic operation, the process required a closer environmental control and considerably more power to maintain the temperature at 55°C[3]. Since plants treating spent wine must be simple to operate, thermophilic digestion does not appear to be justified in small plants with uncertain control.

3. pH may be a strong inhibiting agent in anaerobic processes[8][9]. The activity of anaerobic digestion in general is not significantly affected in the pH range 6,5 to 7,5, but the activity falls off rapidly outside this range. If corrective measures are not taken when the pH moves outside this range, the process progressively deteriorates until complete inhibition results. Adjustment of pH to the optimum range is especially critical during starting-up operations of the process.

   Although volatile fatty acids and ammonia may inhibit a process by affecting the pH, they may also be toxic in their own right[10][11]. The undissociated forms of these compounds appear to be more toxic than the dissociated ionic form. Toxic concentrations of volatile fatty acids and ammonia are not clearly defined, since pH affects the dissociations and therefore toxicity. Volatile fatty acid concentrations tend to increase in processes subjected to stress, so that close control over this parameter is required for successful operation.

4. A period for acclimatization and growth is required by the micro-organisms after the start-up of a process. This is particularly important if the process is seeded with micro-organisms from another process treating a different waste, or if the mass of seed is small. It is necessary to ensure that the feed rates are only gradually increased to the maximum loading capacity of the plant, so that the assimilation capacity of the organisms is at no time exceeded.

Plants treating spent wine are generally decentralized and it is often more convenient to seed them with active anaerobic digestion sludge derived from domestic sewage, which is usually readily available. A process treating spent wine and seeded with active domestic sludge required a period greater than 30 days to attain maximum load capacity[1].

5. Re-inoculation of the anaerobic process treating spent wine with fresh active sludge was not required after a dormant period of approximately 6 months[1]. Reactivation of the process was achieved by merely resuming the feed at a low loading rate. A period of less than 20 days was necessary for the process to achieve its maximum load capacity. This period was reduced (a) for shorter dormant periods, and (b) as the sludge became progressively acclimatized to spent wine over a period of years.

6. Overloading the micro-organisms by substantial increases in feed rates was found to be the primary cause for the failure of the spent wine treatment processes operated by the CSIR[1]. They were unable to identify the mechanism causing the extremely rapid (within one day) decline of the process. Inhibition of the activity of overloaded anaerobic processes is usually attributed to the toxic effects of either pH or acetic acid in its dissociated or undissociated form[8][11]. The exact mechanism of failure of a process, especially in relation to pH, was not clearly described.

7. Anaerobic processes showing a decline in activity due to overloading may recover by applying one or a combination of the following corrective measures:

(a) re-inoculation of the process with fresh digesting sludge - probably the most rapid and effective method[1].

(b) reduction of the loading rate,

(c) adjustment of the pH to 7,0,

(d) increasing the temperature - this temporarily increases the activity of the micro-organisms.

The last three measures are only effective in processes which have not deteriorated extensively. Re-inoculation with a well-acclimatized and sufficiently massive inoculant, however, was always found to be successful[1].

8. The maximum permissible loading rate on anaerobic processes is limited by the micro-organism mass in the reactor. As the loading rate increases, so the steady state mass of micro-organisms concomitantly increases. However, the micro-organism concentration is eventually limited by the washout rate exceeding the production rate, thus also limiting the maximum loading rate. Later in this thesis this sequence of events, and its influence on the progressive failure of the process with increasing load will be thoroughly discussed.

Plants treating spent wine showed failure characteristics consistent with the above descriptions[1]. At high loads, the volatile suspended solids concentration did not increase proportionally with the loading rates, indicating loss of solids[1]. Eventual failure can be credited to excessive washout of solids.

9. The volatile solids concentration in an anaerobic process treating spent wine is composed mainly of active micro-organisms. This is due to the fact that (a) spent wine is virtually completely soluble or solubilized in the process (a maximum of 1,5% of the influent COD is insoluble), and (b) the endogenous respiration of the micro-organisms is low relative to the generation of cell mass, and consequently, there is a low generation of unbiodegradable dead cell material (about 0,5% of the influent COD). A maximum total of about 2% of the influent COD remains in the reactor as inactive mass, compared to about 10% of the influent COD which is converted to active micro-organisms. (These approximate figures are obtained from Part G of this thesis.)

10. Behaviour of an anaerobic process is monitored by measuring the parameters pH, volatile fatty acids, gas production per unit feed rate, and percentage methane in the gas. Stable conditions in a process give rise to low volatile fatty acids concentrations, a pH near 7,0, and a gas production and percentage methane consistent with the loading rate (1 kg COD is equivalent to 350 l of CH_4 at STP)[4]. A decline in the process is identified by decreases in pH, gas production and percentage methane, and an increase in the volatile fatty acids. The first indication of reduced activity is usually given by the volatile fatty acids, but the other parameters are soon affected since they are all inter-related. For continuous successful operation, it is essential that these parameters be frequently monitored, so that upsets in the process may be identified quickly, and the necessary remedial actions taken immediately.

11. Methane production from the anaerobic treatment of spent wine provides more than sufficient energy to maintain a temperature of 35°C in a digestor. Since approximately 6000 mg/l COD is required to raise the temperature of a waste by 10°C[12], it is evident that the 23 000 mg/l present in spent wine will be sufficient to heat the waste from 15°C to 35°C. For this reason, treatment of spent wine at 35°C is an economical and practical proposition.

The observations and deductions made from, (a) the properties of wine distillery waste, and (b) the operational experiences in anaerobic processes reported by others, provided the background to the requirements for operating an anaerobic process treating spent wine. These were used as guidelines for the selection of suitable operating conditions for the anaerobic filter process reported in this thesis.

An example of the typical plant capacity requirements for an anaerobic contact process treating spent wine is supplied by the CSIR[1]:

(a) Suggested volumetric requirements for the reactor and settling tank are for 7,5 and 4 days hydraulic retention time respectively.

(b) A volatile suspended solid concentration of 15 000 mg/l in the reactor is recommended.

Under these operating conditions, reduction of 98,5% in the COD of the influent spent wine should be obtained.

C. THE ANAEROBIC FILTER

The goal of an anaerobic waste treatment system design is to retain the biological solids in the reactor independent of the waste flow, to mix the solids intimately with the waste, and to maintain at all times a high mass of micro-organisms in the reactor relative to the waste treatment rate. To achieve these objectives, several anaerobic systems have been designed, viz. the conventional digestor, the anaerobic contact and anaerobic filter systems.

In order to appreciate a discussion on the relative merits of the different anaerobic systems, a very brief and qualitative description of the principles of anaerobic digestion is necessary. Detailed discussions on the mechanism of anaerobic treatment and on the process simulation by a model based on continuous culture theory are presented in Chapter II - Part A, and Chapter I - Part G of this thesis respectively.

In the anaerobic process, wastewater is stabilized in sequential steps by the micro-organism population. The slowest growing organisms in the sequence (usually the methane forming organisms) place a limitation on the whole process. Thus, the process must allow sufficient time (the solids retention time) for these micro-organisms to multiply, i.e. the washout rate of the micro-organisms from the reactor must be slower than the rate of production of the slowest growing micro-organism. By maintaining a high mass of micro-organisms in the reactor relative to the rate of waste treatment, the efficiency and stability of the process is increased.

1. Conventional Digestor System

Historically, the anaerobic process found its most useful application in the treatment of raw domestic sludges and organic solids derived from aerobic processes. Both originate from the underflows from sedimentation tanks, and thus contain a high concentration of suspended organic solids. An appreciable fraction of these influent solids are unbiodegradable. It is not possible to separate out the anaerobic biological mass from the inert mass. Hence, it is not practically feasible to have a solids retention time different from the hydraulic retention time - a flow through system only is feasible. This system is

called the conventional system (Figure 1). The hydraulic retention time of the reactor, which equals the solids retention time in this process, is governed by the slowest growing micro-organism in the sequential breakdown of the waste.

Depending on the temperature at which the process operates (15°C to 35°C) and the nature of the wastewater treated, a minimum solids retention time of 3 to 10 days is required[13]. These minimum values have been established from laboratory studies on well mixed processes with closely controlled environmental conditions of temperature and rate of loading. Plants operating in the field require longer retention times to provide stability for the process under adverse conditions such as improper mixing, and temperature and loading rate fluctuations. Generally, conventional digestors operating at ambient temperature with no mixing require hydraulic retention times greater than 60 days. Heating the process to the optimum temperature for micro-organism activity (about 35°C for the mesophilic temperature range) improves the efficiency of the process, and the hydraulic retention time may be reduced to about 30 days. In the 'high-rate' digestion process, the reactor contents are well mixed, the temperature is kept at optimum level, and the retention time can be further reduced to between 10 and 30 days.

The conventional digestor system is not economically feasible for the treatment of low strength wastes for the following reasons:

(a) The volumetric requirement of the reactor per unit COD treated increases with decreasing strength of waste, since the hydraulic retention time remains unchanged by the concentration of the wastewater. (The hydraulic retention time is governed by the minimum solids retention time only.)

(b) Methane gas production from the treatment of low strength waste (COD < 5000 mg/l) is insufficient to heat the reactor contents to optimum temperature, and thus, an outside source of heat is required.

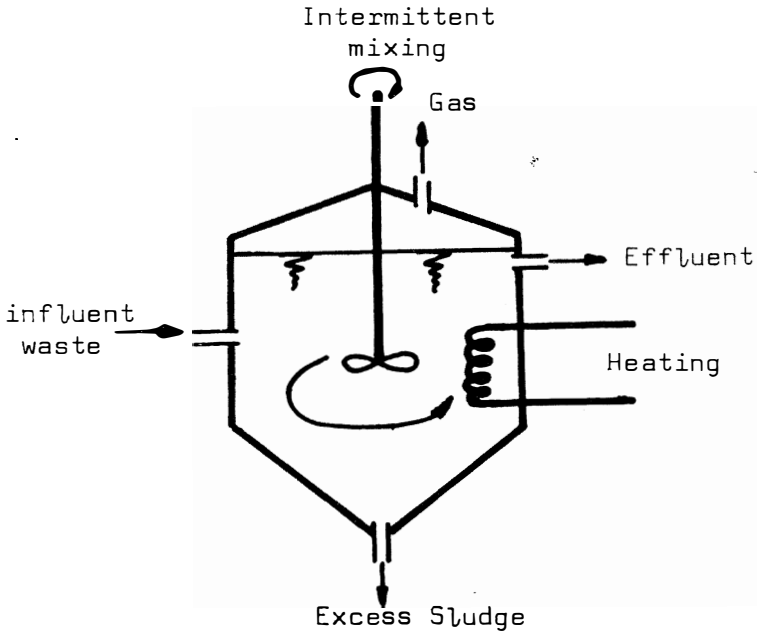

CONVENTIONAL DIGESTOR

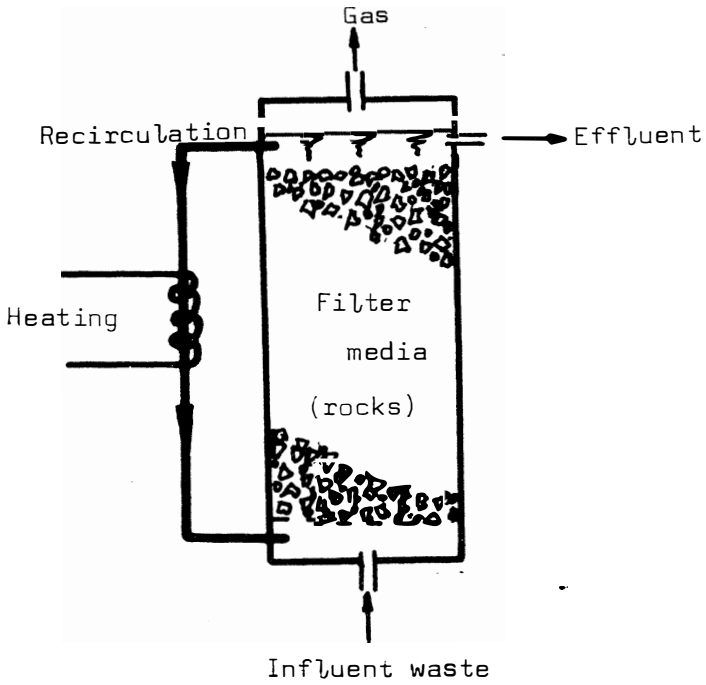

ANAEROBIC FILTER

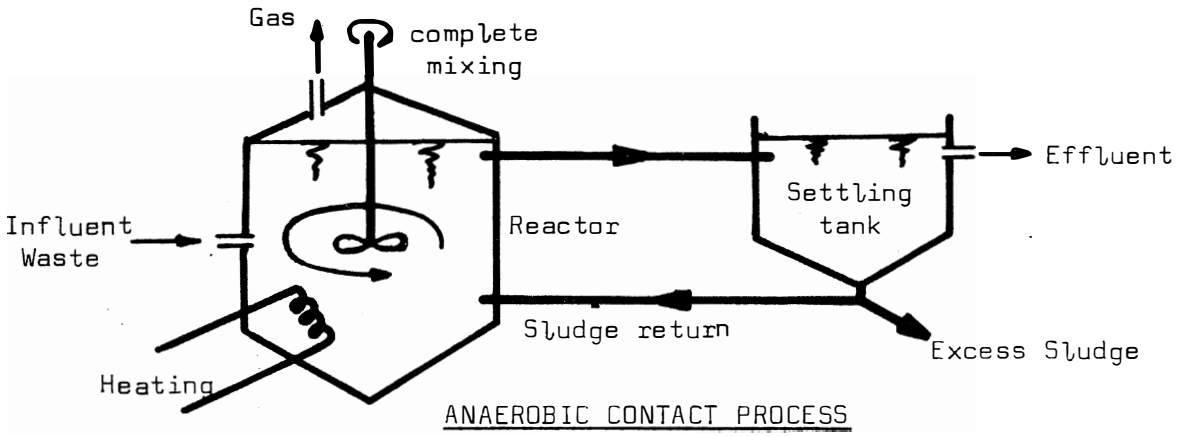

ANAEROBIC CONTACT PROCESS

FIGURE 1: Three Anaerobic Systems

2. The Anaerobic Contact System

The organic suspended solid concentration in an anaerobic reactor treating a completely biodegradable waste consists almost entirely of biomass. For this reason, it is practically feasible to separate out the organic solids from the reactor effluent, and to return them to the reactor. This feature allows the solids concentration and the solids retention time (which control the process) to be increased independently of the hydraulic retention time. (This results in a considerable saving in the tankage of the reactor.) This system is similar to the aerobic activated sludge process with solids recycle, and called the anaerobic contact process.

The contact system consists basically of a completely mixed suspended growth reactor, a sedimentation tank for solid-liquid separation, and solids recirculation from the sedimentation tank to the reactor (Figure 1).

Provided that separation of the solids from the effluent can be efficiently achieved, then theoretically, any waste loading rate may be applied to the reactor, even at ambient temperatures. Practically, the loading rate is limited by either the inefficient operation of the solid-liquid separation unit, or too high a concentration of biological solids in the reactor, which hampers effective mixing of biological solids with the waste.

Contact processes may be usefully employed for the treatment of low strength wastes provided that sufficiently long solids retention times are maintained in the reactor irrespective of the hydraulic retention times, however short. Low strength wastes (COD $<$ 5000 mg/l) are economically treated at ambient temperatures. The limitation of an insufficient methane production from the process to heat the reactor appreciably, is overcome by retaining the biological solids in the reactor. The ratio of the micro-organism mass to the rate of substrate treatment must be very high to compensate for the low activity of micro-organism at low temperature.

A low strength unsettled urban wastewater with a BOD of about 350 mg/l and a suspended solids concentration of 600 mg/l has been treated successfully in a pilot-scale anaerobic contact plant at Durban, South Africa[14]. (These experiments indicate that although the contact system was developed principally for the treatment of soluble wastes, it may also be applied to wastewater with significant suspended solids concentrations.) With a 12 hr hydraulic retention time and a suspended solid concentration of 18 000 mg/l in the reactor, 80% reduction of the influent BOD was obtained. Vacuum degasification was necessary to aid settling. A settling time of 1 hour was found to be optimum[14].

Although the discussion above indicates that it is feasible to anaerobically treat low strength wastes, the anaerobic process is far more efficient at temperatures of about 35°C, and thus suited to naturally warm and high strength wastes. A meat packing waste with a BOD of 1381 mg/l has been treated in a full-scale anaerobic contact process at Alberta Lea, U.S.A.[15]. The waste was naturally warm (27°C to 31°C), and produced sufficient methane to heat the digestor contents to about 35°C. With a 12 to 13 hour hydraulic retention and a suspended solids concentration of 7000 to 12 000 mg/l in the reactor, a 91% reduction of the influent BOD was obtained. Vacuum degasification was needed to promote settling in a sedimentation tank with a 1,2 hour retention.

In all cases it has been found that the capacity of the contact system is severely limited by the settling characteristics of the solids in the sedimentation tank. Anaerobic biological solids are difficult to settle out since they remain dispersed and do not flocculate readily. Settling is further hindered by the gas generation of the biomass which buoys the solids to the surface.

In general, settling characteristics of the reactor effluent from a process treating completely soluble wastes may be improved by (a) degasifaction, (b) the addition of flocculating agents, and (c) the addition of suspended solids to the wastewater to provide a site for biological growth. However, even with these possible modifications to the settling process, solid-liquid separation puts a limitation on the treatment capacity of the plant.

3. The Anaerobic Filter

Recent research investigations have led to the development of the anaerobic filter as a means for retaining solids without the use of sedimentation tanks[2]. In this system the solid-liquid separation unit is eliminated by combining it with the reactor to form one single unit. The unit consists of a submerged bed of rocks through which the waste is passed in an upward direction (Figure 1). Biological solids are retained on the surface area of the media and in the interstices. (The efficacy of the solids retention properties of these two mechanisms is discussed in Parts D and G.) Reports on the operation of this system indicate that the biological solids are efficiently retained[2][16]; so that the system may be operated at high waste loading rates, either with or without heating.

Young and McCarty conducted comprehensive laboratory studies to determine the performance of filters treating low-strength synthetic soluble wastes[2]. The filters were operated under plug-flow conditions at a temperature of 25°C. Behaviour of the waste stabilization mechanism of the filter was interpreted as follows[2][12]:

The bulk of the waste was removed in the lower levels of the filter, which was consequently also the site of profuse micro-organism growth. Some of the solids synthesized in the lower layers were carried upwards through the filter and made available for further waste treatment. Thus, the wastewater was progressively stabilized as it passed upwards through the filter. In the upper layers of the filter, waste concentration was low, and the net biological solids was negative (more solids were degraded by endogenous respiration than synthesized). The effluent was highly stabilized and contained a low solids concentration of mainly unbiodegradable decayed cell mass.

In these studies[2], wastes were fed to the filters at COD concentrations ranging from 1500 to 6000 mg/l, and loading rates ranging from 0,425 to 3,40 kg COD/day/m^3 of total volume (including stone). The temperature was maintained at 25°C, since the methane production from the anaerobic treatment of such low strength

waste insufficient to heat the waste significantly. The efficiency of COD removal under these conditions varied between 98,4% and 63,0% at low and high loading rates respectively. The maximum permissible loading rate of 3,40 kg/day/m^3 compares favourably with other biological processes in general.

In the treatment of raw domestic sewage (500 mg/l COD), Pretorius used the anaerobic filter successfully by operating it in series with a digestor[17]. The first stage of this laboratory scale process - the digestor - retained the influent solids, and hydroloysed a fraction of these solids. Little waste COD was removed in this section. The effluent from this stage was passed to the second stage of the process - the anaerobic filter - where methane fermentation stabilized a large fraction of the waste COD. Thus the purpose of the digestor was to remove and solubilize solid material from the wastewater so as not to cause blockages in the filter. The combined process yielded 90% reductions of the COD of the raw sewage water with 24 hours total retention at a temperature of 20°C.

Although experiments on the anaerobic filter have generally been successful, the system appears to have the following inherent disadvantages:

(a) Solid-liquid separation is not independent of waste flow, and no positive external control over the separation is possible, i.e. the solids concentration and solids retention time in the reactor is not positively controlled.

(b) Only soluble wastes may be treated in the filter, since high influent solids concentrations can cause clogging of the voids. Channelling of flow, and consequently, inefficient treatment results from such blockages.

(c) High concentrations of biological solids associated with high treatment capacities, are also likely to cause blockages.

(d) The media generally occupies more than half the reactor volume. Thus for the same treatment efficiency and total reactor volume, the anaerobic filter requires twice the concentration of sludge compared to the contact system.

Initially, anaerobic filters were designed with the objective of treating low strength soluble wastes. However, the anaerobic filter would appear to be suitable also for the treatment of high strength soluble wastes such as spent wine. For this adaptation of the process, certain modifications appear to be necessary:

(a) Recirculation of the waste distributes the concentrated influent load evenly over the filter. This should minimise adverse conditions, such as low pH, which tend to develop at the wastewater influent end (bottom) of the filter. At high recirculation rates the process is virtually completely mixed, and should show increased stability against shock loads and other environmental changes. Furthermore, the micro-organisms should be distributed more evenly along the whole length of the filter, thus allowing for higher maximum loading capacities on the system. It is, however, inevitable that the effluent quality will deteriorate compared to a plug flow system.

(b) Maintaining the temperature at 35^{o}C instead of at ambient increases the performance of the process. Heating would be economically feasible, since the methane production from a process treating spent wine is sufficient to provide the necessary heat to raise the temperature of the reactor to 35^{o}C (see Part B).

D. DESCRIPTION OF FILTERS AND APPARATUS

Three anaerobic filter reactors were used in this project. Each consisted of an identical filter shell filled with different media. The basic shell consisted of a perspex tube with an internal diameter of 140 mm, a height of 620 mm, and sealed with perspex conical caps at both ends (Figure 2).

Filter Media

Filter media used in Filter No.1 consisted of a 16 mm to 19 mm Malmesbury quartzite (Figure 3). This media resembles the quartzite media used by Young and McCarty[2], and has a relatively low surface area to volume ratio. Although filter media with relatively high surface area to volume ratios have been tested (such as Raschig rings)[16][18], no extensive experimental studies have been conducted to compare the performance of filters when using various types of media.

Filter No.2 was filled with a 10 mm to 25 mm clinker media (Figure 3). (Clinker, i.e. the remains of burnt coal, is readily available from any coal-burning factory.) In comparison to the Malmesbury quartzite, the surface area to volume ratio of the clinker is relatively high, and has a more intricate surface structure. The widely differing surface characteristics of the stone and clinker media were used to identify the significance of surface effects on filter behaviour.

The stone and clinker media of Filters No.1 and 2 were packed on a perforated plate 30 mm from the bottom, to a height of 50 mm below the top (Figure 2). Respective hydraulic volumes of the stone and clinker filters were 4920 ml and 5690 ml.

Filter No.3 used two types of media in series:

(a) perforated plates (Figure 4) were stacked in the lower section of the filter,

(b) a 14 to 18 mesh quartzite sand was packed in the top section.

The plate and sand media of Filter No.3 were positioned as shown in Figure 2. Plates were packed in the bottom 300 mm of the filter at

All measurements in mm

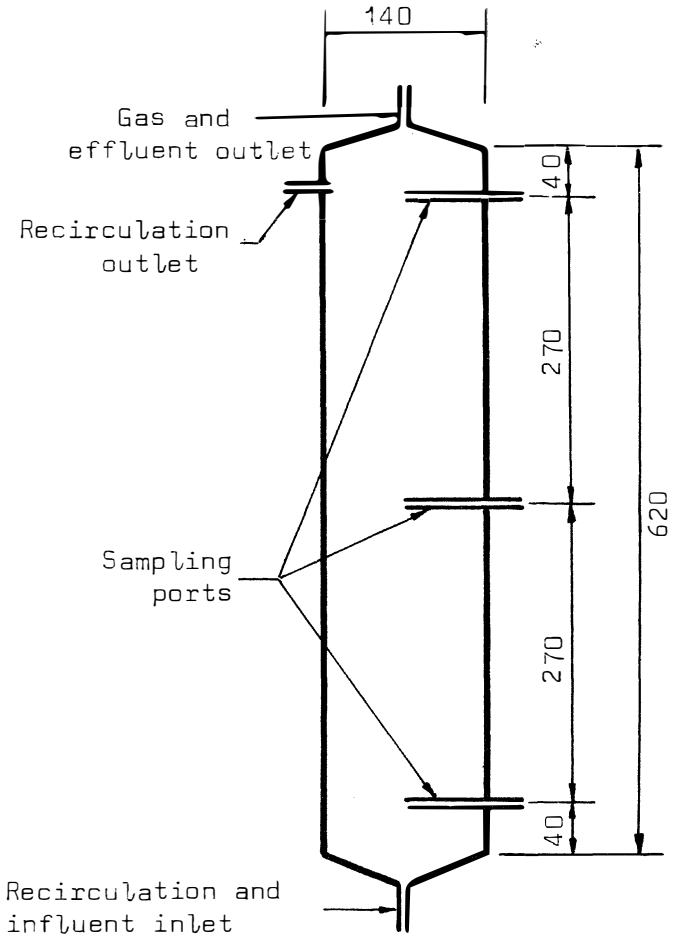

BASIC FILTER SHELL

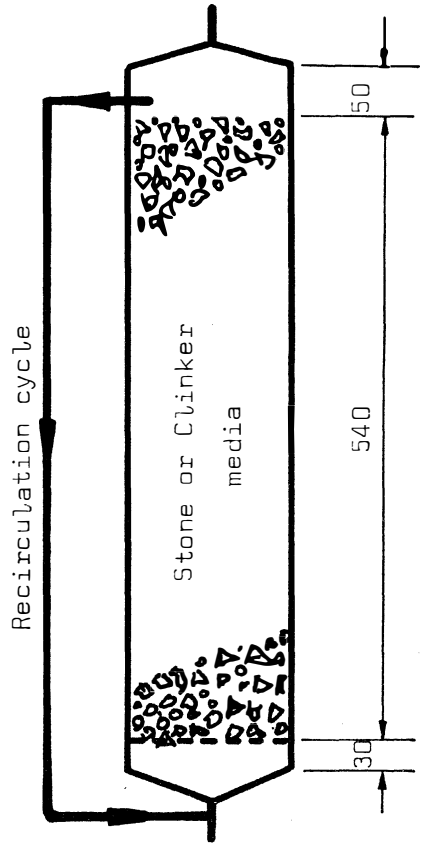

FILTERS NO. 1 and 2

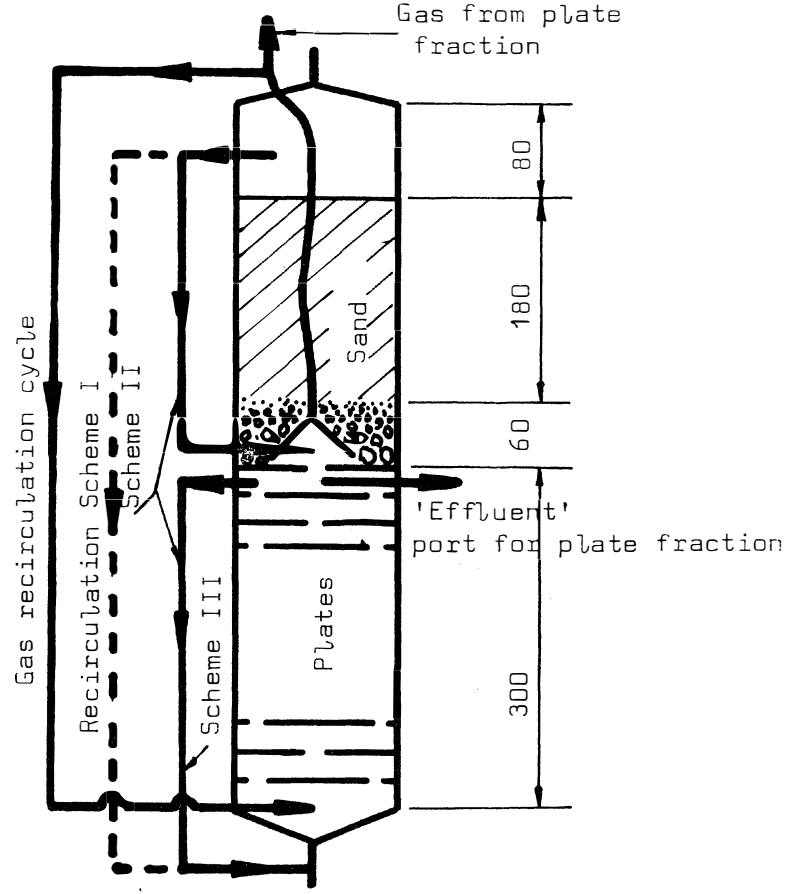

FILTER NO. 3

FIGURE 2: The Experimental Filter Units

CLINKER MEDIA

MALMSBURY QUARTZITE MEDIA

FIGURE 3: Photographs showing the Surface Area Characteristics of the Clinker and Malmsbury Quartzite Media

25 mm intervals. The plates with a 25 mm hole in the centre were alternated with those having 13 mm holes around the periphery. A 180 mm thick layer of sand was placed above the plate section of the filter. In order to prevent the sand from falling through the filter, the sand was packed over a 60 mm thick layer of stone, graded coarse at the bottom and fine at the top. The total volume of the plate section and sand section of the filter was respectively 4500 and 5300 ml, while the hydraulic volume of each was 4080 and 2890 ml.

Solid-Liquid Separation Mechanisms

The media used in each filter generally utilized different mechanisms for solid-liquid separation.

1. Stone Media

The stone media utilized the following two basic mechanisms for the separation of biological solids from the liquid phase[12]:

(a) Anaerobic micro-organisms tend to adhere to surfaces.

(b) Biological flocs are trapped in the interstices of the stone with the following action. Flocs in the void spaces are borne up by the rising gas, but on striking an overlying stone the bubbles break, and re-deposit the flocs. This rolling action of the flocs in the interstices causes them to take a granular shape. These biological granules become large (0,32 cm in diameter) and settle readily[2].

2. Clinker Media

Solid-liquid separation by clinker media was achieved with the same two basic mechanisms as the stone media. However, since the surface area of the clinker was much higher than that of the stone, the surface adhesion mechanism of the clinker played an increased role in the solid-liquid separation.

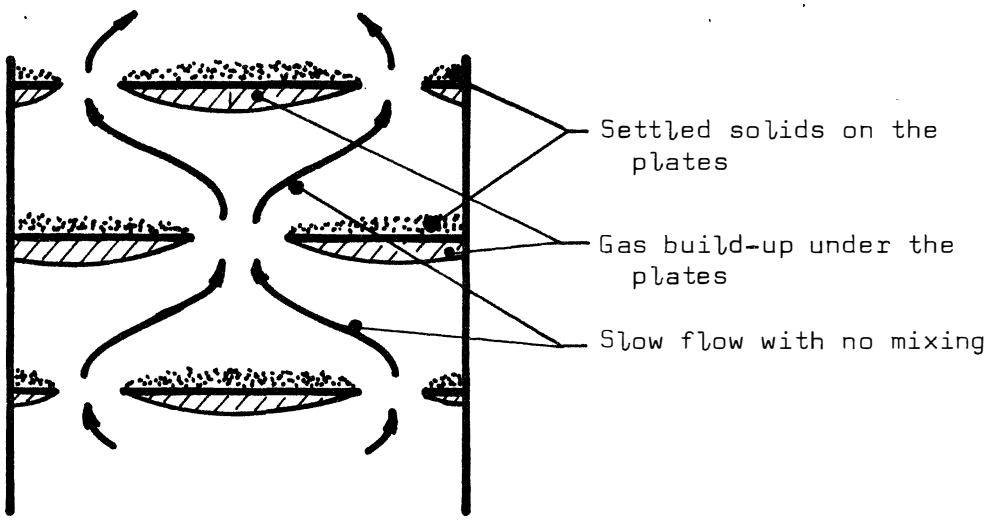

Phase I

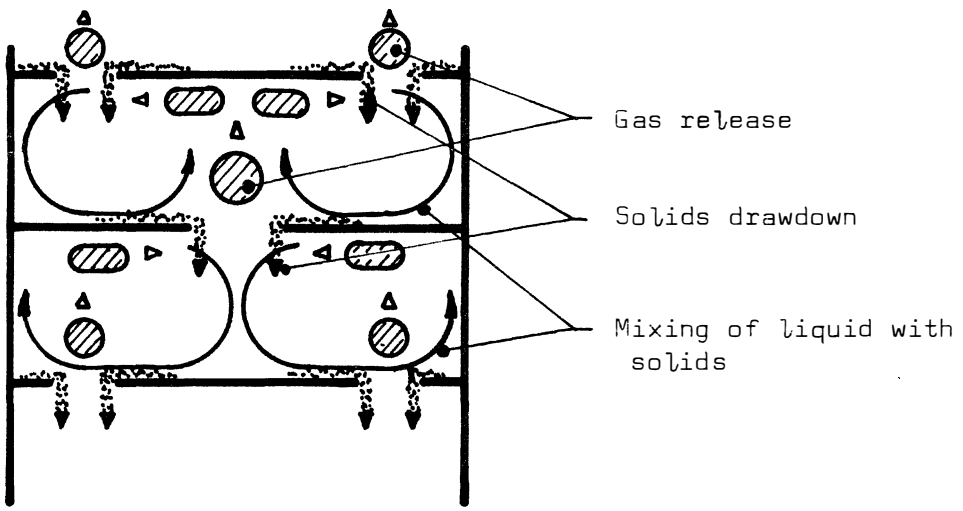

Phase II

ACTION OF PERFORATED PLATES

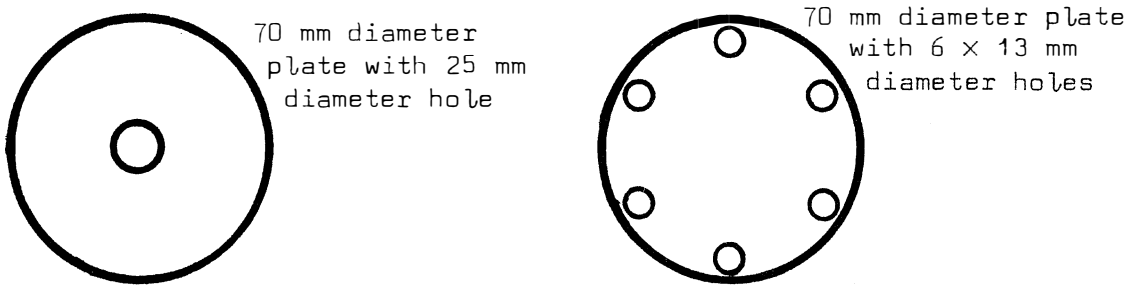

PERFORATED PLATES

FIGURE 4: Perforated Plates of Filter No. 3, and their Mechanism of Operation

3. Perforated Plate Media

The effect the perforated plates have on the hydraulic pattern of the filter is illustrated in Figure 4. In phase I, fermentation gases collect on the underside of the plates, while sludge settles down on the topside. Liquid moves through relatively slowly, causing no disturbances. In phase II, the bubbles have increased to unstable sizes, and are suddenly released through the holes. Voids left by the displaced gas are taken up by the settled sludge which is sucked down through the holes. As a result of the turbulence caused by the sudden rise of gas bubbles, the contents of the filter are mixed quite thoroughly. The net result of this intermittent bubble action is the transfer of sludge down the filter. To verify the action, experiments were conducted in the filter with water containing ferric chloride flocs. Intermittent large air bubbles were introduced at the bottom of the filter by means of a hydraulic 'air gun'[19]. The downward movement of the flocs was clearly apparent after the system operated for an hour or more, and eventually the greater mass of flocs was concentrated in the lower part of the reactor.

4. Sand Media

The sand media was used primarily to provide a physical filter for the stabilized effluent from the plate media section of the filter.

General Apparatus

The general layout of one filter and its related equipment is schematically represented in Figure 5. A photograph showing all three filters and general apparatus is shown in Figure 6.

Positions of the 5 mm perspex tube inlet, outlet and sampling ports for each filter are shown in Figure 2. A single outlet at the top of each filter served both the effluent and gas flows. (Gas-liquid separation was required subsequently.) In Filter No.3, the gas generated in the plate media section of the filter was measured separately by providing a collecting cone over the centre hole in the

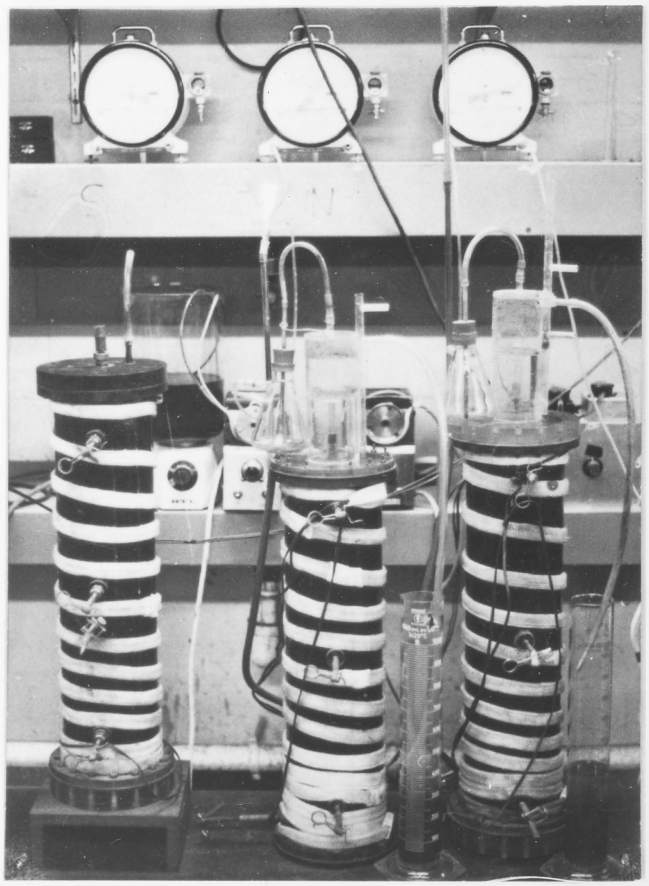

FIGURE 6: Photograph Showing General Layout of Filters

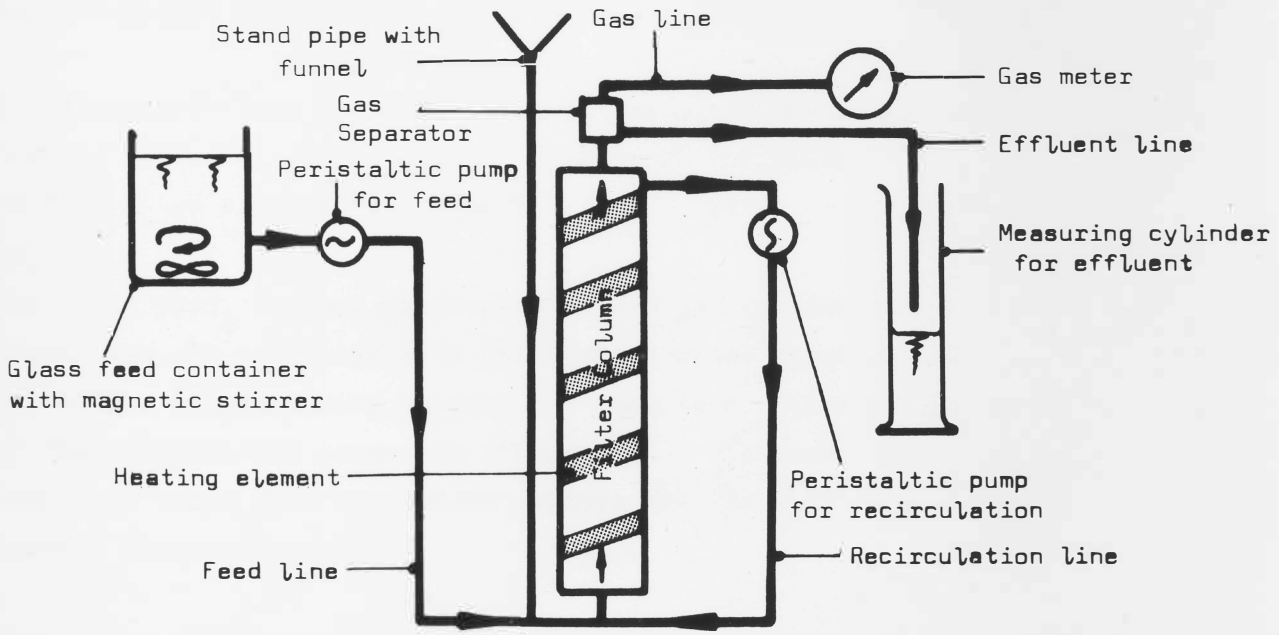

FIGURE 5: Schematic Layout of One Filter with Related Apparatus

last plate, and a pipe leading away from the cone to the gas meter. The 'effluent' sampling port for the plate fraction of Filter No.3 was inserted below the last plate (Figure 2). Influent and recycled flows were combined and passed through one inlet at the bottom of the filter. A stand pipe connected to the inlet was used to replace samples removed from the filter, and also as a trap for air accidently introduced by the pumps.

Recirculation cycles in Filters No.1 and 2 were from top to bottom, i.e. from the effluent to the influent point. In Filter No.3, several cycles were used at different stages during the filter operation (Figure 2):

Scheme I: Separate recirculation cycles for the plate and sand fractions of the filter.

Scheme II: Recirculation in the plate fraction of the filter only, with the sand fraction operating under plug-flow conditions.

Scheme III: One recirculation cycle from the top of the sand fraction (i.e. effluent point of filter) to the bottom of the plate section (i.e. influent point).

A gas recirculation cycle was used in the plate section of Filter No.3. The gas collected from the plate section of the filter was recirculated to the bottom plate (see Figure 2).

The waste feed, reactor recirculation and gas recirculation flow rates were all regulated with peristaltic pumps manufactured by Scientific Manufacturing Company, of Cape Town. In the last phase of the experimental programme (Chapter II), the power supply for the pumps was taken from a constant voltage regulator to dampen out voltage fluctuations.

Separation of the gas from the effluent was achieved in a sealed perspex cylinder with a gas outlet on top, and a water outlet (via a U-tube), on the bottom (Figure 7). Foam carried over in the gas line was collapsed by passing the gas through a conical flask containing a small quantity of alcohol.

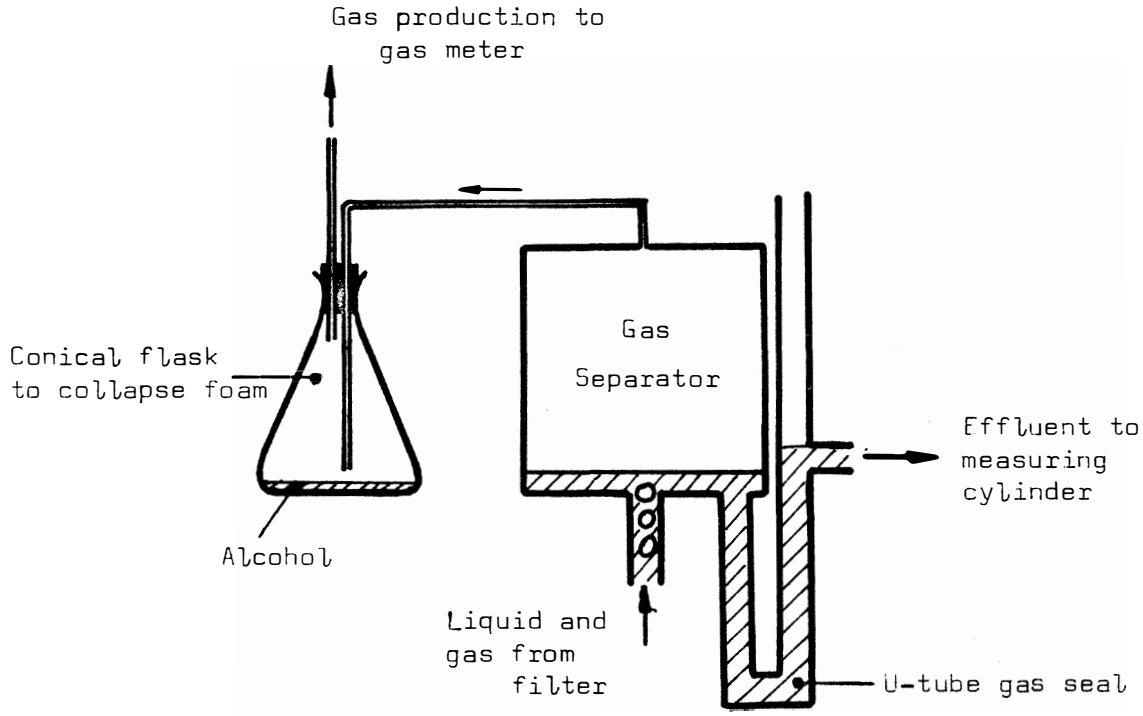

FIGURE 7: Gas-Liquid Separator for the Filter Effluent

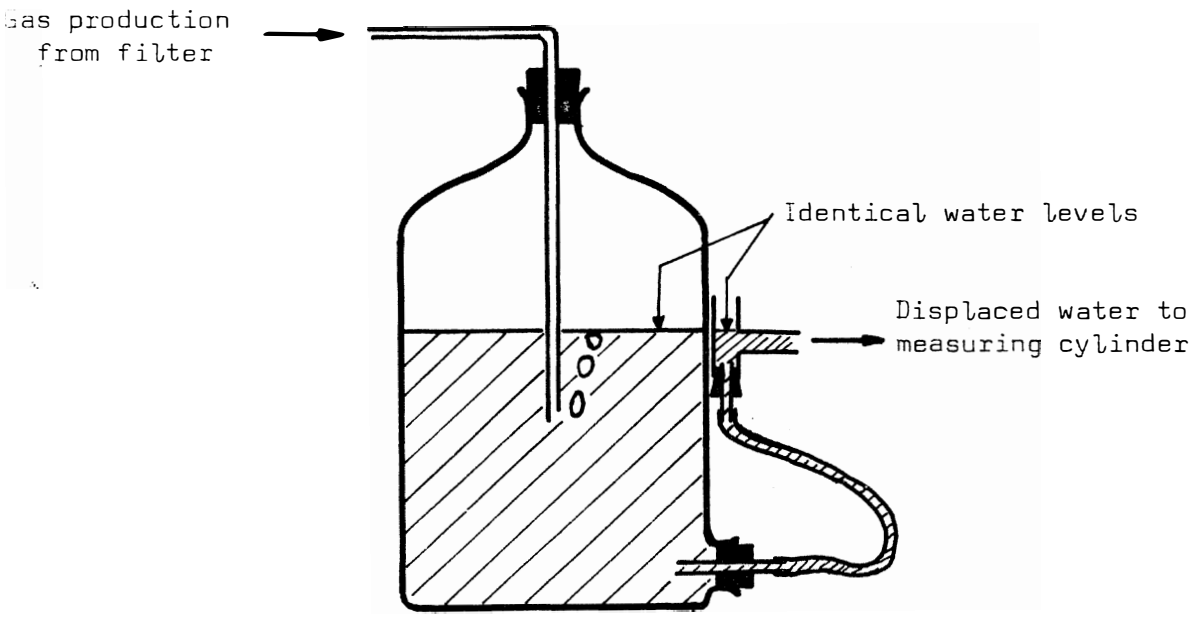

FIGURE 8: Apparatus for Gas Measurement by the Water Displacement Method

Gas measurements were initially made by measuring the water displaced from bell-jars (Figure 8). Before each measurement was taken, the pressure in the bell-jar was adjusted to atmospheric by adjusting the height of the outlet overflow from the jar. The water was not acidified, so that it may be expected that some CO_2 in the gas dissolved into the water. This apparatus was later replaced by wet-type laboratory gas meters manufactured by Alexander Wright and Company (Westminster) Limited, of London.

All the apparatus and equipment were operated in an air-conditioned laboratory at 20°C. The temperature was not constant, and found to vary by up to 2°C, depending on the external air temperature.

Heating of the filters was first accomplished by passing the recirculating filter contents through a coil (1 m long and 50 mm in diameter) submerged in a constant temperature hot water bath at 50°C. This system was later replaced by external heating elements wrapped around the filter. The elements were insulated electrically, and to a lesser degree thermally, with a glass-fibre cloth sheath. Power to the element of each filter was controlled with a rheostat.

The wine distillery waste was stored in drums kept in a cold storage room at 4°C. A quantity was transferred daily to a glass container next to the filter, and stirred continuously with a magnetic stirrer.

Plastic tubing of 2 mm diameter was used for both the liquid and gas lines. The lengths of these lines were kept as short as possible so as to (a) minimise biological growth in the tubes, (b) minimise heat losses in the recycle lines, and (c) detect changes in the gas composition immediately.

E. OPERATING PROCEDURES

The filters were operated with the objective of incrementally increasing their load until failure of the process occurred. At each increment sufficient time was allowed for stable or perhaps 'steady state' conditions of operation to be achieved. During these periods of stable operation, the treatment efficiency of the filter process was measured. Periods of unstable operation, such as during start-up, and load and temperature fluctuations, were useful for determining the response of the filter to changes in operating conditions.

Measurements of the treatment efficiency during 'steady state' were not taken until at least 10 days had elapsed from the time of the load increase. Stable, or 'steady state' conditions of operation were assumed when:

(a) waste flow and gas production remained relatively constant,

(b) CO_2 to CH_4 ratio in the gas remained constant,

(c) low volatile fatty acid concentrations prevailed,

(d) pH remained constant near 7,0,

(e) temperature remained approximately constant at $35^{o}C$.

Feed could be kept fairly constant at any one loading rate, but the loading rate level could not be pre-determined accurately because of the changes in the concentration of the waste, and because of inaccurate pump operation. However, hydraulic retention times were generally decreased from 15 to 2 days, and COD load rates per unit total volume increased from 0,8 to 10,0 kg/day/m^3.

Although start-up of an anaerobic process is often troublesome[20][21], the following operating procedure was successful. Each filter was seeded with 300 ml of actively digesting domestic sludge obtained from the Athlone Sewage Works of Cape Town, and topped up with anaerobic domestic sewage. Recirculation and heating of the filter were started simultaneously, but the spent wine feed was not commenced till one day later. At this stage, the gas production indicated that

the micro-organisms were becoming active. A low loading rate of 0,8 kg/day/m^3 was applied for 3 to 4 weeks to allow the micro-organisms a period of acclimatization and growth. During the first five days of operation, the pH was depressed and required frequent adjustments to pH 7,0. The quantity of 1 N $NaHCO_3$ required to adjust the pH was calculated by removing a sample from the filter and titrating it to pH 7,0. The sodium bicarbonate was fed intermittently to the filters through the sampling ports with a syringe.

The filters were shut down simply by stopping the feed, and 12 hours later the recirculation and heating. Filters were stored in the laboratory at 20°C.

Reactivation of the process was achieved by starting up the recirculation and heating, and a day later the waste feed. A low loading rate of 0,8 kg COD/day/m^3 was initially imposed on the filter, but this was rapidly increased over two days to 4 kg COD/day/m^3. No pH control was required.

Four batches of wine distillery waste were used, the characteristics of each being given in Table II. Batch No.3 was discarded after a few days since it was too dilute. Batches No. 2 and 3 were obtained from the Paarl Sewage Works, and Batches No. 1 and 4 from the Stellenbosch Sewage Works.

The composition of spent wine feed from any one batch was kept constant by following the procedure described below:

Waste in the cold storage room was mixed thoroughly before removing the quantity required each day. This was transferred to a clean glass feed container, and stirred slowly and continuously while being fed to the filters. Every week, the wall growths on the feed lines were cleaned either by squashing the tube, or by passing a strong jet of water through them.

Slow speed peristaltic pumps were used to feed the waste continuously at rates ranging from 360 to 4600 ml/day. Often, the operation of these pumps was erratic due to voltage fluctuations in the power-supply, leakages past the roller and tube of the pump, and other general breakdowns.

TABLE II

Chemical analysis of the four spent wine batches used in this investigation.

TEST	WASTE BATCH NO.			
	1	2	3	4
Total COD mg/l	23 200	28 600	12 200	32 650
Soluble COD mg/l	21 000	21 700	-	30 800
Volatile Suspended Solids mg/l	3 400	2 270	-	1 303
Volatile Fatty Acids mg/l (as acetic acid)	3 010	4 250	-	-
pH	5,6	4,75	-	4,30

Rates of recycle for Filters No. 1 and No. 2 were kept constant at 70 ml/min to give hydraulic flow through times of 1,17 and 1,35 hours respectively. During the first 64 days of operation of Filter No. 3, two separate recirculation cycles were used; one for sand, and the other for the plate media section (recirculation Scheme I - see Figure 2). Rates of recycle were in both cases 21 ml/min, giving hydraulic flow through times of 2,30 and 3,24 hours for the sand and plate sections respectively. From day 64 to 110, recirculation to the sand media section was discontinued, and plug flow conditions were allowed to exist (recirculation Scheme II). Recirculation in the plate fraction continued at 21 ml/min. On day 110, following blockages in the sand, recirculation was changed to a cycle from the top of the sand to the bottom of the plate section at a rate of 21 ml/min (recirculation Scheme III). Since the blockage in the sand caused the filter contents to escape via the gas line from the plate sector, the gas line was shut off. This action forced all the gas to pass through the sand sector, which further assisted in unblocking the sand.

The high speed peristaltic pumps used for the recirculation cycles operated satisfactorily, except for the tubes which had a tendency to split frequently at irregular intervals.

To assist in mixing, recirculation of gas in Filter No. 3 was used for the first 17 days of operation. Gas production was then considered sufficient to operate the mixing and solid-liquid separation action of the plate media, and recirculation was terminated.

Temperatures in the filter were controlled as closely as possible to $35^{o}C$, but variations in the temperatures of the laboratory altered the filter temperatures accordingly. Disruptions in the temperatures were mainly due to failures of the recycle system. With the hot water bath system of heating, breakdown of recycle lowered the temperature of the filter to ambient, i.e. $20^{o}C$, while with the external heating element system, breakdown of the recycle caused the temperatures at the top and bottom of the filters to change from $35^{o}C$ to approximately $36^{o}C$ and $42^{o}C$ respectively.

Replacing the hot water bath system of heating with the heating element system reduced the temperature gradient along the length of the filter and eliminated the long recirculation line.

The only sludge leaving the system regularly was that escaping in the effluent. No sludge was wasted as a routine, but sludge was occasionally wasted following blockages in the filter, and also as a result of accidents.

Tests carried out on the filter were conducted in a specific order so as to minimise their effect on each other. The order in which the tests were carried out is as follows:

1st - Gas analysis for its components.

2nd - Gas flow measurement.

3rd - Waste flow measurement.

4th - Removal of samples from the top, middle and bottom sampling taps, in that order, for the measurement of pH and temperature.

5th - Removal of samples from 4 above and from the effluents for miscellaneous tests.

Gas analysis for the methane, carbon dioxide and nitrogen components was conducted using a gas chromatograph (Appendix I). During 'steady state' operation of the filters, an analysis of the gas was performed every second or third day so as to obtain its average composition. During the periods of unsteady operation, analyses were conducted more frequently, since the composition of the gas was used as an indication of the stability of the process.

Average flows of waste treated and gas produced were recorded daily by measuring their volumes over specific time periods. The ratio of gas production rate to waste flow rate supplied an accurate indication of the performance of the process. The volume of gas from the plate section of Filter No.3 was measured separately to determine the fraction of the waste stabilized in that section of the filter.

The temperature and pH of the filter contents were measured by opening the sampling ports into beakers containing a thermometer and pH electrode. Readings were taken immediately to prevent loss of heat and carbon dioxide, so as to increase the accuracy of the temperature and pH measurements respectively. To obtain a representative sample

from the filter, the liquid in the sampling port was wasted into a container before the actual sample of ± 50 ml was removed. All the mixed liquor withdrawn from the ports was returned to the filter via the stand pipes. Readings of the temperature and pH (mainly on samples from the centre sampling port) are recorded daily. However spot checks were conducted more frequently during unstable conditions.

Chemical oxygen demand and volatile suspended solids tests were conducted on representative samples of the effluent (Appendix I). These tests were performed only during periods of 'steady state' operation of the process, so as to obtain the average quality of the effluent.

Volatile fatty acids concentrations were measured mainly on samples taken from the centre sampling ports, but occasional measurements were made along the length of the filter to determine the concentration profile. Since the test was used only to indicate the stability of the process, daily readings were taken during unstable conditions, but less frequently during stable operation of the process.

Volatile solids concentration measurements of the mixed liquor in the filters were abandoned since the concentrations in consecutive samples taken from one sampling port at any one time showed wide fluctuations. An accurate measure would have required many large samples from the filters, and the process performance would have been affected by the solids removed.

F. RESULTS

The routine measurements recorded during the operation of the three filters are graphically represented in Figures 9, 10 and 11. There seemed little merit in tabulating daily results, since individual results give only an approximate indication of the filter performance. Trends in the performances of the filters, which are of more value than individual results, are easily followed on the graphic presentations (Figures 9, 10 and 11).

Testing periods during which the processes were assumed to be operating in a steady state are shown by the shaded areas in Figures 9, 10 and 11. Filters No.1, 2 and 3 were operated at 5, 6 and 5 'steady-state' levels respectively. Average results describing the treatment efficiency and general performance of the filters during these 'steady state' periods are summarized in Table III, and graphically represented in the figures of the Discussion (Part G).

The diagrams of the daily results (Figures 9, 10 and 11) are particularly useful for following the behaviour of the filter during unstable conditions such as start-up, and temperature and loading rate fluctuations

The arithmetic mean was used to obtain an average of the readings recorded during the 'steady state' period. While this is the obvious method for obtaining the average for the waste flow, gas production and gas composition measurements, the method can be applied also to the COD and VSS measurements, as shown below: Plots of the total and soluble COD measurements for waste batches No.1, 2 and 4 on the cumulative percentage probability paper yield straight lines (Figure 12). Therefore, the measurements are normally distributed, and the arithmetic mean is the best estimate of their average value. Similar probability distributions were generally obtained from the COD's and volatile suspended solids concentrations in the effluents, as shown for Test 4 of Filter No.2 (Figure 13). The arithmetic mean is therefore also a valid estimate of the average effluent COD and VSS values. Standard deviation from the mean was in all cases in the order of 15%.

Small fluctuations in the ratio of the gas produced to the waste treated may originate from inaccuracy of measurements, minor fluctuations in the temperature, and general random fluctuations usual in biological

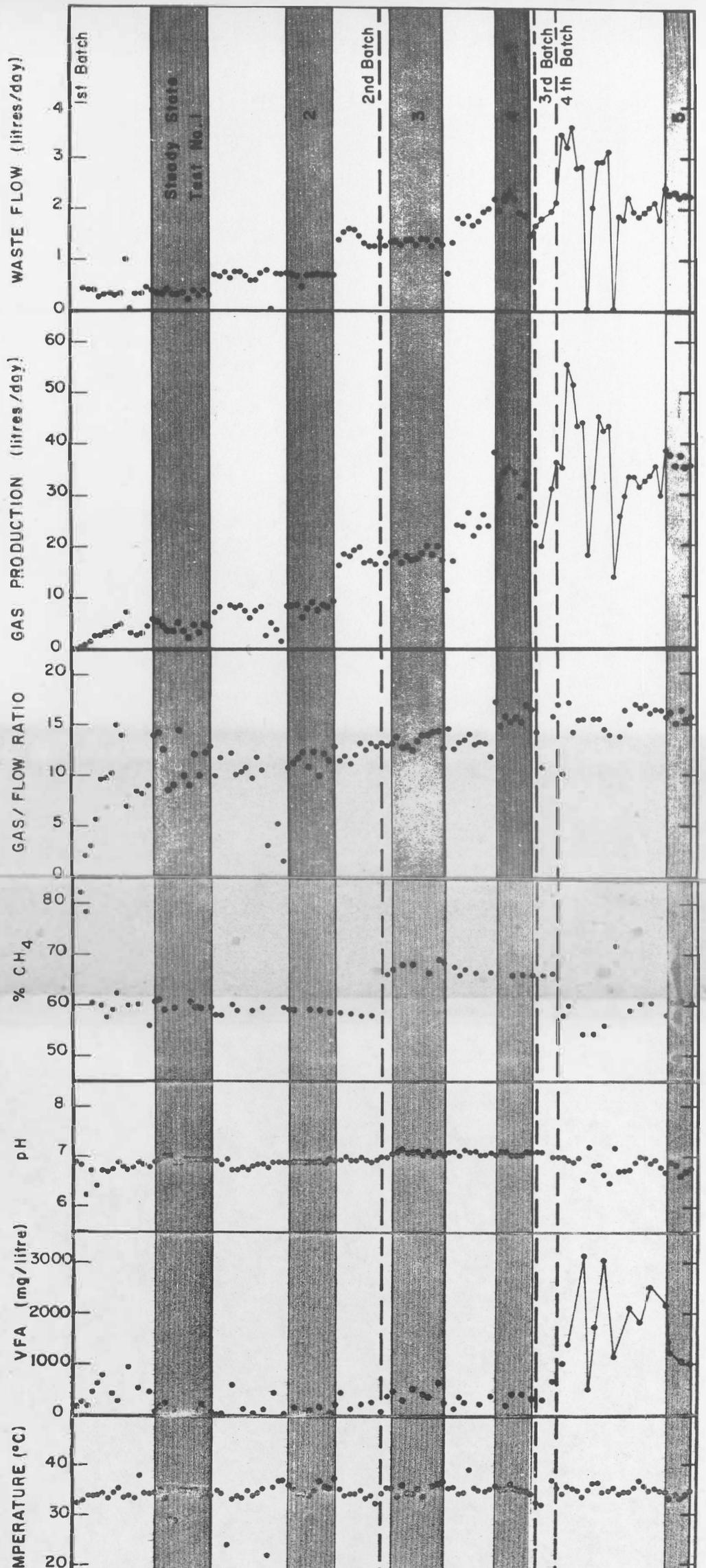

FIGURE 9: Daily Routine Measurements of the Performance of Filter No. 1

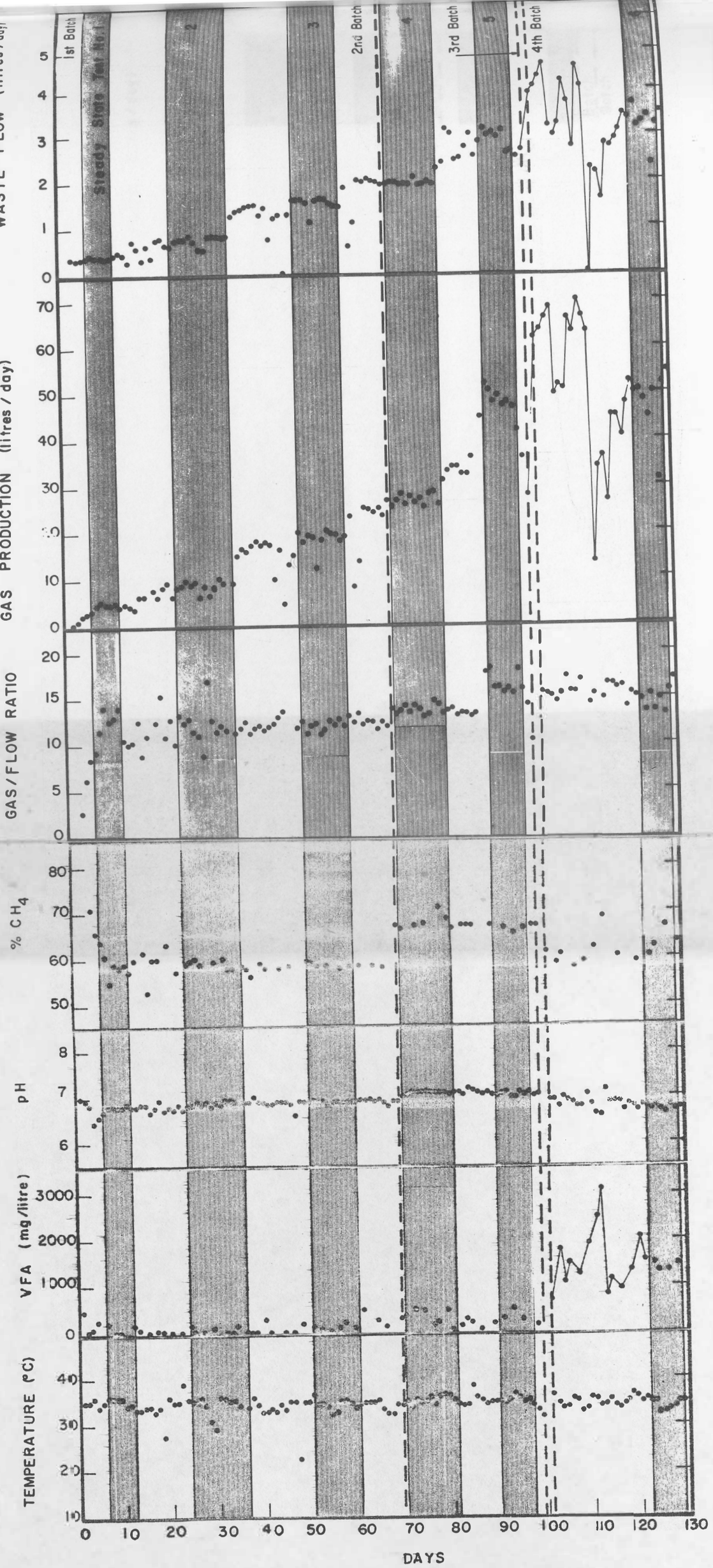

FIGURE 10: Daily Routine Measurements of the Performance of Filter No. 2

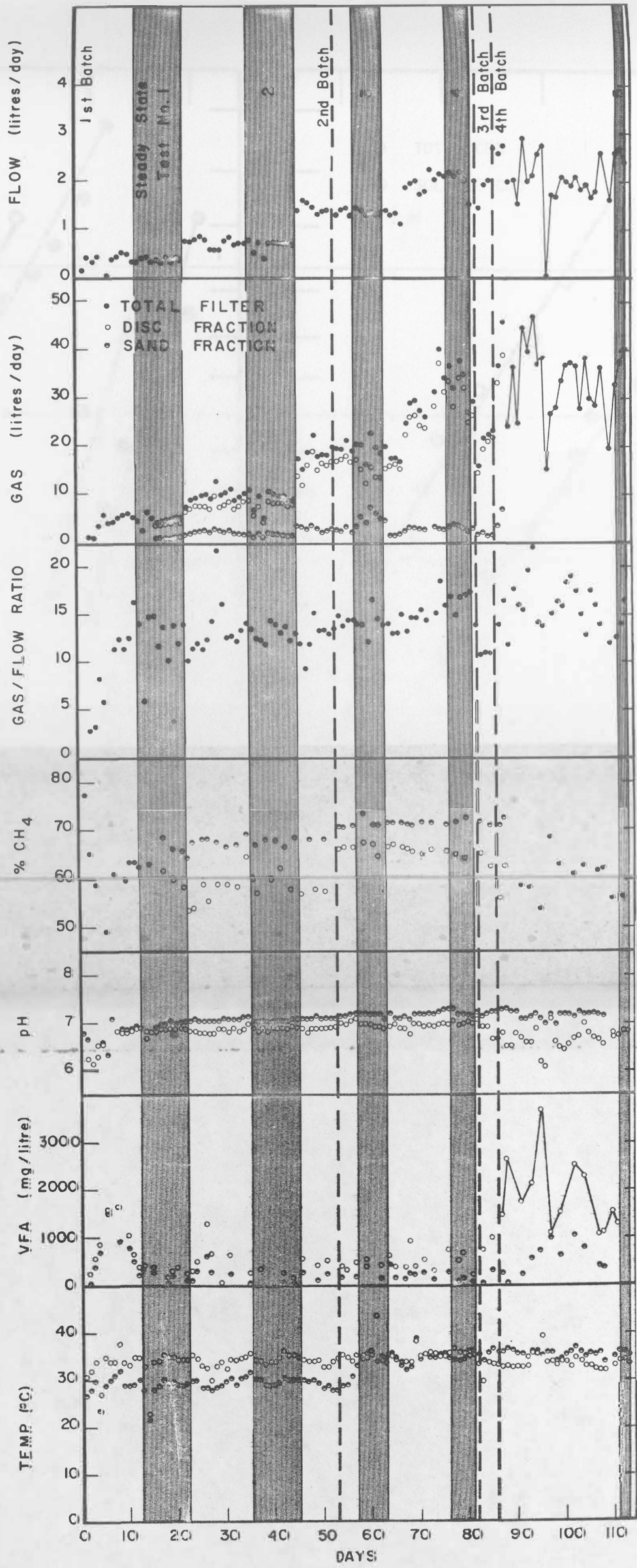

FIGURE 11: Daily Routine Measurements of the Performance of Filter No. 3

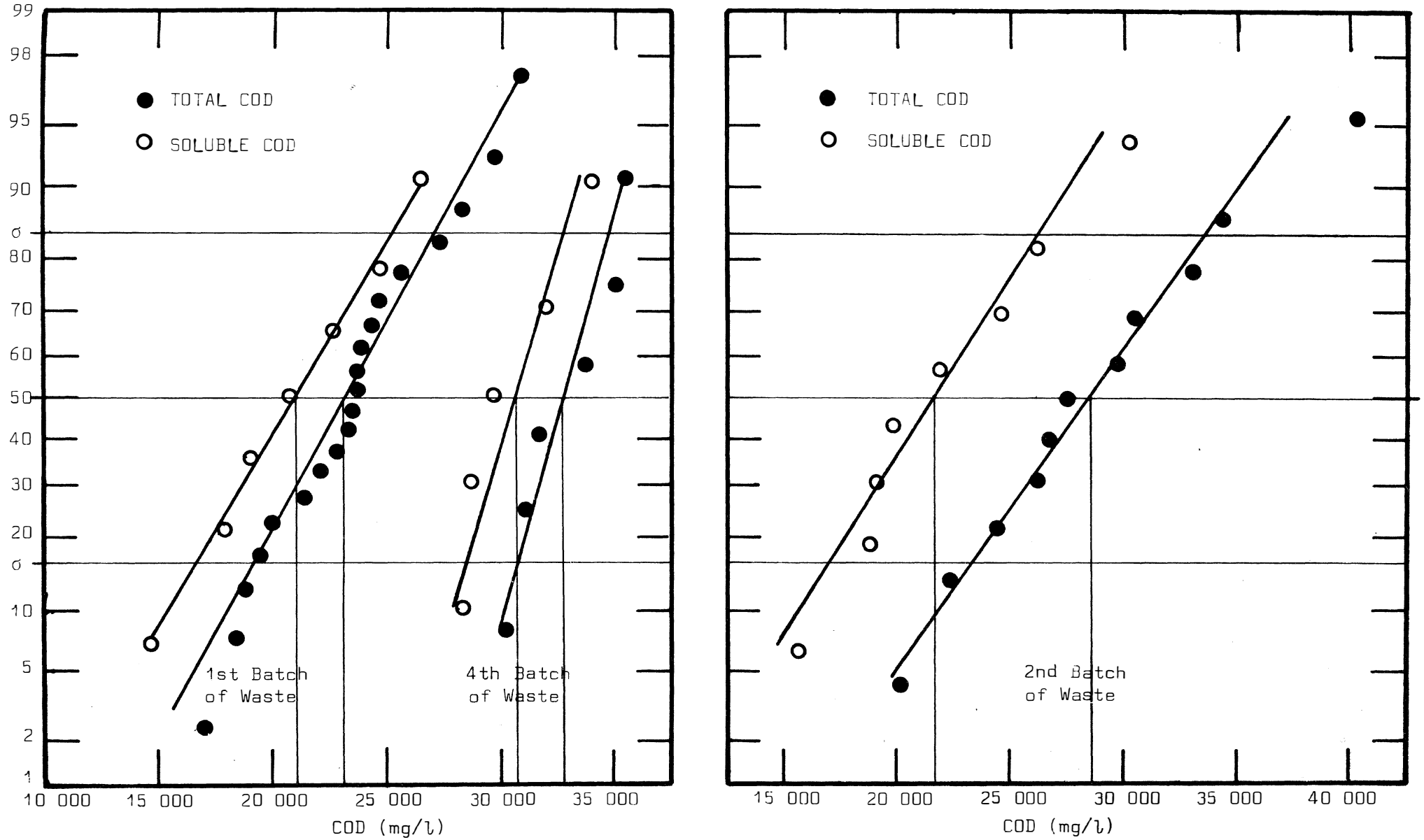

FIGURE 12: Normal Probability Distributions of the COD Measurements for the Three Spent Wine Batches. Mean and standard deviations are shown.

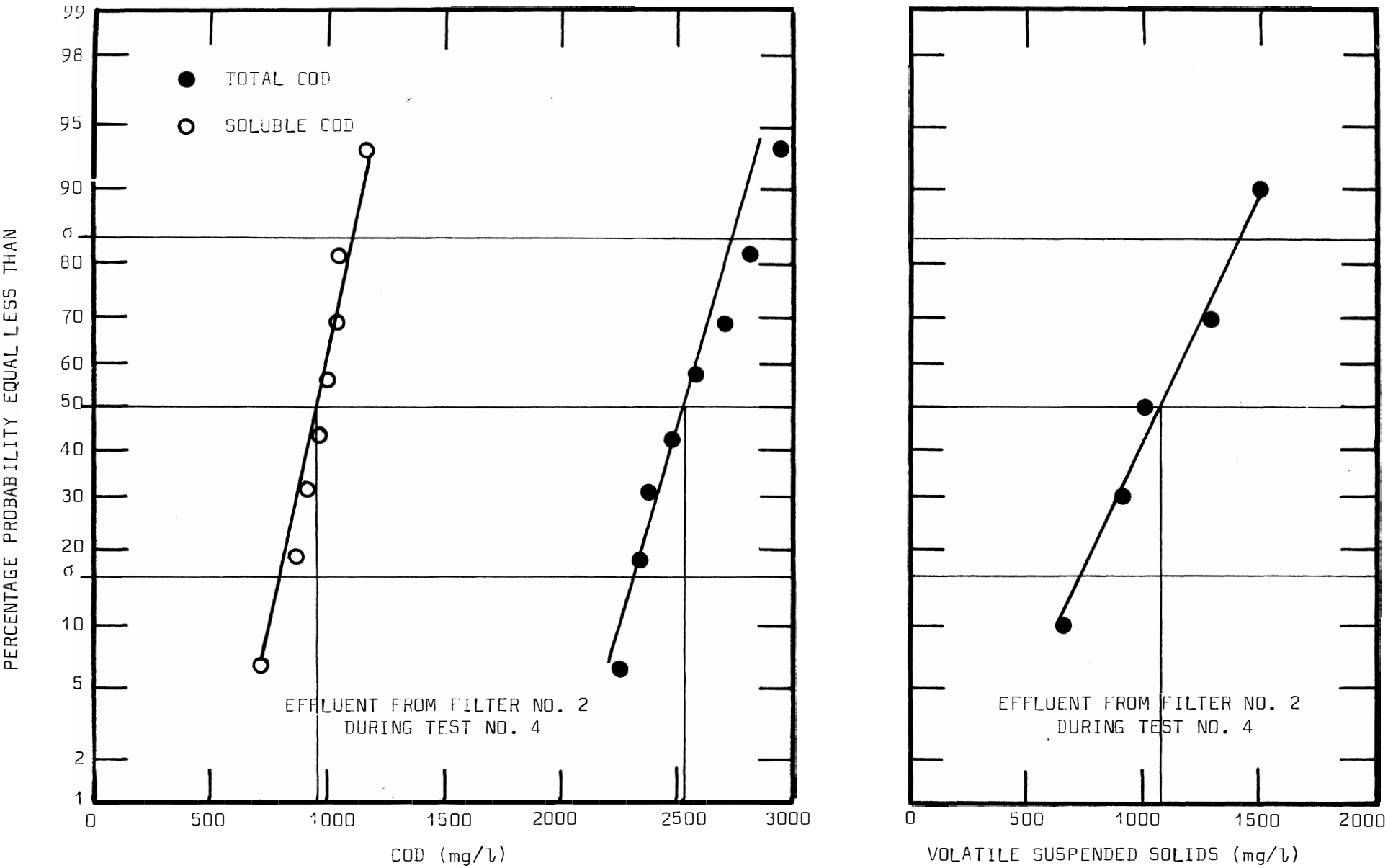

FIGURE 13: Typical Normal Probability Distributions of Effluent COD and Volatile Suspended Solids Concentration for One Steady-State Loading Rate

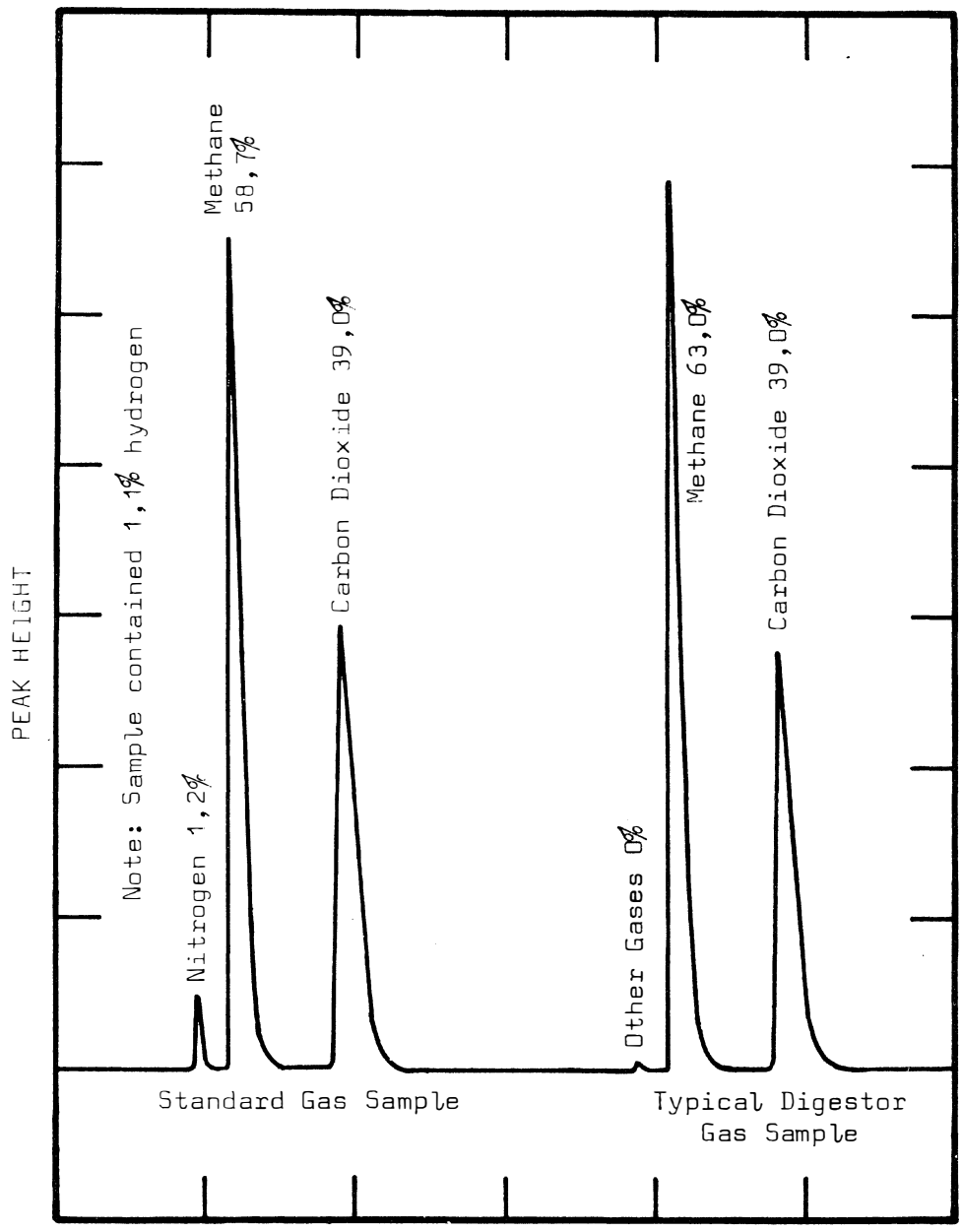

FIGURE 14: Chromatograms of a Standard Gas Sample and a Typical Digestor Gas Sample

TABLE III

Results of 'steady-state' tests conducted on the three filters at various loading rates.
(see overleaf for explanation of symbols)

TEST NO.	WASTE BATCH NO.	WASTE FLOW	GAS FLOW(a)	CH_4	VSS EFF.	TOTAL COD	SOLUBLE COD	HYD. RET.(b)	LOAD RATE(c) kg COD/DAY/m^3		RATIO(d) GAS/ WASTE	RATIO(e) COD/ VSS	COD(f) DESTR.	CH_4(g) PROD.	RATIO (g)/(f)	(h)
		ml/d	ml/day	%	mg/l	mg/l	mg/l	DAYS	HYD.	TOTAL			g COD/ DAY	g COD/ DAY	%	%
FILTER NO. 1 (STONE)																
1	1	360	4 244	59,9	-	1068	-	13,67	0,85	1,70	11,78	-	8,16	6,72	82,4	-
2	1	706	8 170	59,0	771	1841	766	6,97	1,67	3,33	11,57	1,40	15,85	12,42	78,2	98,2
3	2	1364	18 441	67,8	901	1998	943	3,61	3,98	7,93	13,51	1,17	37,70	32,10	85,2	98,2
4	2	2025	32 430	66,0	1084	3218	1447	2,43	5,91	11,77	16,00	1,63	55,10	55,10	100,0	96,4
5	4	2322	36 850	60,0	831	5752	4538	2,12	7,74	15,41	15,86	1,46	65,30	56,90	87,0	87,4
FILTER NO. 2 (CLINKER)																
1	1	383	4 689	59,1	-	584	-	14,86	0,91	1,56	12,24	-	8,73	7,12	81,5	-
2	1	733	9 550	59,1	-	1103	-	7,76	1,73	2,99	13,03	-	16,65	14,50	87,0	-
3	1	1529	18 840	58,7	1128	2252	724	3,72	3,62	6,23	12,32	1,36	35,00	28,40	81,3	98,4
4	2	1993	27 530	68,1	1078	2563	952	2,85	5,82	10,02	13,81	1,50	55,20	48,10	87,0	98,1
5	2	2931	48 160	66,5	1709	3998	1437	1,94	8,55	14,73	16,43	1,50	79,50	82,30	103,0	96,4
6	4	3253	47 910	63,4	1151	8224	6060	1,75	10,84	18,67	14,73	1,88	86,40	78,10	90,5	82,7
FILTER NO. 3 (PLATE-SAND)																
1	1	368	4 960	-	-	540	-	18,94	0,87	1,23	13,48	-	8,43	7,81	92,5	-
2	1	690	9 165	-	517	684	517	10,10	1,63	2,30	13,28	0,32	15,65	14,30	91,5	99,3
3	2	1377	19 614	-	624	1083	618	5,06	4,02	5,65	14,24	0,75	38,60	39,14	88,5	99,3
4	2	2057	33 820	-	453	1566	925	3,89	6,00	8,44	16,44	1,42	57,00	56,88	100,0	98,2
5	4	2567	37 000	56,5	1078	6512	6070	2,72	8,55	12,03	14,40	0,41	68,3	53,80	78,8	82,7
3(a)*	2	1262	17 296	-	-	1233	731	5,52	3,68	5,18	13,71	-	-	-	-	-
PLATE SECTOR OF FILTER NO. 3																
3(a)	2	1262	15 833	66,7	780	2450	1432	3,23	8,02	8,85	12,55	1,32	-	-	-	-
4	2	2057	30 792	64,8	7789	15900	2898	1,98	13,07	14,42	14,97	1,67	-	-	-	-
5	4	2567	-	-	1391	7813	6320	1,59	18,62	20,54	-	1,07	-	-	-	-

TABLE III (continued)

(a) Gas volume as measured by the gas-meters at 20°C.

(b) Hydraulic retention time of the filters in days.

(c) Load rates/unit volume of filters are given in terms of both hydraulic and total volumes of the filters.

(d) Ratio of gas produced to hydraulic flow of waste.

(e) Ratio of suspended solids COD (i.e. difference between total and soluble COD) to volatile suspended solids concentration.

(f) COD destroyed is approximated by the difference between the total COD in the influent and the soluble COD in the effluent. (Soluble COD in the effluents at low loading rates was not measured, but it is assumed to be low for the purpose of the calculation.)

(g) Methane production is corrected to STP (page 46), and converted to COD (350 l of CH_4 at STP is equivalent to 1 kg COD).

(h) Treatment efficiency is measured in terms of biodegradable COD reductions in the waste.

* Test 3(a) was conducted on days 65 to 67 with the sand sector under plug flow conditions.

processes. Significant deviations from the established stable pattern have assignable causes such as significant temperature changes, starting-up conditions, changes in the batches of waste, and changes in the loading rates. The exact cause for each deviation may be identified on Figures 9, 10 and 11. The unrealistically high ratios recorded in Tests No.4, 5 and 4 of Filters No. 1, 2 and 3 were probably caused by incorrect settings on the gas meters.

Chromatograms for the analysis of a standard gas and a typical gas obtained from the filters are shown in Figure 14. Calculation of the composition of the gas is based on the approximation that peak heights of the gas components registered by the chromatograph are proportional to their concentrations. This is a valid approximation, since the composition of the standard gas is nearly the same as that of the digestor gas. Factors causing variations in the composition of the gas were the same as the factors mentioned above as also causing the variations in the gas production.

The volumes of methane produced were adjusted to STP for comparative purposes. Adjustment was made for an assumed average gas temperature of 25°C, and a corresponding water vapour pressure of 24 mm mercury. The correction was applied by assuming the gas to be ideal, i.e.

$$V_2 = V_1 \left(\frac{T_2}{T_1} \cdot \frac{P_1}{P_2} \right)$$

where subscript 1 refers to the measured conditions, and subscript 2 to the STP conditions. Corrected volume is therefore:

$$V_2 = V_1 \left(\frac{273}{298} \cdot \frac{736}{760} \right)$$

or $$V_2 = 0{,}888\ V_1$$

i.e. the measured volume must be reduced by 88,8% for STP conditions.

G. DISCUSSION

The discussion on the performance and behaviour of the three filters operated in this thesis is divided into three parts:

1. Performance of the filters with regard to 'steady-state' treatment efficiencies and capacities. A comparison is made between the three filters and between the filters and other anaerobic systems.

2. Application of the continuous culture kinetic model to the anaerobic filter process. On this basis, steady-state performance of the filters is described.

3. Behavioural characteristics exhibited by the filters, especially during unstable conditions of operation.

1. Steady-State Treatment Efficiencies and Capacities

The steady-state treatment efficiencies and capacities of the three filters during incremental increases in the waste loading rates are summarized in Table III.

Treatment capacities of the processes were measured in terms of waste loading rates per unit hydraulic volume of reactor (kg COD/day/m^3), not in terms of the more usual parameter, waste loading rate per unit mass of organisms in the reactor, since no accurate measure of the solids concentrations in the filters was possible. The hydraulic volumes of the filters were used as a basis for the treatment capacity measurements of the processes, since the volume of the media is inert.

Treatment efficiencies of the processes were measured in terms of percentage reductions obtained in the biodegradable COD of the spent wine influent, assuming 1,5% of the COD of spent wine to be unbiodegradable. As the COD of the spent wine was virtually completely in a soluble or solubilizable form, the soluble COD in the effluent could be used as a reliable measure to determine the efficiency.

The relationships between treatment efficiencies of Filters No. 1, 2 and 3 versus (a) COD loading rates and (b) hydraulic retention times are graphically represented in Figures 15 and 16. In examining

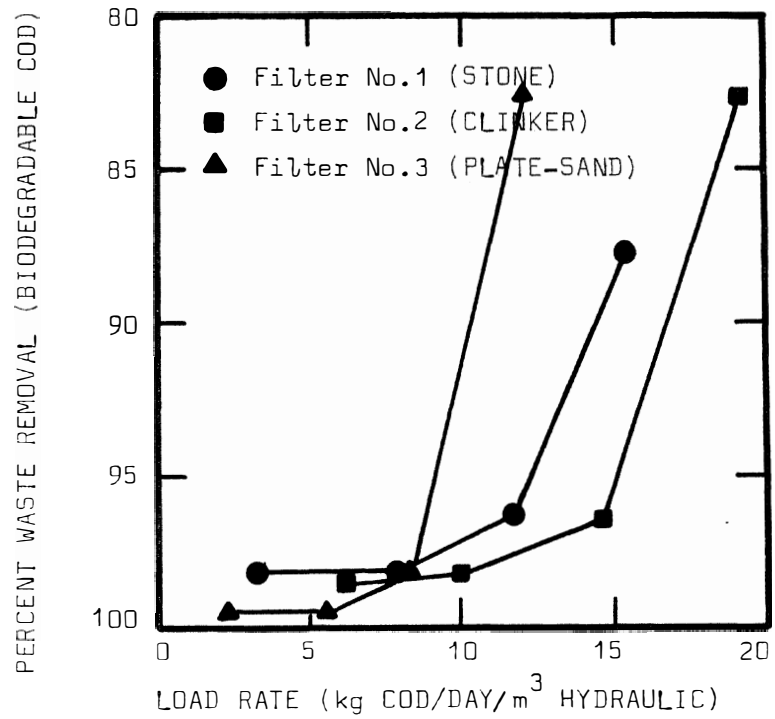

FIGURE 15: Variations in the Waste Removal Efficiencies at Different Load Rates for Filters No. 1, 2 and 3

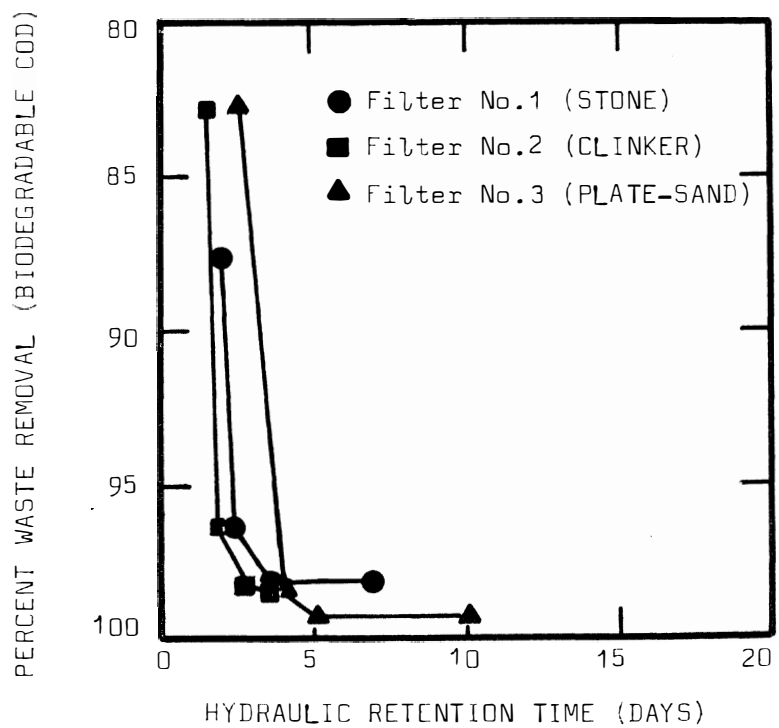

FIGURE 16: Variations in the Waste Removal Efficiency for Different Hydraulic Retention Times for Filters No. 1, 2 and 3

Figures 15 and 16, it should be noted that as the loading rate increases, the hydraulic retention time decreases correspondingly. All three filters generally exhibited the same trend:

(a) Under low loading rates of approximately 4 kg/day/m^3, treatment efficiencies were high - about 98,5% COD removals (Figure 15). These loading rates correspond to fairly long retention times of approximately 6 days (Figure 16).

(b) As the loading rates were increased from the initial low values (4 kg/day/m^3), the processes proved to be relatively insensitive to loading rate, and the treatment efficiencies showed only minor reductions. However, when the loading rate was increased to a certain level (which differed between the three filters), the treatment efficiency exhibited rapid deterioration, indicating that process failure was imminent. The loading rate just before failure was taken to be the maximum permissible for the process. Maximum loading rates for the stone, clinker and plate-sand filters were 11,8; 14,7; and 8,3 kg/day/m^3 respectively, corresponding to 2,5; 1,9; and 3,8 days of hydraulic retention time (Figures 15 and 16). At higher loading rates treatment efficiency showed further rapid deterioration, to 85% COD reductions and less.

Total COD (i.e. soluble plus suspended solid COD) in the effluents from the filters were considerably higher than indicated by the treatment efficiencies, since the effluent contained a significant concentration of suspended solids. The relationships of total COD and volatile suspended solids concentrations in the effluents versus (a) COD loading rates and (b) hydraulic retention times are shown in Figures 17, 18, 19 and 20.

Within the range of loading rates imposed on the filters, the volatile suspended solids concentration in the effluents from all three filters remained fairly constant (Figure 20). The stone, clinker and plate-sand filters delivered effluents with volatile suspended solids concentrations of approximately 900, 1300 and 700 mg/l respectively.

Since the suspended solids concentrations in the effluents remained fairly constant, total COD's in the effluents necessarily show the same

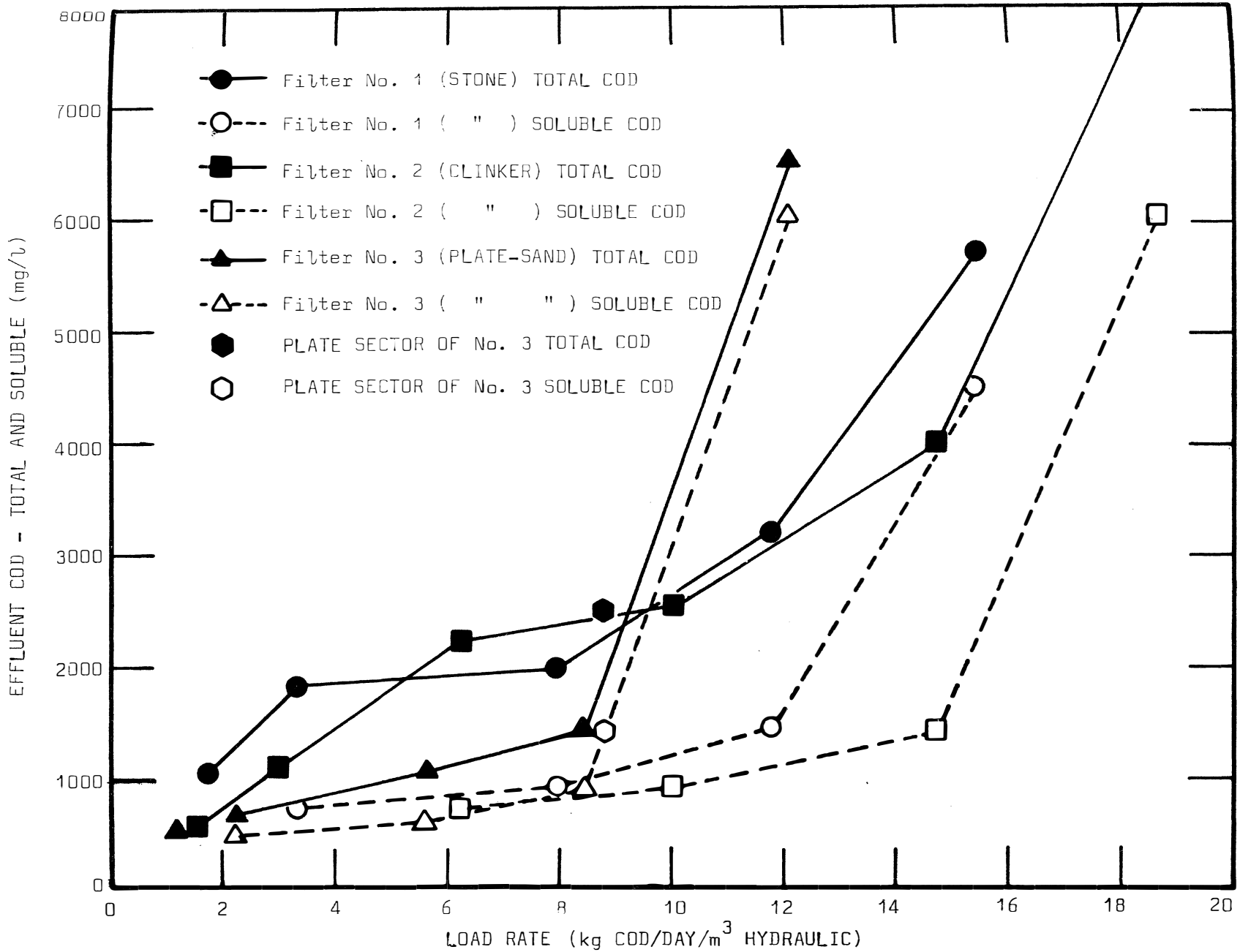

FIGURE 17: Effect of Different Filter Media on the Effluent COD at Different Load Rates/ Hydraulic Volume of Filter

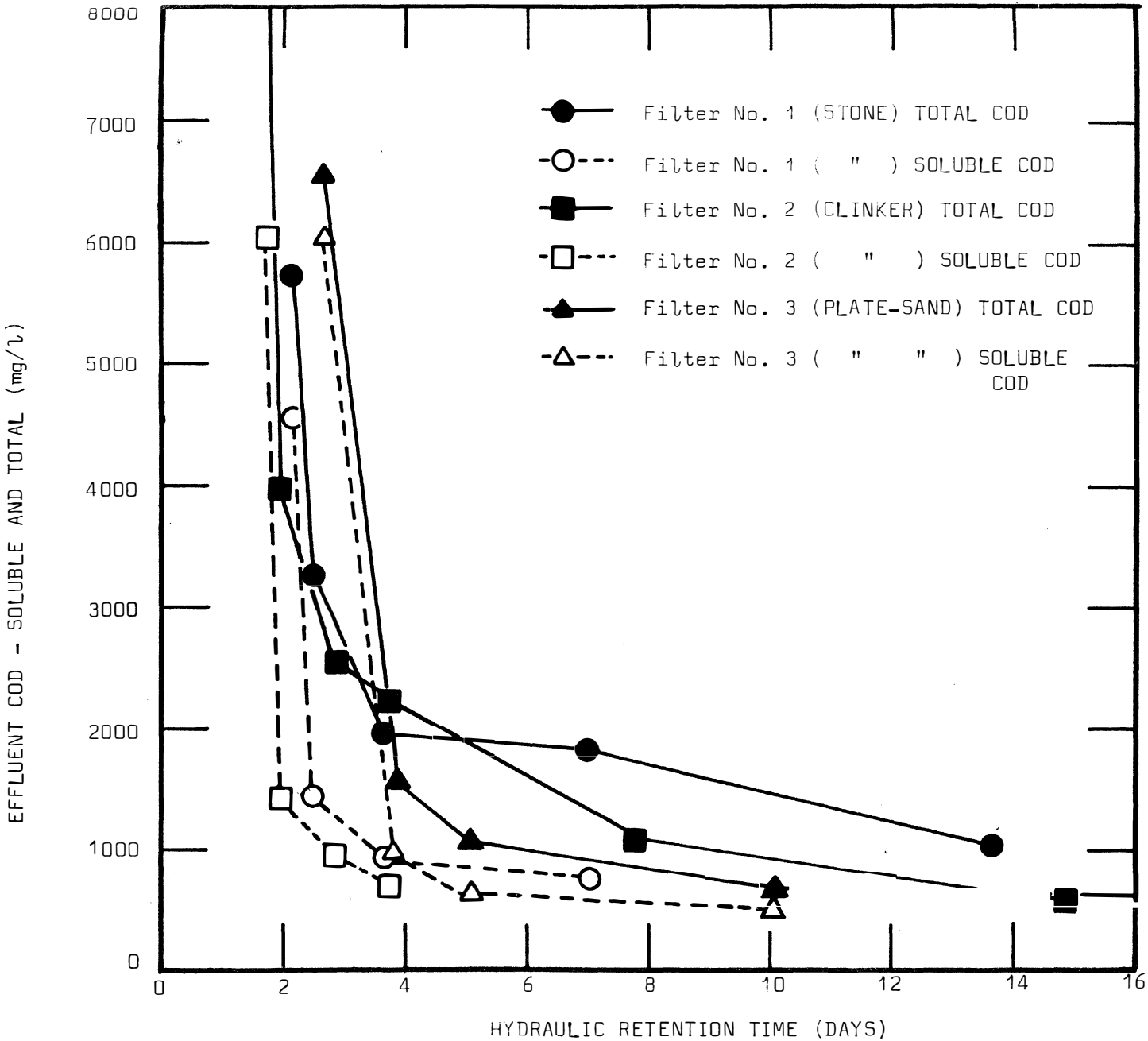

FIGURE 18: Effect of Filter Media on Effluent COD at Different Hydraulic Retention Times

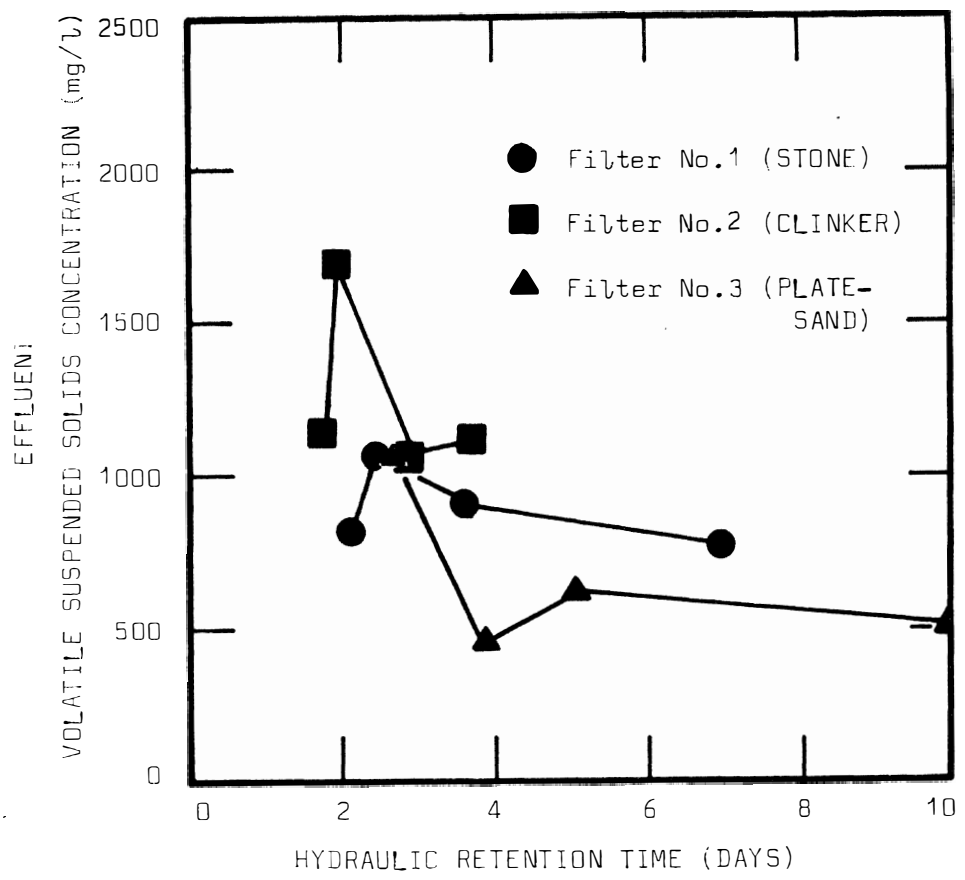

FIGURE 19: Effect of Different Filter Media on the Effluent Volatile Suspended Solids Concentration at Different Hydraulic Retention Times

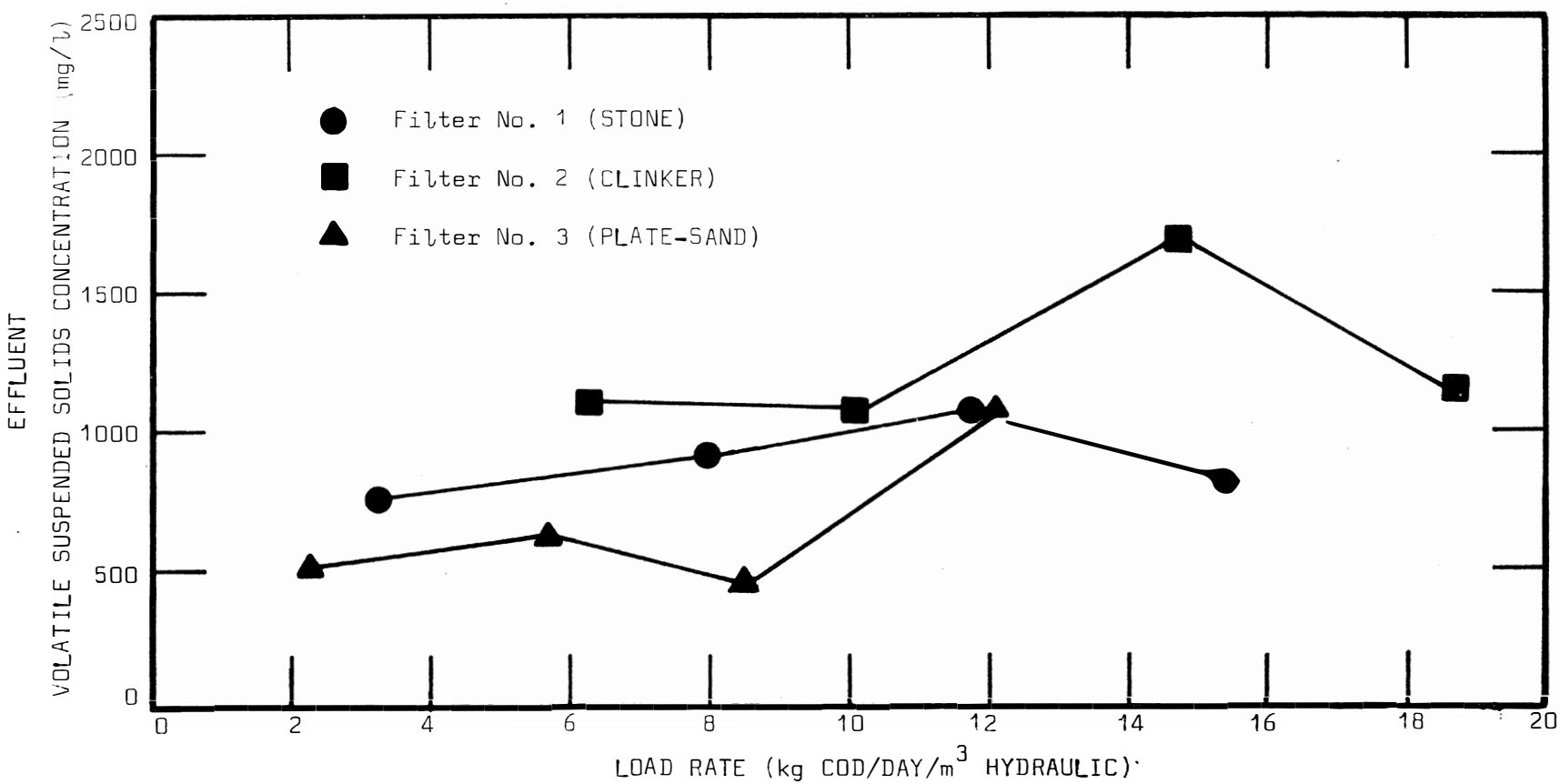

FIGURE 20: Effect of Different Filter Media on the Effluent Volatile Suspended Solids Concentrations at Different Load Rates/Hydraulic Volume of Filters

trend and behaviour as the soluble COD's (Figures 17 and 18), and consequently also the same trend as the treatment efficiency (compare Figure 15 with Figures 17 and 18). At loading rates above maximum permissible, the effluent quality deteriorated rapidly to 6000 mg/l of total COD and more, while below the maximum permissible, the effluent quality remained fairly constant at 2000, 2000 and 1,200 mg/l of total COD for the stone, clinker and plate-sand filters respectively. Thus failure was not evident from the rate of loss of the suspended solids, but from the concentration of the soluble COD in the effluent.

The fact that the solids concentration in the effluent did not increase significantly when the process showed incipient signs of failure (compare Figures 17 and 20) is not contrary to the predicted theoretical behaviour. The theory described in Section 2 of the discussion indicates that failure is almost wholly dependent on the solids retention time; failure occurring when the solids retention time is reduced to low levels. Also, the theory shows that significant reductions in the solids retention time may be achieved with minor increases in the volatile suspended solids concentration in the effluent. These increases in the volatile suspended solids concentrations are of the same order observed in the experimental data presented in Figure 20.

Surface Area Effect

A valid comparison of the solid-liquid separation capacities of the different filter media can be made only on a basis of volatile solids concentration (or mass) measurements in the filter. Unfortunately, solids determinations in the filters were not possible because:

(a) solids concentrations in consecutive samples removed from one sampling port varied widely. Also, the concentrations varied along the length of the filters.

(b) a fraction of the solids remained attached to the surface of the media.

However, the effects of surface area and surface characteristics on the process performance of the three filters can be qualitatively investigated by comparing soluble COD, treatment capacity, and volatile

suspended solids concentration in the effluents from the three filters. Comparisons are made on a basis of hydraulic retention times, and COD loading rates in terms of the hydraulic volume of the filter. The volumes of the media are thus excluded from the comparison.

Soluble COD concentrations in the effluents from Filters No. 1 and 2 (which contain stone and clinker media respectively) are compared on Figures 17 and 18. These figures clearly demonstrate that the soluble COD in the clinker filter effluent was consistently lower than that from the stone filter, especially at the higher loading rates. Also, the maximum permissible loading rate for the clinker filter is seen to be about 20% higher than that for the stone media (Figure 17). Since the filter which contains the higher mass of organisms will deliver the better quality effluent, and also treat the higher loading rate, it appears that the clinker media was more efficient in retaining micro-organisms.

Contrary to the above conclusion, a comparison of the volatile suspended solids concentrations in the effluents shows that the stone filter in fact wasted less solids than the clinker filter (Figures 19 and 20). A possible explanation is that the clinker was able to retain high concentrations of active micro-organisms on its surface, while releasing the inactive solids to the effluent stream. Thus, although the clinker filter wasted more volatile suspended solids, it is possible that less active micro-organisms were wasted than from the stone filter.

A visual examination of the clinker and stone (Figure 3) indicates that the specific surface area of the clinker is considerably higher than that of the stone. However, the maximum permissible loading capacity for the clinker filter was only 20% higher than the maximum for the stone filter. It thus appears that biological solids adhesion to surface area does not play an important role in the solid-liquid separation system of the filter. It follows that the bulk of the micro-organisms are retained in the void spaces provided by the media.

This deduction is supported by examining the performance of the plate media (very low surface area) of Filter No. 3. Soluble and total COD in the effluent at a loading rate of 8,8 kg/day/m^3 were in the same range as the COD from the stone and clinker filters (Figure 17).

The conclusion from the comparisons is that filter media should not be chosen with the objective of providing large surface area, but rather with the objective of improving the solid-liquid separation mechanism in the voids. Of importance also is the fact that stone and clinker occupy about 50% of the reactor volume. Reduction of media volume would provide additional treatment capacity to a much greater extent than the possible improvement based on surface characteristics of the media.

Comparison Between the Three Filters

In order to make a practical comparison between the performances of the filters, one should compare the behaviour using the total volume of the reactor. Even though a process may be more efficient per unit hydraulic volume, the system may in fact be less efficient per unit total reactor volume since media such as stone and clinker occupy a significant fraction of the reactor volume. Comparisons between the performances of the filters are made in terms of soluble COD, volatile suspended solids and total COD in the effluents, and treatment capacity.

Treatment capacity: The maximum permissible loading rates obtained from Filters 1, 2 and 3 were 5,9; 8,55 and 6,0 kg/day/m^3 (Figure 21). Thus highest loading rate was achieved by the clinker filter, followed by the combined plate-sand filter and the stone filter. In making this comparison, it should be noted that the plate-sand filter gave the best performance until the highest loading rate was attained (8,55 kg/day/m^3). (At this loading rate there was in evidence a sharp drop in the filter performance.) During the early period of operation (i.e. at loading rates below 8,55 kg/day/m^3), recirculation in the sand fraction of Filter No. 3 was kept separate from the plate fraction (recirculation Schemes I and II - see Figure 2). However, at the highest loading rate, the sand blocked up with solids, forcing the effluent to escape through the gas-line of the plate sector (see Figure 2). To free the blockage, the gas-line from the plate sector was shut off, and recirculation changed to include the sand fraction (i.e. from the top of the sand sector to the bottom of the plate sector - see recirculation Scheme II in Figure 2). The solids concentration in the effluent increased significantly with the latter system of recirculation, which accounts for the poor performance of the filter at the highest loading rate.

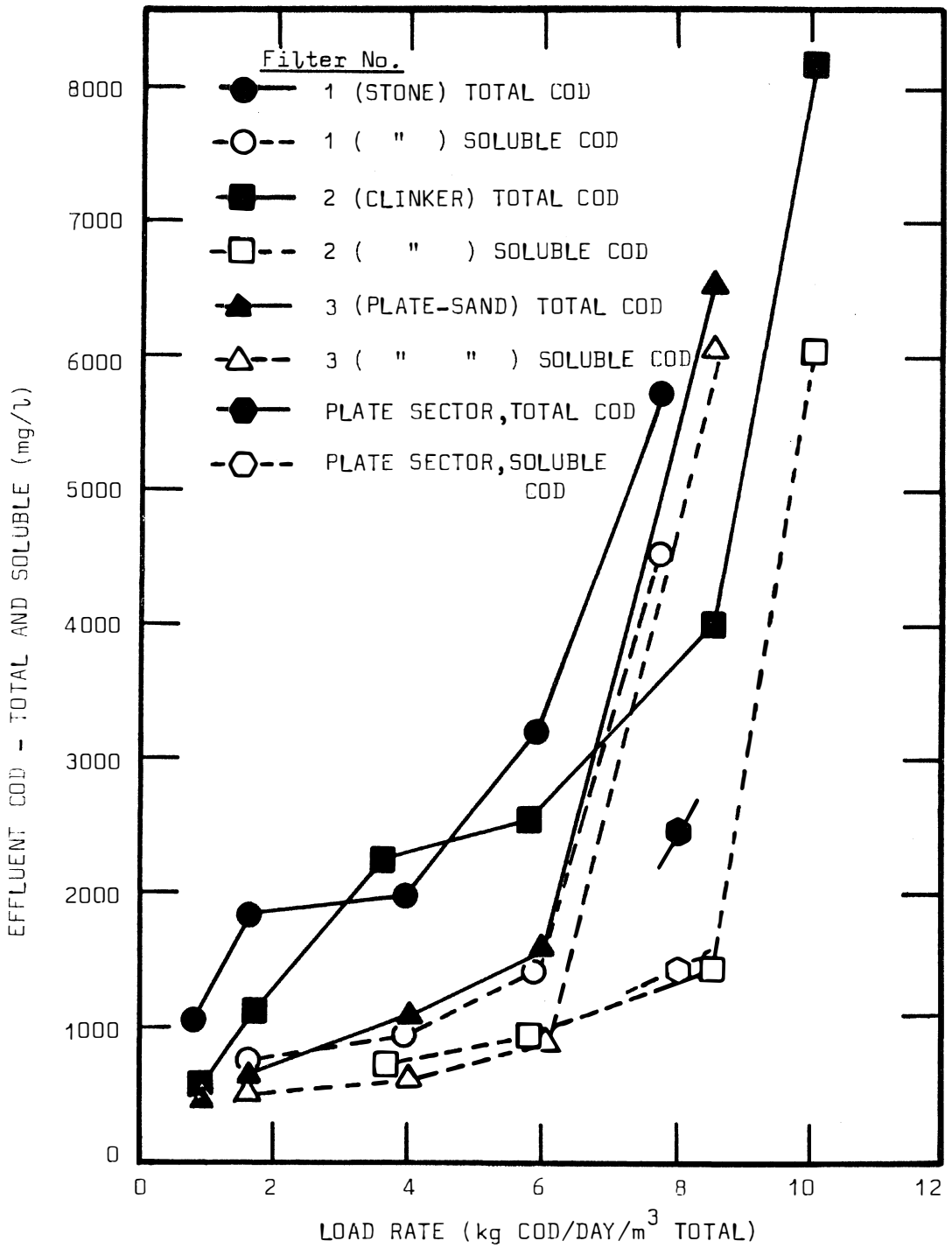

FIGURE 21: Comparison of the Effluent COD's from Filters No. 1, 2 and 3 at Different Load Rates/Total Volume of Filter

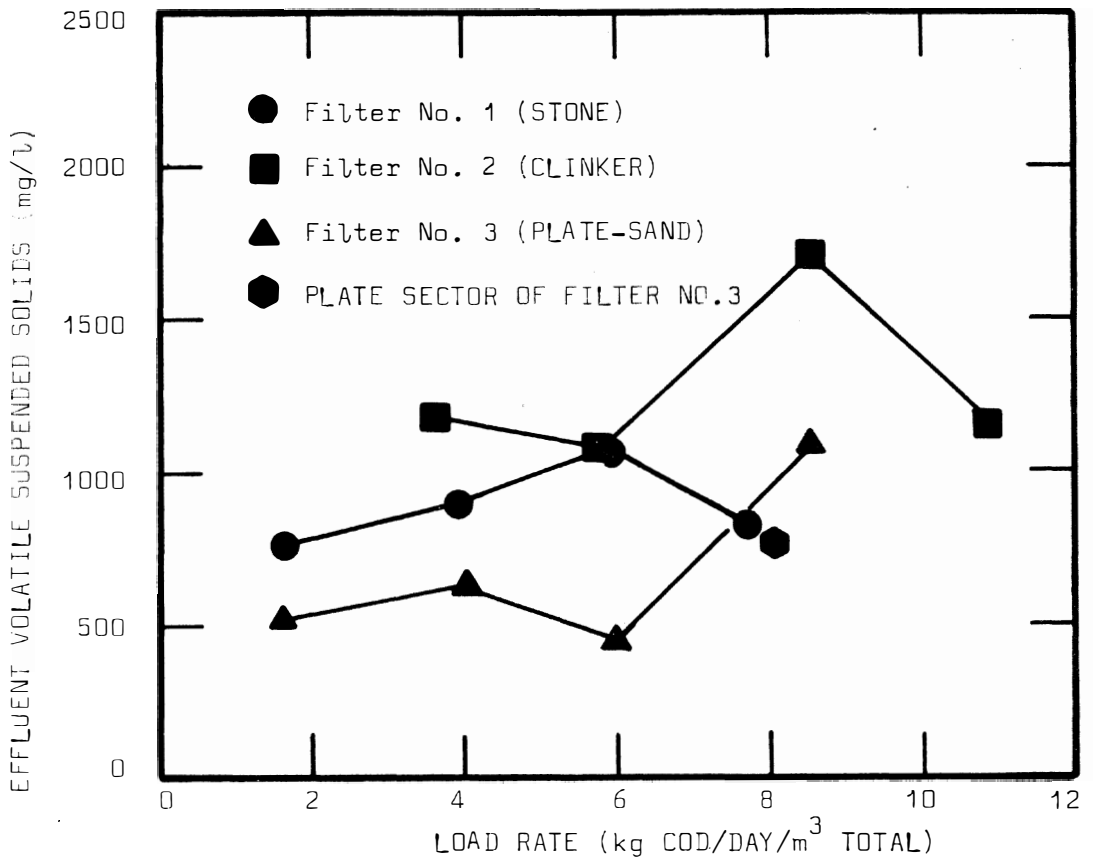

FIGURE 22: Comparison of the Effluent Volatile Suspended Solids at Different Load Rates/Total Volume of Filter

Soluble COD: If the anaerobic filters are to be operated under continuous stable conditions, the loading rates imposed on the process must be below maximum. Thus, soluble COD in the effluents are compared at low loading rates of about 3 kg/day/m^3. Filters No. 1, 2 and 3 delivered effluent soluble COD's of 900; 700 and 500 mg/l respectively (Figure 21). Best treatment efficiency was obtained from Filter No. 3 (with sand fraction operation under plug-flow or with separate recirculation), followed by the clinker and then the stone media filter.

Volatile suspended solids: The relationship between volatile suspended solids concentrations in the effluents and COD loading rates is represented in Figure 22. The plate-sand filter consistently delivered the lowest concentration during the period when recirculation of the sand fraction of the filter was kept separate, i.e. until the highest loading rate on the filter. Hence, the plate-sand filter should have been able to retain the highest mass of organisms, and consequently operate with the longest solids retention time of the three filters. This assumption is substantiated by the fact that the plate-sand filter delivered the lowest effluent soluble COD (Figure 21). A possible explanation for the fact that volatile solids concentrations in the effluents from Filters No. 1 and 2 were inconsistent with the relative treatment efficiencies has already been offered (page 55).

Total COD: The ranking of the filter performances based on total COD is the same as the ranking found with soluble COD, since the COD associated with the suspended solids in the effluent remains approximately constant.

Generally, the best performance was given by the combined sand-plate filter, followed by the clinker filter and then the stone filter. However, it should be remembered that the sand of Filter No. 3 is more prone to blockages than the stone and clinker of Filters No. 1 and 2.

To compare the effect of plug-flow and separate recirculation in the sand sector of the plate-sand filter (recirculation Schemes I and II - see Figure 2), measurements were made during the operation of both systems for a loading rate of 4,0 kg/day/m^3. Virtually no difference was detected in the soluble and total COD's of the effluents (compare Test 3 and 3(a) in Table III).

Since it was realized that blockages in the sand of Filter No. 3 could be an adverse feature affecting the whole filter, it was decided to test the 'effluent' from the plate section of the filter, i.e. test the mixed liquor before it passed into the sand sector. At a loading rate of 8 kg/day/m^3 on the total disc sector volume the 'effluent'

soluble COD and volatile suspended solid concentrations were 1432 mg/l and 780 mg/l respectively. The soluble COD at this loading rate is considerably better than the effluent soluble COD from the stone filter, and almost identical to that obtained from the clinker filter (for a loading rate based on total volume) (Figure 21). The volatile suspended solid concentration was in the same range as that from the other filters (Figure 22). Thus at this loading rate, the plates appeared to operate satisfactorily as a method for solid-liquid separation and mixing. (Compared on a basis of hydraulic volume, the performance of the plate sector was inferior to the clinker and stone filter performance.)

At the next loading rate (13 kg/day/m^3) the effluent quality of the plate sector deteriorated to a soluble COD of 1930 mg/l, and a volatile suspended solid concentration of 7740 mg/l. The high volatile solid concentration indicated that a large fraction of the biological solids in the reactor would have been lost in the effluent had the sand layer not held them back. Thus at this loading rate, the process would have deteriorated far more than indicated by the soluble COD. These experiments show that there is an upper limit to the solids retention ability of the plate filter.

One can conclude that, based on total filter volume, the general performance of the plate sector of Filter No.3 is similar to that of the stone and clinker filters. However, the plate media has more potential for possible improvements in design:

(a) Mixing the contents of a plate filter can be achieved by fitting an 'air-gun'[19] (operating on digestor gas) at the bottom of the filter. The intermittent nature of the gas discharge from the gun assists in the separation of the solids from the liquid. A different design of the plates, such as inclined plates, could further improve the solid-liquid separation mechanism.

(b) Plate media have a low volume compared to stone or clinker media. Thus, for the same concentration of micro-organisms in the mixed liquor of a fixed <u>total</u> volume of reactor, the plate media reactor is able to retain a higher <u>mass</u> of micro-organism than the stone and clinker media reactors. Since treatment performance is dependent on the mass of micro-organisms, the plate media should give a higher performance in terms of total volume of reactor, providing sufficient mass of micro-organisms can be retained.

Comparison of the Filters with Other Systems

Comparisons between the filters of this project and other types of reactors should be made on the basis of COD loading rates per unit total volume of reactor. In this way, the total volumetric capacities of the reactors are compared. Furthermore, when comparing the contact system with the filters (as a system), due account must be taken of the volumetric capacity of the sedimentation tanks required in the contact system.

The maximum permissible loading rates which the stone, clinker and plate-sand filters were able to sustain, before showing signs of failure, were respectively 5,9; 8,6; and 6,0 kg/day/m^3 (Figure 21). In practice, full-scale processes are usually operated well below their maximum permissible loading rates. A safe loading rate for the filters would be about 2 kg/day/m^3, which gives a 'factor of safety' of about 3[13]. All three filters, when operated at this loading rate, gave treatment efficiencies of approximately 98,5%, and delivered effluent total COD's and suspended solids concentrations of approximately 1500 mg/l and 700 mg/l respectively (Figures 21 and 22).

These results can now be compared with:

(a) a full-scale anaerobic contact process treating spent wine at 35°C, as operated by the CSIR (see Part B)[1].

(b) laboratory scale filters treating synthetic wastes at 25°C, as operated by McCarty and Young (see Part C)[2]. (Reports on filters operated at 35°C are not available.)

(a) Contact Process Treating Spent Wine

The suggested maximum loading rate consistent with stable field operation, for the full-scale contact process treating spent wine at 35°C, was 3,1 kg/day/m^3 of reactor, or 2,0 kg/day/m^3 of reactor and sedimentation tank volume[1]. The latter value is approximately the same as the maximum loading on the filters, assuming a factor of safety of 3.

In calculating the treatment efficiency for the full-scale contact process, it was assumed that the reported COD in the effluent was the soluble fraction only. The treatment efficiency thus calculated (for a loading rate of 2 kg/day/m^3) is virtually identical to that of the anaerobic filters, i.e. 98,5% COD removals.

A comparison is not possible between the total COD's in the effluents, since the suspended solids concentrations in the effluent from the contact process were not reported. The report indicates that no solids were purposely wasted from the process[1]. If one therefore accepts the assumption that the treatment efficiencies (based on soluble COD) of the filter and contact system are itentical, it may be concluded that the solids concentration in the effluents from the two systems was of the same order.

Thus, for stable process operation, the anaerobic contact and filter systems appear to offer almost identical treatment efficiencies and loading capacities.

(b) Anaerobic Filters Treating Synthetic Wastes

The anaerobic filters operated by Young and McCarty treated a relatively low strength synthetic waste (COD between 1500 and 6000 mg/l) at 25°C, under plug-flow conditions[2]. The maximum loading rates, at which the process showed an excessive washout of organisms and a deterioration in process performance, was found to be 3,4 kg/day/m^3. In comparing this loading rate with the maximum permissible loading capacity of filters treating spent wine, it should be remembered that process performance is significantly increased by raising the temperature from 25°C to 35°C - it is usually assumed that the loading capacity is doubled for a 10 deg C rise in temperature. Thus for operation at 35°C, the maximum loading rates for the filters operated by Young and McCarty would be of the same magnitude as those operated in this thesis (i.e. 5,9 to 8,6 kg/day/m^3).

Reported treatment efficiencies for the Young and McCarty filters varied between about 70% COD removal (at maximum loading rate) to 98,5% removals at low loading rates of 0,43 kg/day/m^3). These

treatment efficiencies are lower than those obtained from the filters operated in this thesis (Figure 15). The cause for this difference in treatment efficiency can probably be attributed to the low temperature of operation of the reported filters, and also to the fact that the reported filters were treating a relatively low-strength waste.

Reported total COD values in the effluents from the filters operated by Young and McCarty varied between about 100 mg/l at low loading rates, to 1000 mg/l at maximum permissible loading rates. These effluent total COD's are considerably better than those from the filters operated in this thesis, since the effluents from the reported filters (Young and McCarty) contained low solids concentrations (generally less than 100 mg COD/l). The reason for the low solids concentration in the reported filters is probably due to the fact that recirculation of filter contents was not employed.

Anaerobic filter systems treating low and high-strength wastes must necessarily operate under different flow regimes (i.e. plug and completely mixed, respectively) and for economic reasons at different temperatures (i.e. 25^{o} and $35^{o}C$ respectively). As a consequence, treatment characteristics and effluent qualities also differ. However, the anaerobic filter appears to be equally suited to both low and high-strength wastes.

2. Kinetic Model and Applications

Fundamental Growth Kinetics[13][22][23]

The growth of micro-organisms is usually limited by some nutrient requirement for synthesis. For micro-organisms growing from a wine distillery waste, the limiting nutrient may be assumed to be the carbonaceous energy available to the organisms, measured as biodegradable COD. Nitrogen, phosphorous and micro-nutrients are present in relative abundance (see Part B).

The growth kinetics of micro-organisms from the above limiting substrate is based on four fundamental considerations:

(a) The utilization of substrate energy by micro-organisms for synthesis is inefficient, so that only a fraction of the substrate utilized is converted to micro-organisms. This fraction remains constant.

(b) Micro-organisms decay at a constant specific rate.

(c) A constant proportion of the energy in decaying organisms is again made available as substrate for the surviving organisms.

(d) The rate of substrate utilization per unit concentration of micro-organisms is a function of the remaining substrate concentration only.

These four principles describe, at any stage of micro-organism growth, the distribution of the energy originally present in the substrate into (i) the energy bound up in micro-organisms; (ii) energy remaining in the substrate, and (iii) energy lost from the system due to inefficiencies.

Formulation of these four principles follows:

(a) Yield of micro-organisms: Since micro-organisms are inefficient in their utilization of substrate energy, only a fraction of the energy is converted to new organisms, i.e.

$$dX' = -Y\,dS \qquad \ldots(1)$$

where dX' = change in the concentration of micro-organisms due to growth

dS = change in concentration of unmetabolized substrate

Y = micro-organisms synthesized (as COD) per unit COD of substrate utilized - a constant value.

Since the fraction Y of the substrate utilized reappears as micro-organisms, only the fraction (1 - Y) is in fact stabilized, or made unavailable to micro-organisms for further use. The stabilized fraction of the substrate is lost from the system as a consequence of (a) the inherent inefficiencies of all conversions, (b) providing irrecoverable heat or mechanical energy for the micro-organism, and (c) conversion to high-energy waste products, such as methane, which are released from the aquatic system.

(b) Micro-organism decay: The rate of change in the concentration of micro-organisms due to a constant endogenous respiration rate of decay is proportional to the concentration, i.e.

$$\frac{dX''}{dt} = - b X_a \qquad ...(2)$$

where dX''/dt = rate of change in the concentration of micro-organisms due to endogenous respiration decay.

X_a = concentration of micro-organisms

b = endogenous respiration decay constant for micro-organisms.

(c) Unbiodegradable fraction of micro-organisms: A constant fraction of the decaying organism is again utilized as a substrate source, while the remaining fraction remains unbiodegradable (termed the the endogenous residue), i.e.

$$\frac{dX_e}{dt} = - f \frac{dX''}{dt} \qquad ...(3)$$

where dX_e/dt = rate of change in the concentration of endogenous residue

f = fraction of decayed organisms which remains unbiodegradable

By substituting equation (2) into (3)

$$\frac{dX_e}{dt} = f b X_a \qquad ...(4)$$

(d) Rate of substrate utilization: The rate of substrate utilization per unit concentration of micro-organisms is a function of the substrate only, and was shown by Monod[24] to be approximated by:

$$\frac{dS}{dt}/X_a = \frac{- K_m S}{K_s + S} \qquad ...(5)$$

where K_m = maximum substrate utilization rate, i.e. when S is large

K_s = substrate concentration where substrate utilization rate equals $\frac{1}{2} K_m$.

Net change in the concentration of micro-organisms due to both growth and decay is given by the addition of equations (1) and (2) i.e.

$$\frac{dX_a}{dt} = -Y \frac{dS}{dt} - b X_a \qquad ...(6)$$

where dX_a/dt is the net change in the concentration of micro-organisms due to both growth and decay. Substitution of equation (5) into the above yields

$$\frac{\frac{dX_a}{dt}}{X_a} = Y \frac{K_m S}{K_s + S} - b \qquad ...(7)$$

A complete distribution of the utilized substrate energy may be obtained from the equations developed above. The fractions of utilized substrate bound up with micro-organisms and endogenous residue are given respectively by equations (7) and (4), while the fraction lost due to inefficiency is given by the remainder of the utilized substrate.

Process Kinetic Model[25][26]

The above growth kinetic equations become useful when applied to a specific biological process. An anaerobic filter with high recycle rate can be approximated by a completely mixed process with solids retention; diagrammatically shown in Figure 23. Although the micro-organisms have a more or less fixed position in the filter, the reactor is completely mixed in the sense that the substrate concentration remains virtually uniform in the whole filter.

The kinetic model of the completely-mixed-solids-retention process (Figure 23) will be used to derive relationships between concentrations of influent substrate, micro-organisms in the reactor and effluent, unmetabolized substrate, and substrate lost due to inefficiency.

Equations describing the growth of organisms from substrate for the process shown in Figure 23, may be derived from mass balance expressions. The net rate of change in micro-organism concentration and net rate of change in endogenous residue concentration in the reactor is given by:

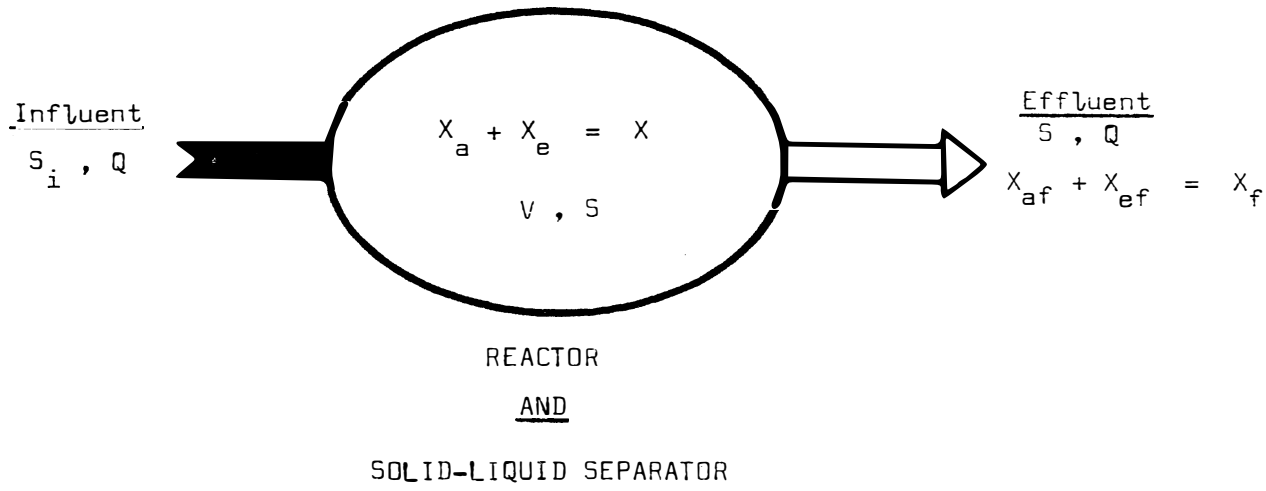

FIGURE 23: Schematic Representation of a Combined Completely Mixed Reactor and Solid-Liquid Separator (e.g. an Anaerobic Filter)

$$\left(\frac{dX_a}{dt}\right) V = \left(-Y \frac{dS}{dt} - b X_a\right) V - X_{af} Q \qquad \ldots(8)$$

$$\left(\frac{dX_e}{dt}\right) V = (f b X_a) V - X_{ef} Q \qquad \ldots(9)$$

where V = volume of the reactor

Q = flow rate through the reactor

X_a = concentration of organisms in the reactor

S = concentration of substrate in the reactor and effluent stream

X_{af} = concentration of organisms in the effluent stream

X_{ef} = concentration of endogenous residue in the effluent stream

Under steady state conditions of operation there are no changes in the above two concentration, i.e.

$$\frac{dX_a}{dt} = 0 \qquad \text{and} \qquad \frac{dX_e}{dt} = 0$$

Equations (8) and (9) can therefore be rewritten as:

$$-Y \frac{dS}{dt} V - b X_a V = X_{af} Q = \left(\frac{dX_a}{dt}\right)_p V \qquad \ldots(10)$$

$$f b X_a V = X_{ef} Q = \left(\frac{dX_e}{dt}\right)_p V \qquad \ldots(11)$$

where $(dX_a/dt)_p$ and $(dX_e/dt)_p$ are respectively the rates of production of the micro-organism concentration and endogenous residue concentration in the reactor. (These production rates are equivalent to the rates of wastage from the reactor.)

Definition of two important parameters, namely hydraulic retention time and solids retention time, simplify the understanding of steady state equations considerably. Hydraulic retention time R is defined as the average time a liquid (such as substrate) is retained in the reactor, and is given by:

$$R = V/Q \qquad \ldots(12)$$

Similarly, solids retention time is defined as the average time any solid (such as micro-organisms) is retained in the reactor, and is given by the total quantity of solids in the reactor divided by the rate at which they are produced or wasted, i.e.

$$R_s = \frac{X_a V}{(dX_a/dt)_p V} = \frac{X_e V}{(dX_e/dt)_p V} \qquad \ldots(13)$$

The solids retention time assumes that all the solids in a reactor (such as micro-organisms and endogenous residue) are retained for the same period.

By using the solids retention time parameter, the concentration of micro-organism in the reactor may simply be derived from equation (10), i.e.

$$X_a = \frac{Y\,(dS/dt)\,R_s}{1 + b\,R_s} \qquad \ldots(14)$$

Under steady state conditions the average rate of change of substrate is given by the substrate utilized divided by its retention time, i.e.

$$\frac{dS}{dt} = \frac{(S_i - S)}{R} \qquad \ldots(15)$$

and therefore, equation (14) may be rewritten as:

$$X_a = \frac{Y\,(S_i - S)}{1 + b\,R_s} \cdot \frac{R_s}{R} \qquad \ldots(16)$$

The concentration of unbiodegradable decayed organisms may be given also as a function of the solids retention time by substituting equation (13) into (11), i.e.

$$X_e = f\,b\,X_a\,R_s \qquad \ldots(17)$$

In practice, micro-organisms and endogenous residue are usually measured together as the volatile suspended solid material, i.e.

$$X = X_a + X_e \qquad \ldots(18)$$

where X is the volatile suspended solid concentration in the reactor.

In this discussion the units of the volatile material and substrate are identical, both expressed as mg COD/l.

As can be seen from equation (18), the model does not take into account the volatile suspended solids of the influent. This simplification seems justified since the volatile suspended solids of spent wine are virtually completely biodegradable (see Part B). The exact fraction of unbiodegradable volatile solids in spent wine was not measured. To obtain an approximation of the error in X introduced by the above assumption, it is necessary to determine how influent unbiodegradable solids accumulate in a reactor. This is done by considering the solids retention time as applied to this fraction of the solids, i.e.

$$R_s = \frac{X_u V}{X_{ui} Q}$$

where X_{ui} = unbiodegradable concentration of solids in the influent

X_u = unbiodegradable concentration of solids in a reactor arising from X_{ui}

The above equation may be rewritten as:

$$X_u = X_{ui} \cdot \frac{R_s}{R} \qquad \ldots(19)$$

The magnitude of X_u which can be expected in the filters described in this thesis is calculated later.

Concentration of volatile suspended solids in the effluent, X_f, is derived by considering equations (13) and (10) or (11), i.e.

$$R_s = \frac{X_a V}{X_{af} Q} = \frac{X_e V}{X_{ef} Q} = \frac{X V}{X_f Q}$$

or $$X_f = \frac{X R}{R_s} \qquad \ldots(20)$$

This equation is valid for the system in which solids are wasted in the effluent stream only. The composition of X_f remains the same as that of X in the reactor.

Unmetabolized substrate concentration in the reactor, and therefore effluent, is derived from equations (5), (10) and (13), and is shown to be a function of micro-organism or solids retention time only, i.e.

$$1/R_s = Y \frac{K_m S}{K_s + S} - b \qquad ...(21)$$

Breakdown of influent substrate into unmetabolized substrate, micro-organisms, unbiodegradable decayed organisms, and substrate lost due to inefficiency may be traced with the equations developed above. Diagrammatic representations of the substrate breakdown will be shown later. However, if the above equations are to be used, prior knowledge is required of the five constants Y, b, K_m, K_s and f, and the hydraulic and solids retention times. The unbiodegradable fraction, f, of most micro-organisms (aerobic and anaerobic) has been reported to be about 20% by mass[27][29]. This value is used throughout subsequent calculations.

Experimental Approximation of Growth Constants

Suitable values for the constants Y, b, K_s and K_m were chosen by inspecting reported value[13], and by applying the above kinetic model to the experimental results obtained from steady state operation of the filters (see Part F). A comparison of the experimental results with the theoretical results (derived with assumed values for the constants), was made as follows:

(a) Measured influent total COD and effluent soluble COD concentrations were corrected by subtracting the unbiodegradable fraction of COD from them (1,5% of the original COD - see Part B).

(b) Solids retention time R_s was calculated from the corrected effluent substrate concentration S by using equation (21).

(c) Solids concentrations X_a and X_e in the reactor were calculated from equations (16) and (17) respectively, using the measured values of R, S_i and S, and values of R_s calculated in (b) above.

(d) Volatile suspended solids concentration in the effluent X_f was finally calculated from equations (18) and (20).

(e) Volatile suspended solid concentrations in the effluent were measured in mg/l, and converted to mg COD/l by assuming 1 mg of volatile suspended solids to have a COD of 1,4 mg[29]. Also, the difference between measured total and soluble COD in the effluent (which is the COD of the suspended solids) may be used for comparison with the calculated values. (It is interesting to note that the COD equivalent of the volatile suspended solids found in this investigation for Filters No. 1 and 2 is 1,48 mg COD/mg of solids. This compares favourably with the theoretical average COD value of 1,42 mg VSS found by Eckenfelder and Weston[29].)

Calculated and measured values of volatile suspended solids concentrations in the effluent, X_f, were compared at each loading rate for the three filters. Table IV lists measured and calculated data for the following assumed values of the constants:

Y = 0,06 mg/mg as COD

b = 0,015 $days^{-1}$

K_m = 4,0 $days^{-1}$

K_s = 1000 mg/l as COD

Discrepancies between measured and calculated results may have arisen from:

(a) experimental errors in the measurement of COD and VSS.

(b) True steady state operation not being achieved - excessively long periods are required to reach steady state at long solids retention times.

(c) Temporary short-circuiting and channelling of flow giving rise to unstable conditions.

(d) The inaccurate assumption that volatile suspended solids is a measure of X_a and X_e only. In the filters, the maximum solids concentration arising from the accumulation of unbiodegradable solids in the influent (X_{ui}), may be calculated as follows: With a typical ratio of the solids

TABLE IV

Comparison of effluent volatile suspended solids concentration, as measured from the three filters, with the values calculated from the steady-state kinetic model.

TEST NO.	MEASURED VALUES					CALCULATED VALUES				
	S_i mg COD/l	S mg COD/l	R days	X_f mg COD/l	Total COD-Soluble COD mg COD/l*	X_f mg COD/l	X mg COD/l	X_a mg COD/l	X_e mg COD/l	R_s days
FILTER No. 1										
2	22 950	418	6,97	1079	1075	1119	2865	2719	146	17,85
3	22 950	514	3,61	1261	1055	1415	5941	5683	258	15,15
4	22 950	1018	2,43	1766	1771	1468	5698	5541	157	9,43
5	22 950	4048	2,12	1163	1214	1588	3902	3842	60	5,21
FILTER No. 2										
3	28 170	376	3,72	1579	1528	1059	5695	5373	322	20,0
4	28 170	523	2,85	1509	1611	1413	7407	7089	318	14,93
5	28 170	1008	1,94	2392	2561	1466	7195	6995	200	9,52
6	28 170	5570	1,75	1163	2164	1502	4565	4494	72	5,32
FILTER No. 3										
2	32 160	169	10,10	724	167	893	4421	3844	577	50,0
3	32 160	189	5,06	873	365	1150	9885	8744	1141	43,48
4	32 160	496	3,89	634	641	1412	5586	5339	247	15,39
5	32 160	5580	2,72	1509	442	1501	2920	2874	46	5,29

* (Total COD-Soluble COD) = Suspended solids COD $\doteq X_f$

Diagrammatic Representation of Model

Behaviour of anaerobic filters or similar systems treating spent wine may be followed on Figure 24. Unmetabolized substrate concentration in the reactor (or effluent) is plotted against the solids retention time according to equation (21). Several important characteristics of the process become clear immediately.

(a) A minimum solids retention time of 4,8 days is required if any substrate is to be utilized. For retention times less than this value, complete failure of the process is due to micro-organisms being washed out of the reactor at a faster rate than the rate at which they are being synthesized.

The minimum solids retention time may be calculated by setting $S = S_i$ in equation (21), i.e.

$$1/R_s = Y \frac{K_m S_i}{K_s + S_i} - b$$

For a process treating spent wine, $S_i >> K_s$, and the above equation is approximated to

$$R_s = \frac{1}{Y K_m - b}$$

With the assumed kinetic constants of $Y = 0,06$; $K_m = 4,0$ days^{-1} and $b = 0,015$ days^{-1}, the approximate value of R_s (for $S_i >> K_s$) is calculated from the above equation, i.e.

$$R_s = 4,5 \text{ days}$$

(b) Substrate utilization in the process (i.e. the treatment efficiency) deteriorates rapidly below a solids retention time of 7 days.

(c) Effluent quality from the process does not improve significantly for solids retention times greater than 9 days.

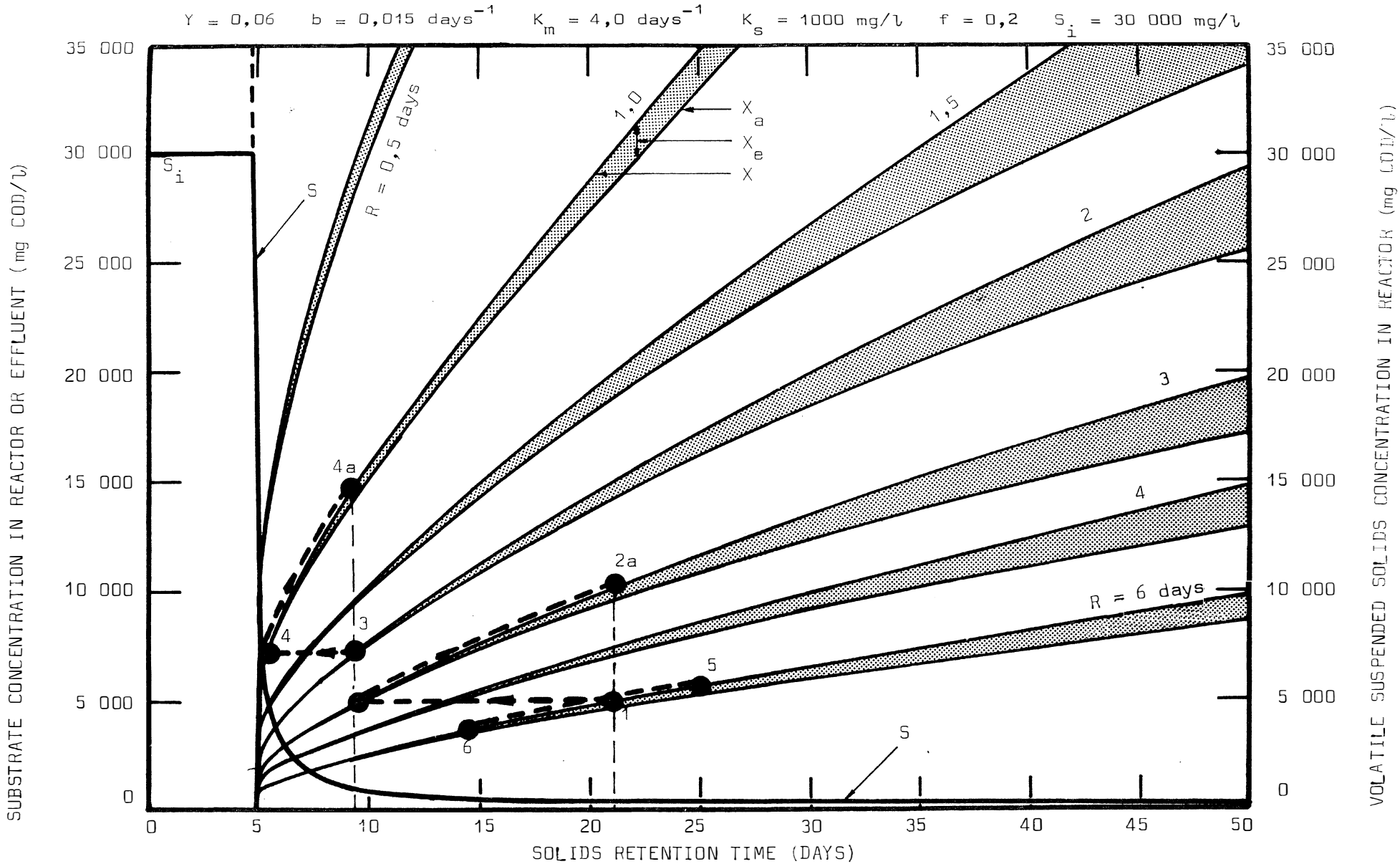

FIGURE 24: Representation of the Steady State Kinetic Model Showing the Variations in Substrate Concentrations and Volatile Suspended Solids Concentrations for Different Solids and Hydraulic Retention Times. Effect of Shock Loads and Sludge Wastage on Process Performance is Also Shown

(d) The slope of the substrate utilization versus solids retention time curve gives a good indication of the stability of the process. For retention times longer than 9 days, a nearly horizontal slope indicates stable conditions. Below this retention time, the sharply increasing slope is indicative of an increasing instability in the process.

The instability of the process is characterized by the production of toxins (pH and acetic acid) from an unbalanced population of micro-organisms. The toxins cause the process to deteroriate rapidly, with eventual failure resulting. A discussion of the mechanism of failure is found in Chapter II of this thesis.

The concentrations of solids X_a, X_e, and their total, X (for different loading rates) may also be represented on the diagram by using equations (16), (17), and (18). In drawing the curves, influent substrate concentration was assumed to be constant at 30 000 mg/l COD, and loading rates were altered by altering the hydraulic retention time in the reactor. The solids concentration required by any loading rate for any effluent quality (established by the solids retention time), may be read off directly from Figure 24.

The graphical representation of the model on Figure 24 is usefully applied to explain some of the behavioural characteristics of the anaerobic filters operated in this thesis.

Treatment Efficiency

Deterioration of the treatment efficiency (measured as soluble COD) with decreasing hydraulic retention times may be followed for Filters No. 1 and 2 on Figure 18. The shape of the curve may be qualitatively compared to the curve of unmetabolized substrate versus solids retention time for the model (Figure 24), by assuming the following approximations:

(a) The solids retention time is governed mainly by the hydraulic retention time. This approximation seems justified by considering equation (20), i.e.

$$R_s = \frac{X}{X_f} \cdot R$$

and by examining the measured values of X_f and R, and the calculated value of X (Table IV). Of the three variables, hydraulic retention time, R, is seen to have the most influence on the solids retention time, R_s. Thus, solids and hydraulic retention times may be used interchangeably for the purpose of qualitative comparisons.

(b) Adjustment of the soluble COD measurements of the effluent to unbiodegradable COD concentrations does not alter the shape of the curve significantly.

Although a quantitative comparison between the theoretical and experimental results is not possible, the shape of the curves is similar, and thus general behavioural trends may be compared.

The unstable conditions which are identified with the steep slope of the curve at short hydraulic retention times are characterized in the highest loading rates on the filters (Figure 18). During this period (see Figures 9, 10 and 11), volatile fatty acids increased sharply, and pH, percentage CH_4 and gas production tended to decrease. This conforms to the operating characteristics predicted by the model at short solids retention times (Figure 24).

At long hydraulic retention times, the substrate concentration from the filters remained essentially constant (Figure 18) and process operation was stable, (Figures 9, 10 and 11). This also is consistent with the trend exhibited by the model at long solids retention times (Figure 24).

Shock Loads

The diagrammatic representation of the model in Figure 24 is extremely useful for determining the stability of the process against shock increases of the loading rate. Operation of the filters during periods of shock loading rates may be followed below:

First consider the reaction of the filters when shock loads were applied at low loading rates. A hydraulic retention time of 6 days and an effluent containing 350 mg/l of unmetabolized substrate and 1350 mg/l of volatile suspended solids was typical of these low loading

rates. This corresponds to a solids retention time of 22,5 days and a solids concentration of 5000 mg/l in the reactor (point (1) in Figure 24). The instantaneous effect of doubling the load, by halving the hydraulic retention time, leaves the solids concentration in the reactor unchanged. As a consequence, the process operates as if the solids retention time had been reduced to 9,5 days (point 2).

Unmetabolized substrate concentration in the effluent is increased only slightly to 1000 mg/l, so that the methane production from the process must necessarily double. The process should show no adverse effects to the shock load, since it is still in the stable region of operation. These behavioural characteristics may be verified by referring to the step-increases of the loads at low loading rates for all three filters (Figures 9, 10 and 11). The hypothetical conditions described by point 2 are unstable, but given enough time, a new equilibrium point will be established depending on the solids retention efficiency of the system. If solids are retained with an efficiency equal to that of before the load increase, the solids retention time will return to 22,5 days and the solids concentration in the reactor will double (point 2a).

Now consider the reaction of the filters when shock loads were applied at the high loading rates. A hydraulic retention time of 2 days and an effluent containing 1000 mg/l of substrate and 2000 mg/l of volatile suspended solids was typical of these loading rates. This corresponds to a solids retention time of 9,5 days, and a solids concentration of 7,440 mg/l in the reactor (point 3). Doubling the load has the equivalent effect of reducing the solids retention time to 5,5 days (point 4). Substrate concentration increases to 5000 mg/l, and the process becomes unstable as indicated by the steep slope of the substrate curve. The instability of the process and the increase in the unmetabolized substrate may be verified by referring to the operation of the filters after the last step-increase in load (Figures 9, 10 and 11). Changes in the volatile fatty acid concentration, pH, percentage CH_4 and gas production all indicated that the process was under stress.

If the process overcomes its instability, and if solids are retained with unchanged efficiency, the equilibrium conditions of the process will eventually be given by point 4a, i.e. a doubling of the solids concentration in the reactor at unchanged solids retention times.

From the above examples, it becomes clear that long solids retention times offer a buffer against shock loads. This is important in anaerobic processes, since processes overloaded to instability will fail of their own accord due to the toxins (pH and volatile fatty acids) which the micro-organisms produce.

Solids Concentration in the Reactor

Solids concentrations in the filters could not be measured, so that in this respect no comparison with the model was possible. However, it is useful to follow the changes in the volatile solids concentrations which occur for changes in (a) loading rates and (b) solids retention times, on the diagrammatic representation of the model (Figure 24).

(a) For the same influent and effluent substrate concentration (or solids retention time), the solids concentrations X_a and X_e in the reactor increase linearly with increasing hydraulic load. This is clearly demonstrated by equations (16) and (17):

For a constant solids retention time,

$$X_a \alpha \frac{(S_i - S)}{R} \qquad ...(22)$$

i.e. the concentration of active micro-organisms is directly proportional to the substrate utilization rate. Since the effluent quality for one solids retention time remains unchanged, micro-organism concentration is inversely proportional to the hydraulic retention time (for a constant S_i), i.e.

$$X_a \alpha 1/R \qquad ...(23)$$

The unbiodegradable fraction of decayed organisms is directly proportional to the active micro-organism concentration (for constant solids retention time), and is thus also inversely proportional to the hydraulic retention time. Thus, for a constant volume reactor ($R = V/Q$), both X_a and X_e are directly proportional to the hydraulic flow rate.

(b) From Figure 24, the solids concentration are seen to decrease non-linearly with decreasing solids retention times. At minimum solids retention time, the concentration is zero since the washout rate of the micro-organisms is faster than the production rate.

It is evident that for practical considerations such as mixing and general handling of the solids, a reactor is limited to a maximum concentration of solids. Therefore, indefinitely increasing the load on a reactor, while keeping the solids concentration constant at the maximum permissible concentration, has the effect of reducing the solids retention time. As a consequence, the effluent quality and stability of the process are reduced. Eventual failure results when the solids retention time approaches the critical minimum retention time (Figure 24).

Solids Concentration in the Effluent

Volatile suspended solid concentration in the effluent is an important parameter controlling the solids retention time in the filter, and thus the process behaviour. The model is best applied to this aspect of process control by referring to a diagrammatic representation of the effluent solids concentrations X_{af}, X_{ef} and X_f versus solids retention time (Figure 25). (The influent COD is again assumed constant at 30 000 mg/l.) Two points of interest arise from the diagram:

(a) For a constant COD concentration in the influent and a constant solids retention time, solids concentration in the effluent does not vary with hydraulic retention time, and therefore loading rate. This may be shown by considering equations (23) and (20) together, i.e.

$$X_a \alpha 1/R \quad ; \quad X_e \alpha 1/R \qquad \ldots(23)$$

and

$$X_{af} = \frac{X_a R}{R_s} \quad ; \quad X_{ef} = \frac{X_e R}{R_s} \qquad \ldots(20)$$

It is obvious that for a constant solids retention time, a combination of the above two equations give:

$$X_{af} = \text{constant} \quad \text{and} \quad X_{ef} = \text{constant}$$

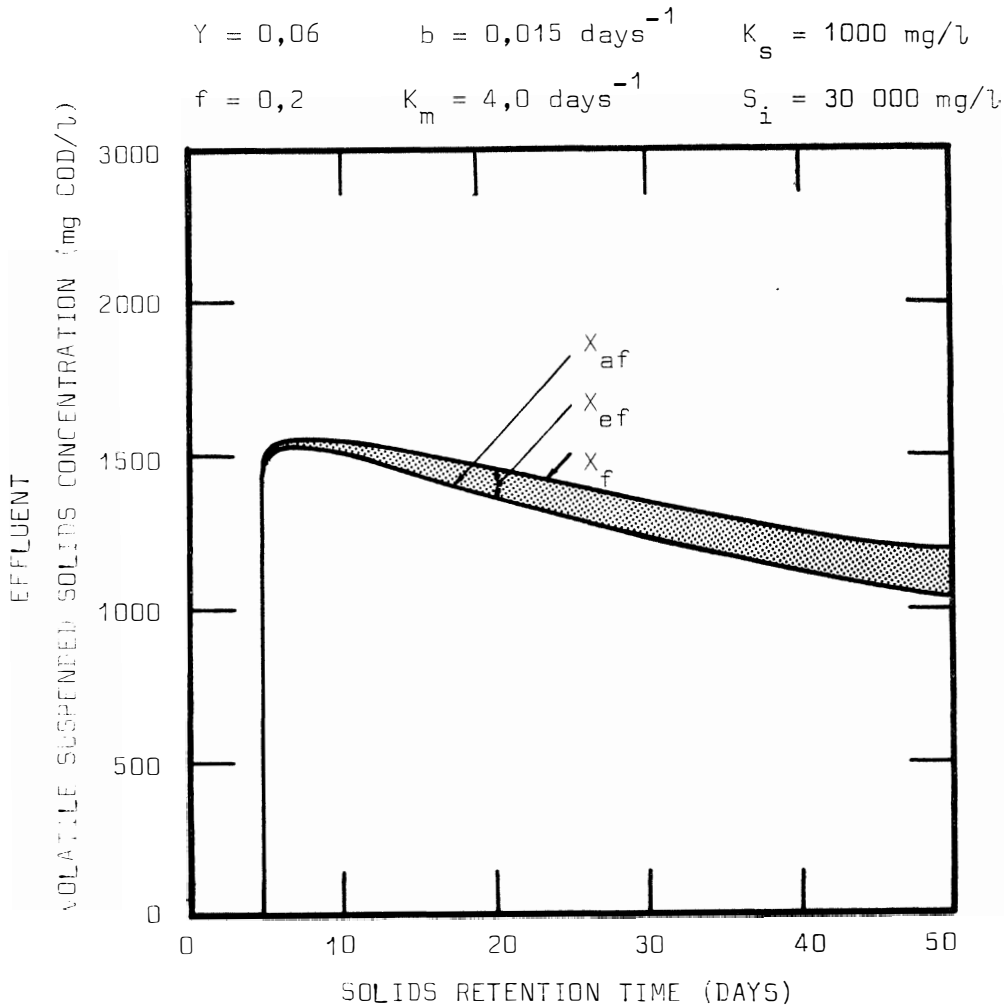

FIGURE 25: Representation of Steady-State Kinetic Model Showing the Variations in Volatile Suspended Solids Concentrations in the Effluent at Different Solids Retention Times (Valid for Any Hydraulic Retention Time)

An anaerobic filter process with a certain treatment efficiency (or unmetabolized substrate concentration) must therefore have an associated constant effluent volatile solids concentration. (The mass of solids wasted will increase in direct proportion to the waste flow.)

(b) Effluent suspended solids concentrations are not altered appreciably by varying the solids retention time, except at very low solids retention times.

These two points show the importance of controlling the suspended solids concentration in the effluent; even small increases in the effluent suspended solids concentration may significantly reduce the solids retention time (Figure 25), and therefore the performance of the filter. For example: An effluent volatile suspended solid concentration of 1400 mg/l fixed the solids retention time at 25 days which implies good process performance (Figure 24). If the solids concentration increases to 1550 mg/l (a 10% increase only), the solids retention time is reduced to 10 days or below, which implies unstable process operation and impending failure due to pH and acetic acid toxicity. Large increases in the solids concentration in the effluent are indicative of excessively high micro-organism washout rates. Rapid failure is the result of the rapidly diminishing micro-organism concentration in the reactor being unable to cope with the treatment of the waste flow. In an anaerobic system discharging solids in the effluent only, increase in the solids concentration in the effluent will probably give the first indication of a potential deterioration in the process.

Results of the effluent volatile suspended solids concentrations from Filters No. 1 and 2 (Figure 19) may be compared with theoretical results of the model (Figure 25), by again assuming that the solids retention time is dependent largely on the hydraulic retention time (page 77). Although a quantitative comparison is not possible, the results appear to follow similar trends.

Effluent Quality

Total biodegradable COD is a convenient measure of the overall effluent quality, since it includes both the soluble and suspended solid fractions of the COD. The effluent quality from an anaerobic filter does not improve significantly with increases in the solids retention time beyond a retention time of about 9 days:

(a) Figure 24 indicates that only small reductions are achieved in the effluent COD by increasing the solids retention time beyond 9 days.

(b) Figure 25 indicates that the effluent solids concentrations are not appreciably altered between the normal operating limits of 10 and 40 days of solids retention.

Thus, from an effluent quality point of view, there is no advantage in maintaining very long solids retention times.

Conclusions

Conclusions which may be drawn from the behaviour of the anaerobic filter treating spent wine and its kinetic model may be summarized as follows:

(a) Unmetabolized substrate concentration in the effluent is not significantly reduced for solids retention times greater than 9 days. If a shock load does not decrease the equivalent solids retention time to below 9 days, the treatment efficiency of the process remains virtually unchanged, and the methane production from the process must accordingly increase.

(b) Solids retention times below 7 days should be avoided since operation of the process is irregular, and complete failure could easily result. This applies also to equivalent solids retention times after shock increases in load.

(c) The main advantage of a long retention time is in the stability it lends to the process during increases in the loading rates. This advantage is possibly extended to changes in other environmental conditions such as temperature.

(d) Solids concentrations in the reactor increase both with increasing loading rates and solids retention times. A limitation on the maximum possible solids concentration in a process limits the solids retention time and maximum load capacity of the process.

(e) Volatile suspended solids concentrations in the effluent are not affected by changes in the hydraulic retention time (provided the influent COD concentration remains constant), and are only slightly affected by changes in the solids retention time.

(f) Increases in suspended solids concentration in the effluent, however small, are indicative of significant reductions in the solids retention time and therefore process performance. Significant increases are a sign of impending failure.

The six points listed above form the fundamental qualitative criteria for the design and operation of any anaerobic system. Solids retention time features prominently as the fundamental control parameter which governs the process.

Failure of the anaerobic filters was caused by the solids retention time approaching the critical micro-organism washout retention time. Reductions in the solids retention times were due to the concomitant increase in the solids concentration washout rates with reduced hydraulic retention times (Figure 19). This emphasizes that the major drawback of the filter system is the fact that no positive external control, independent of hydraulic retention time, can be kept over the solids retention time. Reductions in recirculation rates could increase the solids retention capacity of anaerobic filters, but this is undesirable since it would decrease the mixing efficiency.

An ideal anaerobic system would require a completely independent control over the solids retention time. The final treatment capacity of this ideal system would be limited only when the concentration of micro-organisms in the process became unmanageably high.

Substrate Removal in Aerobic and Anaerobic Processes

Besides describing the behaviour of anaerobic systems, the kinetic model finds an interesting application for the comparison of the pathways of carbonaceous substrate reduction employed by anaerobic and aerobic processes[25]. For this purpose, the distribution of substrate utilized versus solids retention time is diagrammatically represented on Figure 26 for both aerobic and anaerobic systems.

The proportion of utilized substrate wasted in the micro-organisms and endogenous residue is given by equations (16), (17) and (20) respectively. Yield constants and decay rate constants for the anaerobic treatment of spent wine are taken respectively as 0,06 mg COD/mg COD and 0,015 days^{-1}. No information on the aerobic treatment of spent wine is available, but a yield constant of 0,5 mg COD/mg COD (0,35 mg VSS/mg COD) and a decay rate constant of 0,15 days^{-1} is typical of an aerobic process[13][22]. In the anaerobic process, experimental results (Table III) show that approximately 85% of the utilized substrate is converted to methane and thus lost to the organisms. This gives a yield constant of 0,4 (mg VSS as COD/mg COD) on the 15% of the substrate actually utilized by micro-organisms, which is in agreement with the general efficiency of aerobic micro-organisms.

Since processes are usually operated to give a low effluent substrate concentration, the effluent substrate forms a negligible portion of the total substrate passing through the system and is consequently omitted from the following discussions of substrate distribution.

Figure 26 clearly demonstrates that aerobic processes rely on the inefficiency of micro-organisms for the stabilization of substrate. A considerable proportion of the substrate utilized is merely converted to biological solids which still requires further treatment. In contrast, stabilization in the anaerobic process is achieved mainly by the conversion of substrate to methane. The methane gas is spontaneously separable from the aquatic system, and is easily disposed by burning. Since only the remainder of the substrate is actually available to the micro-organisms, the growth of biological solids is low. The problem of solids disposal is thus minimized. One concludes that stabilization of waste in the anaerobic process is more efficient than in the aerobic process, the difference being particularly noticeable at low solids retention times.

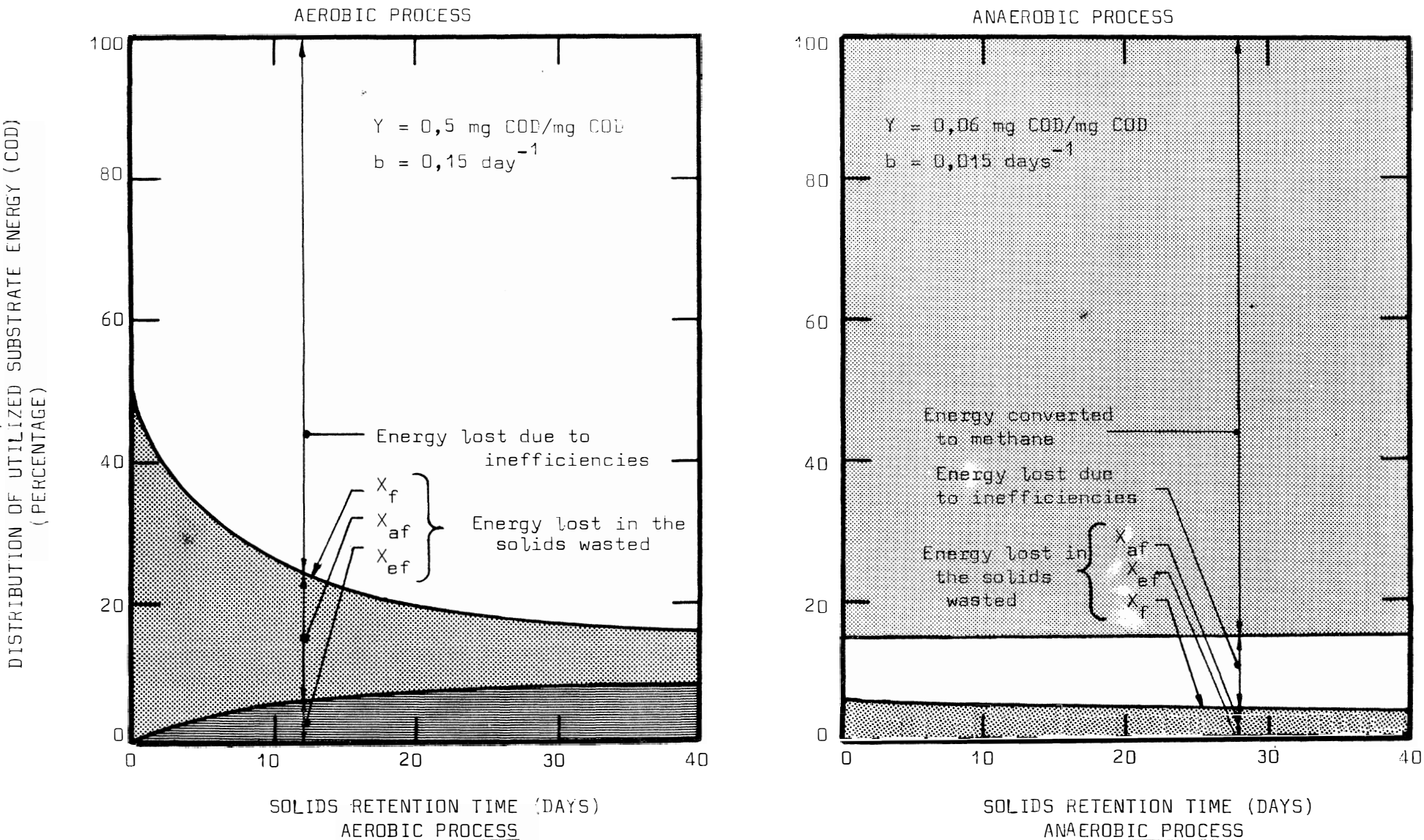

FIGURE 26: Comparison of the Respective Pathways Employed by the Aerobic and Anaerobic Processes in the Stabilization of Carbonaceous Waste Energy

(a) Start-Up

The pH value during start-up is crucial to satisfactory inauguration of the process. At initial start-up the pH has a tendency to decline, and therefore to inhibit the process. Start-up with a pH below 6,5 appeared to be impossible, or to require an inordinately long time. The most rapid start-up was obtained by maintaining the pH at or close to 7,0.

During the first 5 days in the operation of the filters, sodium bicarbonate additions were required to adjust the pH to 7,0. A total of approximately 150 ml of 1 N $NaHCO_3$ was added to each filter during this period, the daily quantity added decreasing each day. During this period, gas production increased gradually (Figures 9, 10 and 11), and after 5 days complete waste stabilization was being achieved.

It should be noted that filters were seeded with a large inoculant of actively digesting sludge from domestic origin and that initial loading rates were low - about 0,8 kg/day/m^3 of total filter volume. Details of start-up are found on page 31. Under the conditions of seeding, loading, temperature and mixing used in these experiments, it is therefore clear that a plant treating spent wine should operate satisfactorily within 1 to 2 weeks. To attain maximum treatment capacity, a longer period would be required with gradually increasing loads. The rate at which the load is increased should be slow enough to ensure that a stable state in the process is maintained at all times (see page 77); a sufficiently high micro-organism concentration is required to prevent the equivalent solids retention time from being reduced to below the recovery level.

If the pH is not controlled at, or near 7,0, grave difficulties may be experienced with start-up operations. Start-up of a similar filter was attempted with the pH maintained at about 6,5. After 3 weeks of operation the process still showed no indication of achieving full waste stabilization; gas production remained near zero, and the volatile fatty acids concentration continued to increase. These conditions indicated complete failure of the process.

The mechanism causing the decline in pH during start-up is not easily identified. However, the following observations and deductions can be made: With the commencement of waste feed (pH 4,5) the pH in the filter showed a sudden decline from 7,0 to below 6,5 (see Figures 9, 10 and 11). Initial gas production was low, indicating incomplete waste stabilization. At this stage, gas evolved from the digestor was composed mainly of methane, which suggested that the CO_2 had dissolved in the water, thereby also reducing the pH. Despite pH adjustment, this phenomenon of pH decline occurred with with decreasing intensity during the first 5 days of operation. Gas production and CO_2 content were at the same time increasing and after 5 days full gas production (with a stable CO_2 content) was achieved (i.e. complete waste stabilization). This coincided with the process being able to maintain a pH of 7,0 of its own accord. The pH decline during this period was not due to the volatile fatty acid concentration, since measurement showed no undue changes in concentration (see Figures 9 and 10). In conclusion, it appears that incomplete waste stabilization is the cause for the decline in pH, and that CO_2 dissolving into the water further depresses the pH.

The fact that the process could maintain a constant pH of 7,0 when operating in a stable regime seemed to indicate that either hydrogen ions were abstracted or hydroxyl ions were generated in the process (to raise the pH of spent wine from 4,5 to 7,0 in a 40% CO_2 atmosphere). This hypothesis merited further investigation, and is quantitatively examined in Chapter II. It is not discussed further at this stage, since it requires lengthy investigations and discussions which deviate from the main objectives of the Chapter.

(b) Loading Rate Fluctuations

The response of Filters No. 1 and 2 during periods of loading rate fluctuations near maximum permissible load capacities may be followed on Figures 9 and 10 during days 90 to 110 and days 97 to 120 respectively. Overloading the metabolic capacities of the micro-organisms with high feeds caused unbalanced activities in the micro-organism population. This inbalance was exhibited

by the accumulation of volatile fatty acids in the processes and by a decrease in the methane productions. Both parameters indicate a breakdown in the sequential steps of substrate conversion to methane (as performed by the micro-organisms).

Since volatile fatty acids and low pH (caused by the volatile fatty acids and incomplete waste stabilization) could have still further retarded the conversion of substrate to methane, the feed was temporarily discontinued after a period of overloading. The process showed rapid recovery (within one day). This was indicated by the sharp decreases in the volatile fatty acids concentrations and the increases in the percentage methane (Figures 9 and 10). With feed rates resumed at lower loading rates, the process behaviour and performance continued normally. This behavioural pattern (for short-term load fluctuations) is consistent with that reported in literature[8], in that a method for the recovery of overloaded processes is to reduce the loading rate. However, it is likely that if the overload is maintained for a long period, the recovery period will also be increased.

The behaviour of a process under overloaded conditions is so intimately related to pH changes, that this aspect also is relegated for a detailed investigation and discussion to Chapter II (Part J).

(c) Temperature Fluctuations

Sudden drops in temperature induced almost immediate retarded activity in the process. Uniform inhibition of the process was indicated, as there was decreased gas production but unchanged pH, volatile fatty acid concentration and percentage methane. Recovery of the process, after the temperature was returned to normal (35^{o}), appeared to be complete in less than one day and no residual effect on the process was noted. This behaviour can be followed in Figures 9 and 10 (days 38 and 47 respectively) for a temperature decline to $22^{o}C$.

The behaviour described above is typical of the response of the anaerobic process to short-term temperature changes[7]. No investigation was made into maintaining the temperature continuously

below 35°C. However, it has been indicated that organisms adapt to temperatures below 35°C, providing the loading rates are adjusted down appropriately - see Part B[1].

Temperature increase from 35°C occurred on several occasions (for example see days 76 and 84 on Figures 9 and 10 respectively). The behaviour of the process showed no response to these short-term fluctuations. This behaviour is to be expected: although increases in temperature induce greater activity[7], the treatment efficiency in the filters was already so high (about 98% biodegradable COD removals), that the slight increase in efficiency would not have been discerned from the experimental data. However, long periods of high temperature will reduce the treatment efficiency due to thermal death of the organisms[1].

General Comment

The steady state model developed in Part 2 of the discussion cannot be applied to the transient responses of processes under start-up operations and during loading rate fluctuations. The behaviour of a process under these conditions may be described by a dynamic model offered by Andrews[11]. The model is based on the same fundamental kinetic principles as the steady state model, but also includes a toxin limiting condition for growth. Acetic acid is assumed to be the nutrient source, and undissociated acetic to be the toxin. This model, however, has not been widely used, mainly because there is a controversy as to whether pH or acetic acid is the toxin which inhibits growth[30][31]. Both models omit the effect of temperature fluctuations. Prediction of process behaviour under conditions of temperature changes is particularly difficult, since micro-organisms undergo a transient period of adaptation after a temperature change.

Operational Behaviour

Behavioural characteristics of the anaerobic filter system treating spent wine include (a) mixing conditions, (b) blockages of voids, (c) reactivation after a dormant period, and (d) process changes due to changes in the composition of spent wine arising from different distilleries.

(a) Mixing Conditions

Completely mixed conditions in the filters were ensured by instituting high recycle rates. Hydraulic flow-through times of about 1,5 hr were employed at all times giving flow rates approximately 35 times higher than the maximum influent flow rates. The high recycle rates ensured that adverse effects (such as low pH at the influent point), which are encountered with plug-flow or partial plug-flow conditions, were eliminated. This investigation did not enquire into the minimum rate of recycle which could be employed before adverse effects became evident.

Completely mixed conditions were verified by measuring pH and volatile fatty acid profiles along the length of the filter. The profiles showed almost no variations: pH varied by not more than one tenth of a pH division, and volatile fatty acid concentrations by not more than 10%.

The necessity of recirculation was demonstrated during periods of recirculation failure: pH at the bottom of the filter (i.e. the influent point) was immediately depressed to below 6,0. It can reasonably be assumed that process failure was initiated at this point and would have gradually spread upwards as the feed moved in a plug flow fashion through the filter.

(b) Blockages of Voids

Partial blockages and consequential channelling of flow was noted in the stone and clinker filters. These situations were identified by feeling the warmth of the filters along the length of the shells during the period when the hot water bath system of heating was being used. Cold patches indicated regions through which the waste was not flowing. The blocked regions did not remain constant, but changed slowly and continuously, probably as a result of the active regions clogging up with biological solids. Despite the gradual changes in the channelling of the flow no undue fluctuations in the performances of the processes were noted. Partial blocking must, however, be a disadvantage, since it implies that the whole volume of the filter is not used efficiently. Predictions cannot be made on the effect which partial blockages will have on the performance of full-scale filters.

The plate section of Filter No. 3 did not exhibit this tendency for blockages.

Total blockage of the flow through the filters occurred occasionally due to (a) a slow build-up of unbiodegradable solids material, (b) the high concentrations of biological solids required for the high loading rates. The interval between blockages depended on the type of media, the solids concentration in the influent, and the loading rate on the filter. The filters were operated over too short a period to determine accurately the time interval between blockages, but the following general impression was formed:

(i) The plate sector of Filter No. 3 did not show any tendency to become blocked, even though it was completely filled with biological solids at the higher loading rates.

(ii) Filter No. 1 with stone media seldom blocked.

(iii) Filter No. 2 with clinker media was more prone to blockages than the stone filter. This was due to the fact that the clinker tended to disintegrate into grit, thus clogging the voids.

(iv) The sand sector of Filter No. 3 operated sucessfully on the effluent from the plate sector provided the solids concentration was low. With high solids concentrations in the plate sector effluent, the sand choked up and ceased to function.

The time interval between blockages in the stone and clinker filters was in the order of about two months.

Blockages in the stone and clinker filters were easily cleared by wasting sludge from the bottom of the filters. The volume of sludge wasted varied, but even volumes of up to one-third the filter capacity did not upset the process at reasonably low loading rates (corresponding to periods of long solids retention times). This effect is similar to the shock increases in load, and may be followed on Figure 24:

Consider a filter operating at a constant hydraulic retention time of 6 days, with an influent COD of 30 000 mg/l, an initial solids concentration in the reactor of 5600 mg/l and a corresponding solids retention time of 25 days (Point 5 on Figure 24). If one-third the mass of micro-organisms is wasted, the solids concentration in the reactor is reduced to 3730 mg/l, so that the solids retention time must instantaneously decrease to an equivalent retention time of 14,5 days (Point 6). The effluent COD does not increase significantly with this reduction in solids retention time, and the process is thus not adversely affected. It should be noted that at low solids retention times failure could result after solids wastage (compare to shock-loads at low solids retention times).

The blockage in the sand sector of Filter No. 3 was cleared by (a) closing the gas outlet from the plate sector, thus forcing all the gas to pass through the sand, and (b) recirculating the effluent from the sand sector to the bottom of the plate sector. Under this system of operation, the sand ceased to operate as an effective method of solid-liquid separation due to the disturbances caused by the gas passing through the sand. It was also observed that liquid tended to short-circuit through one or two paths in the sand.

In conclusion, (i) sand media appears to be undesirable since blockages cannot be cleared effectively; (ii) blockages in the stone and clinker media are easily cleared without upsetting the process performance; (iii) plate media is not prone to blockages.

(c) Reactivation

Reactivation of the anaerobic filter after a dormant period was not a problem. Filters No. 1 and 2 were reactivated after dormant periods of 31 and 45 days respectively by first raising the temperature to 35°C, and then by slowly increasing load over two days. The process showed no signs of stress, and continued to

operate satisfactorily at a loading rate of approximately 4,0 kg/day/m^3 (about half maximum permissible loading rate). A possible reason for the fast rate of reactivation was the fact that the filters were cooled from 35°C and stored at 20°C. Under this temperature reduction biological activity is initially halted[7] and generally low. As there is no food available, the organisms have no opportunity to adjust to the lower temperature, and thus tend to remain dormant. In time, however, micro-organisms will adapt to the low temperature but such an adaptation would probably need an energy source to take place within a reasonable period. As a result, the original population remains virtually intact throughout the dormant period, providing the period is reasonably short. This investigation did not enquire how the length of the dormant period affects reactivation of the process. It seems reasonable that in order to reduce endogenous respiration in a dormant digestor, the reactor must be immediately cooled at the start of the dormant period.

(d) Spent Wine Composition

A peculiarity noted in the treatment of spent wine from different distilleries (Paarl and Stellenbosch) was the difference in gas composition which each yielded during treatment. This did not appear to have any other effect on the process other than adjusting the pH slightly - the pH changes appear to be due to the change in the partial pressure of CO_2. (See 2nd batch of waste - from Paarl - in Figures 9 and 10).

General

During the experimental work conducted for this part of the investigation, Filters Nos. 1, 2 and 3 were operated for a total of 121; 130 and 114 days respectively. Filters No. 1 and 2 were also operated during the experimental work reported in Chapter II for a total of 72 and 57 days respectively. In Chapter II, measurements on the performance of the process were taken for the purpose of investigating pH control in anaerobic digestion, and the results do not contribute to the substance of this Chapter.

CHAPTER II

pH CONTROL IN ANAEROBIC DIGESTION

A. MECHANISM OF ANAEROBIC TREATMENT

The complete anaerobic decomposition of organic matter has traditionally been regarded as a two-step process - an 'acid fermentation' phase, followed by a 'methane formation' phase[32]. Thus, at least two large, physiologically different, bacterial populations must be present for the overall conversion of complex organic matter to methane. In the first stage, a heterogeneous group of micro-organisms hydrolyse and ferment proteins, carbohydrates and lipids to fatty acids, CO_2 and H_2O. In the second stage, the end products from the micro-organisms of the first stage are converted to methane, CO_2 and H_2O by a unique group of strict obligate anaerobic bacteria termed the methanogenic bacteria. A schematic representation of the breakdown of complex organic matter during anaerobic digestion is given in Figure 27.

Knowledge of the microbiology and biochemistry of the 'acid fermentation' of complex waste is limited[32][33]. Although many micro-organisms in the 'acid fermentation' phase have been isolated and some pure culture studies carried out, there is still ignorance and confusion as to the pathways micro-organisms use in the conversion of a complex waste to end-products (fatty acids, CO_2 and H_2O). However, it appears that a great many different types of micro-organisms are required to bring about the multidue of reactions required for the degradation of complex wastes. The end products of the metabolism of the 'acid fermentation' microbial population are important, since they are the substrate sources for the subsequent bacterial growth in the 'methane formation' phase. In general, acid fermentation micro-organisms are more tolerant to environmental changes and also grow more rapidly than the methanogenic micro-organisms. They therefore never limit the rate of an anaerobic digestion process.

A considerable amount of research has been done on the methanogenic micro-organisms, but the difficulties in the isolation and maintenance of pure cultures have made their study extremely difficult, with the result that conclusions are generally not specific. It is now believed that the substrates utilized by methanogenic bacteria are limited to H_2, CO_2, CO, methanol, acetate and formate[34], with acetate and CO_2 being the major methane sources for complex wastes such as domestic sludge.

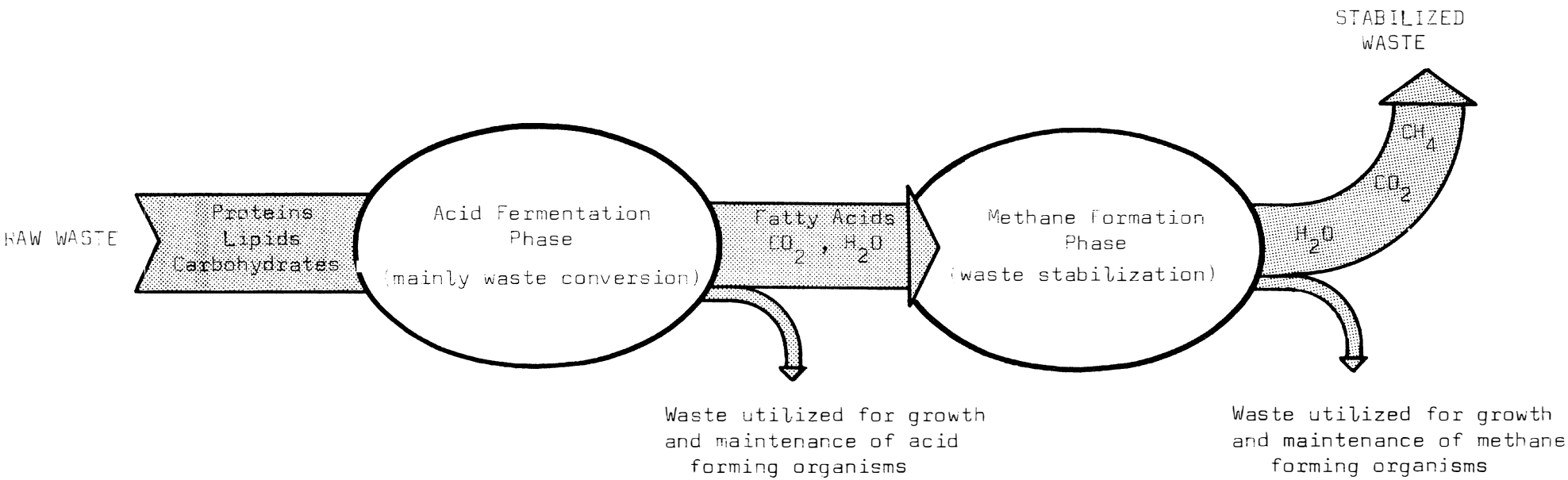

FIGURE 27: Breakdown of Complex Organic Matter in Anaerobic Digestion

Whatever the mechanisms of methane fermentation, there exists ample evidence to show that the methanogenic micro-organisms require exact environmental conditions, and that they grow more slowly than the 'acid fermentation' micro-organisms[23]. Thus, methane formation forms the critical or rate limiting step in the anaerobic digestion process. Its importance is emphasized by the fact that it is only in this phase that the waste is stabilized by its conversion to methane (Figure 27).

The activities of the methanogenic micro-organisms are inhibited either by toxins or by other adverse environmental conditions. Toxins which may be introduced to the process include[10]:

1. dissolved oxygen
2. heavy metals such as copper, nickel and zinc
3. alkali and akali earth metals such as sodium, potassium, calcium and magnesium
4. hydrogen ions
5. volatile fatty acids and ammonia, either in the ionized or unionized form, or both
6. dissolved hydrogen sulphide

Inhibition by each toxic material occurs only above a certain threshold concentration. Below this concentration the toxins do not show any inhibitions, and may in fact stimulate the activity of the organisms.

Other environmental conditions which could cause inhibition are sudden changes in temperature and overloads on the metabolic capacity of the micro-organisms (i.e. high food/micro-organism ratios). As will presently be shown, even partial inhibition of methane formation causes further toxic conditions to develop, so that the mechanism of failure is generally the same irrespective of the original cause of inhibition.

With the introduction of toxins or other adverse environmental conditions, the sensitive methanogenic organisms are the first to come under stress, causing the methane production to diminish. The acid-forming organisms are affected to a far lesser degree and continue with their production of volatile fatty acids and CO_2. Thus there is a build up of volatile fatty acid concentration and an increase in partial pressure of CO_2.

These two factors, and possibly incomplete waste stabilization, cause the hydrogen ion concentration to increase - i.e. the pH to drop. As volatile fatty acids and hydrogen ions can both be toxic, there is a progressive increase in the inhibition of the methane formation. Eventually, the methanogenic organisms cease to function, causing complete failure of the process.

The controversy as to whether hydrogen ions or volatile fatty acids are more toxic to methanogenic organisms is still not resolved, but latest indications are that the unionized fraction of volatile fatty acids acts as the toxin[11]. The unionized fraction, however, is solely dependent on the hydrogen ion concentration, and therefore, pH emerges as the most valuable single parameter for indicating toxic conditions in a declining anaerobic process.

Under exceptional circumstances failure could occur due to an excess concentration of ammonia or some other strong alkali. In this case, failure would occur in a high pH range.

As corrective measures for returning a declining process to normal operation, it is necessary to remove the extraneous cause of the malfunction (e.g. removal of toxin from waste, re-establishing correct temperature and food/organism ratio) and also to adjust the pH to the optimum value. The environment is thus returned as near as possible to the condition existing before the upset occurred.

It is clear that pH is an important controlling factor in the operation of anaerobic digestion processes. To adjust the pH of an unbalanced process in a satisfactory manner, it is necessary to understand how the pH in a normally operating process is established and controlled.

B. pH CONTROL BY ORGANISMS

pH in the aquatic system of an anaerobic process is essentially established and controlled by (a) the chemical composition of the waste being treated and (b) the chemical products released during the metabolic activities of the organisms. The type and quantity of each chemical product released will be dependent on the operating conditions in the process, and again on the chemical composition of the waste. Of the products released, the acid-base systems are the most important in the control of pH[35].

Important weak acid-base systems released during digestion are[36]:

1. carbonic species in the form of carbon dioxide
2. ammonia
3. orthophosphates
4. hydrogen sulphides
5. volatile fatty acid species, mainly in the form of acetic and propionic acid

Besides releasing the above weak acid-base systems, it is conceivable that strong acid-base systems are also released during the process.

Generally, the acid-base systems present in the waste being treated, and which remain unaffected during the process, are include in the above list.

Interaction of all the weak and strong acid-base systems present will establish and govern the pH. Once the pH is established, resistance to pH change will be governed solely by the weak acid-base systems. The mechanism by which weak acids and bases control the pH will be discussed before considering their interaction with strong acids and bases to establish the pH.

C. WEAK ACID-BASE SYSTEMS[37][38][39]

Dissociation and Equilibrium

Weak acids and bases in aqueous solutions are partially dissociated into their component ions. Dissociation equations of the systems listed in the previous section, are summarized in Table V. Monoprotic, diprotic and triprotic systems show step-wise dissociation in one, two and three steps respectively.

The equilibrium expressions for each dissociation are derived by considering the usual mass-action or thermodynamic concepts. These equilibrium expressions, together with the values of the equilibrium constant K (for a temperature of 25°C), are listed in Table V[40][41]. It should be noted that the dissociation equilibria constants require adjustment for different temperatures and for total ionic concentrations significantly greater than zero. The correction factors which must be applied are discussed in Appendix II.

In addition to the dissociations of the weak acids and bases, the water itself dissociates to a small degree. The dissociation equation and equilibrium expression for water are also listed in Table V. Because the unionized fraction of water is very high, it is assumed constant and incorporated into the equilibrium constant K_w.

Examination of the equilibrium-constant values for acetic and propionic acids shows that they are almost equal. In this investigation they are assumed equal, and the sum of the acetic acid and propionic acid species will be referred to as the volatile acid species or sometimes simply as acetic acid species.

Dissociations of the weak acids, weak bases and water can be visualized by their graphical representation on a pH versus negative log species concentration diagram. (pH is defined as the negative log of the measured hydrogen ion concentration.) Each of the systems in Table V is separately represented in Figure 28 for a total species concentration C_T equal to 0,01 moles/l. The pH versus log species concentration diagram is useful for the following reasons:

TABLE V

The weak acid-base systems encountered in the aquatic systems of anaerobic processes.

Species	Dissociation Equations	Equilibrium Expression	Equilibrium Constant at 25°C*	
			K	pK
Carbonic	1st $H_2CO_3 \rightleftharpoons HCO_3^- + H^+$	$[HCO_3][H]/[H_2CO_3] = K_1$	$4,5 \times 10^{-7}$	6,35
	2nd $HCO_3^- \rightleftharpoons CO_3^= + H^+$	$[CO_3][H]/[H] = K_2$	$4,7 \times 10^{-11}$	10,33
Ammonia	$NH_4^+ \rightleftharpoons NH_3 + H^+$	$[NH_3][H]/[NH_4] = K$	$5,5 \times 10^{-10}$	9,26
Ortho-phosphates	1st $H_3PO_4 \rightleftharpoons H_2PO_4^- + H^+$	$[H_2PO_4][H]/[H_3PO_4] = K_1$	$5,9 \times 10^{-3}$	2,23
	2nd $H_2PO_4^- \rightleftharpoons HPO_4^= + H^+$	$[HPO_4][H]/[H_2PO_4] = K_2$	$6,2 \times 10^{-5}$	7,21
	3rd $HPO_4^= \rightleftharpoons PO_4^= + H^+$	$[PO_4][H]/[HPO_4] = K_3$	$4,8 \times 10^{-13}$	12,32
Sulphide	1st $H_2S \rightleftharpoons HS^- + H^+$	$[HS][H]/[H_2S] = K_1$	$1,1 \times 10^{-7}$	6,96
	2nd $HS^- \rightleftharpoons S^= + H^+$	$[S][H]/[HS] = K_2$	$1,0 \times 10^{-4}$	14,0
Acetic Acid	$HAc \rightleftharpoons Ac^- + H^+$	$[Ac][H]/[HAc] = K$	$1,8 \times 10^{-5}$	4,74
Propionic Acid	$HPr \rightleftharpoons Pr^- + H^+$	$[Pr][H]/[HPr] = K$	$1,3 \times 10^{-5}$	4,9
Water	$H_2O \rightleftharpoons OH^- + H^+$	$[OH][H] = K_w$	$1,01 \times 10^{-14}$	14,00

K is the equilibrium constant of the acid dissociation

[ ] denotes the total concentration in moles/l

H_2CO_3 includes the dissolved CO_2 concentration

* ionic concentration of approximately zero is assumed

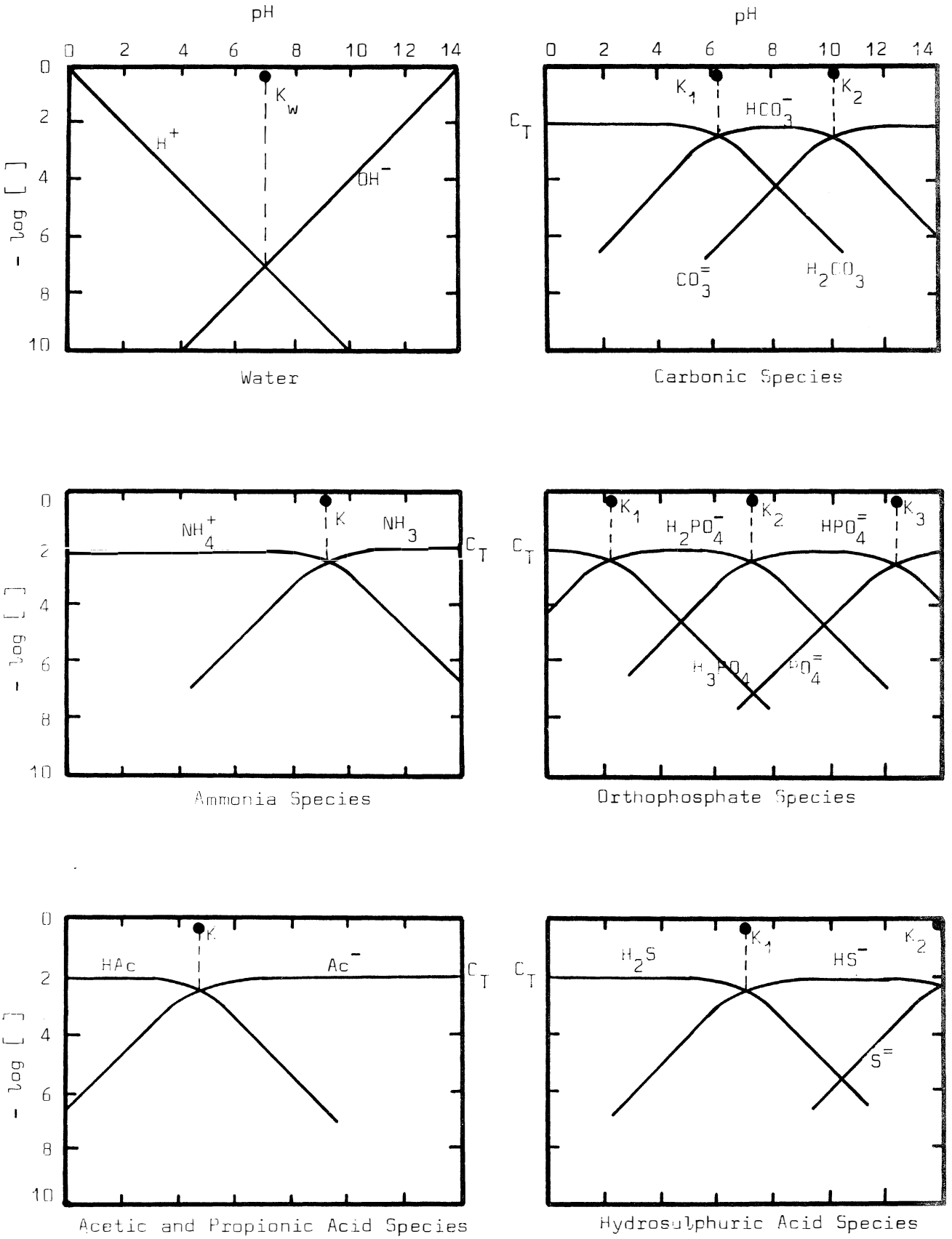

FIGURE 28: pH Versus Negative Log Species Concentration Diagrams for Weak Acid-Base Systems Encountered in the Aquatic Systems of Anaerobic Processes (Temperature 25°C; C_T = 0,01 moles/l; Ionic Strength Near Zero)

1. The concentration of each specific species in a particular system can be easily evaluated through the whole pH range.

2. The equilibrium constant for each dissociation is given by the intersection of the species lines involved. Since the scales are in negative log units, the negative log of the equilibrium constant (pK) is also listed in Table V.

3. Varying the total species concentration of a system does not alter the shape of the species concentration lines, but merely shifts them up or down.

4. The different systems do not interfere with each other, and can therefore be represented on one diagram. The diagram in Figure 29 represents the carbonic, ammonia and acetic acid systems (in aqueous solution) with total species concentrations of 0,1; 0,05; and 0,01 moles/l respectively.

Now that the dissociation of weak acid-base systems has been briefly described, the reasoning into how they tend to resist pH changes can be discussed.

pH Buffer Capacity

Resistance to pH change is described by the pH buffer capacity and measured in terms of the buffer index. The buffer index, β, is defined as the change in monovalent strong base (or acid) concentration with respect to the change in pH, i.e.

$$\beta = \frac{dC_b}{dpH} = -\frac{dC_a}{dpH}$$

where C_b and C_a are the additions of monovalent strong base and acid respectively (units are moles/l). An average buffer index (for a finite change in pH) will define the moles/l of strong base or acid addition required to cause that change in pH.

In any weak acid-base dissociation reaction, the buffer index of the system is directly related to the equilibrium constant, total species concentration and hydrogen ion concentration as follows:

$$\beta = 2{,}303 \frac{C_T K [H]}{(K + [H])^2}$$

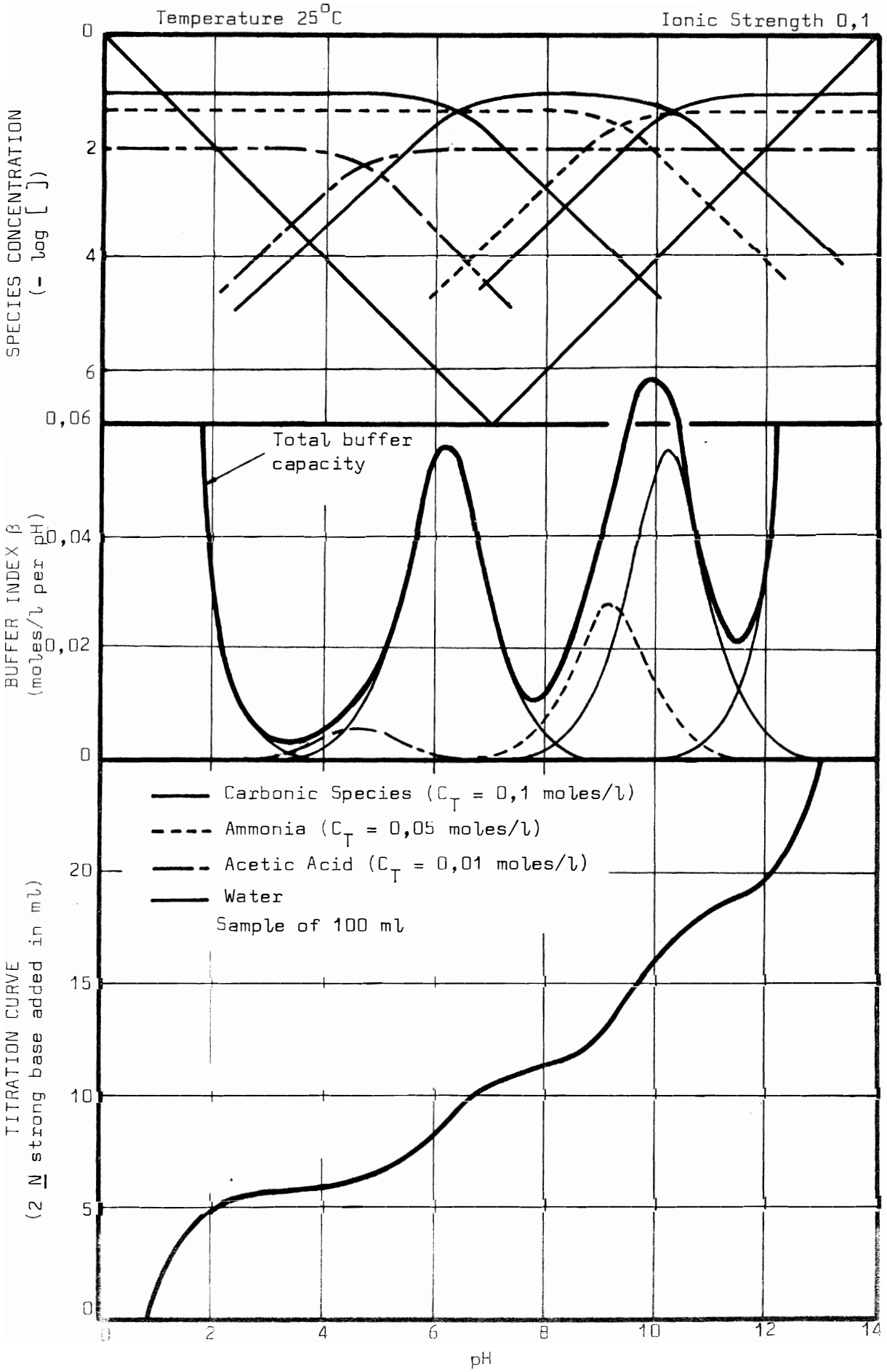

FIGURE 29: Relationship Between Species Concentration, Buffer Index and Titration Curve (on a pH Basis) for an Aqueous System Containing Weak Acids and Bases

A graphical representation of the buffer index and species concentration versus pH for a unit total species concentration of any weak acid-base system is shown in Figure 30. The diagram can be used to illustrate the following points:

1. Buffering capacity is a maximum where the pH equals the equilibrium constant pK, i.e. where the component species of the weak acid-base system are in equal concentration. For a unit C_T, the curve has the same shape irrespective of the pK value.

2. Buffering index decreases rapidly on either side of the pK value and becomes negligible within 2 pH divisions. The decrease in buffer capacity coincides with the concentration of one species of the system becoming dominant over the other.

3. Altering the total species concentration has the effect of altering the height of the bell-shaped buffer index curve.

Buffer index versus pH curve for any weak acid-base can be obtained simply by drawing the parabola of Figure 30 (corrected for total species concentration) with the pK value of the weak acid-base coinciding with the pH. Figure 31 represents the buffer index for the dissociation of the ammonia species (pK = 9,26) with total species concentrations of 0,08 moles/l.

The dissociation reaction of water offers buffering capacity at very high and very low pH's. Buffer index is related to the equilibrium constant and hydrogen ion concentration as follows:

$$\beta = 2{,}303\left([H] + \frac{K_w}{[H]}\right)$$

K_w is a constant, and the buffer index of water is therefore dependent on pH only, as shown in Figure 32.

Since different acid-base dissociation reactions do not interfere with each other, the buffer indecies of the different systems can all be represented on one diagram and simply added to give the total buffer index. The buffer indecies of the systems represented in Figure 29 are shown in the same figure, together with the total buffer index curve.

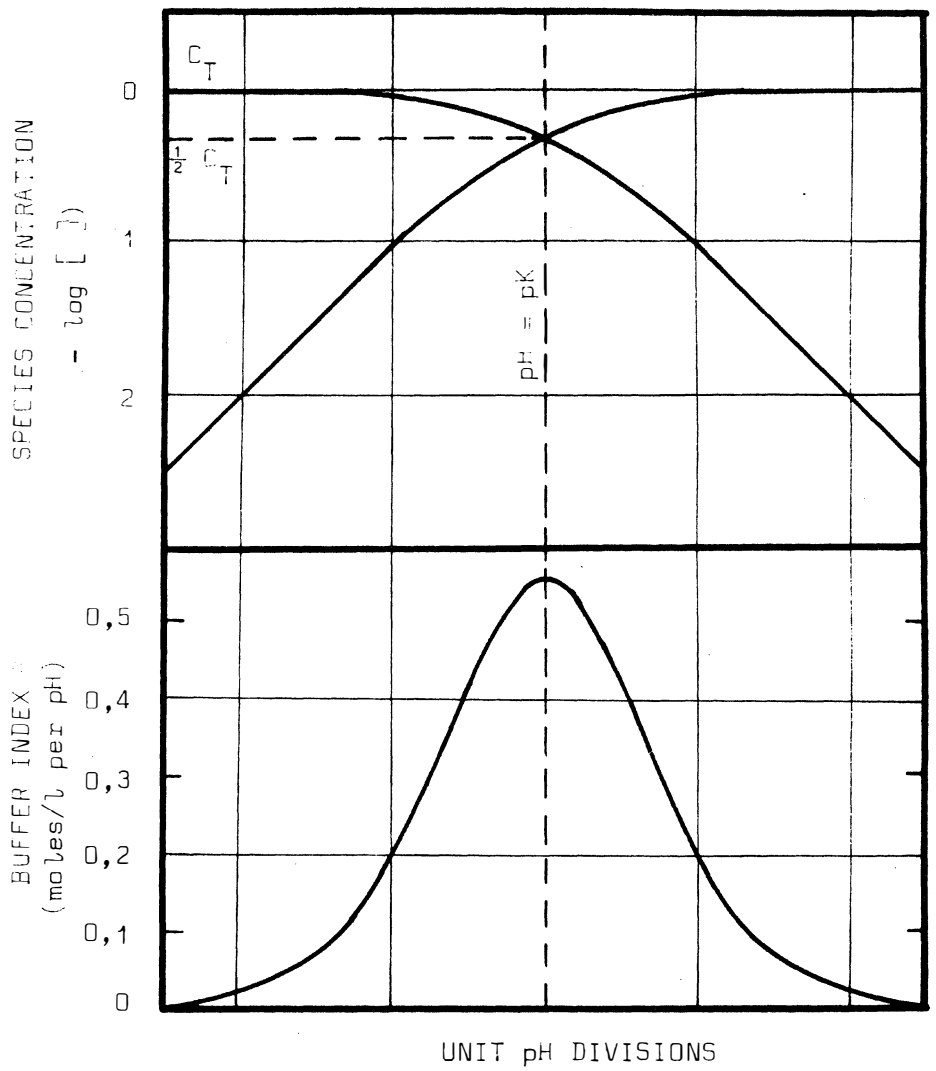

FIGURE 30: Relationship Between Species Concentration and Buffer Index (on a pH Basis) for Any Weak Acid/Base System with a Unit Total Species Concentration

Assuming that the mechanism of the weak acids/bases is the only mechanism buffering the anaerobic aquatic system, the resistance which the process shows to pH change may be quantitatively described by the total buffer index. Knowledge of the concentrations and dissociation constants of the weak acids and bases is required for the calculation of the buffer capacity of a system.

Experiments were conducted to ascertain to what extent the buffer capacity in the aquatic system of an anaerobic process is provided by the weak acid and base systems discussed above. The same experiments were used to identify the relative importance of systems, so as to simplify subsequent calculations for the determination of pH.

TABLE VI

Titration curve for a 0,1 moles/l aqueous solution of acetic acid as calculated from the buffer index.

pH	β_w moles/l/pH	β_a moles/l/pH	β_T moles/l/pH	β_T * ΔpH moles/l	C_b moles/l
2,0	0,025	-	0,025	0,013	0,013
2,5	0,008	0,001	0,009	0,005	0,018
3,0	0,003	0,004	0,007	0,004	0,022
3,5	-	0,013	0,013	0,007	0,029
4,0	-	0,032	0,032	0,016	0,045
4,5	-	0,054	0,054	0,027	0,072
4,7	-	0,058	0,058	0,011	0,083
5,0	-	0,052	0,052	0,016	0,099
5,5	-	0,028	0,028	0,014	0,013
6,0	-	0,011	0,011	0,006	0,119
6,5	-	0,004	0,004	0,002	0,121
7,0	-	0,001	0,001	0,001	0,122
8,0	-	-	-	-	0,122
9,0	-	-	-	-	0,122
10,0	-	-	-	-	0,122
11,0	0,003	-	0,003	0,001	0,123
11,5	0,008	-	0,008	0,004	0,127
12,0	0,025	-	0,025	0,013	0,140

β_w is the buffer capacity of water

β_a is the buffer capacity of acetic acid

β_T is the total buffer capacity

ΔpH is the step-increase in pH

C_b is the cumulative total of (β_T * ΔpH) and is equal to the moles/l of strong monovalent base required in the titration

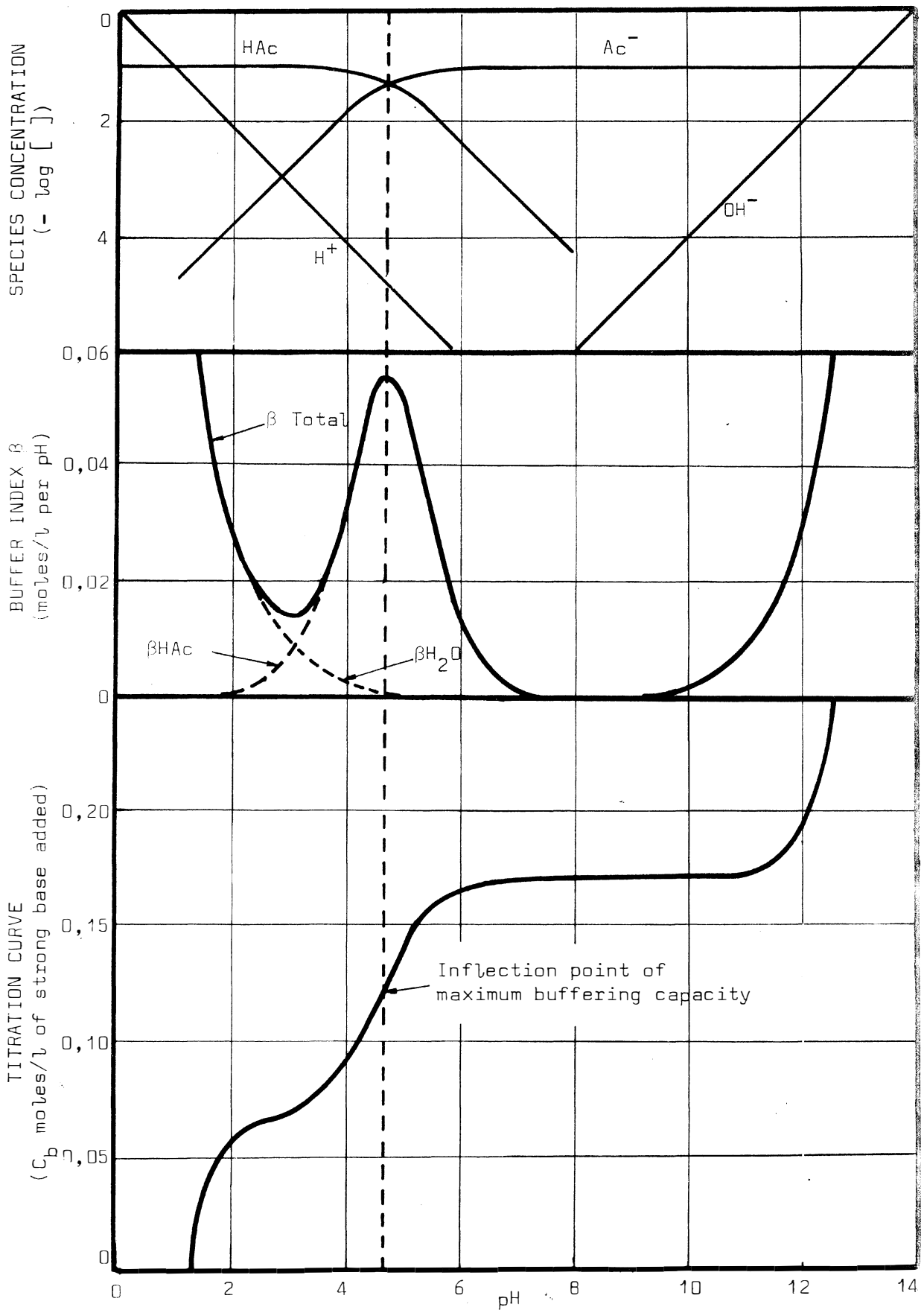

FIGURE 33: Relationship Between Species Concentration, Buffer Index and Titration Curve (on a pH Basis) for a 0,1 moles/l Aqueous Solution of Acetic Acid

titration curve, indicating the point of maximum buffer capacity. At very high and low pH's, the system is seen to have high buffer capacity due to the high buffer index of water.

Manual calculation of the titration curve becomes tedious when several weak acid-base systems are present. A computer programme used to facilitate these calculations is given in Appendix III. The programme includes the necessary corrections for temperature and ionic strength which must be applied to the equilibrium constants.

The titration curve for the weak acid-base systems presented in Figure 29 was calculated by this programme. As expected, the diagram indicates that in high buffer index regions, large quantities of strong base or acid are required to effect small pH changes, and vice versa.

A comparison of the theoretical titration curve for the aqueous system of an anaerobic process (as determined above) and an experimental titration curve performed on the same system, determines the accuracy of the assumption that weak acid-base systems provide the buffer capacity in anaerobic digestion processes.

Experimental verification of the above assumption was conducted on samples from two anaerobic processes. Samples were extracted from an experimental bench-scale anaerobic filter treating a wine distillery waste (see Chapter I) and from a full-scale digestor of the Athlone Sewage Works, Cape Town, treating a domestic sludge. Both processes were in normal stable operation at the time of sampling.

Samples from the process treating spent wine were prepared by removing a sample from the filter and immediately diluting it ten times with de-ionized (CO_2 free) water. This was done to reduce the loss of CO_2 and NH_3 to the atmosphere during titrations. The samples were centrifuged, and then considered ready for use. Samples from the process treating domestic sludge were stored for several days before use. For this reason, they were submitted to an atmosphere containing 39% CO_2 and 71% CH_4 (approximate composition of a digestor gas) for several hours to ensure CO_2 saturation. The samples were then prepared in the same way as the spent wine samples.

Measurements to determine the concentrations of total carbonic, ammonia, orthophosphate and volatile fatty acid species were conducted according to the methods in Appendix I. Hydrosulphuric measurements were omitted since concentrations reported in literature have been very low[36]. (Confirmation of its insignificance was obtained from the experiments conducted.) Results of the analysis for the total species concentrations of the two samples (from spent wine and domestic sludge treatment processes) are recorded in Table VII. Temperature and conductivity were measured to correct the equilibrium constants as per Appendix II.

The samples were titrated upscale and downscale with NaOH and H_2SO_4 respectively, and the titration curve recorded on an automatic recorder coupled to the titrator (see Appendix I). The experimental titration curves for the two wastes are shown in Figure 34, and are compared with the theoretical curve as predicted by the weak acid/base systems measured.

Close correlation of the theoretical and experimental curves was obtained for both samples, confirming that the measured weak acid-base systems control the buffer capacity. Since the two processes were treating widely different wastes, it seems probable that most anaerobic processes are buffered by weak acid-base systems of carbonic acid, acetic acid, ammonia and orthophosphate.

From the species concentration and buffer index diagrams of the undiluted sample extracted from the process treating spent wine (Figure 35), it is possible to identify the important weak acid-base systems: (the sample from the domestic sludge process will yield similar diagrams, since the species concentrations are of the same order).

Orthophosphates were insignificant in providing any buffer action due to their low total species concentration. This is demonostrated in the buffer index diagram. The total species concentration of the hydrosulphuric acid is probably still lower, since its effect cannot be discerned on the titration curves in Figure 34.

The pH in anaerobic processes rarely falls outside the range 6,0 to 7,5. Correction to pH in an unbalanced process should be always applied before the pH falls outside these limits.

TABLE VII

Chemical analysis of undiluted samples extracted from processes treating spent wine and domestic sludge.

Weak Acid/Base Species	Total Species Concentration moles/l	
	Spent Wine	Domestic Sludge
Carbonic	$57,5 \times 10^{-3}$	$78,0 \times 10^{-3}$
Ammonia	$11,6 \times 10^{-3}$	$24,3 \times 10^{-3}$
Acetic Acid	$10,0 \times 10^{-3}$	$2,1 \times 10^{-3}$
Orthophosphate	$2,5 \times 10^{-3}$	$2,1 \times 10^{-3}$
Temperature ^{o}C	20	20
Conductivity milli-siemens	5,8	5,1

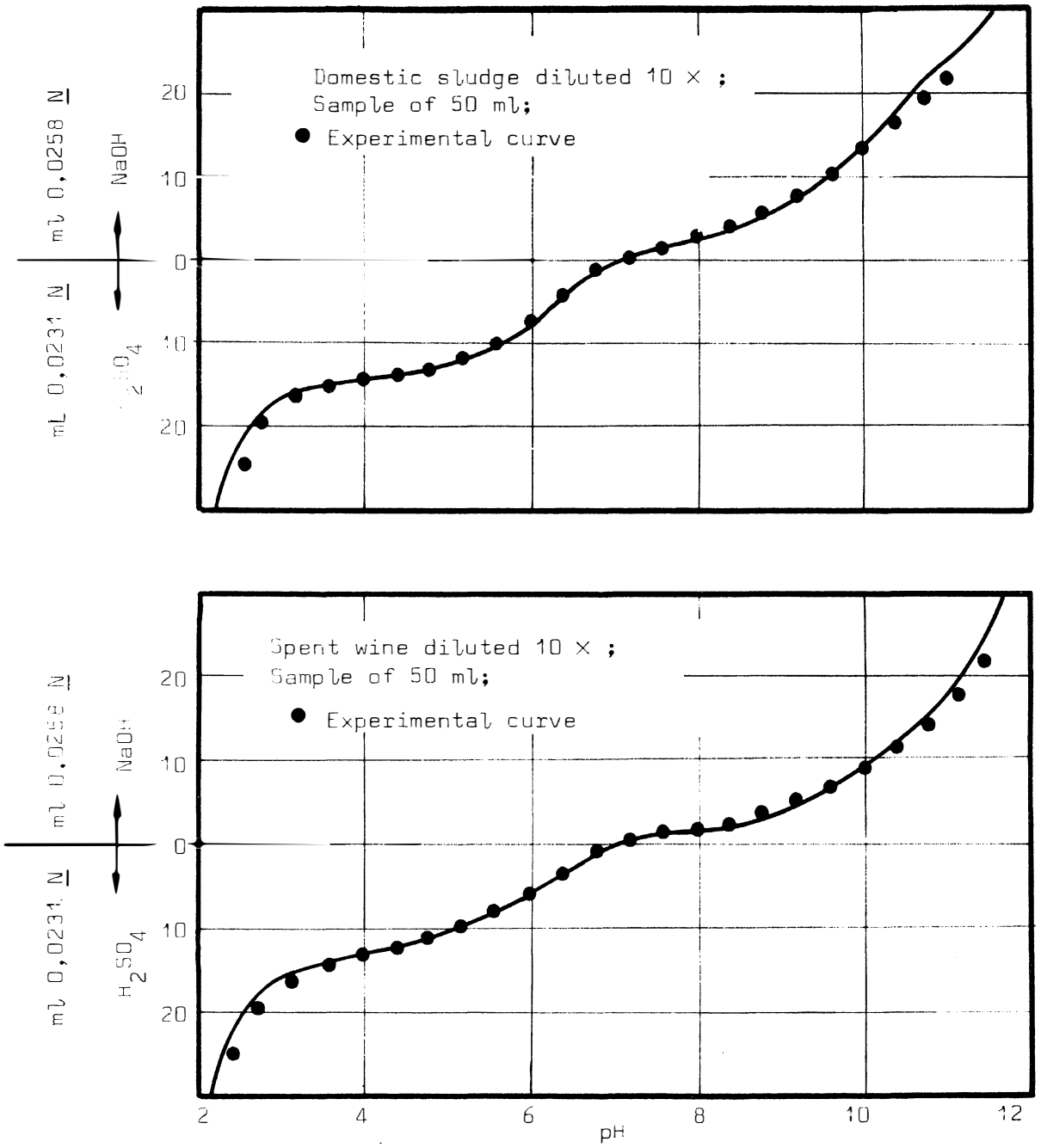

FIGURE 34: Comparison Between Experimental and Theoretical Titration Curves for the Aquatic Systems of Anaerobic Processes (Domestic Sludge and Spent Wine)

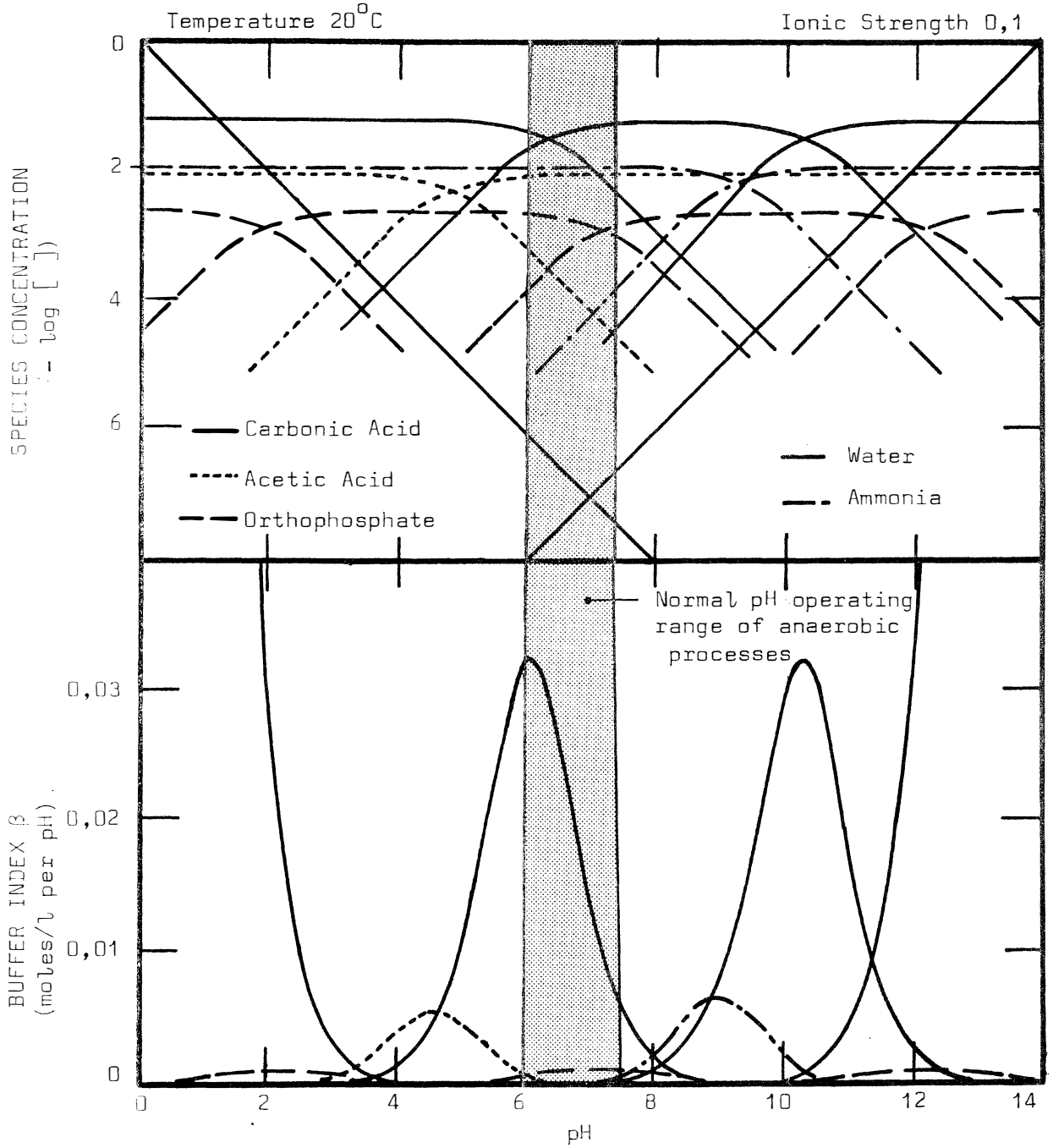

FIGURE 35: Relative Significance of the Weak Acid/Base Systems Normally Present in the Aquatic Systems of Anaerobic Processes (Sample Taken from a Process Treating Spent Wine)

The buffer index diagram in Figure 35 demonstrates that the buffer capacity in the pH range 6,0 to 7,5 is almost completely supplied by the first dissociation constant of carbonic acid. It is in fact the only system in this pH range which operates as a weak acid. Buffer capacity afforded by the acetic acid and ammonia will generally be insignificant in this pH range, and particularly so if their species concentrations are low. Even at higher concentrations, such as 3000 mg/l of acetic acid, the contribution to buffer capacity at pH 6,0 will be approximately 15% only.

The species concentration diagram in Figure 35 demonstrates that in the pH range 6,0 to 7,5, the acetic acid and ammonia species are almost completely dissociated. This accounts for the fact that (a) they provide no buffering capacity, and (b) they may be considered to act as a strong acid and base respectively (in that specified pH range only).

From the behaviour pattern described above, it is clear that for the aquatic system of anaerobic processes, resistance to pH change in the range pH 6,0 to 7,5, is governed by the carbonic weak acid system only. Acetic acid and ammonia act as a strong acid and base respectively, and thus, do not influence the buffer capacity.

The pH which is established in an anaerobic digestor will be dependent on the interaction of the carbonic weak acid system and the strong acid-base systems (including the acetic acid and ammonia systems).

E. pH ESTABLISHMENT AND CONTROL

The simplified aqueous system controlling the pH of an anaerobic process in the region 6,0 to 7,5 consists of the carbonic weak acid and the strong acid-base systems (in which are included acetic acid and ammonia). The system is further simplified by considering the summation of the strong acids and bases to yield a net acidic or basic concentration. In the aquatic system of anaerobic processes, it will become evident that the summation yields a net basic concentration. The carbonic and strong base systems used to define and control the pH are sketched in Figure 36.

A proton balance from the zero-ion conditions of the carbonic and strong base systems in water defines the ionic equilibrium* point of the two systems, and hence the pH. Zero-ion condition is given by the ionic condition of species before their addition to water. Since the carbonic species are derived mainly from the carbon dioxide gas (released during the digestion process), their zero-ion condition will be the dissolved carbon dioxide or carbonic acid species. Zero-ion conditions of the water and strong base are obviously their undissociated species. The following dissociations from zero-ion conditions are considered in the proton balance:

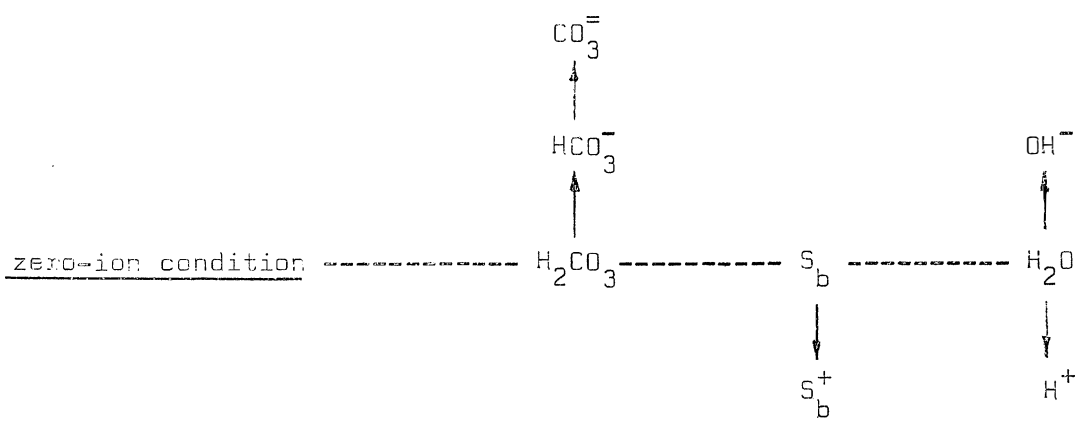

where S_b is the concentration of a monovalent strong base.

The proton balance yields:

$$2[CO_3] + [HCO_3] + [OH] = [H] + S_b$$

---

* Ionic equilibrium is defined as a steady-state dynamic balance between the reacting compounds and their ions.

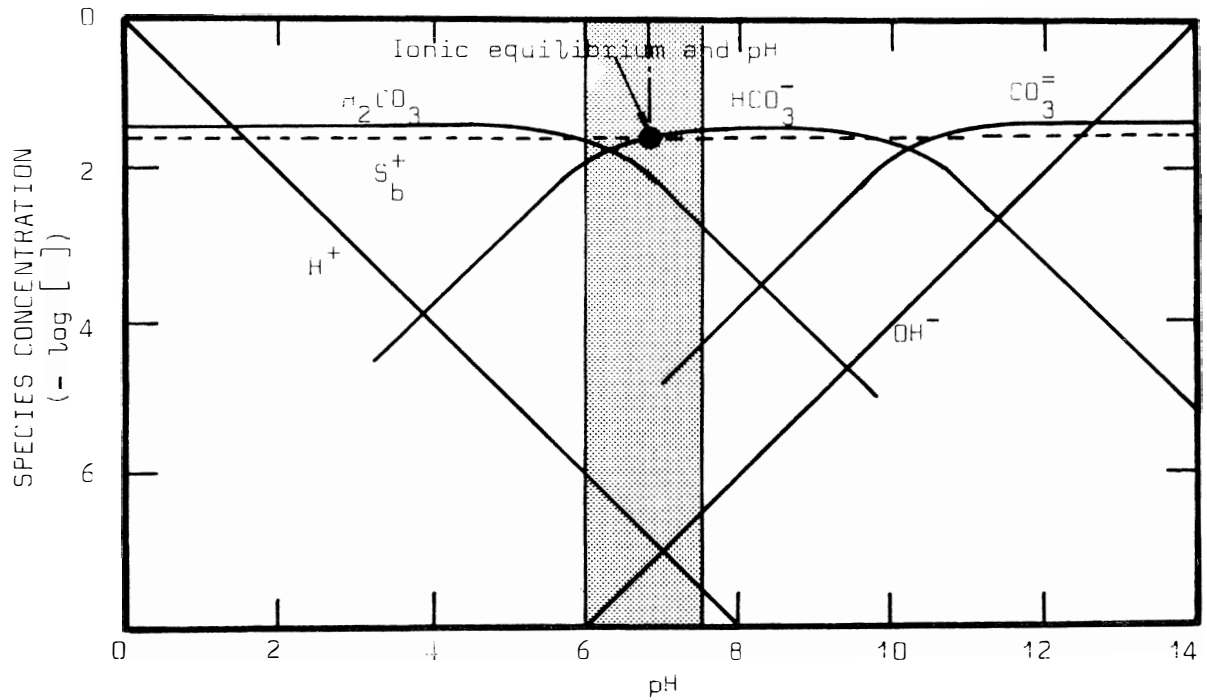

FIGURE 36: Simplified Aqueous System of an Anaerobic Process for the pH Range 6,0 to 7,5, i.e. Carbonic Species and a Net Strong Base Species Only

Consulting Figure 36, in the pH range 6,0 to 7,5, shows that the $CO_3^=$, H^+ and OH^- concentrations are negligible, and the equation above can therefore be reduced to:

$$[HCO_3] = S_b \qquad ...(24)$$

In Figure 36, the ionic equilibrium point, and therefore the pH, are defined by the intersection of the HCO_3^- and S_b^+ lines. (It is now obvious that if a net strong acid concentration were present, no solution in the pH range 6,0 to 7,5 would be possible.) The above graphical solution for the ionic equilibrium point and pH requires knowledge of the total carbonic species concentration, and either the net strong base or HCO_3^- concentration. Appendix I considers the difficulties encountered in measuring the above three variables.

Measurement of the CO_2 partial pressure (over the aquatic system of the process) and the pH is the easiest method for defining the ionic equilibrium point. The equilibrium expressions for the first dissociation reaction of carbonic acid and the equilibrium equation for free and dissolved CO_2 relate the two variables, CO_2 and pH, i.e.

$$\frac{[HCO_3][H]}{[H_2CO_3]} = K_1 \qquad ...(25)$$

$$[H_2CO_3] = K_G * P_{CO_2} \qquad ...(26)$$

where K_G* is the solubility equilibrium constant of CO_2 in water and P_{CO_2} is the partial pressure of CO_2 (atmosphere).

Combining equations (24), (25) and (26) we arrive at:

$$S_b = [HCO_3] = (K_1 * K_G) * \frac{P_{CO_2}}{[H]} \qquad ...(27)$$

Equation (27) is graphically represented in Figure 37. Corrections for temperature and ionic strength, as set out in Appendix II, are applied to constants K_1 and K_G before being used in equation (27). The diagram is extremely useful in clarifying various points in pH establishment and control:

---

* The value of pK_G at 25°C is 1,46 moles/l/atmosphere.

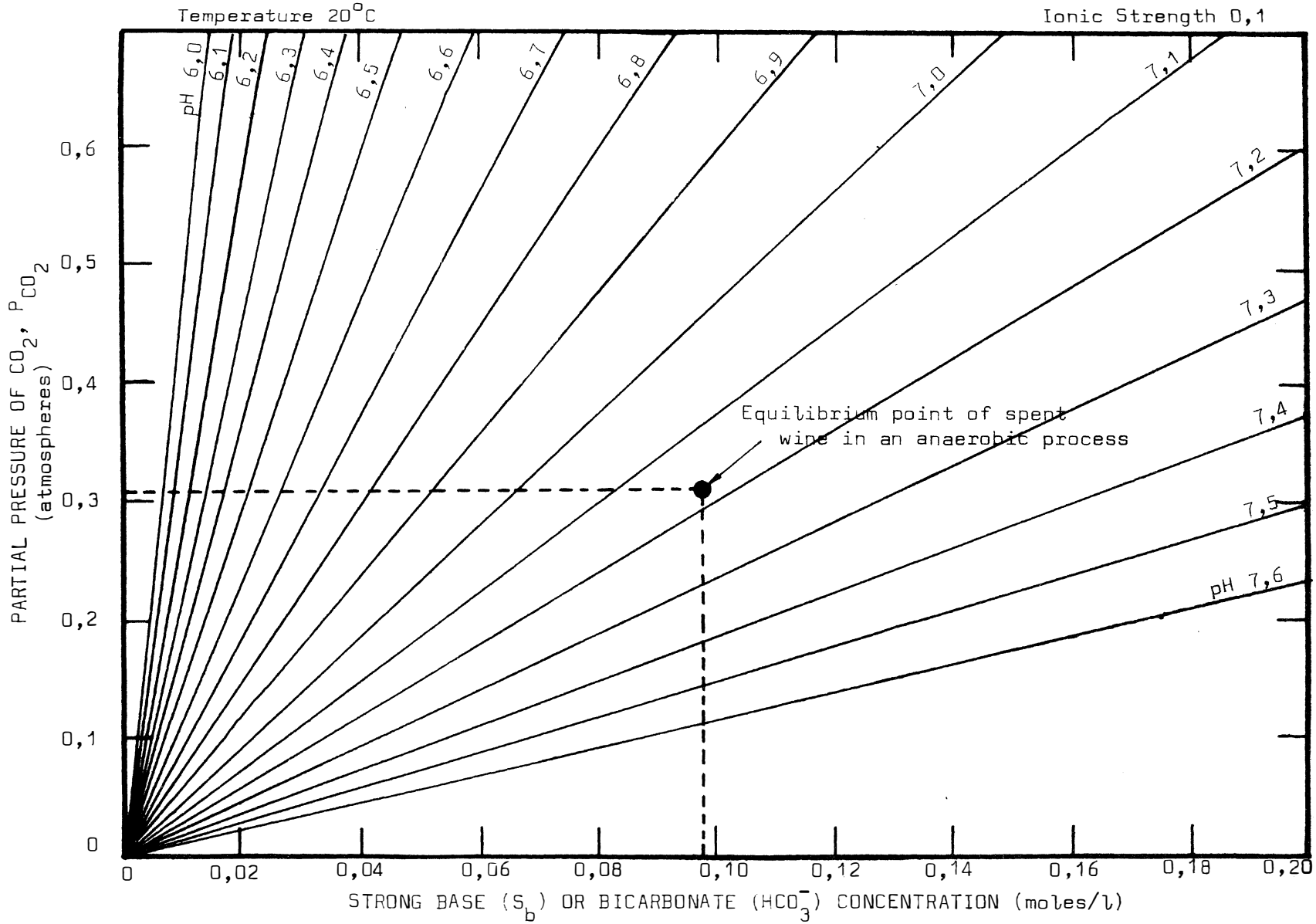

FIGURE 37: Relationship Between Partial Pressure of CO_2, Strong Base (or Bicarbonate) Concentration and pH for the Simplified Aquatic System of an Anaerobic Process (pH Range 6,0 to 7,5 Only) - Diagram after McCarty[8]

The net concentration of strong base S_b is not provided by the ammonia and acetic acid alone. This may be experimentally verified as follows: in the treatment of spent wine, a P_{CO_2} of 0,31 atmospheres and a pH of 7,18 were recorded. These values are plotted on the diagram (Figure 37) to define the ionic equilibrium point, and hence the S_b value of 0,098 moles/l. Measured values of ammonia and acetic acid were 0,011 and 0,018 moles/l respectively, giving a net measured S_b concentration of 0,001 moles/l. The difference between the calculated and measured values of S_b, i.e. 0,097 moles/l gives the concentration provided by some other strong base. Treatment of domestic sludge was found to give similar results.

From the data developed above, the assumption that the equivalent of some strong base is released (or hydrogen ions removed) during anaerobic digestion seems to be verified, but the findings disagree with those of Pohland[42]. The origin of the strong base, however, is not clear. Its relation to the anaerobic process during periods of overload is investigated in Park K.

Examination of Figure 37 shows that the buffer capacity decreases with decreasing pH, i.e. at low pH's, a unit change in S_b causes a larger change in pH than at high pH's. This seems contrary to expectation since the buffer index for unit total carbonic species increases for a decreasing pH between 7,5 and 6,0 (Figure 38). However, the unit species buffer index diagram assume a constant total carbonic species concentration, whereas in the anaerobic process the total carbonic species concentration changes with change in pH for a constant partial pressure of CO_2. The species concentration decreases rapidly with decreasing pH (for an unchanged partial pressure of CO_2), and the buffer capacity is correspondingly reduced. This is illustrated in Figure 38, which shows how (a) the buffer index for unit species, (b) the total carbonic species and (c) the buffer capacities change with pH for different CO_2 partial pressures.

The S_b concentration can be indirectly obtained from HCO_3^- measurements, which in turn are measured by alkalinity titrations. Alkalinity for a pure carbonic species system is defined as:

$$\text{Alkalinity} = 2[CO_3] + [HCO_3] + [OH] - [H]$$

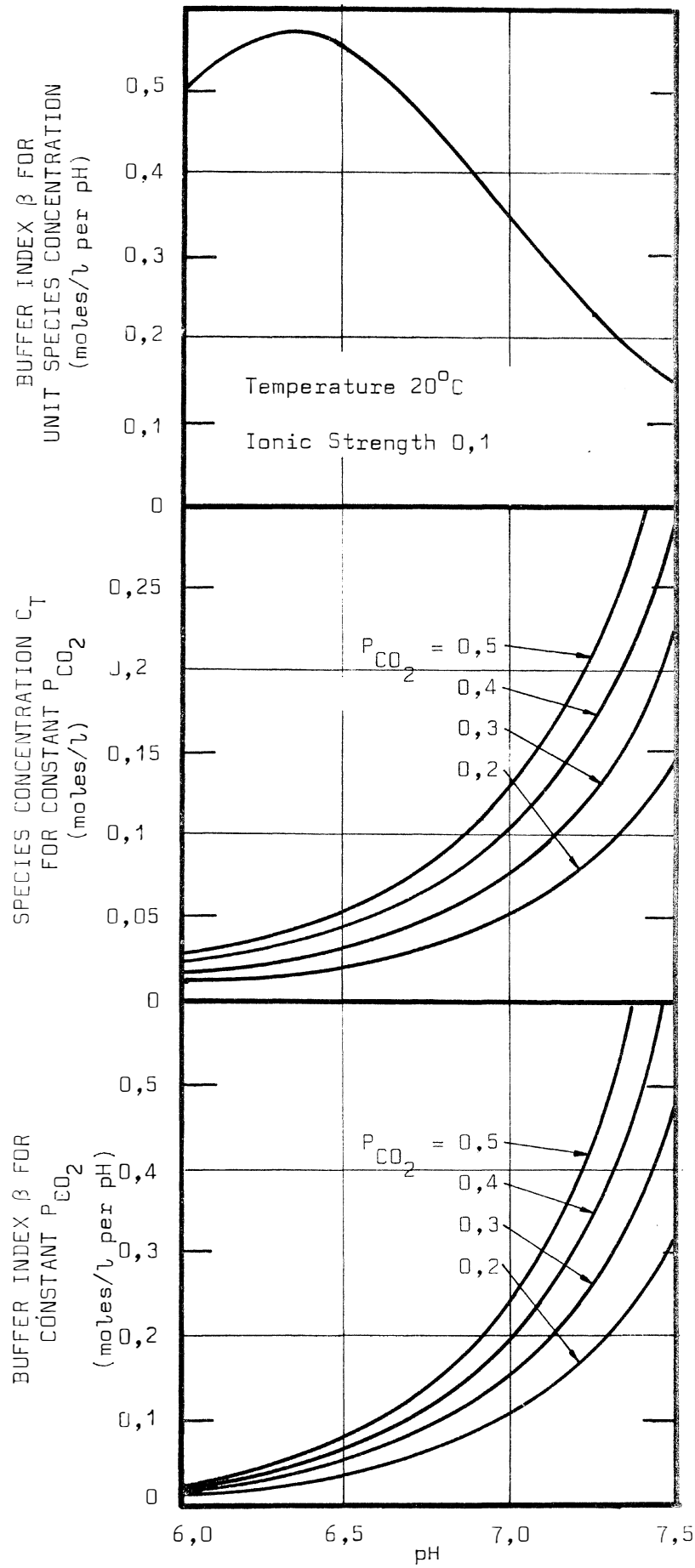

FIGURE 38: Comparison (on a pH Basis) of the Buffer Index of a Constant Concentration of Carbonic Species with the Buffer Index for a Constant Partial Pressure of CO_2 (Change of Species Concentration with pH is also shown)

In the pH region 6,0 to 7,5, $CO_3^=$, OH^- and H^+ concentrations are negligible (see Figure 36), and the above equation reduces to:

$$\text{Alkalinity} = [HCO_3^-]$$

In pure carbonic aquatic systems the alkalinity titration will give an accurate estimate of the HCO_3^- concentration. However, with other weak acid systems present, notably acetic acid, the titration will be some measure of the total alkalinity present, including that provided by the acetic acid. In this case the titration will give a poor estimate of the HCO_3^- concentration, particularly where the acetic acid concentration is high. A correction can be made to the total titration value by subtracting that part of the alkalinity which is ascribed to the titration of the acetic acid fraction. Estimation of the alkalinity due to the acetic acid concentration is not reliable, so that HCO_3^- concentrations are not given accurately. The difficulties in measuring alkalinity makes it a poor parameter for determining the value of HCO_3^- and S_b, and hence for defining the ionic equilibrium point.

Measurements of alkalinity were omitted in this study because it is redundant for calculating the ionic equilibrium point, providing pH and P_{CO_2} are measured. If P_{CO_2} is not measured, then alkalinity measurements can be substituted but this is not satisfactory for accurate work.

Measurement of the partial pressure of CO_2 and pH is the most accurate method for determining the ionic equilibrium point in the aquatic system of the anaerobic process. The diagrammatic representation of the ionic equilibrium point in relation to P_{CO_2} and S_b (Figure 37) will be particularly useful in describing the pH changes which occur in anaerobic processes.

The partial pressure of CO_2 is given by the percentage CO_2 in the gas, only if it can be assumed that the dissolved CO_2 is under atmospheric pressure at sea level. The magnitude of the errors introduced by this approximation at high altidues and in deep digestors is shown in Appendix IV.

pH is established and controlled by the CO_2 partial pressure and the net strong base concentration (Figure 37). Both these parameters are controlled normally by the activities of the micro-organisms in the process. However, during unblanced operation it is possible to adjust the P_{CO_2} and S_b (and hence the pH) by methods described in Part F.

F. pH ADJUSTMENT

The pH in a process can be adjusted by changing the composition of the waste, modifying the environmental conditions for the organisms, direct chemical dosing and changing the CO_2 partial pressure.

Changes in waste composition should be considered where the waste contains excess acids or bases. It may be necessary to partly neutralize the pH by additions of either a strong base or acid as the case requires. Usually, pH adjustment is necessary only with some specific industrial organic waste. The vast majority of organic wastes do not require pH adjustment; it is certainly not required in domestic sludges.

Modification of the environmental conditions of a process usually alters the degree of activity of the acid and methane organisms by different amounts. A decline in pH is caused by an increase in the activity of the acid forming organisms relative to the activity of the methanogenic organisms (see Part A). This usually occurs during periods when the metabolic capacity of the methanogenic organisms is exceeded (e.g. during start-up operations, sudden increases in load rates and temperature reductions - see Chapter I). Since high-rate digestion processes are normally operated under environmental conditions optimum for the methanogenic organisms, any deviation from these conditions is likely to decrease the activity of the methanogenic organisms. This depresses the pH. Short-term temperature increase is an exception, since it temporarily increases the activity of the methanogenic organisms[7]. In an overloaded process with a depressed pH, a short-term temperature increase may be a possible procedure to return the pH to its normal value for the process. (This solution is useful only in processes where the activities of the methanogenic organisms have not been completely inhibited.)

Direct chemical additions to a process is the method most often used to adjust pH in an unbalanced process. The additions immediately change the S_b and carbonic species concentrations, thus alleviating the adverse pH conditions. Relief is only temporary, but it provides time for the cause of the inbalance to be determined and corrected. To increase the pH, the following chemicals can be used: $Ca(OH)_2$, $CaCO_3$, $NaHCO_3$, Na_2CO_3, NaOH and NH_3. A decrease in pH can be obtained

by dosing with any strong acid such as HCl. Direct correction of the CO_2 partial pressure is seldom used as a method of pH adjustment.

The effect on pH of each of the above dosing chemicals, and the effect of P_{CO_2} changes, can be demonstrated by referring to a pH conditioning diagram. This will be considered in the next section.

G. pH CONDITIONING DIAGRAM

pH Conditioning Diagram for Completely Soluble Dosing Chemicals

The basic pH conditioning diagram (Figure 39) is essentially identical to the diagram in Figure 37, except for the units of the axis which require some clarification.

The vertical axis represents either the partial pressure of CO_2, the percentage CO_2 in the gas, or the H_2CO_3 concentration. Percentage CO_2 is assumed to be equal to the CO_2 partial pressure in the digestor atmosphere (see Appendix IV). The H_2CO_3 concentration is obtained from equation (26), i.e.

$$[H_2CO_3] = K_G * P_{CO_2}$$

which expresses the H_2CO_3 concentration in moles/l. Conversion to equivalents/l is obtained as follows:

$$(H_2CO_3) = \text{valency} * [H_2CO_3]$$
$$= 2 * [H_2CO_3]$$

where ( ) represents equivalents/l. Equivalent concentrations can in turn be expressed in mg/l (or ppm) as $CaCO_3$ as follows:

$$(H_2CO_3) * \text{equivalent weight } CaCO_3 * 10^3 = \text{mg/l as } CaCO_3$$

i.e. $(H_2CO_3) * 50 * 10^3 = \text{mg/l as } CaCO_3$

The horizontal axis represents either the HCO_3^- or strong base concentration. These parameters can be expressed either in moles/l, equivalents/l or mg/l as $CaCO_3$. Conversions from one unit to another are the same as for the H_2CO_3 conversions, except that HCO_3^- has unit valency.

Units generally used in calculations will be ppm as $CaCO_3$ on both axes, and CO_2 percentage on the vertical axis.

Since the equilibrium constants change for different temperatures and ionic strengths (see Appendix II), the pH conditioning diagram will change correspondingly. A selection of pH conditioning diagrams for different temperature and ionic strengths are given in Appendix V.

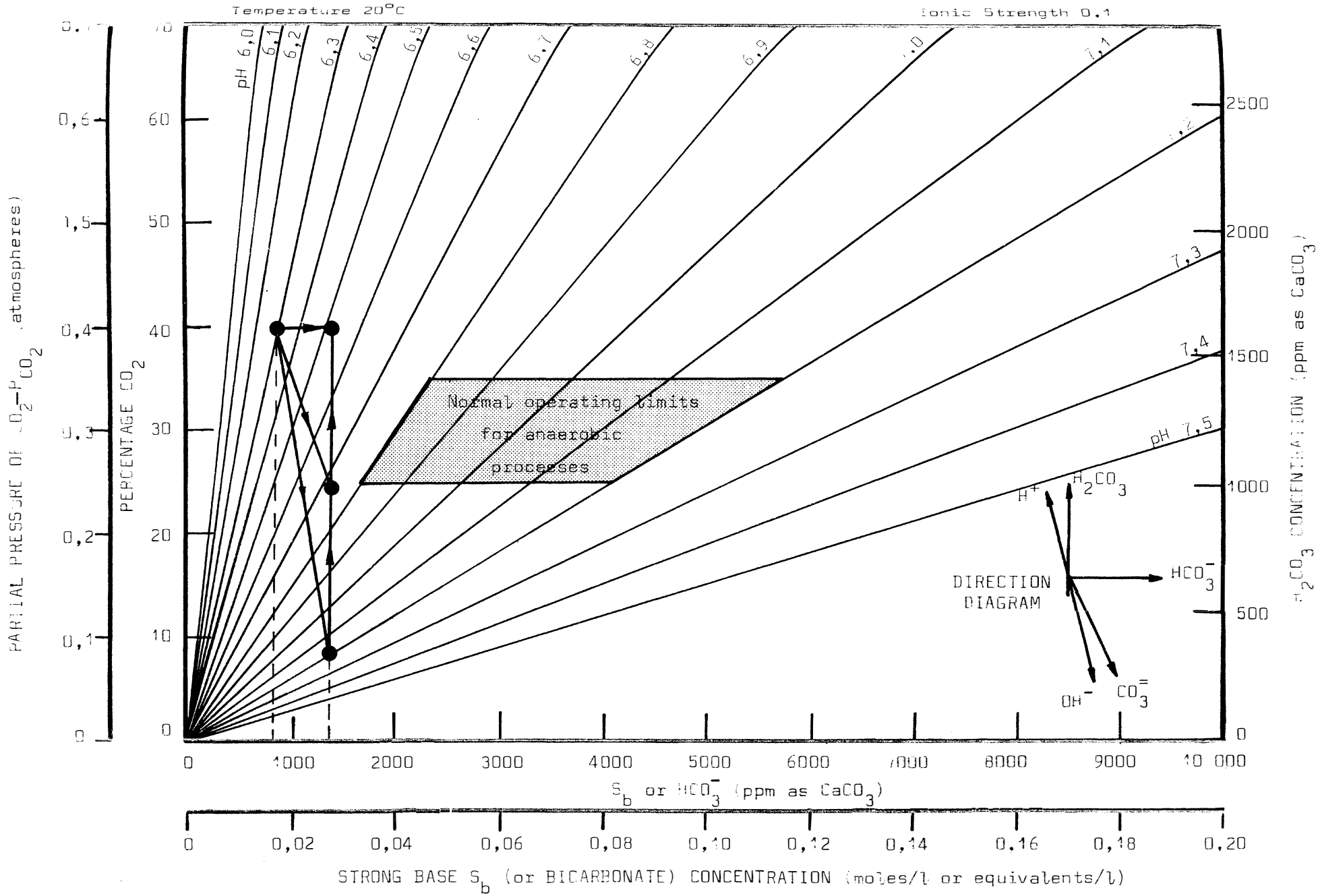

FIGURE 39: pH Conditioning Diagram for the Aquatic System of an Anaerobic Process

These are seen to vary considerably with changing temperature and ionic strengths. The computer programme for plotting the diagrams is given in Appendix VI.

Anaerobic processes normally operate at a pH between 6,8 and 7,2, and within a CO_2 percentage range of 25 to 35%. These limits are shown on the conditioning diagram in Figure 39. A pH outside these limits indicates an inbalance in the process, and adjustment of the pH becomes necessary.

Before adjusting the pH of an anaerobic process, the equilibrium point should be established on the diagram by measuring the percentage CO_2 and the pH. This point represents both CO_2 solubility equilibrium and carbonic species ionic equilibrium.

Additions of chemicals alter the ionic and CO_2 solubility equilibrium points, and hence the pH. It is assumed that ionic equilibrium is immediately satisfied, and that solubility equilibrium is satisfied at a much slower rate, depending mainly on the CO_2 production of the organisms. The direction and magnitude of changes of the equilibrium points for the addition of the following different chemicals will now be considered:

1. a strong base or acid other than a carbonic species acid or base
2. a bicarbonate
3. a carbonate
4. carbonic acid

Firstly, the movement of ionic equilibrium is considered, assuming no CO_2 exchange takes place with the gas. Changes in the concentrations of the HCO_3^- and H_2CO_3 are computed for the addition of each chemical, in order to define the new ionic equilibrium point.

Secondly, the movement of ionic equilibrium is considered while it adjusts to the CO_2 solubility equilibrium. The changes in H_2CO_3 and HCO_3^- are computed for CO_2 exchanges with the gas in order to define the final ionic and solubility equilibrium point.

These calculations assume that the solubilities of the chemicals are infinite.

1. Ionic Equilibrium Movement for the Addition of a Strong Base or Acid

The change in $[HCO_3]$ may be calculated as follows: it was shown earlier in equation (24) that the ionic equilibrium point is given by

$$[HCO_3] = S_b$$

The addition of X moles/l of a strong monovalent base merely alters the above proton-balance equation to

$$[HCO_3] = S_b + X$$

The change in $[HCO_3]$ for the addition of X is therefore given by

$$\Delta [HCO_3] = X \qquad ...(28)$$

Equation (28) assumes that S_b remains unchanged during the addition of the strong base, X. Since S_b is governed by the biological process, it seems valid to assume that the process, and thus S_b, will initially remain unaffected by the addition of a dosing chemical.

The change in $[H_2CO_3]$ may be calculated by considering a mass-balance of the carbonic species:

$$C_T = [H_2CO_3] + [HCO_3] + [CO_3] \qquad ...(29)$$

Since no exchange of CO_2 with the gas is considered, C_T remains constant. In the pH region 6,0 to 7,5, the $[CO_3]$ is again negligible, so that for changes in $[HCO_3]$, equation (29) reduces to

$$\Delta [H_2CO_3] = - \Delta [HCO_3]$$

By substitution of equation (28) into the equation above,

$$\Delta [H_2CO_3] = - X$$

Hence, addition of X moles/l of a strong base changes the $[H_2CO_3]$ and $[HCO_3]$ by equal amounts of X moles/l. The concentrations can be expressed in ppm as $CaCO_3$ as follows:

$$[H_2CO_3] = [H_2CO_3] * 100 * 10^3 \quad \text{ppm as } CaCO_3$$

$$[HCO_3] = [HCO_3] * 50 * 10^3 \quad \text{ppm as } CaCO_3$$

Thus, for the addition of X moles/l of X, the HCO_3 concentration changes by $X * 50 * 10^3$ ppm as $CaCO_3$, while the H_2CO_3 concentration changes by $X * 100 * 10^3$ ppm as $CaCO_3$, i.e. expressed as ppm as $CaCO_3$, the H_2CO_3 change is twice the HCO_3 change.

On the pH conditioning diagram, the direction and magnitude of the ionic equilibrium movement for the addition of a strong base is graphically shown in Figure 40. The addition of a strong acid will merely reverse the direction and magnitude of the ionic equilibrium movement.

It should again be noted that any acid or base with a dissociation constant significantly outside the pH range 6,0 to 7,5 can be taken to act approximately as a strong base or acid.

2. Ionic Equilibrium Movement for the Addition of a Carbonate

Since the addition of a carbonate alters the total carbonic species concentration, it is useful to consider two carbonic species systems - one with a total species concentration C_{Tg} given by the original species present before the addition of a carbonate, and the other with a total species concentration C_{Ts} equal to the carbonate added.

A mass-balance of the two systems, neglecting $[CO_3]$ as being insignificant, is given by

$$[HCO_{3g}] + [H_2CO_{3g}] = C_{Tg} \qquad ...(30)$$

$$[HCO_{3s}] + [H_2CO_{3s}] = C_{Ts} \qquad ...(31)$$

and adding the two systems gives

$$[HCO_3] + [H_2CO_3] = C_{Tg} + C_{Ts} \qquad ...(32)$$

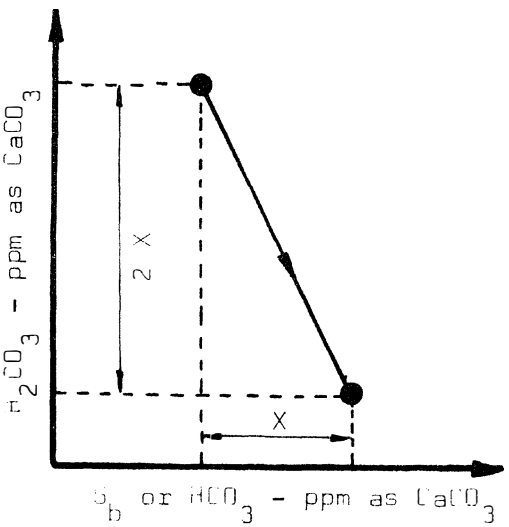

(1) Addition of X moles/l of a strong monovalent base

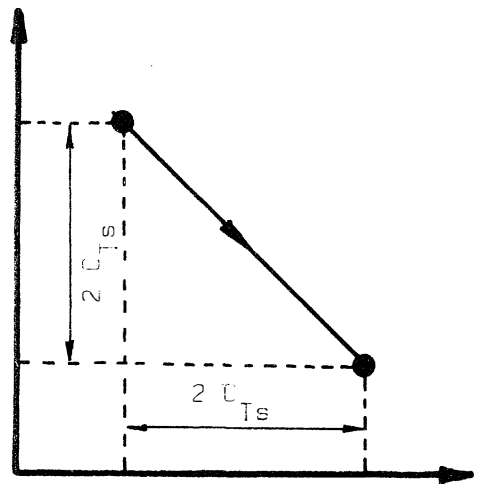

(2) Addition of C_{Ts} moles/l of a carbonate

Note: Scales on both axes have the same divisions

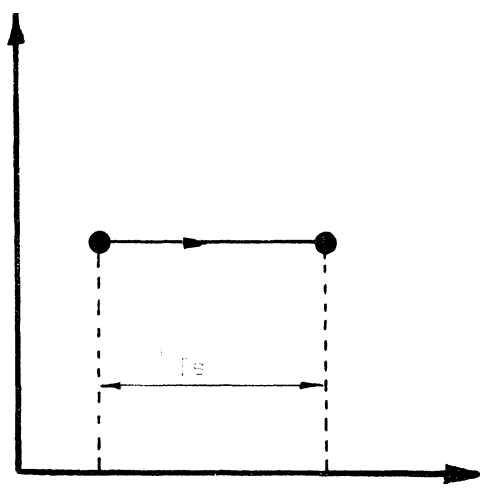

(3) Addition of C_{Ts} moles/l of a bicarbonate

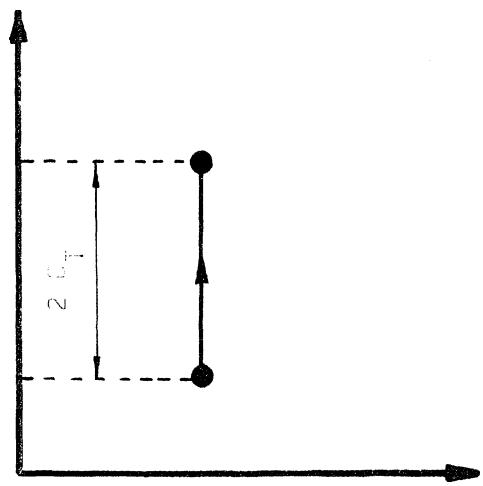

(4) Addition of C_T moles/l of carbonic acid or (CO_2)

FIGURE 40: Movement of Ionic Equilibrium on the pH Conditioning Diagram for Different Dosing Chemicals

Consider also a proton-balance of the complete system:

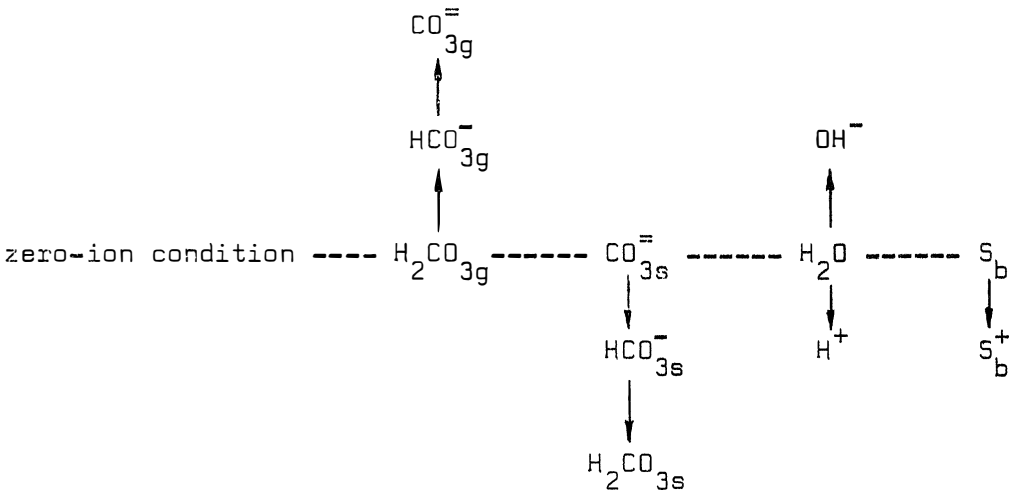

$$\text{i.e. } 2[CO_{3g}] + [HCO_{3g}] + [OH] = 2[H_2CO_{3s}] + [HCO_{3s}] + [H] + [S_b]$$

Neglecting $[CO_3]$, $[OH]$ and $[H]$ simplifies the above equation to

$$[HCO_{3g}] = 2[H_2CO_{3s}] + [HCO_{3s}] + S_b \qquad ...(33)$$

The change in $[HCO_3]$ may now be calculated as follows: considering equations (30), (31) and (32), the following equation is derived

$$[HCO_3] = [HCO_{3s}] + [HCO_{3g}] \qquad ...(34)$$

Substituting equation (34) in equation (33) yields

$$[HCO_3] = 2[HCO_{3s}] + 2[H_2CO_{3s}] + S_b$$

Finally, substituting equation (31) into the above gives

$$[HCO_3] = 2\ C_{Ts} + S_b \qquad ...(35)$$

Assuming that S_b remains constant, the change in $[HCO_3]$ will be given by

$$\Delta\,[HCO_3] = 2\ C_{Ts} \qquad ...(36)$$

The change in $[H_2CO_3]$ may be calculated as follows: substitution of equation (35) into (32) yields:

$$[H_2CO_3] = (C_{Tg} - C_{Ts}) - S_b \qquad ...(37)$$

Again, S_b and C_{Tg} are constant, so that the change in H_2CO_3 is given by

$$\Delta [H_2CO_3] = - C_{Ts}$$

Hence, addition of C_{Ts} moles/l of a carbonate changes the HCO_3^- concentration by 2 C_{Ts} moles/l and the H_2CO_3 concentration by C_{Ts} moles/l. The concentrations can be expressed in ppm as $CaCO_3$ as was shown in the case of strong base addition (page 133).

In the pH conditioning diagram, the direction and magnitude of ionic equilibrium movement is shown in Figure 40. Removal of CO_3, for example by the precipitation of $CaCO_3$, reverses the direction and magnitude of ionic equilibrium movement.

3. Ionic Equilibrium Movement for the Addition of a Bicarbonate

Two carbonic species systems, identical to those in the carbonate addition case (page 133), are considered. The mass-balance equations (30), (31), (32) and (34) remain unchanged.

A proton-balance of the complete systems follows:

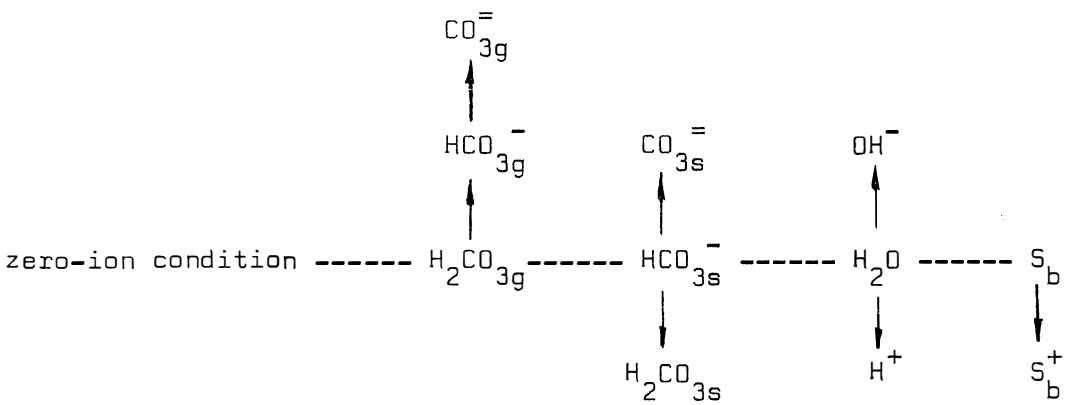

The change in $[HCO_3]$ may now be calculated: omission of the $[CO_3]$, $[OH]$ and $[H]$ ions from the proton-balance yields the following simplified equation:

$$[HCO_{3g}] = [H_2CO_{3s}] + S_b$$

Substituting equations (34) and (31) into the above gives

$$[HCO_3] = C_{Ts} + S_b$$

With S_b remaining constant, the change in HCO_3^- is given by

$$\Delta [HCO_3] = C_{Ts}$$

The $[H_2CO_3]$ remains unchanged: substitution the above equation into equation (32) yields

$$[H_2CO_3] = C_{Tg}$$

and since C_{Tg} remains constant, there is no change in $[H_2CO_3]$.

Hence, addition of C_{Ts} moles/l of bicarbonate changes the HCO_3^- concentration by an amount equal to C_{Ts}, and leaves the H_2CO_3 concentration unaltered. Concentrations may again be expressed in ppm as $CaCO_3$ (page 133). The direction and magnitude of ionic equilibrium movement is shown in Figure 40.

4. Ionic Equilibrium Movement for the Addition or Removal of Carbonic Acid (Dissolved CO_2)

The ionic equilibrium which is established by the addition of H_2CO_3 is defined by the acid-base systems discussed in Part E. The changes in $[H_2CO_3]$ and $[HCO_3]$ may be defined by considering the proton balance equation (24), i.e.

$$[HCO_3] = S_b \qquad ...(24)$$

and the mass-balance equation

$$C_T = [H_2CO_3] + [HCO_3] \qquad \text{(omitting } [CO_3])$$

A combination of the two equations gives

$$[H_2CO_3] = C_T - S_b \qquad ...(38)$$

Assuming S_b constant, equation (24) shows there is no change in the HCO_3^- concentration, while equation (38) shows the H_2CO_3 concentration change is equal to the H_2CO_3 added, i.e. C_T. Concentrations may again be expressed in ppm as $CaCO_3$. The direction and magnitude of the ionic equilibrium movement is shown in Figure 40. Removal of H_2CO_3, for example by CO_2 stripping, reverses the direction and magnitude of the ionic equilibrium point movement.

A combination of the direction diagrams in Figure 40 is shown in the pH conditioning diagram (Figure 39), corrected to scale.

Addition of the above dosing chemicals causes oversaturated, undersaturated or saturated conditions with respect to CO_2 solubility to develop. As CO_2 exchange between the water and gas proceeds, the H_2CO_3 concentration changes as indicated by the CO_2—H_2CO_3 solubility-equilibrium equation (26). In the pH conditioning diagram, the ionic equilibrium point moves vertically up or down, as shown for H_2CO_3 additions in subsection 4 above. The point where ionic and solubility equilibria are both satisfied defines the final pH.

Upward Adjustment of pH

The different effect each dosing chemical has on pH is demonstrated in the following example by referring to the pH conditioning diagram (Figure 39):

Consider an initial ionic and CO_2 solubility equilibrium point given by a pH of 6,3 and a CO_2 percentage of 40 (point 1). A strong base, a carbonate and a bicarbonate are each added in equal amounts (500 ppm as $CaCO_3$) to raise the pH. For the respective chemical additions of strong base, carbonate and bicarbonate, the ionic equilibria initially move to points 2, 3 and 4 (as indicated by the direction diagram).

Addition of the bicarbonate causes no change in the H_2CO_3 concentration, so that CO_2 solubility remains satisfied, and the final pH of 6,52 is given by point 4.

Additions of a strong base and carbonate, however, cause undersaturated conditions to develop. The H_2CO_3 concentrations, after the addition of the strong base and carbonate, are given respectively by 400 and 1100 ppm as $CaCO_3$. pH in both cases is extraordinarily high. As CO_2 comes into solution to satisfy the undersaturated conditions, the H_2CO_3 concentration increases, causing the ionic equilibrium point to move vertically up. At the same time, the pH is decreasing rapidly. CO_2 solubility is eventually satisfied when the CO_2 in solution is in

equilibrium with the original partial pressure, i.e. point 4. Thus, the final pH is the same in all cases.

The decreasing efficacy of the dosing chemicals with increasing pH (for a constant P_{CO_2}) can be noted in Figure 39. For example: with a constant percentage CO_2 of 40, 500 ppm as $CaCO_3$ of some base is required to raise the pH from 6,0 to 6,3, while 4000 ppm is required to raise the pH from 7,0 to 7,3.

Experimental Verification of the pH Conditioning Diagram for the Addition of Soluble Dosing Chemicals

Experimental verification for dosing with completely soluble chemicals was conducted on samples taken from the anaerobic process treating wine distillery waste. The experimental procedure was as follows:

> Samples were subjected to an atmosphere containing 39% CO_2 and 71% CH_4 until CO_2 saturation was achieved. Temperatures were adjusted to 20°C, pH's to the low initial values required, and ionic strengths to 0,1. The gas source was then removed, and samples dosed with NaOH, Na_2CO_3 and $NaHCO_3$ respectively. The pH was allowed to become stable, after which the gas source was re-introduced to saturate the sample with CO_2. After dosing (in the absence of the CO_2 source), ionic equilibrium was attained quickly, and consequently, pH measurements were taken almost immediately. The time taken to reach CO_2 solubility equilibrium under the experimental conditions was of the order of 10 min. Thus, measurement of the final pH (with ionic and CO_2 solubility equilibria both satisfied) was taken after 10 minutes. Samples which were subsequently left for up to 24 hours showed no change in the pH values. Details of the experimental procedure are set out in Appendix I.

pH measurements at (a) ionic equilibrium (with undersaturated CO_2 conditions) and (b) ionic and CO_2 solubility equilibrium are recorded on Table VIII together with the theoretical pH values obtained graphically from the pH conditioning diagram (see example in preceding subsection - page 138). The experimental results are represented on the pH conditioning diagrams in Figures 41, 42 and 43.

TABLE VIII

Comparison of measured and theoretical pH's (as obtained from the pH conditioning diagram) for the addition of soluble dosing chemicals to samples of actively digesting spent wine (ionic strength 0,1; temperature 20°C; 39% CO_2 atmosphere).

Dosing Chemical	Dosing Quantity Added ppm as $CaCO_3$	pH on Addition of Dosing Chemical (CO_2 Undersaturated Conditions)		pH After CO_2 Saturation is Achieved	
		Measured	Theoretical	Measured	Theoretical
Na_2CO_3	0	-	-	6,12	6,12
	500	6,63	6,57	6,42	6,40
	500	6,82	6,73	6,62	6,58
	500	6,93	6,85	6,75	6,71
	0	-	-	6,30	6,30
	3000	8,00	-	7,01	6,94
NaOH	0	-	-	6,30	6,30
	500	6,90	6,95	6,52	6,52
	500	7,12	7,10	6,65	6,64
	500	7,19	7,20	6,76	6,75
	500	7,35	7,28	6,85	6,83
	0	-	-	6,23	6,23
	3000	8,85	-	6,94	6,96
$NaHCO_3$	0	-	-	6,20	6,20
	500	-	-	6,43	6,61
	500	-	-	6,60	6,61
	500	-	-	6,71	6,72
	1000	-	-	6,88	6,88

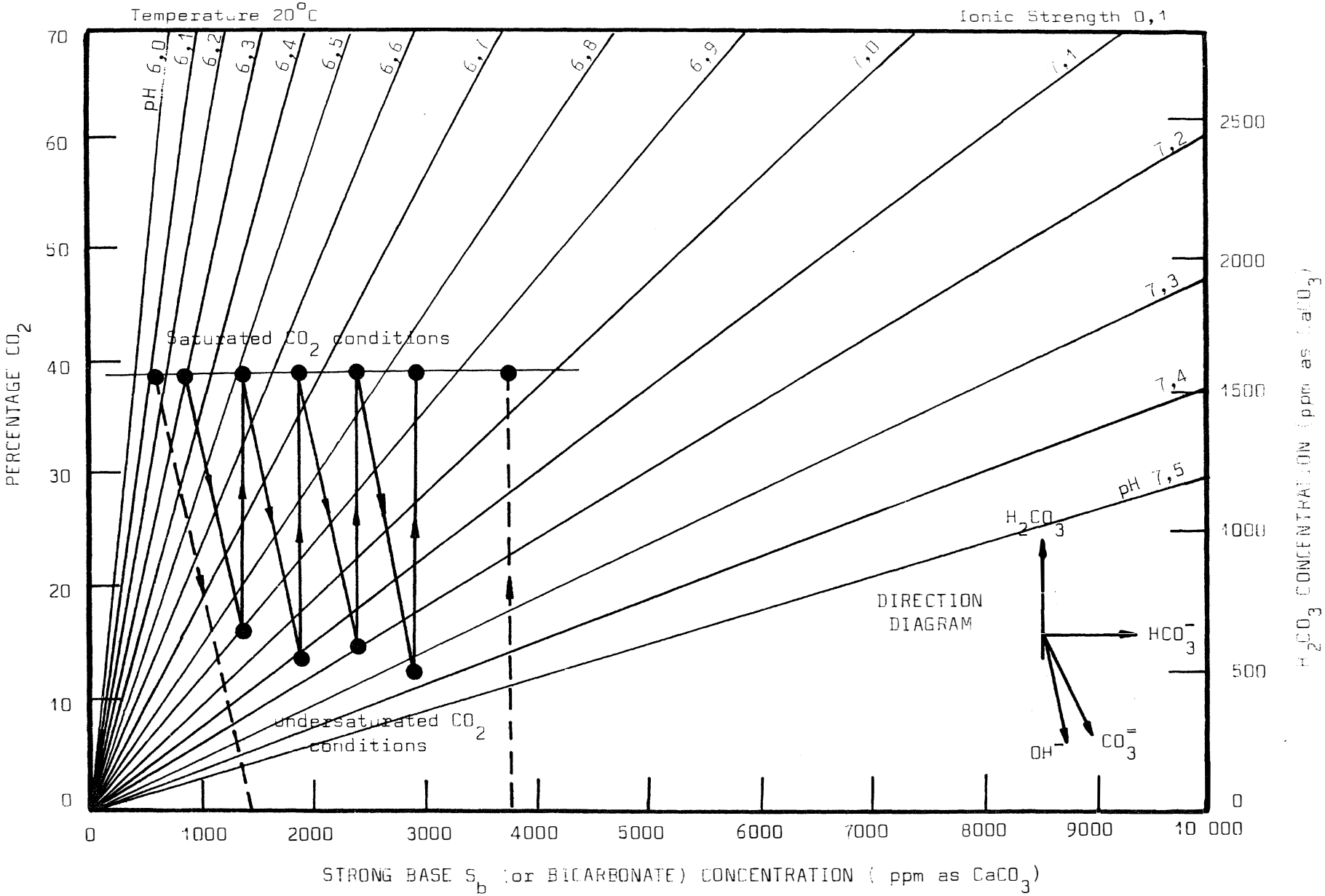

FIGURE 41: pH Movement in an Actively Digesting Spent Wine Sample for Successive Additions of NaOH (see Table VIII)

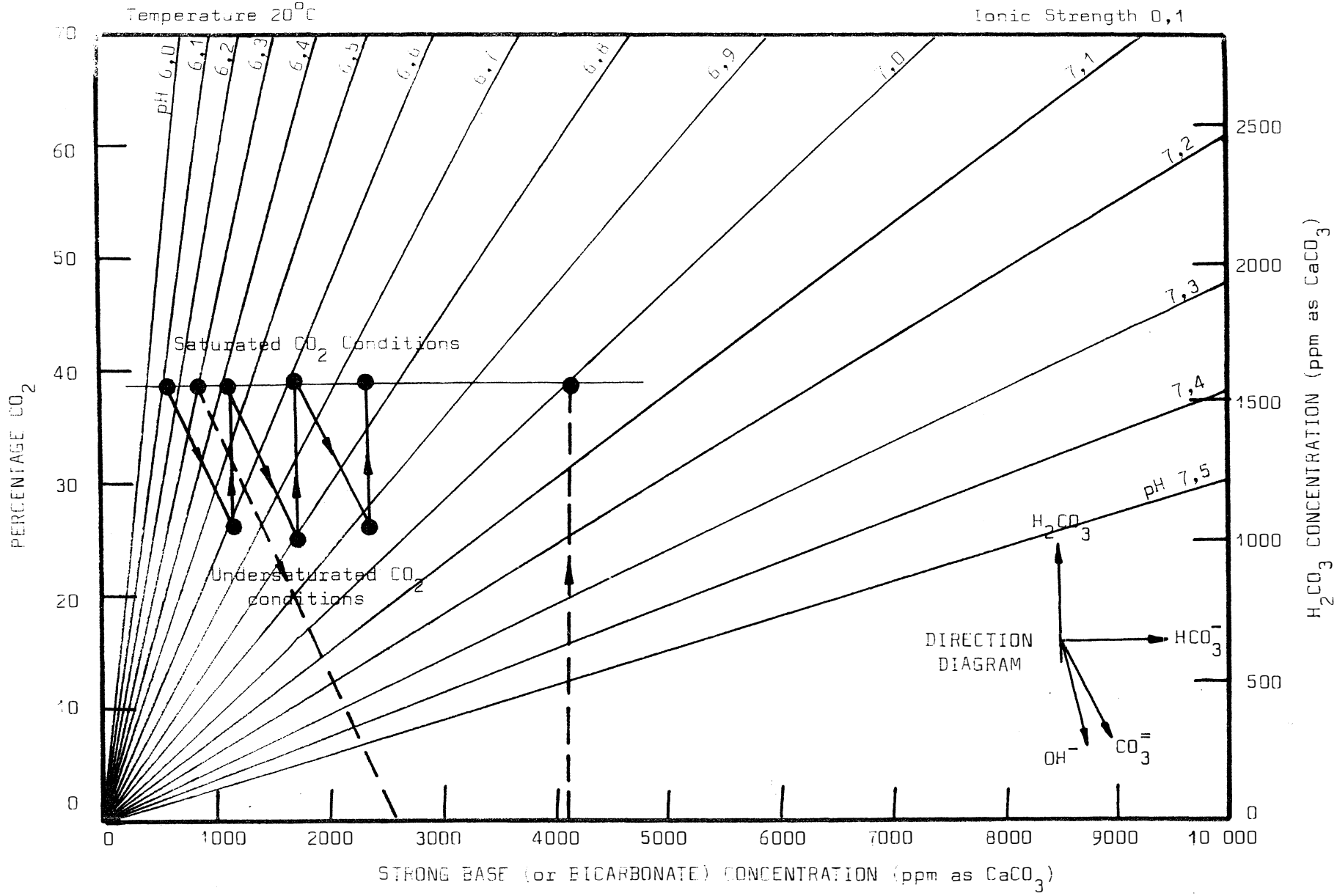

FIGURE 42: pH Movement in an Actively Digesting Spent Wine Sample for Successive Additions of Na_2CO_3 (see Table VIII)

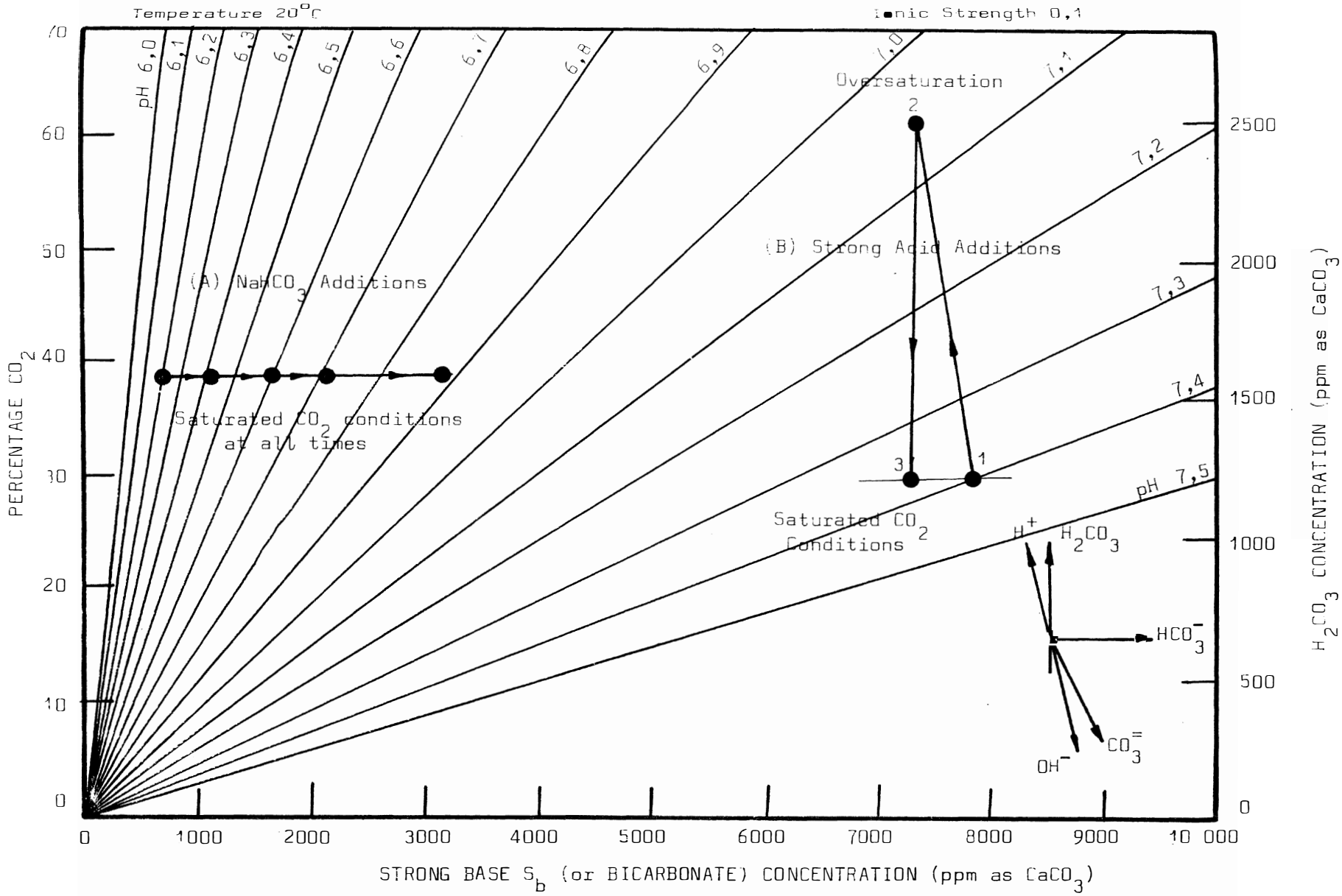

FIGURE 43: (A) pH Movement of an Actively Digesting Spent Wine Sample for Successive Addition of $NaHCO_3$ (see Table VIII)
(B) Theoretical pH Movement for the Addition of 500 ppm as $CaCO_3$ of a Strong Acid

Experimental results obtained in saturated CO_2 conditions (i.e. with ionic and solubility equilibria both satisfied) conformed to the theoretically predicted values closely in all cases. In undersaturated conditions, the pH values for step-wise additions of NaOH and Na_2CO_3 may be followed in Figures 41 and 42. Again, pH values were found to be in agreement with the predicted values from the pH conditioning diagram (Table VII). For large additions of dosing chemicals, the pH in undersaturated CO_2 conditions moves outside the carbonic acid-bicarbonate buffer system (hence off the diagram) and no prediction of the pH in undersaturated conditions can be made.

For the case of pH adjustment with completely soluble dosing chemicals, the pH conditioning diagram appears to provide an accurate method for predicting the pH movement in anaerobic digestors.

Downward Adjustment of pH

The unusual case of pH correction from a high to a low value is graphically shown in Figure 43, for the following theoretical cases:

Initial ionic and CO_2 solubility equilibrium (point 1) is given by a CO_2 percentage of 30 and a pH of 7,40. Addition of 500 ppm as $CaCO_3$ of a strong acid moves the ionic equilibrium in the direction opposite to that for strong base additions, i.e. to point 2. pH at this point is 7,05 and H_2CO_3 concentration 2500 ppm as $CaCO_3$, indicating an over-saturated CO_2 condition. As CO_2 comes out of solution, the H_2CO_3 concentration decreases and the ionic equilibrium point moves verically down. The pH is correspondingly increased until ionic and CO_2 solubility are again both satisfied, i.e. point 3. The final pH is given by 7,37. Large quantities of acid are required to adjust the pH since the buffer capacity in this region is very high.

Anaerobic processes failing at high pH will probably not show signs of failure below pH 7,5. The diagram, however, is limited to a maximum pH of 7,5, so that it will not prove very useful in curing processes failing at high pH. For this reason, and because it is an unusual case, experimental verification of strong acid dosing was omitted. No further consideration is given to pH adjustment at high pH.

pH Conditioning Diagram Incorporating $CaCO_3$ Solubility

Thus far, the discussion and formulations have assumed that the various chemicals are infinitely soluble. Taking the normal dosing quantities into account, the assumption in the case of all sodium compounds is correct. Calcium compounds, however, are relatively insoluble, with $CaCO_3$ forming the solubility limiting condition in the pH range 6,0 to 7,5[37]. Since lime, ($Ca(OH)_2$), is the dosing chemical most often used for adjusting pH in digestors, it is important to investigate the effect of $CaCO_3$ solubility on pH adjustment.

$CaCO_3$ is extremely insoluble, having a solubility product, K_s, of $4,8 \times 10^{-9}$ at 25°C, i.e.

$$[Ca] \times [CO_3] = K_s \qquad ...(39)$$

Permissible calcium concentration lines (i.e. the maximum [Ca] allowable before $CaCO_3$ precipitation occurs) can be plotted on the pH conditioning diagram by relating Ca^{++} with H_2CO_3 and HCO_3^-. The two equilibrium expressions for the dissociation of carbonic acid yield

$$[CO_3] = K_2 \times [HCO_3]/[H]$$

$$[H] = K_1 \times [H_2CO_3]/[HCO_3]$$

and by substituting them into equation (39) we arrive at

$$[Ca] = \frac{K_s \times K_1 \times [H_2CO_3]}{K_2 \times [HCO_3]^2}$$

Permissible calcium concentration lines are plotted on the pH conditioning diagram in Figure 44. Temperature and ionic strength corrections for the equilibrium constants are made as set out in Appendix II, and incorporated into the diagram. The diagram demonstrates that the permissible calcium concentration decreases rapidly with increasing pH, particularly in the low pH regions. In a normally operating process, the maximum permissible Ca^{++} concentration is of the order of 100 ppm as $CaCO_3$.

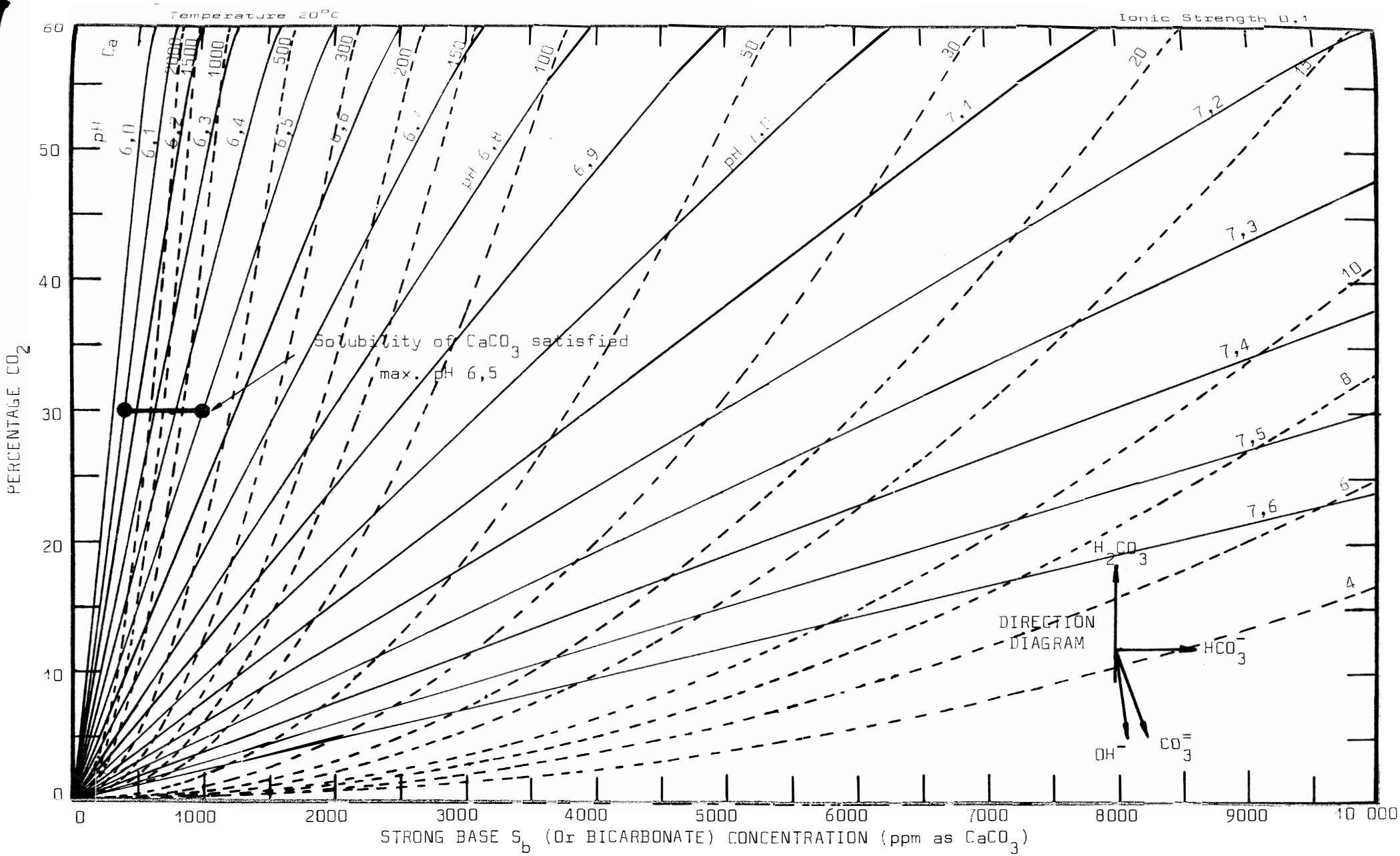

FIGURE 44: pH Conditioning Diagram Including Permissible Ca Concentration Lines (pH Limitation by $CaCO_3$ Solubility for Hypothetical $Ca(HCO_3)_2$ Additions is Shown Also)

Where calcium based dosing chemicals are used, $CaCO_3$ solubility equilibrium, together with ionic and CO_2 solubility, will govern the final pH established. The effect of $CaCO_3$ equilibrium on the final pH is best illustrated by addition of a fictitious chemical, $Ca(HCO_3)_2$, and by referring to Figure 44.

Consider a sample with an initial equilibrium point 1 given by 30% CO_2 and a pH of 6,2. The initial assumed calcium concentration in the sample is zero, i.e. $CaCO_3$ undersaturated conditions exist. The pH is therefore not limited by $CaCO_3$ solubility. $Ca(HCO_3)_2$ is now added slowly, causing the ionic equilibrium point to move in the direction of HCO_3^- increase. The HCO_3^- and Ca^{++} concentration increase by equal amounts. The point where the Ca^{++} concentration added equals the permissible Ca^{++} concentration at ionic equilibrium is also the $CaCO_3$ solubility equilibrium point, i.e. point 2. CO_2 solubility remains satisfied at all times and thus does not affect the pH. Any further addition of $Ca(HCO_3)_2$ will cause the $CaCO_3$ solubility to be exceeded, and $CaCO_3$ will precipitate out. No increase in pH will be achieved since the strong base added as HCO_3^- is removed as $CO_3^=$. pH is therefore limited by $CaCO_3$ solubility.

The order in which the ionic, CO_2 solubility and $CaCO_3$ solubility are satisfied is difficult to establish. Ionic equilibrium is satisfied immediately, but the CO_2 and $CaCO_3$ solubility are very much time dependent reactions. The rate of the reactions will be dependent, amongst other things, on the concentrations of the component species. It is stressed that the rates of reaction only govern the pH while under or oversaturated CO_2 and $CaCO_3$ conditions prevail. The final equilibrium point and pH are independent of the reaction rates. These observations are best illustrated by considering a theoretical example dealing with two extreme cases, one in which CO_2 solubility is completely satisfied before $CaCO_3$ solubility is satisfied; the other in which $CaCO_3$ solubility is first satisfied. The movement of pH is presented on the pH conditioning diagram (Figures 45 and 46).

Consider a process with an initial CO_2 percentage of 40, a pH of 6,4 and a calcium concentration equal to zero. These conditions define the initial equilibrium, point 1 in Figures 45 and 46. Ionic and CO_2 solubility equilibria are both satisfied and undersaturated $CaCO_3$

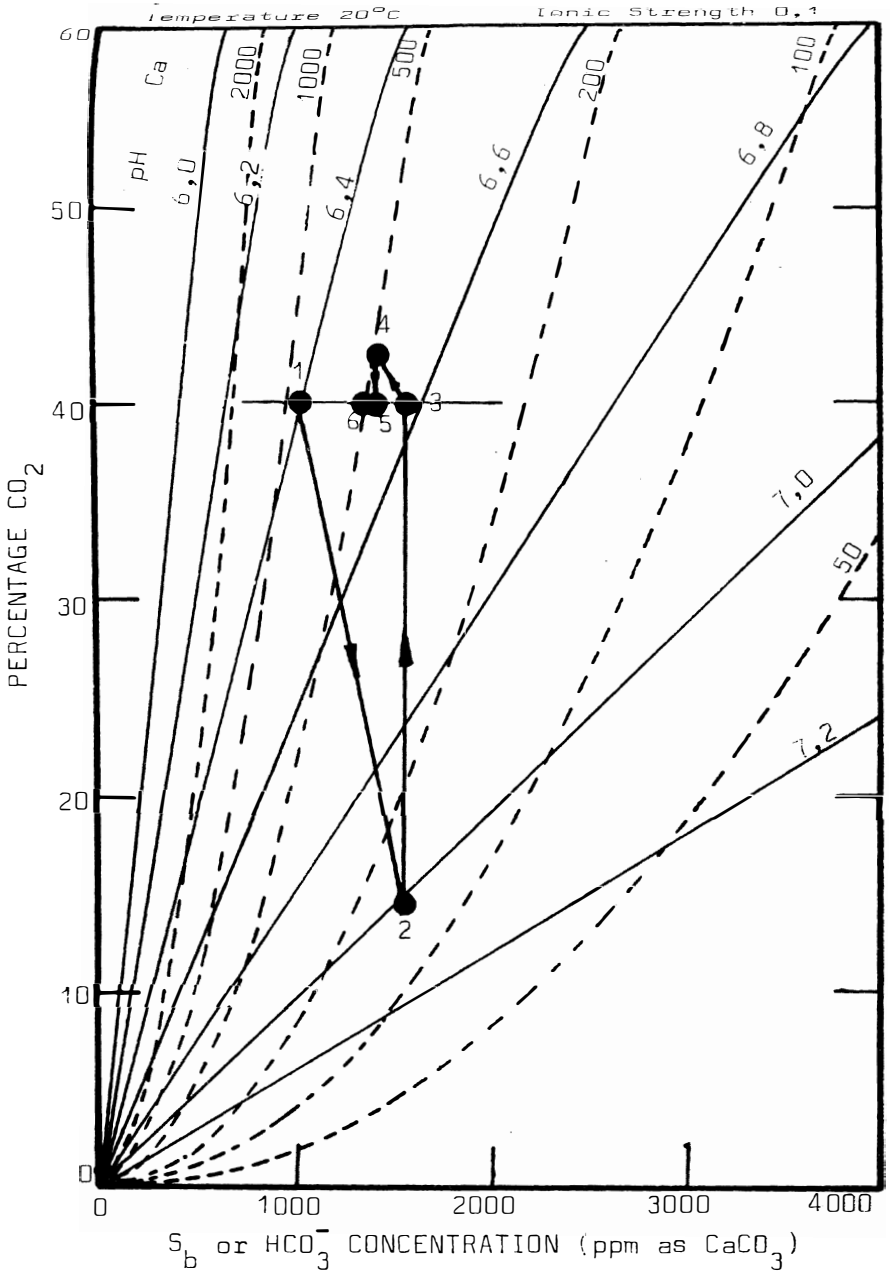

FIGURE 45: pH Movement for $Ca(OH)_2$ Dosing - CO_2 Equilibrium is Satisfied Before $CaCO_3$ Equilibrium

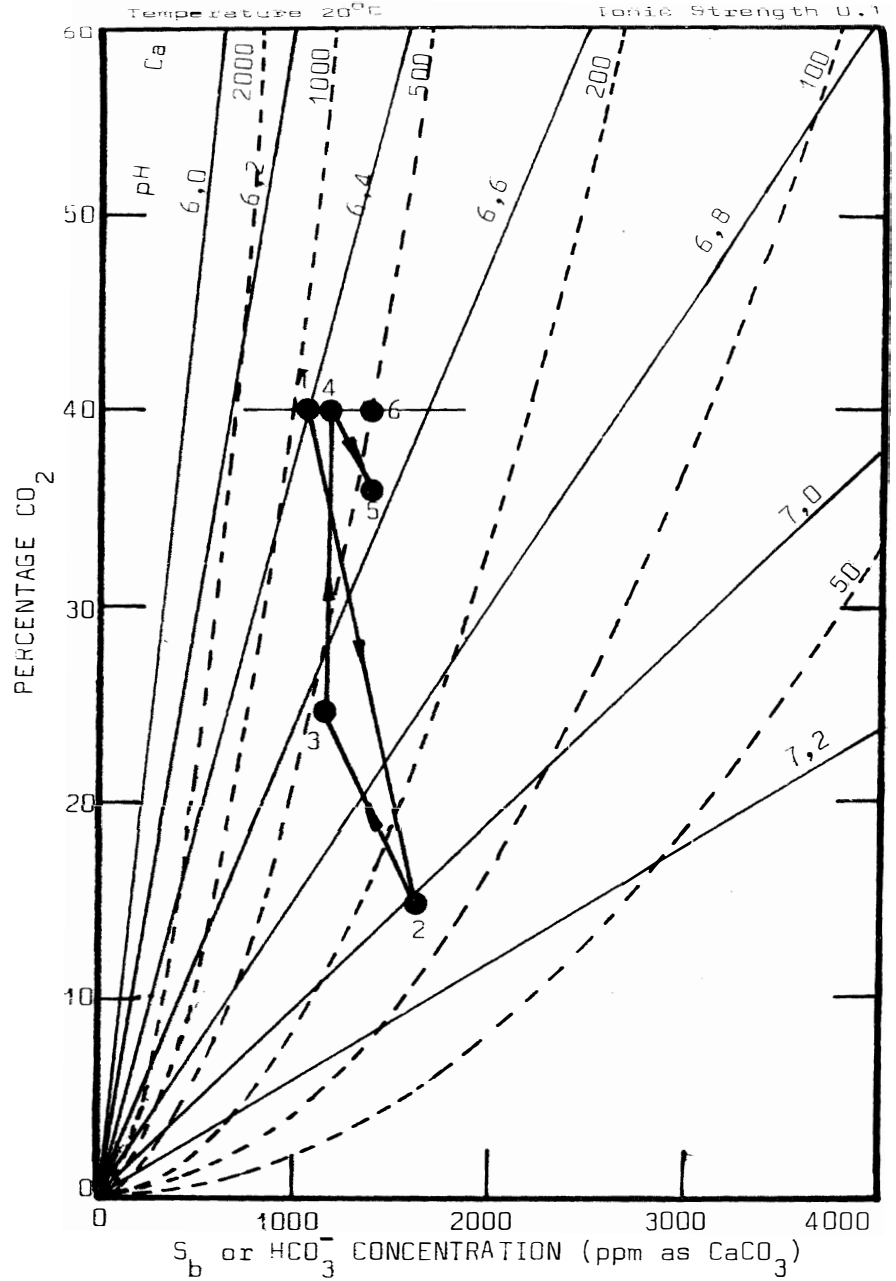

FIGURE 46: pH Movement for $Ca(OH)_2$ Dosing - $CaCO_3$ Equilibrium is Satisfied Before CO_2 Equilibrium

conditions exist. $Ca(OH)_2$ is now added to raise the pH. Addition of 600 ppm of $Ca(OH)_2$ as $CaCO_3$ moves the ionic equilibrium to point 2, as described by the direction diagram. The system is now oversaturated with respect to CO_2.

The case where CO_2 solubility is satisfied will be considered first (see Figure 45). To satisfy the CO_2 solubility equilibrium, H_2CO_3 comes into solution causing the ionic equilibrium point to move vertically up to point 3. The system remains oversaturated with $CaCO_3$, and its precipitation causes the ionic equilibrium to move to point 4 as shown by the direction diagram (reverse direction of $CO_3^=$ added). At point 4, the calcium concentration remaining in the system is equal to the permissible calcium concentration as shown on the diagram. CO_2 must now come out of solution to satisfy the CO_2 solubility, and the ionic equilibrium moves to point 5. $CaCO_3$ solubility will again be exceeded, causing further $CaCO_3$ precipitation and CO_2 oversaturated conditions. These sequential adjustments to pH will proceed until such time as the ionic, CO_2 solubility and $CaCO_3$ solubility equilibria are all satisfied, as shown by point 6.

The case where $CaCO_3$ equilibrium is satisfied before CO_2 equilibrium will now be considered (see Figure 46). As $CaCO_3$ is precipitated out, the ionic equilibrium point moves in the direction of CO_3 removal until such point where the remaining calcium concentration equals the permissible calcium concentration, i.e. point 3. $CaCO_3$ solubility is now satisfied, but the system remains undersaturated with respect to CO_2. Ionic equilibrium now moves vertically up to point 4 to satisfy the CO_2 solubility, which makes the system undersaturated with respect to $CaCO_3$. Dissolution of $CaCO_3$ is extremely slow, but ionic equilibrium will eventually move to point 5 where the $CaCO_3$ solubility is satisfied. CO_2 will again come into solution to satisfy solubility. These adjustments continue till ionic, CO_2 solubility and $CaCO_3$ solubility are all satisfied, as shown by point 6. The final equilibrium (point 6) is identical in both cases (Figures 45 and 46).

The movement of pH in the aquatic system of a normal anaerobic process is likely to fall between the two extreme cases described above. If lime is added slowly so as to maintain CO_2 and $CaCO_3$ solubility-

equilibrium conditions, the equilibrium point moves horizontally across to point 6 on Figures 45 and 46.

Experimental verification for $Ca(OH)_2$ additions (in the form of a slurry) was conducted on a de-ionized water adjusted to an ionic strength of 0,1, a temperature of 20°C, and saturated in an atmosphere containing 39% CO_2. Isolation of the intermediate pH's in over and undersaturated conditions proved difficult, and only final pH's were measured when all the equilibria were considered satisfied. pH generally reached stability after 15 min to 20 min. Details of the experimental procedures are set out in Appendix I.

The final measured pH's for the addition of various quantities of $Ca(OH)_2$ are recorded on Table IX. These values may be compared with the theoretically predicted pH's obtained from the pH conditioning diagram showing the calcium solubility lines (Figure 44). Predicted pH's for the hypothetical case of considering calcium to be infinitely soluble are also recorded in Table IX (i.e. the pH's which would have been recorded had NaOH been used instead of $Ca(OH)_2$).

Experimental and theoretical results are in close agreement, showing that $CaCO_3$ solubility equilibrium limits pH adjustments to relatively low pH's. Thus, in the prepared water samples, pH adjustment to a value of 7,00 is impossible with $Ca(OH)_2$ additions.

The results of experiments performed on samples taken from processes treating spent wine and domestic sludge did not follow the predicted values of the pH conditioning diagram. Inhibition of $CaCO_3$ precipitation by orthophosphates was isolated as the factor causing the discrepancy between measured and theoretical results (see Part H).

TABLE IX

Comparison of measured and theoretical pH's (as obtained from the pH conditioning diagram) for the addition of $Ca(OH)_2$ to water samples (ionic strength 0,1; temperature 20°C; 39% CO_2 atmospheres).

$Ca(OH)_2$ Added ppm as $CaCO_3$	Final pH		Calculated pH for hypothetical infinite Ca^{++} Solubility
	Measured	Theoretical	
0	6,00	6,00	6,00
500	6,35	6,34	6,34
500	6,42	6,43	6,53
500	6,42	6,43	6,67
1000	6,42	6,43	6,85
1000	6,42	6,43	6,92
0	6,40	6,40	6,40
500	6,53	6,54	6,57
500	6,53	6,54	6,69
1000	6,53	6,54	6,87

H. INHIBITION OF $CaCO_3$ PRECIPITATION

The use of lime as a dosing chemical to raise the pH to 7,0 is feasible only if $CaCO_3$ precipitation is inhibited. Fortunately, most wastes appear to contain some inhibitory agent, the principal one probably being orthophosphate.

Inhibition of $CaCO_3$ precipitation by orthophosphate has previously been noted by Stumm[43], Bachra[44] and Schmid[45]. Van Wazer[46], has attributed the inhibition mechanism to the ability of chain phosphates to absorb onto growing surfaces and nuclei of calcium carbonate crystals, thereby preventing the growth of the crystals. However, it will be apparent from the following experiments that a fraction of the dissociated calcium and carbonate species did not even combine to form nuclei, but that they remained in their ionic form.

A series of experiments was run to determine the inhibitory effect of different orthophosphate concentrations on $CaCO_3$ precipitation. (De-ionized water was used to make up the samples.) Also the same experiments were repeated on samples taken from the anaerobic processes treating spent wine and domestic sludge. A comparison of these two sets of results made it possible to determine whether the mechanism of $CaCO_3$ precipitation inhibition by orthophosphates in the artificial solution was the same as the mechanism of inhibition observed in the anaerobic digestor samples.

Water samples were prepared with orthophosphate (Na_2HPO_4) concentrations of $0,1 \times 10^{-3}$; $0,5 \times 10^{-3}$; $1,0 \times 10^{-3}$ and $6,0 \times 10^{-3}$ moles/l (in the same range as that found in anaerobic digestors), ionic strengths of 0,1, temperatures of 20°C, and saturated with CO_2 in an atmosphere containing 39% CO_2. Initial pH's were set to either 6,0 or 6,4 by addition of H_2SO_4. $Ca(OH)_3$ was incrementally fed, in the form of a slurry, and the pH was taken after each addition, once equilibrium was established (in a 39% CO_2 atmosphere). The time taken for the pH to reach stability in each case was of the order of 10 minutes. Details of the experimental procedure are available in Appendix I. The same experimental technique was used on the samples from the anaerobic processes, except that no adjustment to the orthophosphate concentration was made.

The pH movement for the addition of each dose of $Ca(OH)_2$ was graphically analysed on pH versus S_b (or HCO_3^-) diagrams (e.g. Figure 47). These diagrams include

(a) the equilibrium line for NaOH additions, which is equivalent to considering $Ca(OH)_2$ additions if Ca^{++} were infinitely soluble (i.e. no $CaCO_3$ precipitation); and

(b) the equilibrium line for $Ca(OH)_2$ additions to a sample containing no orthophosphates (the dotted line indicates the maximum pH attainable - further increase in S_b is impossible, and $Ca(OH)_2$ additions merely cause $CaCO_3$ precipitation).

Both these lines were obtained from a pH conditioning diagram (for a constant 39% CO_2), and have been experimentally verified - see Tables VIII and IX. The initial equilibrium points of the samples were fixed by the measured pH and the $[HCO_3]$ obtained from the pH conditioning diagram (for 39% CO_2 atmosphere), and plotted on the diagrams (e.g. Figure 47), Thereafter, the recorded pH was plotted against the $Ca(OH)_2$ additions (e.g. Figure 47).

The pH versus HCO_3^- concentration for each experimental run was plotted on these diagrams, as shown by the run with a water sample containing an orthophosphate concentration of 3×10^{-3} moles/l in Figure 47. The difference in HCO_3^- concentrations between this experimental line and the line which considers calcium infinitely soluble, gives the concentration of $CO_3^=$ which was precipitated out, presumably as $CaCO_3$. These values are plotted against the $Ca(OH)_2$ concentration added, as shown in Figure 48 for a 3×10^{-3} moles/l concentration of orthophosphate. The slope of the line indicates that a constant fraction of $Ca(OH)_2$ added was precipitated out as $CaCO_3$. Results for samples containing orthophosphate concentrations of $1,0 \times 10^{-3}$; $3,0 \times 10^{-3}$; and $6,0 \times 10^{-3}$ moles/l are generally similar.

Examination of Figure 48 reveals that $CaCO_3$ precipitation is mainly dependent on $Ca(OH)_2$ additions, and not on pH. The fraction of $CaCO_3$ precipitated to $Ca(OH)_2$ added can be approximated as constant, and was equal to 0,50; 0,60 and 0,61 for orthophosphate concentrations of $1,0 \times 10^{-3}$; $3,0 \times 10^{-3}$ and $6,0 \times 10^{-3}$ moles/l respectively.

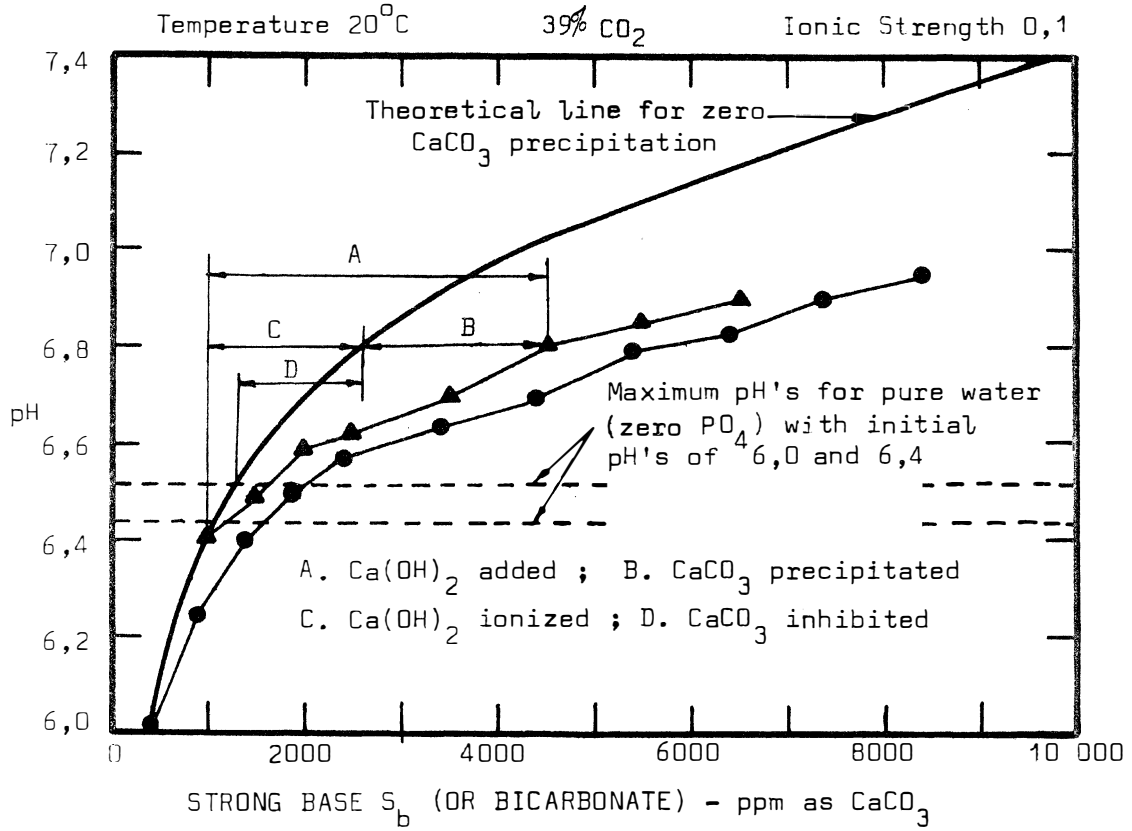

FIGURE 47: Inhibition of $CaCO_3$ Precipitation in Water Containing 3×10^{-3} moles/l of Orthophosphate for $Ca(OH)_2$ Additions

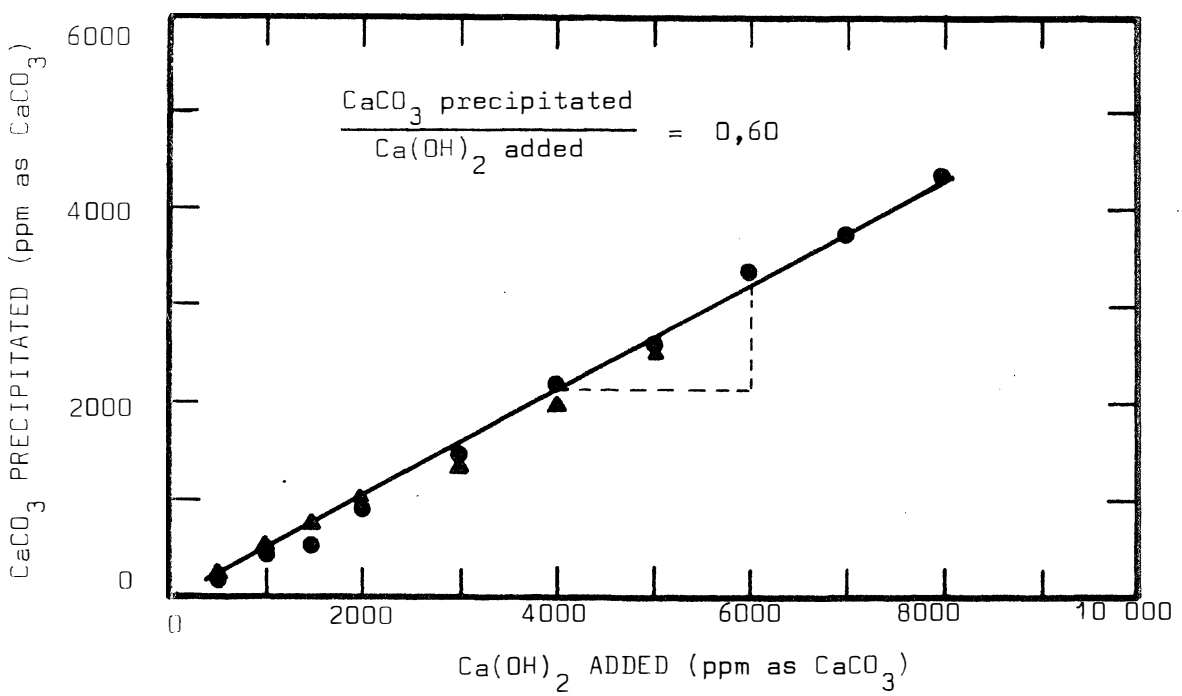

FIGURE 48: Ratio of $CaCO_3$ Precipitated to $Ca(OH)_2$ Added for a Water Sample Containing 3×10^{-3} moles/l of Orthophosphate (see Figure 47)

Results from the samples removed from processes treating spent wine and domestic sludge are shown in Figures 49, 50, 51 and 52. Measured orthophosphate concentrations were $2,5 \times 10^{-3}$ and $2,0 \times 10^{-3}$ moles/l respectively. Results followed trends similar to those of pure water with orthophosphate additions ($1,0 \times 10^{-3}$ to $6,0 \times 10^{-3}$ moles/l). The fraction of $CaCO_3$ precipitated to $Ca(OH)_2$ added was found to be 0,55 in both cases. It thus appears that inhibition of $CaCO_3$ precipitation in most anaerobic processes is caused by orthophosphates.

The mechanism of inhibition of $CaCO_3$ precipitation by orthophosphates is not clear:

(a) From the experiments conducted above, it can be shown that one mole of orthophosphate can keep as much as 30 moles of Ca^{++} from precipitating out. However, compounds or complexes which combine in this ratio, i.e. $(Ca)_{30}(PO_4)$ are not reported in literature.(47)

(b) Prevention of crystal growth of $CaCO_3$ nuclei(46) does not appear to govern the inhibition of $CaCO_3$ precipitation, since it is in fact the formation of the $CaCO_3$ nuclei which is inhibited. This is indicated by the measured pH's in the experiments conducted above, which show that part of the Ca^{++} and $CO_3^{=}$ remained in ionic form, and did not combine to form $CaCO_3$. Had the Ca^{++} and $CO_3^{=}$ completely combined to form $CaCO_3$, no pH increase above the pH defined by the $CaCO_3$ solubility would have been possible.

(c) It therefore appears that orthophosphates have in some way a direct effect on the solubility of $CaCO_3$.

Equilibrium was attained approximately 10 minutes after dosing, and samples subsequently left for up to 24 hours showed no change in pH. The mechanism of inhibition of $CaCO_3$ precipitation appears to be stable and relatively independent of time.

In the samples having orthophosphate concentrations lower than 1×10^{-3} moles/l, the pattern of $CaCO_3$ precipitation changed. Experimental results for concentrations of 1×10^{-4} and 5×10^{-4} moles/l are shown in Figures 53 and 54. $CaCO_3$ initially precipitated

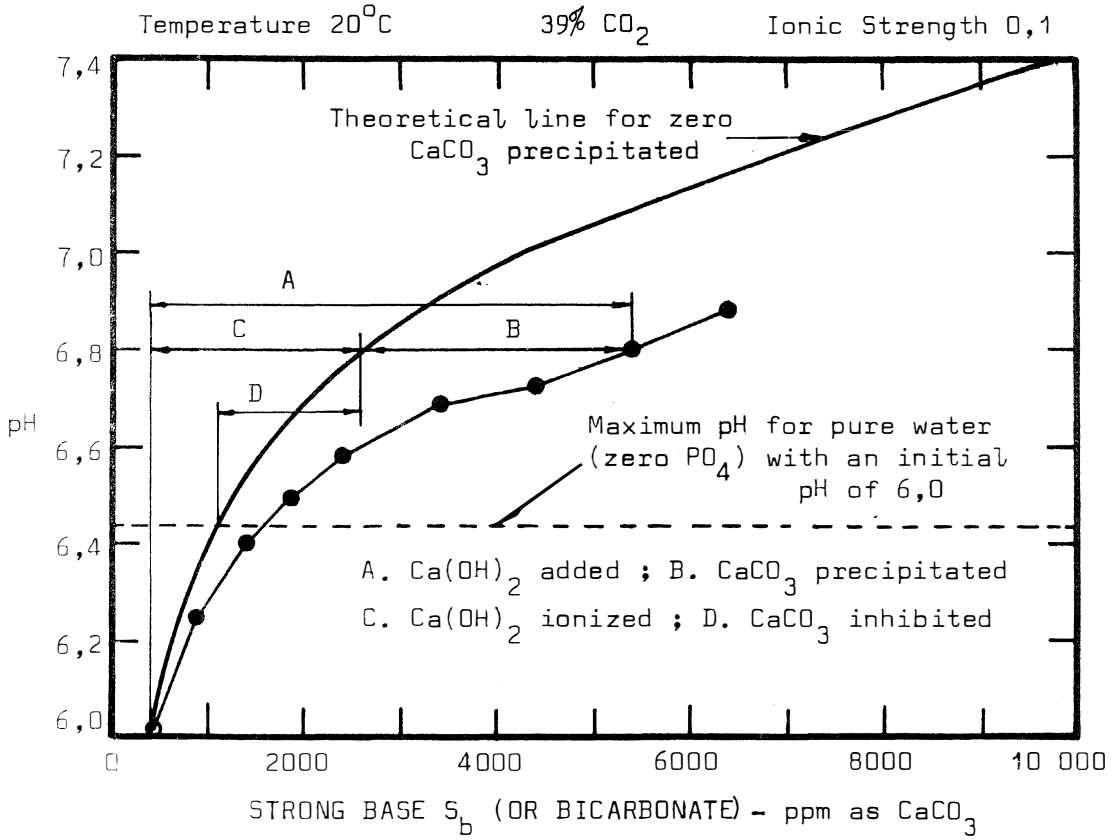

FIGURE 49: Inhibition of $CaCO_3$ Precipitation in Actively Digesting Spent Wine ($[PO_4]$ = $2,5 \times 10^{-3}$ moles/l) for $Ca(OH)_2$ Additions

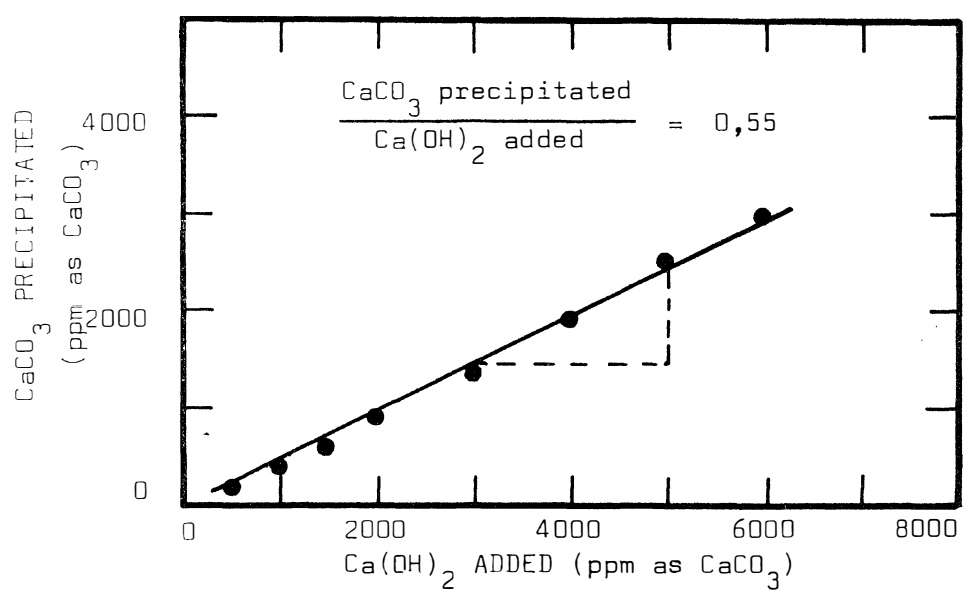

FIGURE 50: Ratio of $CaCO_3$ Precipitated to $Ca(OH)_2$ Added in Actively Digesting Spent Wine ($[PO_4]$ = $2,5 \times 10^{-3}$ moles/l) - see Figure 49.

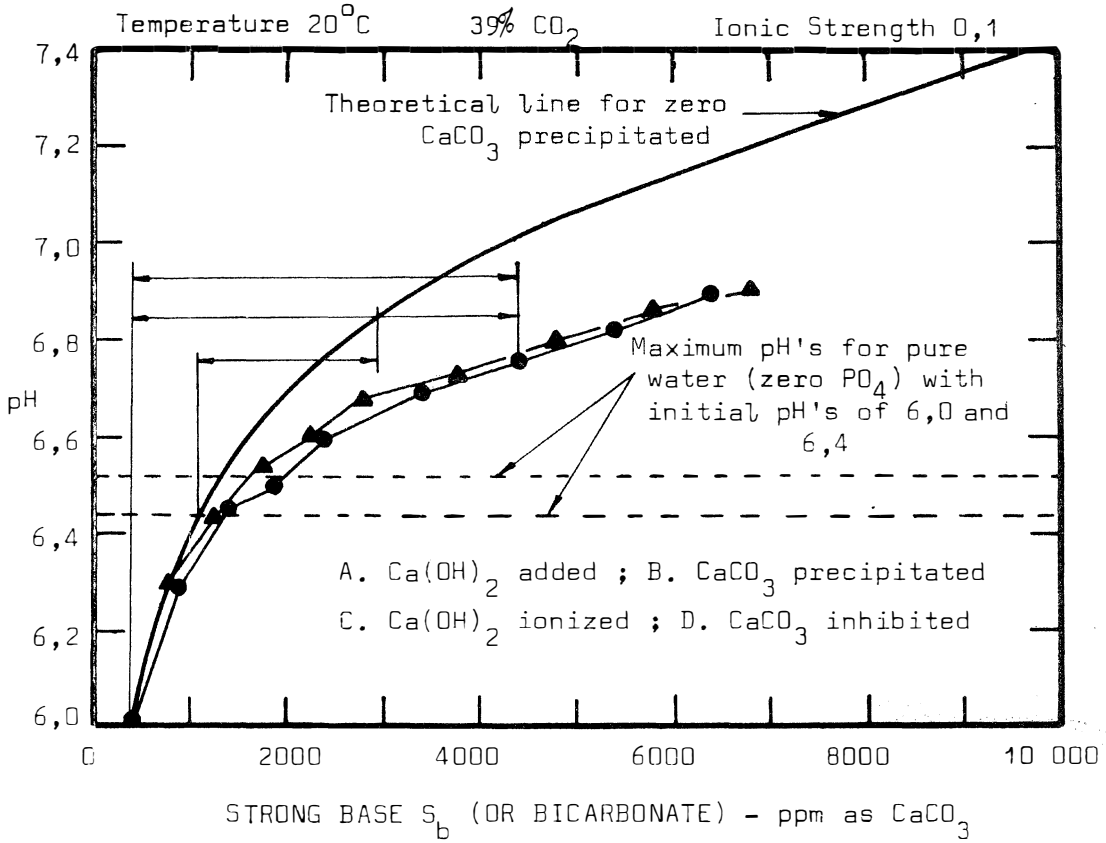

FIGURE 51: Inhibition of $CaCO_3$ Precipitation in Actively Digesting Domestic Sludge ($[PO_4] = 2,0 \times 10^{-3}$ moles/l) for $Ca(OH)_2$ Additions

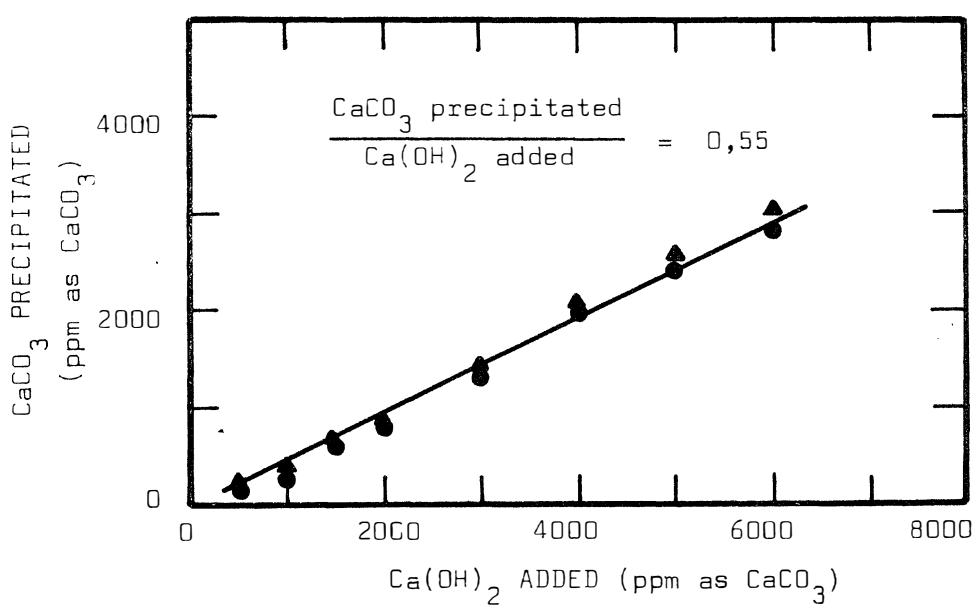

FIGURE 52: Ratio of $CaCO_3$ Precipitated to $Ca(OH)_2$ Added in Actively Digesting Spent Wine ($[PO_4] = 2,0 \times 10^{-3}$ moles/l) - see Figure 51

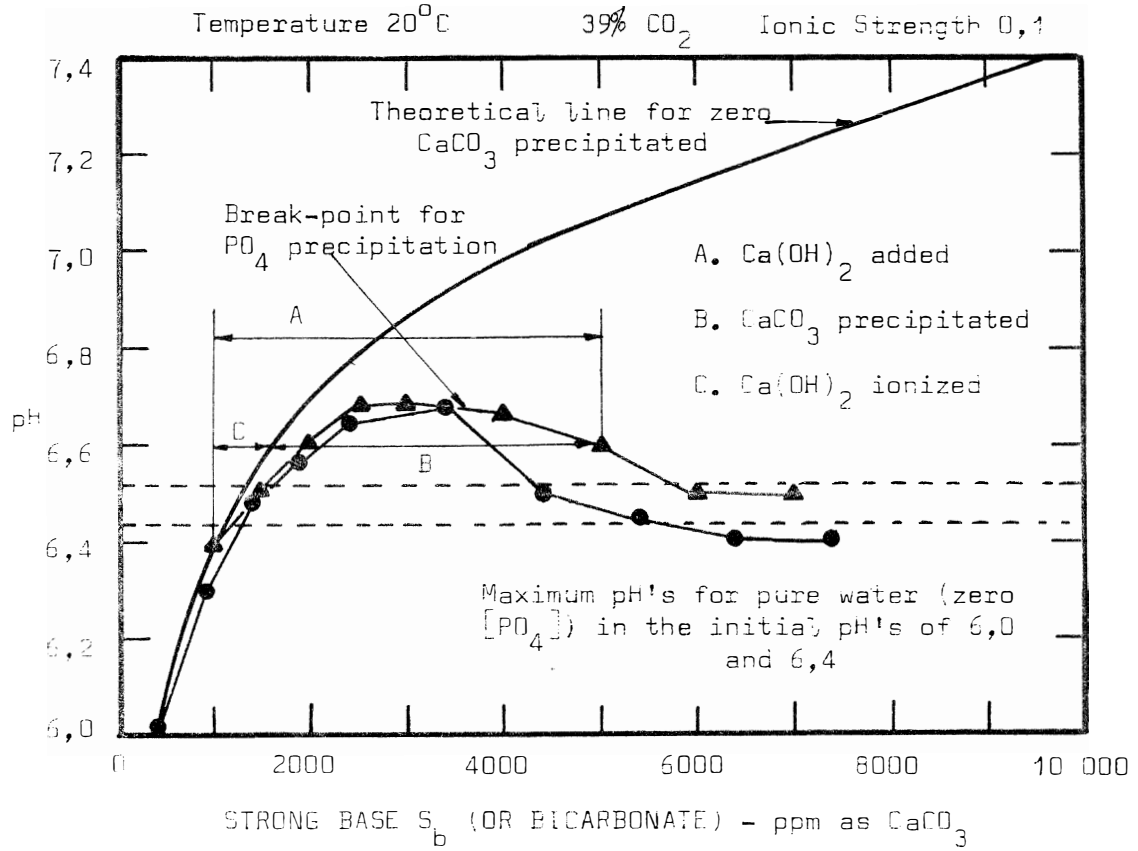

FIGURE 53: Failure of the Mechanism of $CaCO_3$ Precipitation Inhibition in a Water Sample Containing 1×10^{-4} moles/l of Orthophosphate

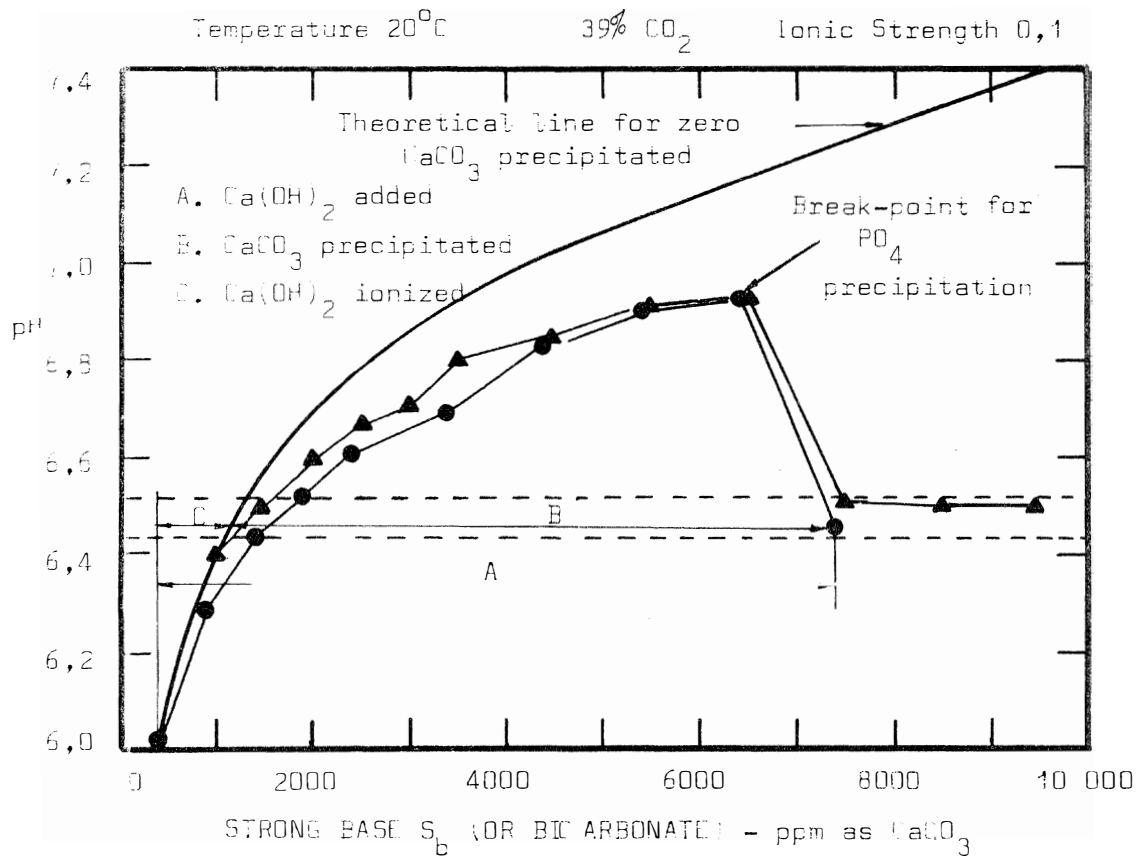

FIGURE 54: Failure of the Mechanism of $CaCO_3$ Precipitation Inhibition in a Water Sample Containing 5×10^{-4} moles/l of Orthophosphate

out in the same proportion to $Ca(OH)_2$ added as in the case of samples with high concentrations of orthophosphates. At a certain point, however, the orthophosphates themselves appeared to precipitate out completely. In so doing, they no longer inhibited $CaCO_3$ precipitation, and the excess Ca^{++} and $CO_3^{=}$ species which were held in solution precipitated out. The system was thus returned to the simple orthophosphate-free system where pH increase above a certain level was impossible because of the limiting $CaCO_3$ solubility equilibrium.

The point at which orthophosphates precipite out is not clear, and probably depends, amongst other factors, on pH, HCO_3^- and Ca^{++} concentrations. The rate of reaction for the phosphate precipitation, and consequently the $CaCO_3$ precipitation which followed, was found to be relatively slow. Up to 3 hours were required before the pH reached stability. Phosphate precipitation, probably in the form of $CaHPO_4$ has been reported to have slow precipitation rates[43].

An investigation was made to determine whether complete phosphate precipitation was possible in a water sample containing $3,0 \times 10^{-3}$ moles/l orthophosphate. Additions of up to 15 000 ppm of $Ca(OH)_2$ as $CaCO_3$ caused an initial increase in the pH, up to 7,2, where it remained stable even after three hours of reaction time. Apparently, sufficient phosphate was left in solution to inhibit $CaCO_3$ precipitation.

In conclusion, it appears that if the aquatic system of an anaerobic process contains about 3×10^{-3} moles/l of orthophosphates, $CaCO_3$ precipitation will always be partially inhibited. A pH increase to 7,0 and higher will therefore be possible with $Ca(OH)_2$ additions. However, if the orthophosphate concentration is below 1×10^{-3} moles/l, the danger exists that the phosphates will precipitate out; inhibition of $CaCO_3$ precipitation would be removed, and $Ca(OH)_2$ additions would merely precipitate out as $CaCO_3$. pH would be limited by the $CaCO_3$ solubility; i.e. in the region of 6,2 (see Figure 44).

Inhibition of $CaCO_3$ precipitation need not be limited to orthophosphates. Polyphosphates, for example, are also strong inhbitors, even in minute concentrations[44]. In anaerobic processes the results of the experiments above indicate that orthophosphate is the principal inhibitor.

I. COMPARISON OF DOSING CHEMICALS

The effect of each dosing chemical on pH has been discussed in detail, and a comparison of their relative merits is now in order. The following list of chemicals was considered as possible dosing agents for raising pH:

NaOH	$Ca(OH)_2$	NH_3
$NaHCO_3$	$CaCO_3$	
Na_2CO_3		

$CaCO_3$ is most unsuitable due to its low solubility and slow rate of dissolution. Consequently, $CaCO_3$ is seldom or never used as a dosing chemical.

$Ca(OH)_2$ is the most frequently used dosing chemical despite some disadvantages. In a process containing more than $1,0 \times 10^{-3}$ moles/l of orthophosphate, $CaCO_3$ precipitation is partially inhibited and approximately 55% of $Ca(OH)_2$ added is precipitated out as $CaCO_3$; only 45% of the lime added contributes towards raising the pH. Besides being inefficiently used, the $Ca(OH)_2$ tends to flocculate the suspended solids in the process and to precipitate them out. Hence, unless proper mixing is maintained in the process, a further deterioration of the process could result. With orthophosphate concentrations lower than $1,0 \times 10^{-3}$ moles/l, the danger exists that the orthophosphates will precipitate out, thus removing the inhibition of $CaCO_3$ precipitation. With the precipitation of $CaCO_3$, the pH is limited to a maximum value where the $CaCO_3$ solubility equilibrium is satisfied. This nowhere near pH 7,0 and the use of lime in this case would prove to be a completely unsatisfactory method of pH adjustment.

Dosing chemicals with sodium cations are all extremely soluble, and do not show the disadvantages of the calcium compounds. $NaHCO_3$ is the most useful of these chemicals since it leaves the H_2CO_3 concentration unchanged. Na_2CO_3 and NaOH cause CO_2 undersaturation, and consequently an abnormally high pH. If only a small supply of CO_2 is available from the gas, the pH may remain permanently high. However, CO_2 production of the organisms is usually sufficient to maintain saturated

CO_2 conditions, providing the dosing chemical is added incrementally over a period of time. The problem of high pH values as a result of large doses of Na_2CO_3 and NaOH is also encountered with $Ca(OH)_2$ additions.

Ammonia, as a dosing agent, will exhibit the same effects on pH as any strong base addition such as NaOH discussed above.

All strong acid additions used to depress the pH react in the same manner. There is therefore no particular advantage in choosing a specific acid, except that toxic chemicals should be avoided.

A disadvantage of all of the dosing chemicals is that they become toxic above a certain threshold concentration. Cation toxicity of sodium and calcium generally becomes significant at concentrations higher than 0,2 and 0,1 moles/l respectively[10]. A combination of cations sometimes alters their toxic threshold, since some cations act antagonistically, and other synergistically with each other. Ammonia and acetic acid (strong base and acid respectively in the pH range 6,0 to 7,5) are especially toxic in their unionized form. The toxic threshold concentrations of ammonia and acetic acid are thus dependent on pH. Care should be taken not to exceed the toxic threshold concentrations for any of the chemicals added. For this reason it may become necessary to add a combination of the dosing chemicals available.

J. pH AND THE MECHANISM OF FAILURE

Anaerobic filters treating wine distillery waste (see Chapter I) were used for this series of experiments. The filters were overloaded by imposing high feed rates to induce conditions of failure in the process. It was hoped that the response of the process under these overloaded conditions would give an indication of the mechanism of failure, and in particular, the influence of pH since it has featured so prominently in past research on failure.

Operating Procedure

To induce initial stable conditions, Filters No. 1 and 2 were operated at a relatively low loading rate of approximately 7,0 kg COD/day/m^3 of hydraulic volume for a period of 35 days. This loading rate corresponds to a hydraulic retention time of 2,7 days.

The processes were overloaded by gradually increasing the loading rates over a period of 20 days. The maximum loading rates (i.e. on the 20th day) were both approximately 65 kg COD/day/m^3 of hydraulic volume, corresponding to a hydraulic retention time of about 0,4 days.

The treatment efficiencies of the processes were monitored by measuring the percentage conversion of waste COD to methane. For this purpose, the waste flow, waste COD, gas production and percentage methane were measured. The gas volume was not corrected for STP, i.e. not reduced by approximately 10%; and no account was taken of the COD converted to organisms - also about 10%. Since these two corrections are of the same order but opposite in action, they are compensatory and the percentage conversion of waste COD to methane (not corrected to STP) thus provides a sufficiently accurate measure of the treatment efficiency.

The following factors governing the pH were measured: percentage CO_2, volatile fatty acids and ammonia. The net strong base S_b was evaluated from the pH conditioning diagram for each particular percentage CO_2 and pH. The contribution to the net strong base S_b by a strong base other than ammonia was calculated as follows (page 124):

$$X = S_b + VFA - NH_3$$

where X = a strong base other than NH_3.

(It has been pointed out that the strong base X is formed, or equivalently hydrogen ions are removed, during the anaerobic waste stabilization process - see page 124).

Past research has indicated that failure of a process is often due to inhibition of methane formation - either by a low pH or by a high volatile fatty acid concentration. Thus, it was hypothesized that eventual failure in the filters would be due to pH, or to factors related to pH. Consequently, all measurements on the mechanism of failure were related to pH. Sludge concentrations in the filter and effluent were <u>not</u> measured; this was an unfortunate omission, for the response of the processes subsequently appeared to indicate that reduction in the organism concentrations in the filters was the dominant factor in the failure mechanism. The volatile fatty acid and pH inhibition mechanism did not appear to contribute significantly to the failure mechanism.

The behaviour of the process was monitored at frequent intervals, since reports have indicated that failure due to inhibition by pH or volatile fatty acids is rapid[48][49]. All parameters monitoring the process were measured three times a day.

For the last ten days of operation of Filter No. 1, a fraction of the solids in the effluent was settled out and returned to the filter. This was initiated when the conclusion was formed that failure was being caused by organism washout and not by the inhibition of the organism activities.

Results

During the initial low loading period (7,0 kg COD/day/m^3), the treatment efficiencies for both filters were approximately 95% COD removals. Subsequently, as the loading intensity increased over the 20 day period of overloading, the efficiency progressively decreased (Figure 55). At the maximum loading rates of 65 kg COD/day/m^3 the treatment efficiencies for Filters No. 1 and 2 were respectively 35% and 25% COD removals.

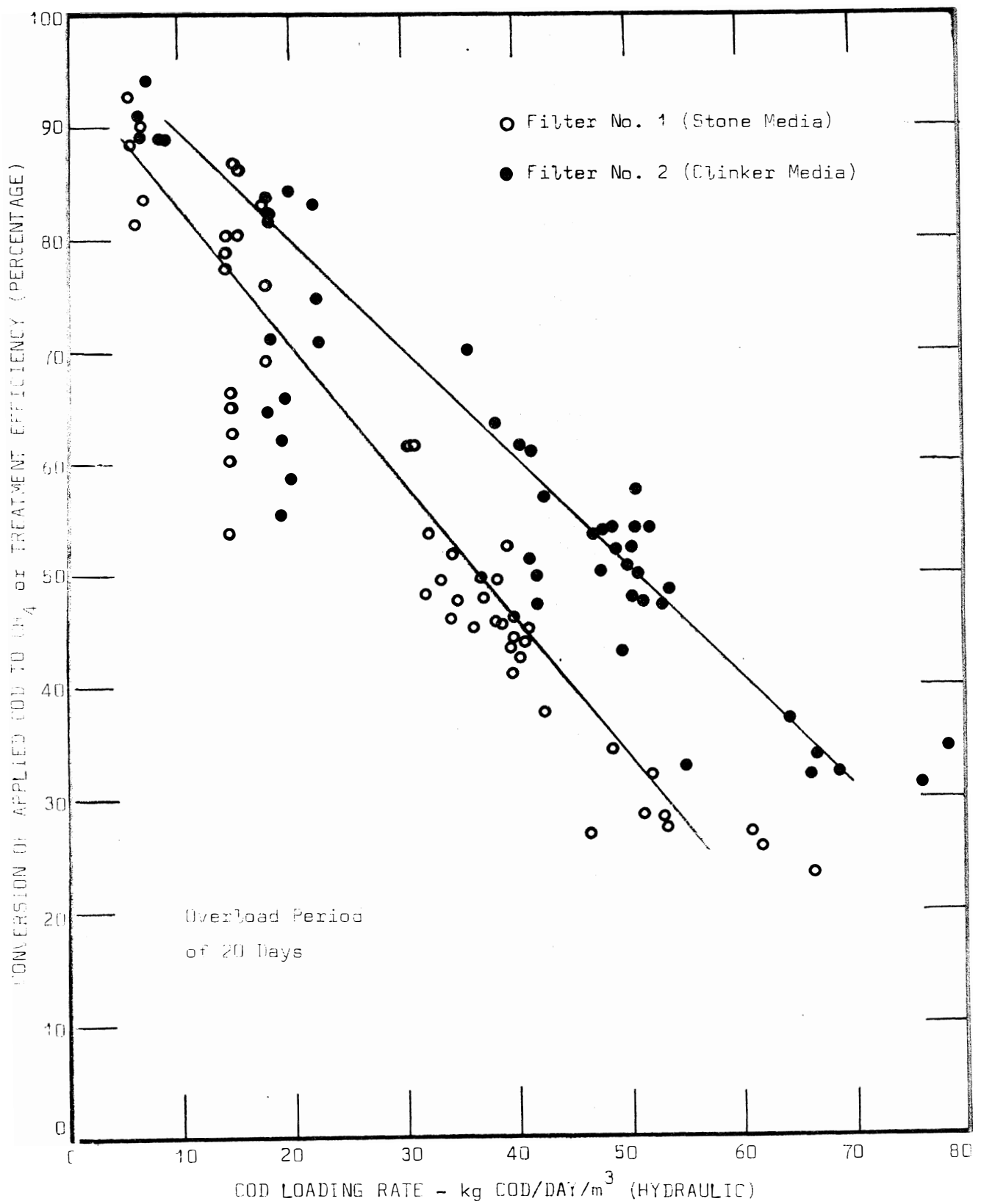

FIGURE 55: Decrease in Treatment Efficiency with Increasing Loading Rate for a Period of Overloading

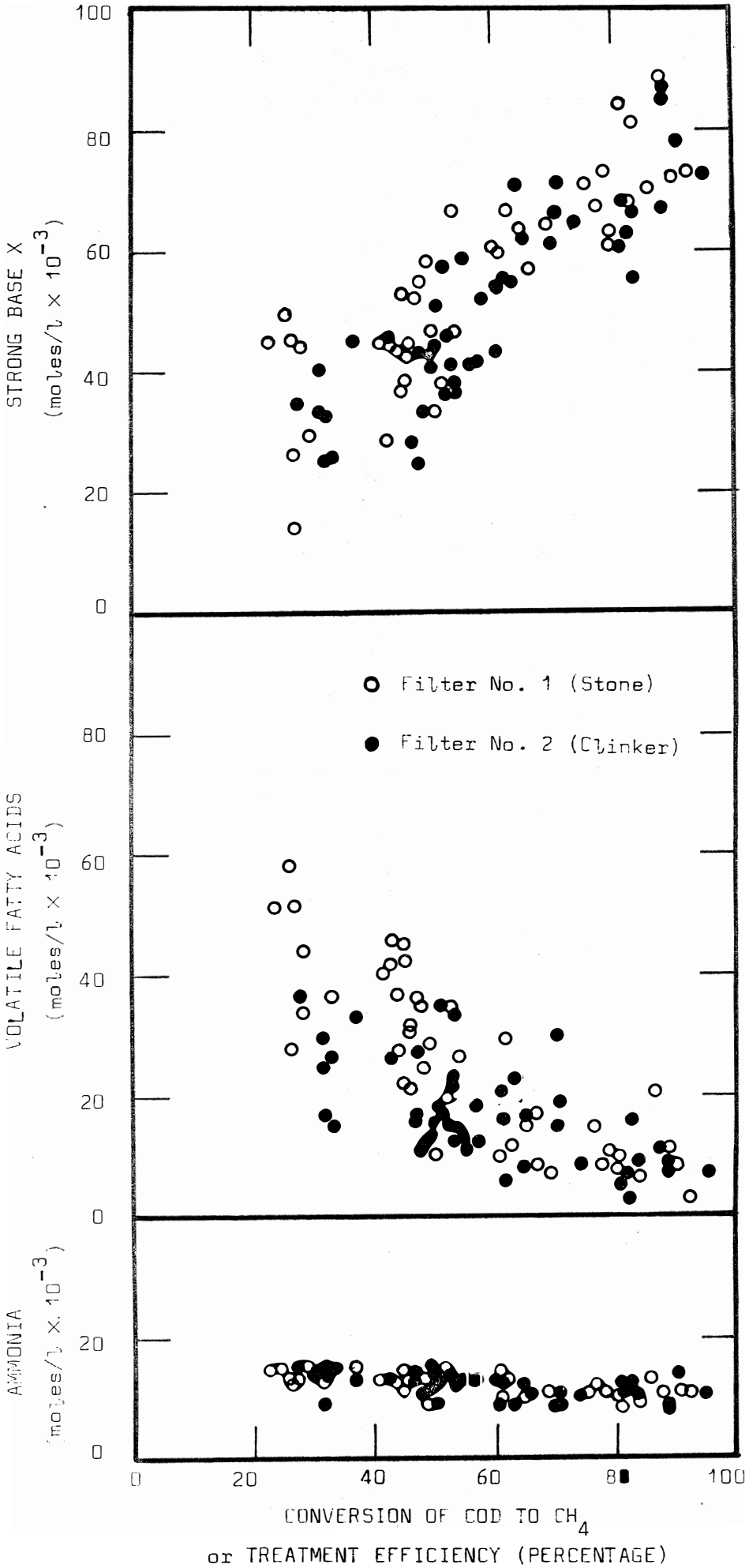

FIGURE 56: Variations in the Concentrations of the Strong Acid-Base Systems Controlling the pH with Decreasing Treatment Efficiency

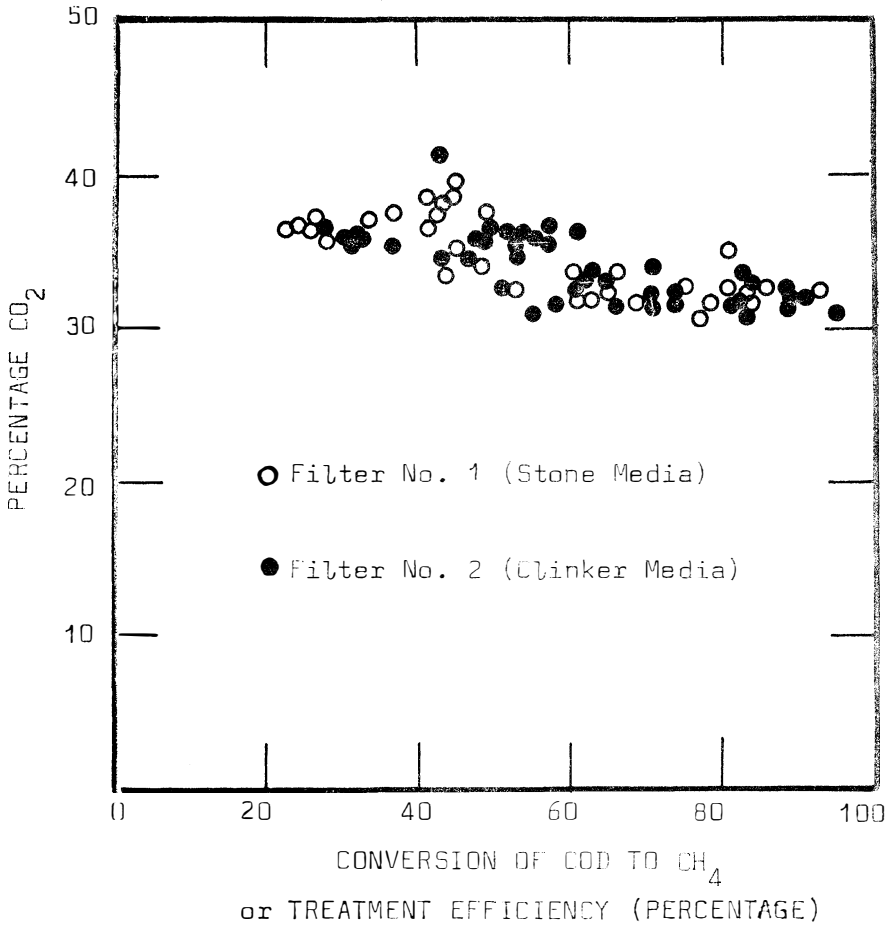

FIGURE 57: Variation in the CO_2 Content of the Digestor Gas with Decreasing Treatment Efficiency for Overloaded Conditions

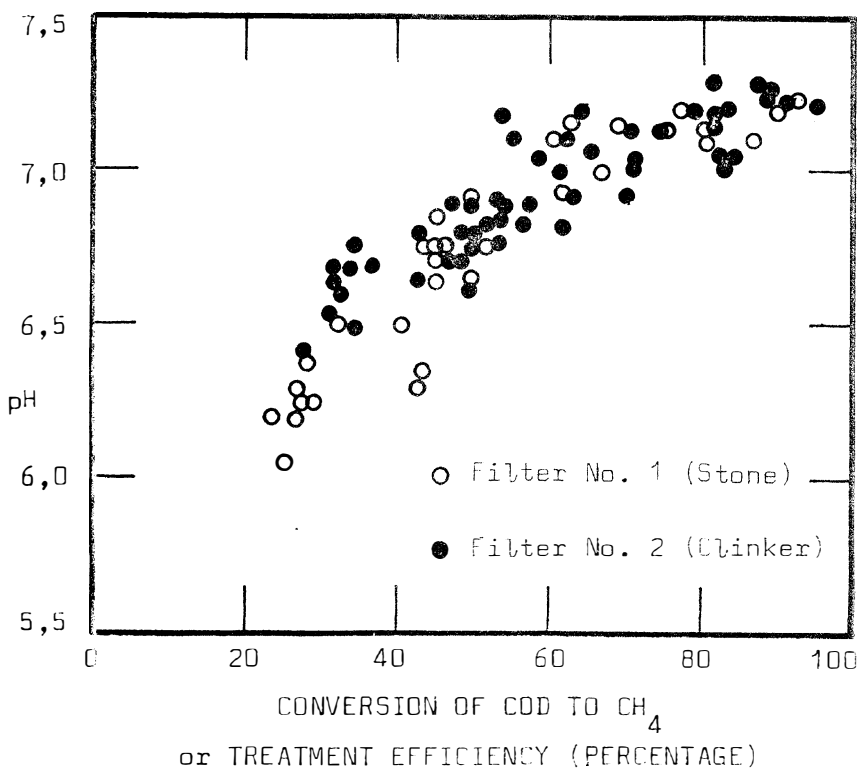

FIGURE 58: Decline of pH with Decreasing Treatment Efficiency for Overloaded Conditions

In order to investigate the mechanism of failure in relation to pH, the measured pH's, and factors controlling pH, were plotted against the treatment efficiency (Figures 56, 57 and 58).

1. The volatile fatty acids concentrations in both filters were relatively low (10×10^{-3} moles/l) at the higher treatment efficiencies (90% COD reductions). As the treatment efficiency deteriorated, so the volatile fatty acids increases; at the lowest treatment efficiency (approximately 30% COD reductions), the volatile fatty acid concentrations in Filters No. 1 and 2 were 35×10^{-3} moles/l and 45×10^{-3} moles/l respectively (Figure 56).

2. The concentration of strong base X in both filters decreased gradually from 90×10^{-3} moles/l at 90% COD reductions, to 25×10^{-3} moles/l at the lowest treatment efficiency (Figure 56).

3. The ammonia concentration in both filters was relatively insensitive to the treatment efficiency, and remained almost constant at 12×10^{-3} moles/l (Figure 56).

4. In both filters the rate of decline in the pH increased progressively as the treatment efficiency deteriorated - see Figure 58. (The is to be expected, since the buffer capacity decreases with decreasing pH - see page 124.) The initial pH in both filters was 7,2. At maximum loading, the lowest pH's obtained in Filters No. 1 and 2 were 6,4 and 6,05 respectively.

5. The percentage CO_2 in the digestor gas from both filters increased slightly from 32% at 90% COD reductions, to 38% at the lowest treatment efficiencies - 30% COD reductions (Figure 57).

Discussion

From the behaviour of the parameters monitoring the response of the filter during the overloaded period, it was not possible to identify the mechanism of failure. It could not be conclusively shown whether the mechanism of failure was due to inhibition of organisms or to

organism washout. However, the following observations support the contention that organism washout was probably the dominant mechanism of failure:

The treatment efficiencies of both filters deteriorated only gradually with increasing load (Figure 55). This contrasts with the sudden and complete process failures reported by the CSIR[1] and Thiel[49]. The implication was that pH and volatile fatty acids were dominant in the mechanism of failure, since their reported failures showed sudden sharp depressions in the pH and increases in the volatile fatty acids. This pattern of failure was not in evidence in the process failure of the filters.

The only alternative explanation for the slow deterioration in the process efficiency is the progressive washout of organisms (both acid and methane forming) from the process.

The relative activities of the methane and acid forming organisms remained approximately in proportion to each other, even at low treatment efficiencies. (The volatile fatty acis, which are the end products of acid fermentation, did not show are sharp increase.) This is contrary to the expected pH and volatile fatty acid inhibition mechanisms, since methanogenic organisms are usually inhibited before the acid forming organisms, with resulting rapid accumulation of volatile fatty acids. (The gradual increase in the volatile fatty acids, however, did indicate that the methanogenic organisms were coping with the load at a slower rate than the acid forming organisms.

When the load was removed after the 20 days of overload, the process showed fast recovery. Methane formation continued at a decreasing rate for the next two days until waste remaining in the reactor was completely stabilized. This appears to indicate that the process was highly overloaded (i.e. high food/organism ratio), and that the organisms were incapable of treating the total waste flow. The activities of the organisms, however, did not appear to be impaired in any way.

Retention of solids in Filter No. 1 appeared to aid the processes; the treatment efficiency of Filter No. 1 was consistently higher than that of Filter No. 2. This further supports the hypothesis that washout of solids definitely contributed to the process failure. Further discussion

on the mechanism of failure due to organism washout is not possible, since vital information on the solids concentrations in the reactor and effluent were not measured.

One may now enquire why the processes reported by the CSIR[1] showed such precipitate failure. A possible explanation is that their processes were operating near the minimum solids retention time before failure. The relative ratio of methane to acid organisms would then be lower than for long solids retention times. Thus, their processes were more sensitive to overloading, since washout of organism further reduces the methane/acid organism ratio. The relative reduction in the concentration of the methanogenic organisms was probably sufficiently high to cause an unbalanced organism population. As a consequence, the volatile fatty acids accumulated in the processes and the pH declined. The pH and volatile fatty acids are both toxins, and probably caused the sudden failure of their processes.

Although pH and volatile fatty acids inhibition did not appear to contribute significantly towards the mechanism of failure, the pH and related measurements remain useful for determining the causes for the decline in pH.

In the anaerobic process, decrease in pH may be caused by either a decrease in the net strong base S_b, or an increase in the partial pressure of CO_2, or both. The percentage CO_2 in the digestor gases did not increase significantly with decreasing treatment efficiency (Figure 57), and thus did not appreciably depress the pH: the effect of the change in CO_2% on pH may be noted on a pH conditioning diagram. The decreasing value of net strong base S_b was thus isolated as causing the depression in pH.

The systems contributing to the S_b concentration, i.e. volatile fatty acids, ammonia and strong base X are shown in Figure 56. A comparison of the three systems (on a basis of treatment efficiency) indicated that the increase in the volatile fatty acids and decrease in strong base X were responsible for the reduction in the <u>net</u> strong base S_b value. The ammonia remained virtually unchanged, and thus did not affect the S_b value. Thus, pH appears to be dependent mainly on the volatile fatty acids and strong base X.

The formation of strong base X, or equivalently the removal of hydrogen ions, has been identified as dependent on the waste stabilization process (Figure 56). Also, it appears that the formation of strong base X is in some way related to the conversion of the volatile fatty acids to methane: a comparison of the increases in the volatile fatty acids with the decreases in strong base X (Figure 56) shows that they are approximately proportional, possibly in the ratio 1 : 1.

In conclusion, it appears that failure of the filter processes can be attributed to the washout of organisms, and not to an inhibition mechanism. This suggests that unbalanced organism activities, which produce the pH and volatile fatty acid toxins, are induced only when the solids retention time in a process is near minimum. The decline in pH was caused by an increase in the volatile fatty acids and a decrease in the strong base X; both as a result of the decrease in treatment efficiency.

K. CONCLUSIONS

1. A high strength waste such as wine distillery waste is amenable to treatment in the anaerobic filter system. For the treatment of spent wine, the treatment efficiencies and capacities (based on the total volume of the system) appear to be almost identical to those of the contact system. On this consideration, there appears to be little advantage in replacing the established contact systems with the filter system. An advantage of the filter system, however, is the simplicity of its operational control.

2. The major site of the stabilization process in the filters appears to be in the interstices of the media, and not on the surface area of the media. Of the four filter media employed, i.e. quartzite, clinker, perforated plate and sand, the plate media gave the most satisfactory performance. Further attention in research should be devoted to developing a positive method for solid-liquid separation rather than providing large surface areas for micro-organism adhesion.

3. The steady-state continuous culture kinetic model can be usefully applied to the anaerobic filter system. As in the contact system, the solids retention time is the governing parameter of the process model, and can be used to describe the following process characteristics:

   (a) Treatment efficiency deteriorates rapidly below a solids retention time of about 7 days, but does not improve significantly at solids retention times greater than 9 days.

   (b) Solids concentration in the reactor increases both with solids retention time and loading rate. The maximum treatment capacity of a reactor with effective solids retention properties is eventually limited by the solids concentration becoming unmanageably high.

(c) Response of a process to shock loads is governed by the solids retention time. At long sludge ages, the process shows stability.

(d) The concentration of solids in the effluent is an extremely sensitive parameter controlling the solids retention time and therefore the process performance. Even small increases in effluent solids concentration is indicative of imminent process failure. For efficiant process operation, it is important that positive and effective control be kept over the solids wasted. Possible methods are the centrifuging of effluent and the return of solids to the reactor

4. Response of the anaerobic filters to changing environmental conditions such as during start-up, and temperature and loading rate fluctuations, was generally the same as the reported behaviour in literature. The parameters, pH, volatile fatty acids, gas production and percentage methane gave good indication of the process behaviour during unstable conditions of operation.

5. The control of pH in the aquatic system of an anaerobic process is intimately related to the activities of the micro-organism population. However, the following factors were isolated as governing the pH:

(a) pH in anaerobic processes is governed by the interaction of the strong and weak acid-base systems. The predominating weak acid-base systems are carbonic acid, acetic acid and ammonia species. As both acetic acid and ammonia species occur in dissociated form in the pH range 6,0 to 7,5, the pH is governed by the carbonic acid system, and the equivalent of a net strong base.

(b) Predictions to pH change using soluble dosing chemicals such as $NaHCO_3$ is facilitated by the use of a pH conditioning diagram. The partial pressure of CO_2 and the pH are used to define the initial equilibrium point before chemical dosing.

(c) Alkalinity is not an essential measurement in the monitoring of a digestor. Equally good control can be achieved by measuring the CO_2 partial pressure and the pH. In fact, total alkalinity measurements are undesirable as they are affected by the volatile fatty acid 'alkalinity'.

(d) Orthophosphate inhibits $CaCO_3$ precipitation. Lime, $Ca(OH)_2$, is only effective if orthophosphate, or some other chemical which inhibits $CaCO_3$ precipitation, is present. In the absence of orthophosphates, $Ca(OH)_2$ is completely ineffective as a dosing chemical to raise the pH above about 6,3, since the $Ca(OH)_2$ added precipitates as $CaCO_3$.

(e) In the presence of orthophosphate, lime is only 45% effective, and its cost should therefore be compared with the cost of dosing chemicals such as $NaHCO_3$ which is 100% effective.

(f) Orthophosphate concentrations greater than $1,0 \times 10^{-3}$ moles/l partially inhibit $CaCO_3$ precipitation for any addition of $Ca(OH)_2$. With concentrations below $1,0 \times 10^{-3}$ moles/l, the danger exists that the orthophosphate itself may precipitate out during the $Ca(OH)_2$ additions, thus removing the $CaCO_3$ precipitation inhibition mechanism. $CaCO_3$ would then precipitate out, and thus depress the pH to about 6,3. No further increase in the pH would be possible with $Ca(OH)_2$ additions.

(g) The mechanism of failure in the overloaded processes appeared to be governed mainly by organism washout and

not by pH and volatile fatty acid inhibition of the methanogenic organisms. However, the gradual depression in pH which did occur appeared to be governed by the volatile fatty acids and the strong base released during the waste stabilization process. The changes in percentage CO_2 in the digestor gas and ammonia did not significantly affect the pH.

oooOOOooo

APPENDIX I

ANALYTICAL TESTS AND EXPERIMENTAL PROCEDURES

1. Orthophosphates

Orthophosphate concentrations were determined by the method described by Edwards, Molof and Schneem in 'Determination of Orthosphate in Fresh and Saline Waters' from the Journal of the American Water Works Association - July 1965.

2. Ammonia

Free and saline ammonia concentrations were determined by the conventional method as described in Standard Methods, 13th Edition, 1971, (p. 186), published by the American Public Health Association, Washington D.C.

3. Volatile Fatty Acids

Total volatile fatty acid concentrations were measured by the method described by Montgomery, Dymock and Thom in 'The Rapid Colorimetric Determination of Organic Acids and Their Salts in Sewage Sludge Liquor' from The Analyst, Vol. 87, 1962.

4. Carbonic Species

A 'Beckman Carbon Analyser' (with Infrared Analyser, Model 215A) was used for the determination of the total inorganic carbon. Samples were centrifuged and diluted with CO_2 free de-ionized water to give readings in the range of 0 - 100 ppm of carbon. For this range of carbon concentration, the scale was approximately linear to carbon concentration (see Operating Manual).

5. Chemical Oxygen Demand - COD

Chemical oxygen demands (COD) were measured by methods described in Standard Methods, 13th Edition, 1971 (p. 501), published by

the American Public Health Association, Washington D.C.

Soluble COD measurements were made on the supernatant of a centrifuged sample (sample was centrifuged for 15 minutes).

6. Volatile Suspended Solids - VSS

Volatile suspended solids concentrations were measured by methods described in Standard Methods, 13th Edition, 1971 (p. 538), published by the American Public Health Association, Washington D.C.

The total suspended solid material was centrifuged from the mixed liquor.

7. Gas Composition

The methane and carbon dioxide components in the digestor gas were measured with a 'Beckman/GC-2A' gas chromatograph. Samples were introduced with (a) a gas-tight syringe (measurements for Chapter I), and (b) an automatic sampling valve (measurements for Chapter II). Hydrogen was used as the carrier gas. The gas component was assumed proportional to its peak height (see operating manual).

8. Conductivity

Conductivity measurements were made with a 'Radiometer' conductivity meter Type CDM2b.

9. pH

pH measurements were taken with 'Radiometer' pH meters Types '26', '28' and '29'. pH meter Type '26' was the most accurate and could determine the second decimal point of a pH division.

10. Temperature

Temperatures were measured with a mercury bulb thermometer graduated in 0,05°C divisions.

11. Titration Curves

The following combination of 'Radiometer' equipment was used:

(a) pH meter Type '28'.

(b) 'Autoburette ABU12' as the automatic burette feeding the titrant.

(c) 'Titratgraph' as the recorder on which the titration curve was plotted.

(d) Gas tight beaker and assembly to hold the sample and electrodes. A stirrer and thermometer were included in the aseembly.

(e) General purpose glass and reference calomal electrodes were used.

Operating procedure is described in the operating manuals of the apparatus.

12. Chemical Dosing

Experiments were conducted in the same beaker assembly of 11(d) above. The gas (39% CO_2 and 71% CH_4) was obtained from a gas cylinder prepared by AFROX and fed into the beaker (below water level) with a diffuser. pH measurements were taken with 'Radiometer' pH meters Type '26' and '28' and general purpose electrodes.

Samples of 50 ml were used in the tests. The samples were diluted with de-ionized water (as required) and the initial pH's adjusted with H_2SO_4 and NaOH. The gas was bubbled through the sample continuously to ensure CO_2 saturation at all times. Chemical additions were introduced through a small hole in the lid of the beaker. Temperature measurements were taken from a thermometer immersed in the sample, and the necessary corrections were made by immersing the sample in either hot or cold water as required.

APPENDIX II

TEMPERATURE AND IONIC STRENGTH CORRECTIONS TO THE EQUILIBRIUM CONSTANTS[37]

Temperature corrections were applied only to the equilibrium constants related to the carbonic system. The pK values for the dissociations of carbonic acid and water are calculated from:

$$pK_1 = \left(\frac{17\,052{,}000}{T}\right) + 215{,}21 \log T - 0{,}12675\ T - 545{,}56$$

$$pK_2 = \left(\frac{2902{,}39}{T}\right) + 0{,}02379\ T - 6{,}498$$

$$pK_w = \left(\frac{4787{,}3}{T}\right) + 7{,}1321 \log T + 0{,}010365\ T - 22{,}801$$

where T is in degrees Kelvin. The pK value for the solubility of $CaCO_3$ in water is given by:

$$pK_s = 0{,}01183\ t + 8{,}03$$

where t is in degrees celcius. The pK_G value for the solubility of CO_2 in water is given by:

$$pK_G = 1{,}12 + 0{,}0138\ t \quad \text{in the range } 0^oC \text{ to } 35^oC$$

and $$pK_G = 1{,}36 + 0{,}0069\ t \quad \text{in the range } 35^oC \text{ to } 80^oC$$

Ionic strength corrections were applied to all equilibrium constants except for the CO_2 solubility constant. Determination of ionic strength concentrations were made from both conductivity and total dissolved solids measurements. Their relationships to ionic strength are:

$$\mu = 2{,}5 \times 10^{-5}\ S_D$$

and $$\mu = 1{,}55 \times 10^{-5}\ C_N$$

APPENDIX III

The computer programme used for the calculation of theoretical titration curves is shown overleaf. The corrections applied to the equilibrium constants for ionic strength are included in the programme. The equilibrium constants (corrected for temperature) are read into the programme. Although only carbonic acid, ammonia, acetic acid and orthosphosphate species are included in the programme it can be easily modified to include any other weak acid-base system.

```
      CALCULATION OFTHEORETICAL TITRATION CURVE FROM THE WEAK
      ACID BASE SPECIES.



      N = 1
   10 REAL NPK, NK

      TEMP= TEMPERATURE OF SAMPLE
      AIS = IONIC STRENGTH OF SAMPLE
      SML= SAMPLE SIZE IN ML.
      CNN = NORMALITY OF TITRANT.
      READ (5, 11) TEMP, AIS, SML, CNN
   11 FORMAT (F5.3, F8.5, F6.1, F8.5)

      CALCULATION OF ACTIVITY COEFFICIENTS.
      FX = -0.5 * ((AIS ** 0.5 / (1.0 + AIS ** 0.5)) - (0.2 * AIS))
      FM = 10.0 ** (FX * 1.0)
      FD = 10.0 ** (FX *4.0)
      FT = 10.0 ** (FX * 9.0)

      WPK = PK FOR WATER.
      CPK 1 = PK1 FOR CARBONIC SPECIES.
      CPK2 = PK2 FOR CARBONIC SPECIES.
      ACPK = PK FOR ACETIC ACID.
      NPK = PK FOR AMMONIA.
      PPK1 = PK  FOR ORTHOPHOSPHATE.
      PPK2 = PK2 FOR ORTHOPHOSPHATE.
      PPK3 = PK3 FOR ORTHOPHOSPHATES.

      READ (5, 12) WPK, CPK1, CPK2, ACPK, NPK, PPK1, PPK2, PPK3
   12 FORMAT (8F7.2)

      CONVERSION OF PK VALUES TO K VALUES AND CORRECTION
      FOR IONIC STRENGTH.
      WK = (1.0 /(10.0 ** WPK)) / (FM ** 2.0)
      CK1 = (1.0 / (10.0 ** CPK1)) / (FM ** 2.0)
      CK2 = (1.0 / (10.0 ** CPK2)) / FD
      ACK = (1.0 / (10.0 ** ACPK)) / (FM ** 2.0)
      NK = (1.0 / (10.0 ** NPK)) / (FM ** 2.0)
      PK1 = (1.0 / (10.0 ** PPK1)) / (FM ** 2.0)
      PK2 = (1.0 / (10.0 ** PPK2)) / FD
      PK3 = (1.0 / (10.0 ** PPK3)) / (FD / (FT * FM))
      WRITE (6, 27) WK, CK1, CK2, ACK, NK, PK1, PK2, PK3
   27 FORMAT (8E10.4)

      CC= CONC. OF CARBONIC SPECIES IN MG/LITRE.
      CAC= CONC. OF ACETIC ACID SPECIES IN MG/LITRE.
      CN= CONC. OF AMMONIA SPECIES IN MG/LITRE
      CP= CONC. OF ORTHOPHOSPHATE SPECIES IN MG/LITRE.
      READ (5, 13) CC, CAC, CN, CP
   13 FORMAT (4F10.5)

      INITIAL PH OF TITRATION.
      PH = 2.0
   40 H = (10.0 ** (-PH)) / FM
```

```
     CALCULATION OF BUFFER INDICES.
50   BW = 2.303 * ((WK / H) + H)
     BC1 = 2.303 * ((CC * CK1 * H) / ((CK1 + H) ** 2.0))
     BC2 = 2.303 * ((CC *CK2 * H) / ((CK2 + H) ** 2.0))
     BAC = 2.303 * ((CAC * ACK * H) / ((ACK + H) ** 2.0))
     BN = 2.303 * ((CN * NK * H) / ((NK + H) ** 2.0))
     BP1 = 2.303 * ((CP * PK1 * H) / ((PK1 + H) ** 2.0))
     BP2 = 2.303 * ((CP *PK2 * H) / ((PK2 + H) ** 2.0))
     BP3 = 2.303 * ((CP *PK3 * H) / ((PK3 + H) ** 2.0))
     BT = BW + BC1 + BC2 + BAC + BN + BP1 + BP2 + BP3

     CALCULATION OF XML STRONG BASE ADDED IN ML.REQUIRED TO CAUSE
     AN INCREASE OF 0.1PH UNITS.
     XML = (0.1 * BT) / CNN * SML
     IF (PH - 2.0) 25, 25, 35

     XMLT = ML. OF STRONG BASE REQUIRED TO RAISE THE PH FROM THE
     INITIAL VALUE OF 2.0
25   XMLT = XML
     GO TO 85
35   XMLT = XMLT + XML
85   WRITE (6, 14) BW, BC1, BC2, BAC, BN, BP1, BP2, BP3, BT, XMLT
14   FORMAT (10E11.4)
     IF (PH - 12.0) 61, 61, 71
61   PH= PH + 0.1
     GO TO 49
71   IF (N - 2) 18, 19, 21
18   N = N + 1
     GO TO 18
21   STOP
     END
```

APPENDIX IV

CORRECTIONS TO CO_2 PARTIAL PRESSURES

This project has considered anaerobic processes to be under an atmospheric pressure of 1 atmosphere. However, atmospheric pressure decreases for increasing altitudes, and gas pressures at the bottom of digestors are not atmospheric.

Correction to atmospheric pressure for different altitudes can be applied with the following formula:

$$H' = 62\ 000 \log \frac{760}{p}$$

where H is the altitude in ft. and p the pressure in mm of mercury. For a rise in altitude from sea level to 6 000 ft the atmospheric pressure drops from 1 atmosphere to 0,8 atmospheres. Partial pressure of CO_2 will be correspondingly reduced by 20%. This could have considerable effect on the pH in a digestor (see any pH conditioning diagram).

Under quiescent conditions the gas pressure increases with increasing depths in a digestor. Since 1 atmosphere approximately equals a pressure of 10,5 m of water, the pressure at the bottom of a 10 m deep digestor is twice the pressure at the top. The partial pressure of CO_2 is correspondingly increased, affecting the equilibrium point and pH significantly. However, digestor contents are normally under completely mixed conditions, so that pH should be uniform throughout. The value of the pH will be dependent on the depth of the digestor, and will probably correspond to the CO_2 partial pressure at mid-depth. Deep digestors could thus depress the pH significantly, as shown by the pH conditioning diagram for an increased partial pressure of CO_2.

APPENDIX V

A selection of pH conditioning diagrams for the different temperatures and ionic strengths which may be encountered in anaerobic processes follow overleaf. The corrections which are applied to the equilibrium constants for different temperatures and ionic strengths are set out in Appendix II.

In each diagram, pH values range from 6,0 to 7,6 in intervals of 0,1 pH divisions, and the permissible Ca^{++} concentration from 2000 to 4 ppm as $CaCO_3$ in the following order:

2000; 1500; 100; 500; 300; 200; 150; 100; 50;
30; 20; 15; 10; 8; 6; 4.

A direction diagram for the addition of various possible dosing chemicals is shown on each diagram.

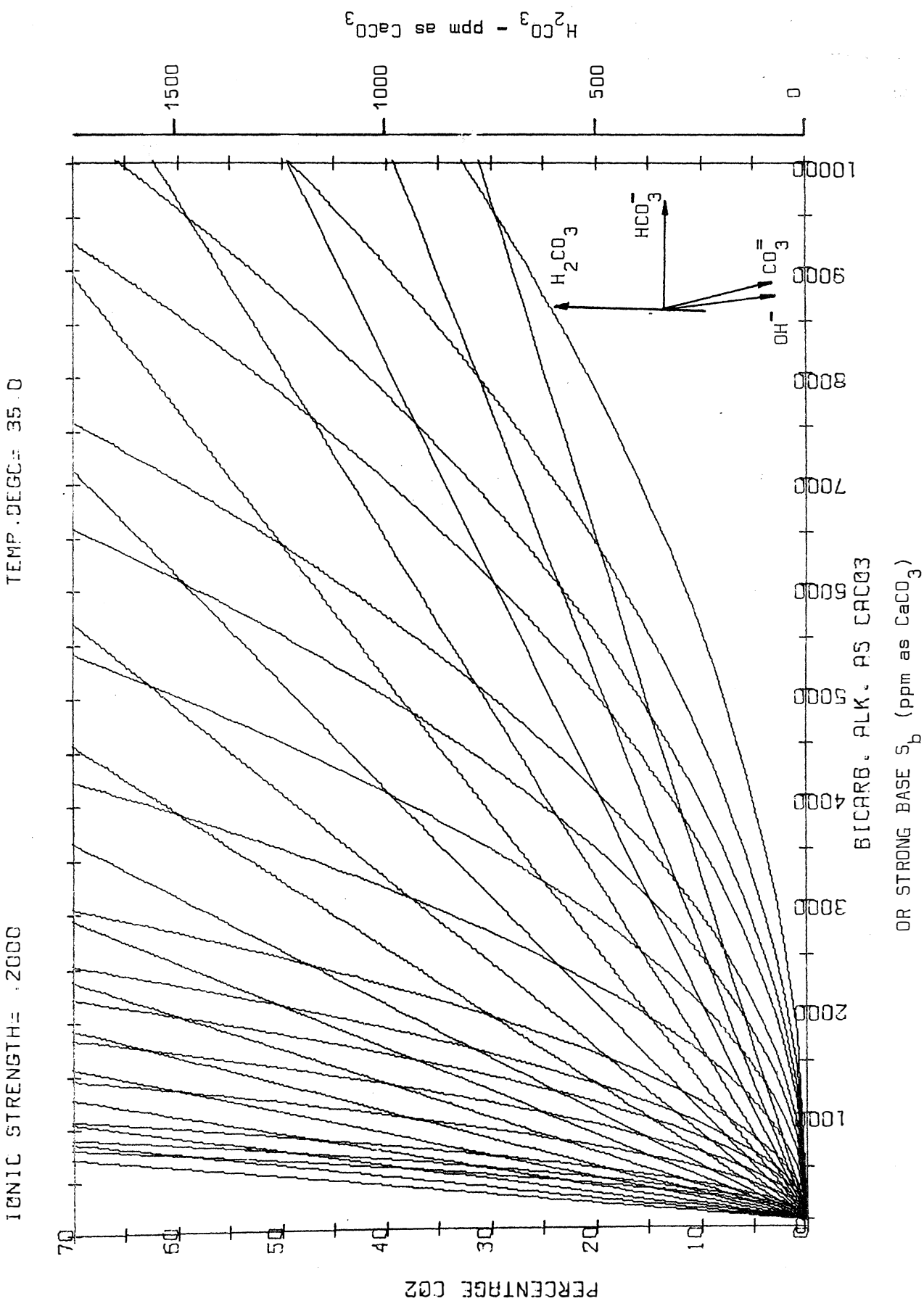
IONIC STRENGTH= .2000
TEMP.DEGC= 35.0
PERCENTAGE CO2
0
10
20
30
40
50
60
70
BICARB. ALK. AS CACO3
OR STRONG BASE S_b (ppm as $CaCO_3$)
1000
2000
3000
4000
5000
6000
7000
8000
9000
10000
H_2CO_3
HCO_3^-
$CO_3^=$
OH^-
H_2CO_3 - ppm as $CaCO_3$
0
500
1000
1500

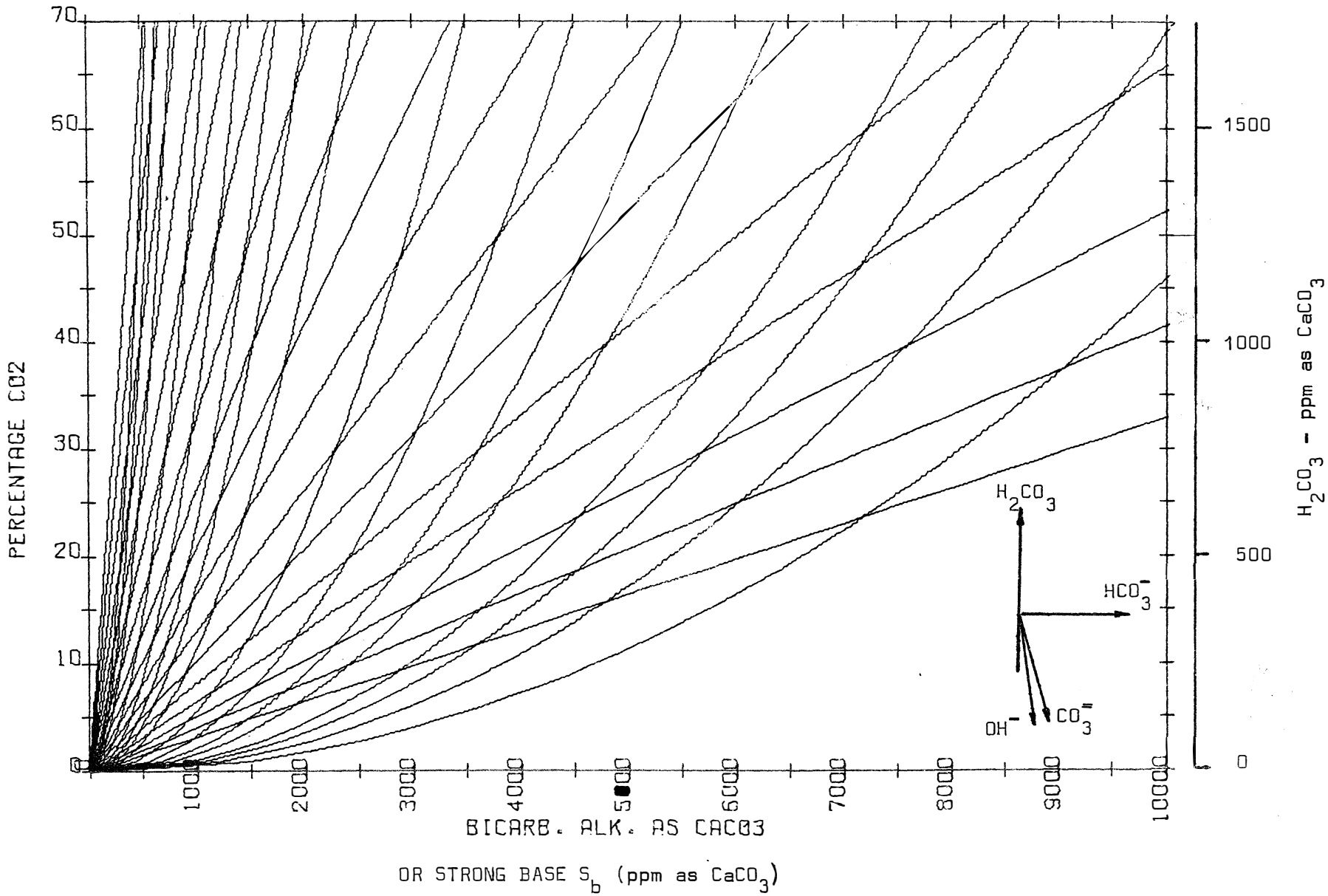
IONIC STRENGTH= .1000
TEMP.DEGC= 35.0
PERCENTAGE CO2
70
50
50
40
30
20
10
0
1000
2000
3000
4000
5000
6000
7000
8000
9000
10000
BICARB. ALK. AS CACO3
OR STRONG BASE S_b (ppm as $CaCO_3$)
H_2CO_3
HCO_3^-
OH^-
$CO_3^=$
1500
1000
500
0
H_2CO_3 - ppm as $CaCO_3$

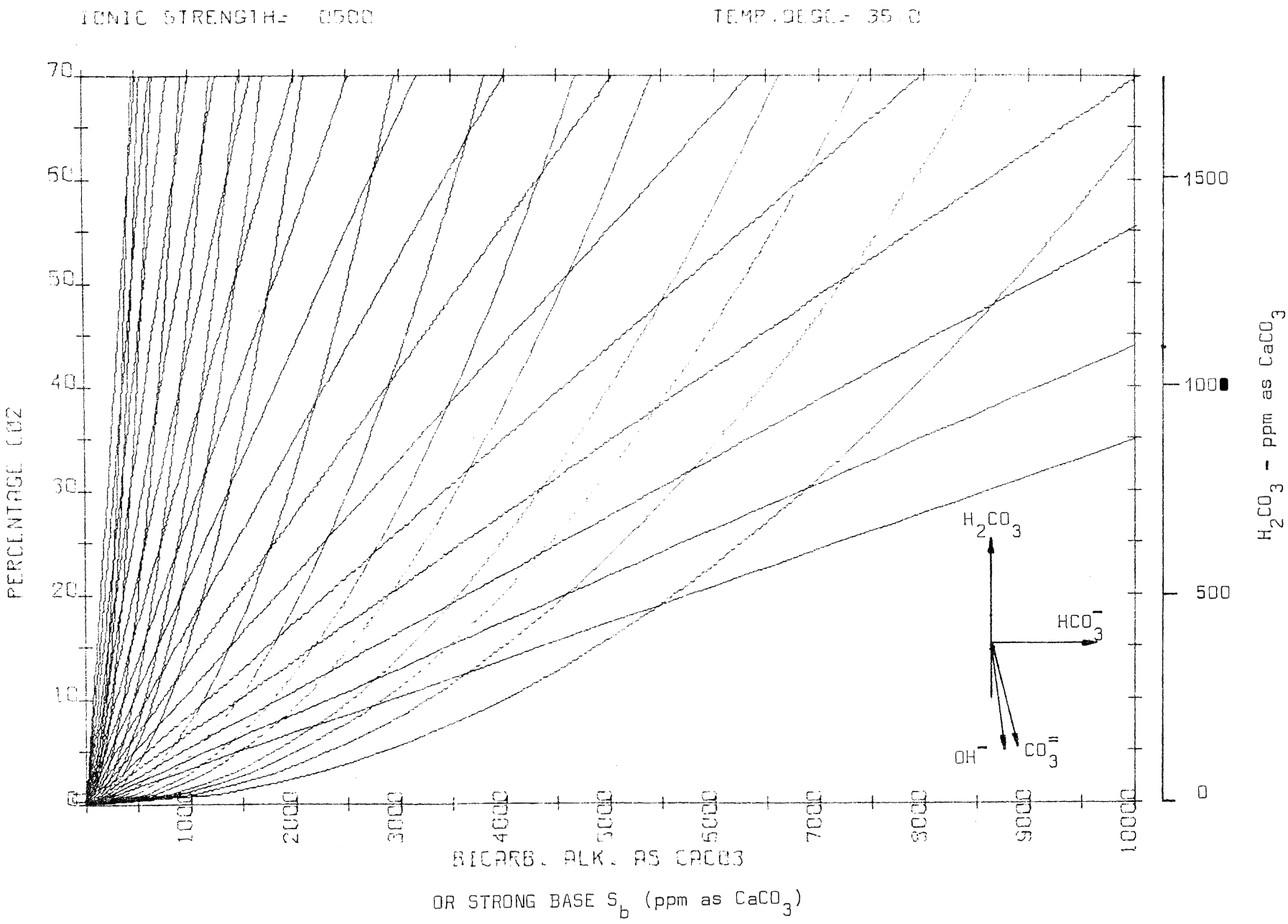
IONIC STRENGTH= 0500
TEMP.DEGC.= 35.0
PERCENTAGE CO2
70
60
50
40
30
20
10
0
1000
2000
3000
4000
5000
6000
7000
8000
9000
10000
BICARB. ALK. AS CACO3
OR STRONG BASE S_b (ppm as $CaCO_3$)
H_2CO_3
HCO_3^-
OH^-
$CO_3^{=}$
1500
1000
500
0
H_2CO_3 - ppm as $CaCO_3$

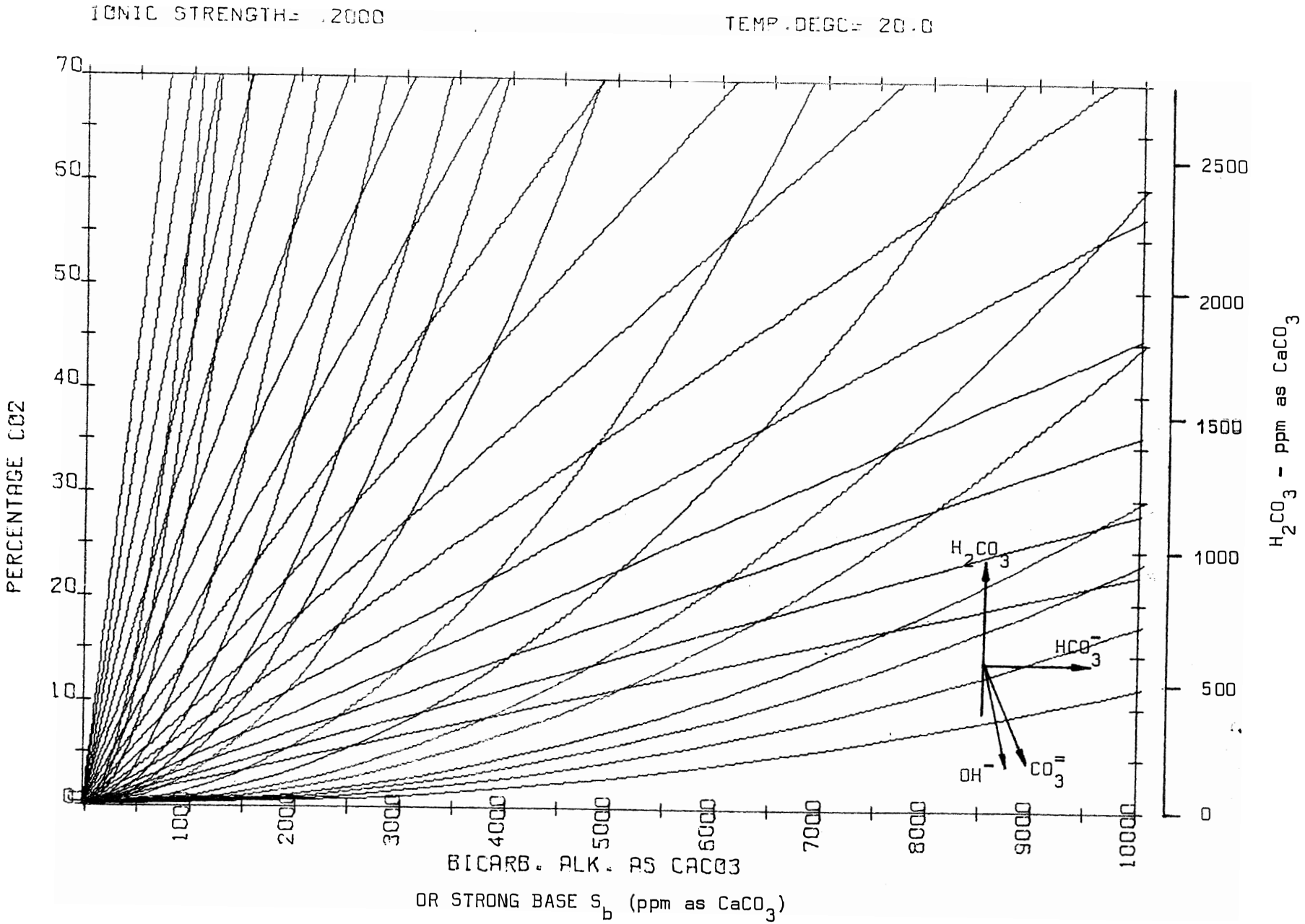
IONIC STRENGTH= .2000
TEMP.DEGC= 20.0
PERCENTAGE CO2
70
60
50
40
30
20
10
0
100
200
300
400
500
600
700
800
900
1000
BICARB. ALK. AS CACO3
OR STRONG BASE S_b (ppm as $CaCO_3$)
2500
2000
1500
1000
500
0
H_2CO_3 - ppm as $CaCO_3$
H_2CO_3
HCO_3^-
OH^-
$CO_3^=$

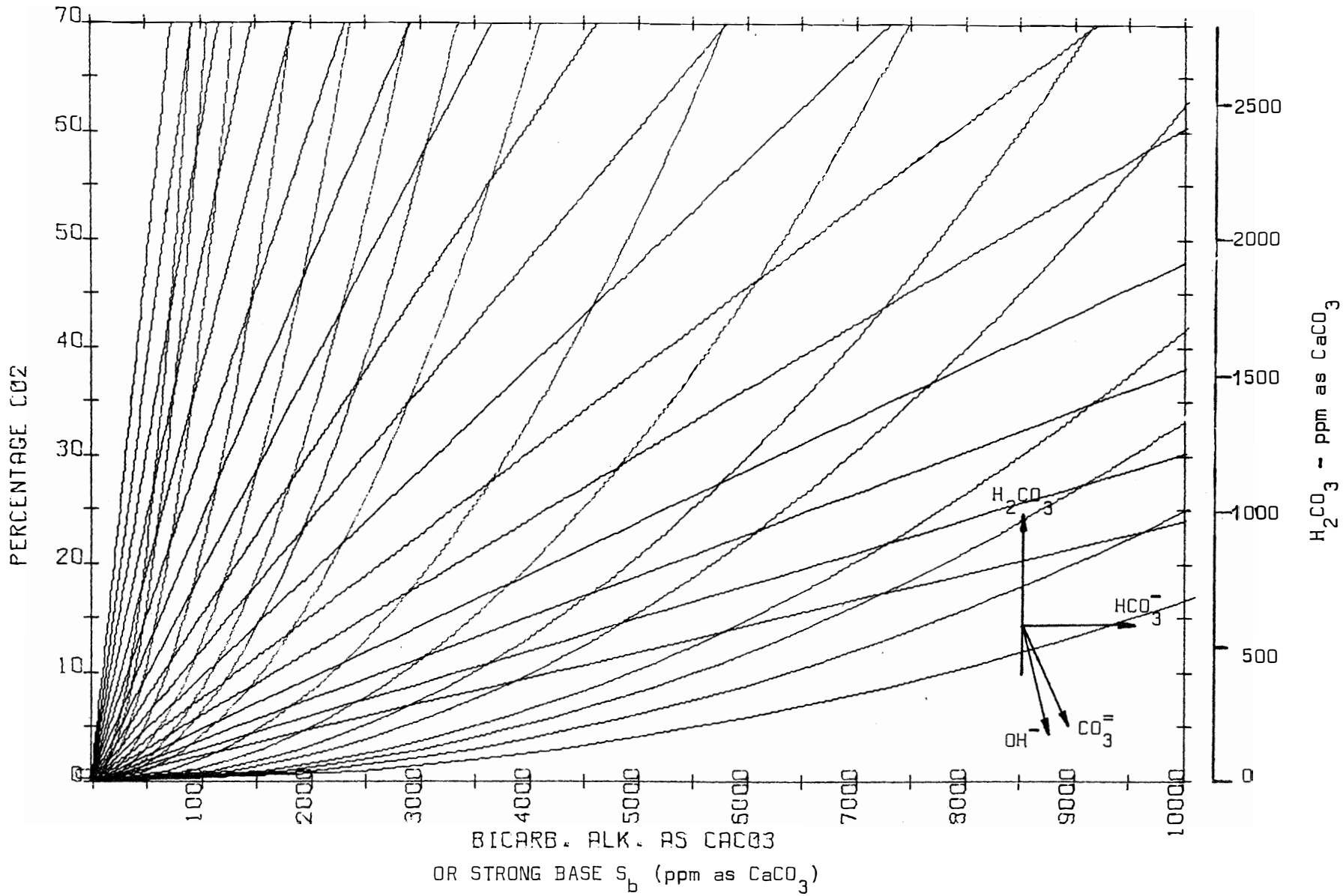
IONIC STRENGTH= .1000
TEMP.DEGC= 20.0
PERCENTAGE CO2
70
50
50
40
30
20
10
0
100
200
300
400
500
600
700
800
900
1000
BICARB. ALK. AS CACO3
OR STRONG BASE S_b (ppm as $CaCO_3$)
H_2CO_3
HCO_3^-
OH^-
$CO_3^=$
2500
2000
1500
1000
500
0
H_2CO_3 - ppm as $CaCO_3$

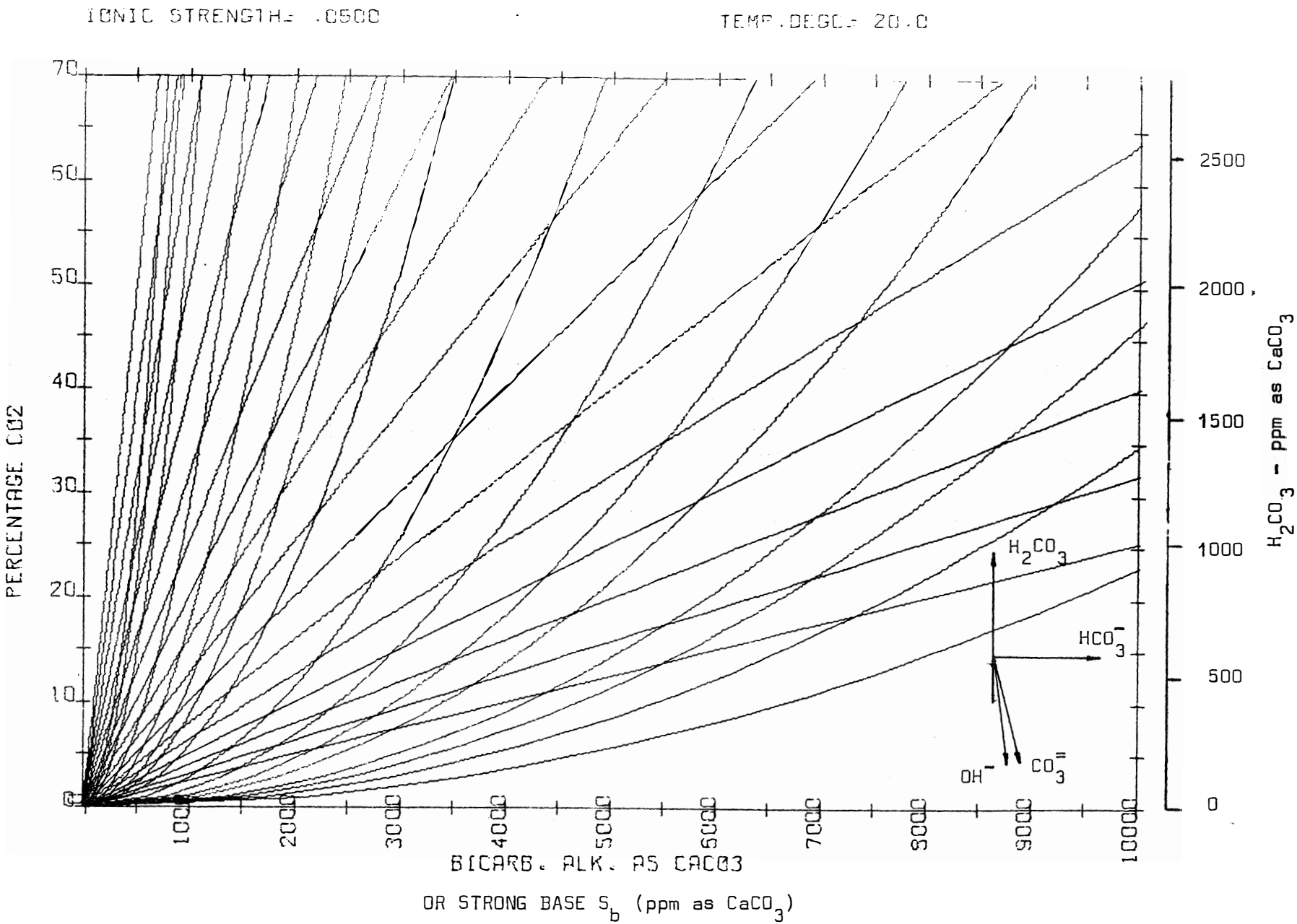
IONIC STRENGTH= .0500
TEMP.DEGC= 20.0
PERCENTAGE CO2
70
60
50
40
30
20
10
0
100
200
300
400
500
600
700
800
900
1000
BICARB. ALK. AS CACO3
OR STRONG BASE S_b (ppm as $CaCO_3$)
2500
2000
1500
1000
500
0
H_2CO_3 - ppm as $CaCO_3$
H_2CO_3
HCO_3^-
OH^-
$CO_3^=$

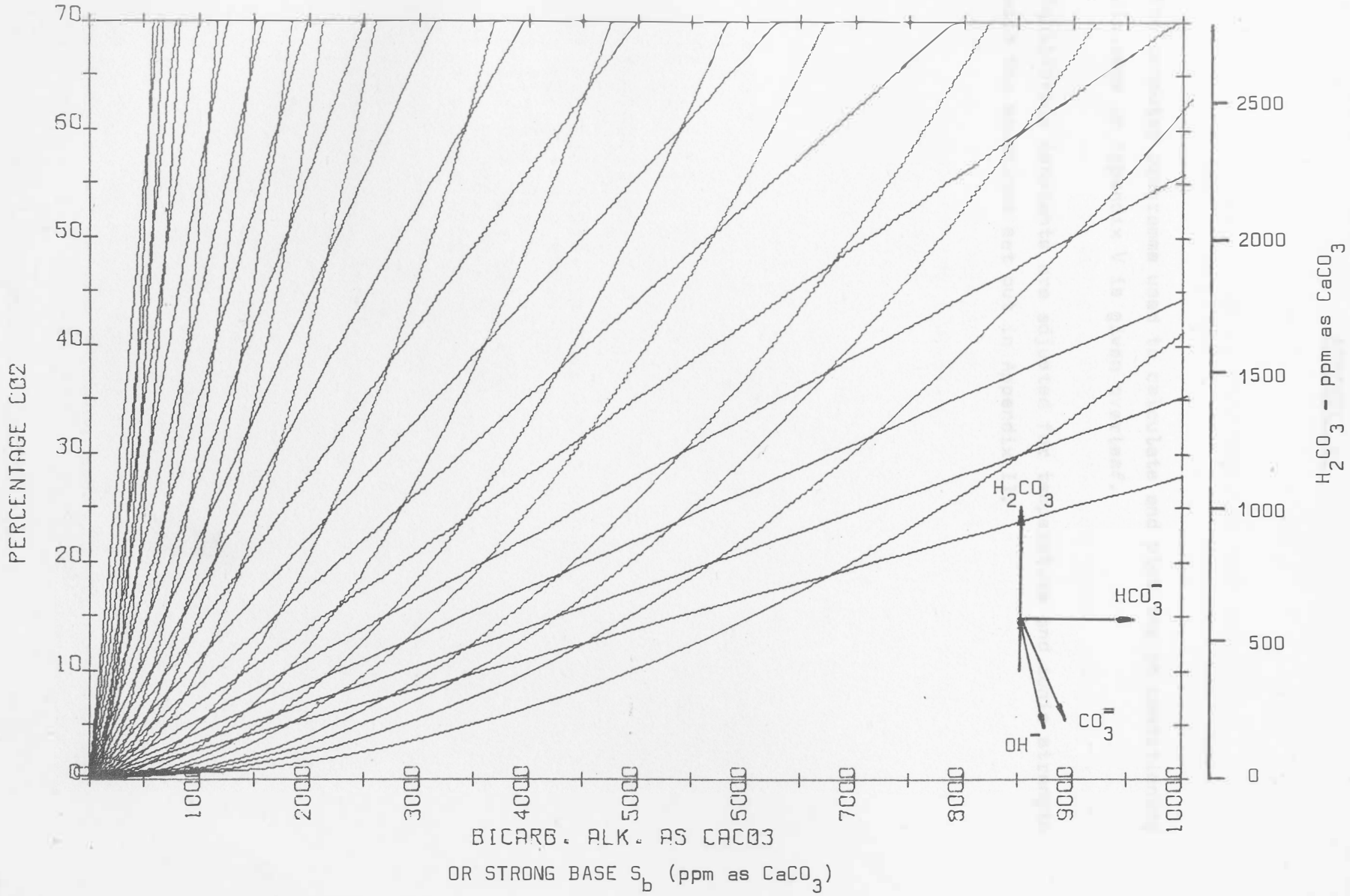
IONIC STRENGTH= .0100
TEMP.DEGC= 20.0
PERCENTAGE CO2
70
60
50
40
30
20
10
0
1000
2000
3000
4000
5000
6000
7000
8000
9000
10000
BICARB. ALK. AS CACO3
OR STRONG BASE S_b (ppm as $CaCO_3$)
H_2CO_3
HCO_3^-
$CO_3^=$
OH^-
2500
2000
1500
1000
500
0
H_2CO_3 - ppm as $CaCO_3$

APPENDIX VI

The computer programme used to calculate and plot the pH conditioning diagrams in Appendix V is given overleaf.

Equilibrium constants are adjusted for temperature and ionic strength with the equations set out in Appendix II.

```
      CALCULATION OF PH CONDITIONING DIAGRAM FOR THE AQUATIC
      SYSTEM OF AN AEROBIC DIGESTOR.


      REAL K1, K2, KG, KS, IS
      DIMENSION PCO2(100), ALK(100), CO3(100), CO2(100), D(100), STRING(
     .6), C(40), T(10), IS(10)
      DO 11 JK = 1, 8

      T= TEMPERATURE IN THE  DIGESTOR.
      IS =IONIC STRENGTH IN THE DIGESTOR.
      READ (5, 20) T(JK), IS(JK)
   20 FORMAT (2F20.5)
   11 CONTINUE
      DO 13 J = 1, 16
      READ (5, 23) C(J)
   23 FORMAT (F20.5)
   13 CONTINUE
      DO 12 JK = 1, 8
      AA = T(JK)
      BB = IS(JK)
      PI = 3.1416

      PLOTTING INSTRUCTIONS.

      CALL SCALE (.00075, .075, -4000., -30.)
      CALL FGRID (0, 0., 0., 500., 20)
      CALL FGRID (1, 0., 0., 5., 14)
      CALL FGRID (0, 0., 70., 500., 20)
      CALL FGRID (1, 10000., 0., 5., 14)
      DO 37 L = 1, 10001, 1000
      ML = L -1
      X = ML
      ENCODE (21, 5) ML
      CALL PCHAR (X, -5., .1, 5, PI/2., 5)
   21 FORMAT (I5)
   37 CONTINUE
      DO 60 L = 1, 71, 10
      ML = L - 1
      Y = ML
      ENCODE (55, 5) ML
      CALL PCHAR (-300., Y, .1, 5, 0., 2)
   55 FORMAT (I2)
   60 CONTINUE
      CALL PCHAR (-600., 20., .1, 'PERCENTAGE CO2', PI/2, 14)
      CALL PCHAR (3500.,  -6., .1, 'BICARB. ALK. AS CACO3', 0., 21)
      CALL PCHAR (-3000., 0., .1, 'M CRAPI', PI/2, 7)
      ENCODE (400, STRING) BB
      CALL PCHAR (0., 75., .1, STRING, 0., 21)
   40 FORMAT ('IONIC STRENGTH=', F6.4)
      ENCODE (500, STRING) AA
      CALL PCHAR (6000., 75., .1, STRING, 0., 15)
   50 FORMAT ('TEMP.DEGC=', F5.1)
      CALL PLTIME(90)
```

```
C
C     CALCULATION OF EQUILIBRIUM CONSTANTS FOR SPECIFIC TEMPERATURES.
C     RK1 =PK1 OF CARBONIC SPECIES.
C     RK2 = PK2 OF CARBONIC SPECIES.
C     RK5= PK5 OF CALCIUM CARBONATE SOLUBILITY.
C     RK6 = PK6 OF CO2 SOLUBILITY.
C
      TK = 273. + T(JK)
      RK1 = 17052. / TK + 215.21 * ( ALOG1C (TK)) - 0.12675 *TK - 545.56
      RK2 = 2902.39 / TK +0.02379 *TK - 6.498
      RK6 = 1.12 + 0.0138 * T(JK)
      RK5 = 0.03 + 0.01133 * T(JK)

C     CALCULATION OF ACTIVITY COEFFICIENTS
      FX = -0.5*((IS(JK)**0.5/(1. + IS(JK)**0.5)) - (0.2*IS(JK)))
      FM = 10. **FX
      FD = 10. ** (FX * 4.)

C     CONVERSION OF PK VALUES TO K VALUES, WITH IONIC STRENGTH
C     CORRECTIONS APPLIED.
      K1 = 10.**(-RK1) / FM**2.
      K2 = 10. ** (-RK2) / FD
      K6 = 10. ** (-RK6)
      K5 = 10. ** (-RK5) / FD ** 2.

C     FOR A CONSTANT PH, THE HCO3(ALK) IS CALCULATED FROM
C     THE PARTIAL PRESSURE OF CO2 (PCO2) INPUTS.
      PH = 6.
   97 H = 10. ** (-PH) / FM
      I = 1
      PCO2(I) = 0.
      M = 1
   85 ALK(I) = K6 * PCO2(I) * K1 / H * 500.
      IF (ALK(1) - 10000.) 95, 95, 99
   95 M = M + 1
   99 IF (PCO2(I) - 30.) 63, 64, 64
   63 PCO2(I+1) = PCO2(I) + 1.
      I = I + 1
      GO TO 85

C     EACH LINE OF CONSTANT PH IS PLOTTED.
   64 CALL FPLOT (3, ALK(1), PCO2(1))
      IF (M - 71) 41, 42, 42
   42 M = 71
   41 DO 52 I = 1, M
      CALL FPLOT (2, ALK(I), PCO2(I))
   52 CONTINUE
      IF (PH - 7.5) 61, 62, 62
   61 PH = PH + 0.1
      GO TO 97
   62 CONTINUE
      J = 1
      DO 67 J = 1, 18
```

```
C
C       FOR A CONSTANT CALCIUM CONCENTRATION, THE HCO3 (ALK) IS
C       CALCULATED FROM THE PARTIAL PRESSURE OF CO2 (PCO2) INPUTS.
      CA = C(J)
      I = 1
      M = 1
      PCO2(I) = 0.
   86 CO3(I) = KS / CA * 10. ** 5.
      CO2(I) = KG * PCO2(I) / 100.
      D(I) = CO3(I) * K1 * CO2(I) / K2
      ALK(I) = SQRT (D(I)) * 50000.
      IF (ALK(I) - 10000.) 97, 97, 98
   97 M = M + 1
   98 IF (PCO2(I) - 80.) 65, 66, 65
   65 PCO2(I+1) = PCO2(I) + 1.
      I = I + 1

      GO TO 86
C
C       EACH LINE OF CONSTANT CALCIUM CONCENTRATION IS PLOTTED.
   66 CALL FPLOT (3, ALK(1), PCO2(1))
      IF (M - 71) 43, 44, 44
   44 M = 71
   43 DO 53 I = 1, M
      CALL FPLOT (2, ALK(I), PCO2(I))
   53 CONTINUE
   67 CONTINUE
      CALL FPLOT (3, 10000., -30.)
   12 CONTINUE
      CALL PEND
      CALL EXIT
      END
```

REFERENCES

1. South African Council for Scientific and Industrial Research, 'Investigation of the Full-Scale Purification of Wine Distillery Wastes by the Anaerobic Digestion Process', Research Report No. 270 (Sept. 1968).

2. YOUNG, J.C. and McCARTY, P.L. 'The Anaerobic Filter for Waste Treatment Journal Water Pollution Control Federation, Vol. 41, Part 2 (May 1969).

3. STANDER, G.J. 'Effluents from Fermentation Industries - Parts III and IV', Journal and Proceedings Institute of Sewage Purification, Part 3 and 4 (1950).

4. McCARTY, P.L. 'Anaerobic Waste Treatment Fundamentals, Part One, Chemistry and Microbiology', Public Works (Sept. 1964).

5. SHINDALA, A. and BYRNE, T.G. 'Anaerobic Digestion of Thickened Sludge', Public Works

6. MALINA, J.F. 'Thermal Effects on Completely Mixed Anaerobic Digestion', Water and Sewage Works, (Jan 1964).

7. SPEECE, R.E. and KEM, J.A. 'The Effect of Short-Term Temperature Variations on Methane Production', Journal Water Pollution Control Federation, Vol. 42 (Nov. 1970).

8. McCARTY, P.L. 'Anaerobic Waste Treatment Fundaments, Part Two, Environmental Requirements and Control', Public Works (Oct. 1964).

9. CLARK, R.H. and SPEECE, R.E. 'The pH Tolerance of Anaerobic Digestion', Proceedings 5th International Water Pollution Research Conference, July-August 1970, Pergamon Press Ltd., Spring 1971.

10. McCARTY, P.L. 'Anaerobic Waste Treatment Fundamentals, Part Three, Toxic Materials and Their Control', Public Works (Nov. 1964).

11. ANDREWS, J.F. 'Dynamic Model of the Anaerobic Digestion Process', Proceedings of the American Society of Civil Engineers, Sanitary Engineering Division, (Feb. 1969).

12. YOUNG, J.C. and McCARTY, P.L. 'Fixed Film Anaerobic Processes for Biological Wastewater Treatment', Preliminary draft of a chapter to be included in a book 'Biological Treatment of Wastewaters', edited by F.G. Pohland, and published by Marcel Dekker, Inc., New York.

13. LAWRENCE, A.W. and McCarty, P.L. 'Unified Basis for Biological Treatment Design and Operation', Proceedings of the American Society of Civil Engineers, Sanitary Engineering Division, (June 1970).

14. Simpson, D.E. 'Investigations on a Pilot-Plant Contact Digestor for the Treatment of Dilute Urban Waste', Water Research, Vol. 5, (1971).

15. STEFFEN, A.J. and BEDKER, M. 'Operation of Full-Scale Anaerobic Contact Treatment Plant for Meat Packing Wastes', Proceedings of the 16th Industrial Waste Conference, May 1962, Purdue Engineering Extension Series 109 (1961).

16. PLUMMER, A.H., MALINA, J.F., Jr. and ECKENFELDER, W.W., Jr. 'Stabilization of a Low Solids Carbohydrate Waste by an Anaerobic Submerged Filter', Proceedings of the 23rd Industrial Waste Conference, May 1968, Purdue Engineering Extension Series 132, (1968).

17. PRETORIUS, W.A. 'Anaerobic Digestion of Raw Sewage', Water Research, Vol. 5 (1971).

18. WARREN, M.P. 'The Treatment of Yeast Factory Effluent by an Anaerobic Submerged Filter', Thesis M.Sc.(Eng), University of Cape Town, 1972.

19. 'Rate of Digestion and Loading', Water Pollution Control Federation Manual of Practise, No. 16 (1968).

20. FILBERT, J.W. 'Procedures and Problems of Digestor Start-up', Journal of the Water Pollution Control Federation, Vol. 39, (March 1967).

21. LYNAM, B., McDONNELL, G. and KRUP, M. 'Start-up and Operation of Two New High-Rate Digestion Systems', Journal of the Water Pollution Control Federation, Vol. 39, (April 1967).

22. MARAIS, G.v.R. 'The Activated Sludge Process at Long Sludge Ages', Unpublished paper.

23. LAWRENCE, A.W. and McCARTY, P.L. 'Kinetics of Methane Fermentation in Anaerobic Treatment', Journal of the Water Pollution Control Federation, Vol. 41, Part 2, (Feb. 1969).

24. MONOD, J. 'Technique of Continuous Culture - Theory and Application' (Translation from French), Ann. Inst. Pasteur, Vol. 79 (1950).

25. McCARTY, P.L. 'Stoichiometry of Biological Reactions', International Conference - Toward a Unified Concept of Biological Waste Treatment Design - Atlanta, Georgia, Oct. 1972.

26. GATES, W.E., SMITH, J.H., SHUN-DAR LIN, and RIS III, C.H. 'A Rational Model for the Anaerobic Contact Process', Journal of the Water Pollution Control Federation, Vol. 39, Part 2, (Dec. 1967).

27. WASHINGTON, D.R. and SYMONS, J.M. 'Volatile Sludge Accumulation in Activated Sludge Systems', Journal of the Water Pollution Control Federation, Vol. 34, (1962).

28. McCARTY, P.L. 'Thermodynamics of Biological Synthesis and Growth', International Journal of Air and Water Pollution, Vol. 9 (1965).

29. ECKENFELDER, W.W., Jr. and WESTON, R.F. 'Kinetics of Biological Oxidation in Biological Treatment of Sewage and Industrial Wastes Vol. I', Edited by Brother Josph McCabe, F.S.C., and Eckenfelder, W.W., Reinhold Publishing Corporation, New York (1956).

30. DAGUE, R.R., Discussion on paper by Andrews, J.F. 'Dynamic Model of the Anaerobic Digestion Process', Proceedings American Society of Civil Engineers, Sanitary Engineering Division (Dec. 1969).

31. POHLAND, F.G. and MARTIN, J.C. Discussion on paper by Andrews, J.F. 'Dynamic Model of the Anaerobic Digestion Process', Proceedings American Society of City Engineers, Sanitary Engineering Division (Dec. 1969).

32. KIRSH, E.J. and SYKES, R.H. 'Anaerobic Digestion in Biological Waste Treatment', Progress in Industrial Microbiology, Vol. 9, (1971).

33. TOERIEN, D.F. and HATTINGH, W.H.J. 'Anaerobic Digestion, I, The Microbiology of Anaerobic Digestion', Water Research, Vol. 3, (1969).

34. BRYANT, M.P., WOLIN, E.A., WOLIN, M.J. and WOLFE, R.S. Arch. Mikrobiol. Vol. 59, (1967).

35. POHLAND, F.G. and ENGSTROM, R.J. 'High-Rate Digestion Control, I Fundamental Concepts of Acid-Base Equilibrium', Proceedings of the 19th Industrial Waste Conference, Purdue University Extension Series, (1964).

36. POHLAND, F.G. 'High-Rate Digestion Control, II, Techniques for Evaluating Acid-Base Equilibrium', Proceedings of the 22nd Industrial Waste Conference, Purdue University Extension Series, (1969).

37. LOEWENTHAL, R.E. 'The Carbonic System in Water Treatment', M.Sc. (Eng) Thesis, University of Cape Town, (1973).

38. STUMM, W. and MORGAN, J.T. 'Aquatic Chemistry', Wiley-Interscience (1970).

39. BUTLER, J.N. 'Ionic Equilibrium', Addison-Wesley Pub. Co., (1964).

40. BARD, A.J. 'Chemical Equilibrium', Harper International Edition, (Dec. 1966).

41. SAWYER, C.N. and McCARTY, P.L. 'Chemistry for Sanitary Engineers', McGraw-Hill Book Co., (1967).

42. POHLAND, F.G. 'High-Rate Digestion Control, III, Acid-Base Equilibrium and Buffer Capacity', Proceedings 23rd Industrial Waste Conference, Purdue University Extension Series, (1969).

43. STUMM, W. Discussion on 'Methods for the Removal of Phosphorus and Nitrogen from Sewage Plant Effluents', Advances in Water Pollution Research, Vol. 2 (1962).

44. BACHRA, B.N. TRANTZ, O.R. and SIMON, S.R. 'Precipitation of Calcium Carbonates and Phosphates', Achiv. Biochem. and Biophys., Vol. 103, (1963).

45. SCHMID, L.A. and McKINNEY, R.E. 'Phosphate Removal by a Lime-Biological Treatment Scheme', Journal of the Water Pollution Control Federation, Vol. 41 (July 1969).

46. VAN WAZER, J.R. 'Phosphorus and its Compounds', Vols. I and II, Interscience Publishers, Inc., New York (1958).

47. FERGUSON, F.J. and McCARTY, P.L. 'The Precipitation of Phosphates from Fresh Waters and Waste Waters', Technical Report No. 120, Department of Civil Engineering, Stanford University, (Dec. 1969).

48. POHLAND, F.G. and BLOODGOOD, D.E. 'Laboratory Studies on Mesophilic and Thermophilic Anaerobic Sludge Digestion', Journal of the Water Pollution Control Federation, Vol. 35, (Jan. 1963).

49. THIEL, P.G., TOERIEN, D.F. HATTINGH, W.H.J., KOTZE, J.P., and SIEBERT, M.L. 'Interrelation between Biological and Chemical Characteristics in Anaerobic Digestion', Water Research, Vol. 2, (1968).